COMPUTATIONALLY EFFICIENT POLYNOMIAL CHAOS FRAMEWORK BASED SFEM FOR STRUCTURAL MECHANICS PROBLEMS WITH RANDOM MATERIAL PROPERTIES

A Thesis Submitted
in Partial Fulfilment of the Requirements
for the Degree of

DOCTOR IN PHILOSOPHY

by

KAMALJYOTI NATH

DEPARTMENT OF CIVIL ENGINEERING
INDIAN INSTITUTE OF TECHNOLOGY GUWAHATI
GUWAHATI-781039, ASSAM, INDIA

SEPTEMBER 2019

Dedicated to my parents

Mr. Harindra Mohan Nath

and

Mrs. Putul Devi

CANDIDATE'S DECLARATION

I do hereby declare that work which is being presented in the thesis entitled "COMPUTATIONALLY EFFICIENT POLYNOMIAL CHAOS FRAMEWORK BASED SFEM FOR STRUCTURAL MECHANICS PROBLEMS WITH RANDOM MATERIAL PROPERTIES" in partial fulfilment of the requirement for the award of the degree of Doctor of Philosophy in Civil Engineering, with specialization in Structural Engineering, is an authentic record of my own work carried out in Department of Civil Engineering at Indian Institute of Technology Guwahati. The work has been carried out under supervision of Dr. Anjan Dutta and Dr. Budhaditya Hazra.

The content presented in this thesis has not been submitted by me for award of any other degree or diploma of this or any other University/Institute.

(Kamaljyoti Nath)

CERTIFICATE

This is to certify that the above statement made by the candidate is correct to best of our knowledge.

(Dr. Anjan Dutta)
Professor
Department of Civil Engineering
Indian Institute of Technology Guwahati
Guwahati-781039

(Dr. Budhaditya Hazra)
Associate Professor
Department of Civil Engineering
Indian Institute of Technology Guwahati
Guwahati-781039

Acknowledgement

This thesis is the outcome of studies carried out in the Department of Civil Engineering, Indian Institute of Technology Guwahati (IITG), Assam, India. I would like to express my deep sense of gratitude to my supervisors Prof. Anjan Dutta and Dr. Budhaditya Hazra for their endless effort in providing suggestions and critical reviews of my work, moral support and constant encouragement throughout the research work. The endless reassurance, recommendations and co-operation have been a great motivation for me while carrying out my research work. I will always be grateful to them for the knowledge they shared from their enormous experience.

Besides my supervisor, I would like to acknowledge the members of doctoral committee comprising of Prof. Sajal K. Deb, Prof. Uday S. Dixit and Dr. Kaustubh Dasgupta for their valuable recommendations and insightful remarks throughout the course of research activities, which has constantly engaged me towards undertaking a meaningful thesis work.

I have very fond memories of my time here. I would like to deeply thank all my friends in IITG. Specially, I would like to thank my friends in the department Pallab, Pranjal, Monjusha, Nishant, Biswajit, Nithin for all the enriching and valuable discussions.

Last but not the least, I owe my gratitude towards my parents Mr. Harindra Mohan Nath and Mrs. Putul Devi, my brother Mr. Bikash Jyoti Nath as well as my sister Miss Bhaswati Devi for their love and support throughout my journey.

KAMALJYOTI NATH

Abstract

Presence of uncertainties in structural systems is one of the major concerns in the safety of any designed structure. The fact that system variables are uncertain, implies that there is consequent uncertainty in structural responses and the designed structure. The structural analyses generally performed considering the characteristic values of system parameters (variables) do not provide true scenarios of reality. With a better understanding of the physical world, the numerical models to represent physical phenomena are also improving, and in many cases, the uncertainties are considered in the mathematical model. Moreover, with the advancement in computational power, demands for a more realistic analysis considering uncertainties of the engineering problems are increasing. Researchers are continuously engaged in exploring more and more realistic consideration of random nature of physical parameters in mathematical models. Such studies provide the basis for finding a safety factor in engineering design. Moreover, the uncertainty study makes it possible for the assessment of alternative strategies in engineering problems. The present study considers systematic studies on linear structural mechanics problems with random material properties.

Stochastic Finite Element Method (SFEM) is one of the branches of the Finite Element Methods, where an approximate solution of the stochastic system is sought to be evaluated. Within the framework of SFEM, Polynomial Chaos (PC) based method is one of the methods, where the solution is approximated using known random orthogonal functions and unknown coefficients. Thus, the evaluation of random responses is equivalent to finding out the unknown coefficient of PC expansion. However, as the number of random variables and/or the order of expansion increases, the number of terms also increases exponentially. This is known as the curse of dimensionality and one of the major drawbacks of PC based method. The present study considers a detailed study of PC based SFEM to improve its computational efficiency and to address the curse of dimensionality. One of the methods for evaluation of coefficients is by utilizing the orthogonal property of the PC expansion, where the stochastic equations may be converted to equivalent deterministic equations. The process is known as an intrusive method.

An iterative method for the solution of stochastic linear structural mechanics problems with random coefficient in the intrusive PC framework is proposed in the present study. The

method solves the problem by constructing the PC expansion iteratively with a reduced number of unknown coefficients. The method is based on an orthogonal expansion of stochastic responses and generation of an iterative PC based on the responses of the previous iteration. The polynomials are formulated using the Gram-Schmidt orthogonalization process. The number of random variables in PC expansion is reduced by considering only the dominant components of the response characteristics, which is evaluated using Karhunen-Loève (KL) expansion. In the case of random material field problem, KL expansion is used to discretize the random field. The usefulness of the proposed method in terms of accuracy and computational efficiency is examined by considering different types of example problems. From these numerical examples considered with Gaussian randomness, the proposed method is observed to be more efficient than conventional PC based method in terms of accuracy and computational demand.

The proposed method is further explored to consider non-Gaussian material properties. In this case, the random field is discretized and simulated using iterative KL expansion. However, the random variables considered to represent the random field may not be independent. Thus, independent component analysis (ICA) is carried out on the random variables of KL expansion. It is observed from numerical studies on linear structural mechanics problem with non-Gaussian system parameters that the proposed method is computationally more efficient than conventional PC based method.

Polynomial dimensional decomposition (PDD) is one of the methods for reduction of the dimension of a stochastic system. The method expresses the multidimensional response by considering a linear combination of responses of mean, univariate, bivariate and higher variate components. These uni-, bi-variates components may be solved using PC based method. In the present study, it is solved using the previously proposed iterative method. Thus, a hybrid approach of PDD and iterative PC based method is considered to solve SFE equations. From the numerical study of linear structural mechanics problem with both Gaussian and non-Gaussian material, it is observed that the proposed hybrid method of PDD and iterative PC can generate appropriate responses with lesser computational demand than PDD-PC based method.

Apart from the curse of dimensionality, another drawback of PC based method is the loss of optimality of polynomial bases as observed in the case of time-dependent problems. The polynomials in PC are optimal for the representation of a random process when the weight functions for the orthogonal polynomials are identical to the probability density function. However, in the case of time-dependent problems, the statistic of the responses change over time and hence the initial assumed PC expansion losses its optimality. Time-Dependent generalised Polynomial Chaos (TDgPC) can be considered to overcome this, where PC is generated again, at a time instant where it fails to appropriately represent with the previously assumed PC bases. The present study considers TDgPC for dynamically loaded structural mechanics problems with random material properties, both Gaussian and non-Gaussian. Numerical studies on linear structural mechanics problems under long duration dynamic loading show that TDgPC can be effectively considered to overcome the drawback of PC expansion.

In the case of random field problems, the random field is discretized using KL expansion. Discretization means an appropriate representation of the continuous random field with a countable number of random variables. The accuracy of the discretized random field can be increased by considering finer discretization with a large number of terms. However, this would increase the computational cost. A study has been conducted to examine the effect of discretization and the number of terms in KL expansion on the accuracy of the simulated random field. Further, an adaptive discretization scheme is proposed where the elements failing to represent the random field for a prescribed accuracy are only further discretized. The proposed method considers all the possible errors in the discretization of random field.

Contents

List of Figures

List of Tables

Abbreviations

Abbreviation	Description
1-D	One Dimension/Dimensional
2-D	Two Dimension/Dimensional
3-D	Three Dimension/Dimensional
c.o.v.	Coefficient of variation
CDF	Cumulative distribution function
DOFs / dofs	Degree of freedoms
FEM	Finite Element Method
FRF	Frequency Response function
gPC	Generalized Polynomial Chaos
ICA	Independent Component Analysis
INP	Interpolation of Nodal Point
IP	Integral Point or Integration Point
KL expansion	Karhunen-Loève expansion
KPCA	Kernal principal component analysis
MAC	Model Assurance Criterion
MCS	Monte Carlo Simulation
ME-gPC	Multi-Element generalized Polynomial Chaos
mPC	Modified Polynomial Chaos
MPD	Mid Point Discretization
ODE	Ordinary Differential Equation
OLE	Optimal Linear Estimation
FE	Finite Element
PC	Polynomial Chaos
PDD	Polynomial Dimensional Decomposition
PDE	Partial Differential Equation

Abbreviation	Description
PDF	Probability Distribution Function
PDD	Polynomial dimensional decomposition
pdf	Probability Density Function
PFEM	Probabilistic Finite Element Method
RMS	Root mean square
SA	Spatial Average
SD	Standard Deviation
SFE	Stochastic Finite Element
SFEM	Stochastic Finite Element Method
TDgPC	Time-Dependent generalized Polynomial Chaos
WI	Weighted Integral
w.r.t.	with respect to

Symbols

Symbol	Description
A	Area of member
$\boldsymbol{B}$	Strain displacement matrix
$\boldsymbol{C}$	Covariance matrix
$\boldsymbol{D}$	Damping matrix
$\widetilde{\boldsymbol{D}}$	Constitutive matrix
E	Elastic modulus or Young's modulus
$\boldsymbol{H}_{mixing}$	Mixing matrix
I	Moment of inertia
$\boldsymbol{K}$	Stiffness matrix
$\overline{\boldsymbol{K}}$	Mean Stiffness matrix
$\boldsymbol{K}_i$	Stochastic part of stiffness matrix
L	Length of member
L_c	Correlation length
L_{c_x}	Correlation length in X direction
L_{c_y}	Correlation length in Y direction
$\boldsymbol{M}$	Mass matrix
$\overline{\boldsymbol{M}}$	Mean mass matrix
$\boldsymbol{M}_i$	Stochastic part of mass matrix
N	Degree of freedoms
$(P+1)$	Total number of terms in PC expansion
Q	Number of terms in KL expansion, Number of random variables
T	Time period
b	Width of member
d	Depth of member
p	Order of PC expansion

Symbol	Description
$\boldsymbol{q}$	Load vector
$\boldsymbol{q}(t)$	Load vector (Time varying)
r	Number of random variables in PC expansion
$\boldsymbol{r}$	Responses under dynamic loading
t	Time
$\lvert . \rvert$	Absolute value
λ	Eigenvalue
$\mathbb{E}[.]$	Expectation operator
δ_{ij}	Kronecker delta
$\Psi_i[\{\boldsymbol{\xi}_r(\theta)\}]$	Polynomial Chaos
$\alpha(x,\theta)$	Random field
$\xi(\theta)$	Random variable
$\boldsymbol{u}$	Response or deflection as applicable
σ	Standard Deviation
$\sum$	Summation operator
$\otimes$	Tensor product

1

Introduction

Contents

1.1 Background

Generally, any physical phenomenon can be represented by a mathematical model subjected to appropriate boundary and initial conditions. A physical system has basic variables (e.g. describing system geometry, loading, material properties) and response variables (e.g. displacement, strain, stresses). The mathematical model represents the relationship among these input basic variables and output response variables of a physical system, which is considered as the governing equation. These equations can be algebraic, differential, trigonometric or any other form depending upon the problem. Mathematical models act as tools for better understanding and reasoning of the real world phenomena and have been extensively used in academia and industries.

A mathematical model can be deterministic or stochastic depending upon whether the input parameters are considered as deterministic or stochastic. In case of a deterministic model, analysis is carried out considering signature values of the input parameters which may be mean, maximum, minimum, mean plus/minus some factor of standard deviation or any characteristic values of the input parameters. This type of analysis does not consider the random nature of the input parameters. On the other hand, in case of a stochastic model, one or more of the input variables are represented in a statistical sense and random nature of input parameters are directly considered in the analysis. Since the inputs are random in case of the stochastic model, the responses are also stochastic in nature. Whether to consider a deterministic analysis or stochastic analysis and the variables to be considered as stochastic, depends on the data available, computational time requirement, the variability of data and importance of the analysed structure etc.

In the case of a deterministic model, uncertainties are not considered, whereas in a stochastic model, one or more uncertainties are considered. Moreover, the basic assumptions in any modelling also violate the reality to some extent, which intern cause some uncertainties. Thus, the model contains some uncertainties either in the form of inherent randomness in the physical quantities or from lack of knowledge. These can be categorized as Aleatory and Epistemic (Ang and Tang, 2014, Kiureghian and Ditlevsen, 2009). The word Aleatory originated from Latin word *alea*, meaning the rolling of dice and Epistemic from Greek word $\varepsilon\pi\iota\sigma\tau\eta\mu\eta$ (*episteme*), meaning knowledge (Kiureghian and Ditlevsen, 2009). Thus, the aleatory uncertainty is associated with the natural randomness, while epistemic is present due to lack of knowledge.

Engineering problems, in general, involve both types of uncertainties. However, it is often difficult to categorize a particular type of uncertainty into a group. The distinction of uncertainty, whether it is aleatory or epistemic, purely depends on the considered model. A particular uncertainty may be treated as aleatory in one model, and the same may be regarded as epistemic in another model. Thus one needs to consider an uncertainty into one category based on scientific knowledge and available data, but it is also important to consider the practical need of model sophistication to the level of engineering importance for the decision to be made out of the model (Kiureghian and Ditlevsen, 2009).

Deterministic analysis carried out considering only one of the realizations of the input variables does not provide complete information about the variability of the output quantities. With the advancement in computational power, there is an increase in demand for a more realistic analysis of engineering problems considering stochasticity in the input parameters. Thus, the random nature of physical parameters are considered in many of the engineering fields, like flow through random porous media (Ma and Zabaras, 2011), modelling soil properties (Popescu et al., 2005, Li et al., 2015) etc. along with material properties in structural engineering (Shinozuka, 1972, Shinozuka and Lenoe, 1976).

Solutions of engineering problems with uncertainties in input parameters are generally obtained using a numerical technique like Stochastic Finite Element Method (SFEM), Stochastic finite difference method etc. The present study explores further to improve computational efficacy of SFEM in solving linear structural engineering problems. SFEM is a branch of FEM, where solutions of governing differential equations with random quantities are sought. The randomnesses in physical quantities are needed to be described through a proper probabilistic model like random variables, fields and/or processes etc. A random field can be considered as a collection of random variables representing the evolution of uncertain values over spatial coordinates. The decision to consider a random variable or field model can be decided on the variability of physical quantities in the spatial domain. The choice of a particular random field model will also depend on the underlying probability distribution of variables that are considered to be uncertain, which can be estimated through experimental measurement. It also depends on the correlation structure of the variables that are considered to be uncertain. However, for simplicity of model, and due to the lack of experimental data, stochastic methods are often built up from assumptions about the probabilistic characteristics of the model.

The formulation of SFEM is similar to that of its deterministic counterpart, where virtual energy principle, minimization of potential energy etc. are considered. The only difference that the stochastic quantity needs to be considered instead of deterministic. However, in the case of random field problem, the random field needs to be discretized before formulation. The discretization converts a continuous random field to a set of random variables forming a random vector (Stefanou, 2009). Karhunen-Loève (KL) expansion (Loeve, 1977) is one of the discretization methods generally consider for discretization of a random field. The method can be applied to Gaussian random field (Spanos and Ghanem, 1989, Ghanem and Spanos, 1991a) and also can be applied to a non-Gaussian random field with marginal probability density with appropriate modifications (Huang et al., 2000, Phoon et al., 2002, 2005). The present study considers KL expansion for discretization of random field. The discussion on KL expansion and other discretization method are included in section 2.3. Once the stochastic finite element equations are formulated, these can be solved to find out the responses. Polynomial chaos (PC) expansion (Wiener, 1938, Ghanem and Spanos, 1991b) is one of the popular method to approximately calculate response in SFEM. The PC based method has received a good amount of attention among the researchers in the last few decades and has been considered in different field of engineering to approximate statistical properties including structural mechanics problem with both static and dynamic loading. The PC based and other approximate solution methods are discussed in section 2.4.

The randomness present in the system parameters of the structural system affects the reliability of design parameters. Thus, it is vital to study their effect to enhance the reliability of designed structures. However, the study of uncertainty is computationally demanding, and closed-form solutions are limited to simple structures. This leads to the importance of computationally efficient numerical method to solve uncertain structural system more efficiently. SFEM, where responses are approximated using PC, is one of the methods to evaluate responses of a stochastic system with random system properties. However, PC expansion experiences the curse of dimensionality with the increase in the number of random variable or/and order of expansion. The present study considers the improvement of PC based numerical method by addressing the curse of dimensionality at multiple levels, starting from the formulation of stiffness matrices so that accurate responses can be evaluated even with much less computational facility. The detailed objective of the present study is discussed in section 1.4

1.2 Uncertainties in structural engineering problems and general framework of probabilistic analysis

As discussed in the previous section, consideration of uncertainties in the analysis and design enhances the reliability of structural system. The deterministic study considering either average, maximum and/or characteristic measure of physical quantities does not consider uncertainties in the physical quantities, and consequentially in the response. This type of analysis and design is considered as appropriate where randomness is very small. The assumption that the responses obtained from the representative measurement considering only a characteristic value for all admissible values of the physical quantities provide a true scenario is not always true. Moreover, the deterministic analysis does not provide a rational basis for deciding on optimal structural design for a given set of loading conditions consistent with desired levels of safety at an economical and affordable cost.

Uncertainty study provides a logical framework for scientifically studying the problem of structural analysis and design, where uncertainties in physical quantities are invariably significant. Fig. 1.1 shows a typical flow chart of the various steps of an engineering process. They are discussed below:

Step 1: First step of engineering design is to collect data about the physical parameters of the system from existing structures and/or from experiments at laboratory level.

Step 2: Identification of uncertain parameters and to decide about the variability of these parameters and modelling. Further, to decide whether a random variable model is sufficient or to model the parameters as a random field.

Step 3: This step consists of idealization of the physical system and mathematical formulation of the governing equation of the system. It also includes the definition of system variable and basic assumptions to be made for the formulation of the governing equation.

Step 4: The formulation of the governing equation is followed by solution and study of responses and its accuracy. In case of random input, the responses are also stochastic in nature and thus need to be represented in terms of statistical parameters.

Step 5: The next step is to arrive at a suitably designed structure, to be followed by construction. There may be alternative design philosophy based on previous experience and knowledge. Thus, some amount of uncertainties are present in this step as well. Moreover, any construction also includes uncertainties regarding skills of labour, construction methodology etc.

In each step of the engineering design processes discussed above, some amount of uncertainties are present. Uncertainty study provides an idea about the nature of the variability of the physical quantities. It also provides the basis of determining the response of physical systems as well as a basis for finding safety factor in engineering design. Many a time it is observed that responses are sensitive to input variability. Moreover, the uncertainty study makes it possible for the assessment of alternative strategy in engineering design (Vanmarcke et al., 1986). It may however be noted that while the uncertainties in a system are inherent, consideration of such uncertainties is not easy due to model complexity, time requirement, lack of data of all the involved physical quantities including input load etc. Thus, the physical quantities to be considered as random are needed to be judged based on available scientific data considering the above criteria.

The mathematical model considered to describe the physical system is also an idealization of the physical world. However, many a time only the significant physical parameters are considered in the mathematical model, which thus introduces uncertainty. Uncertainties related to modelling are not studied in this report and these are assumed to be an appropriate representation of reality or assumed to be sufficiently accurate. The uncertainties pertaining to only input parameters are addressed in this report. Thus, the present study is focussed on step 4, where the structural input parameters are considered as random in nature. A discussion on considered random input parameters is presented in section 2.2.

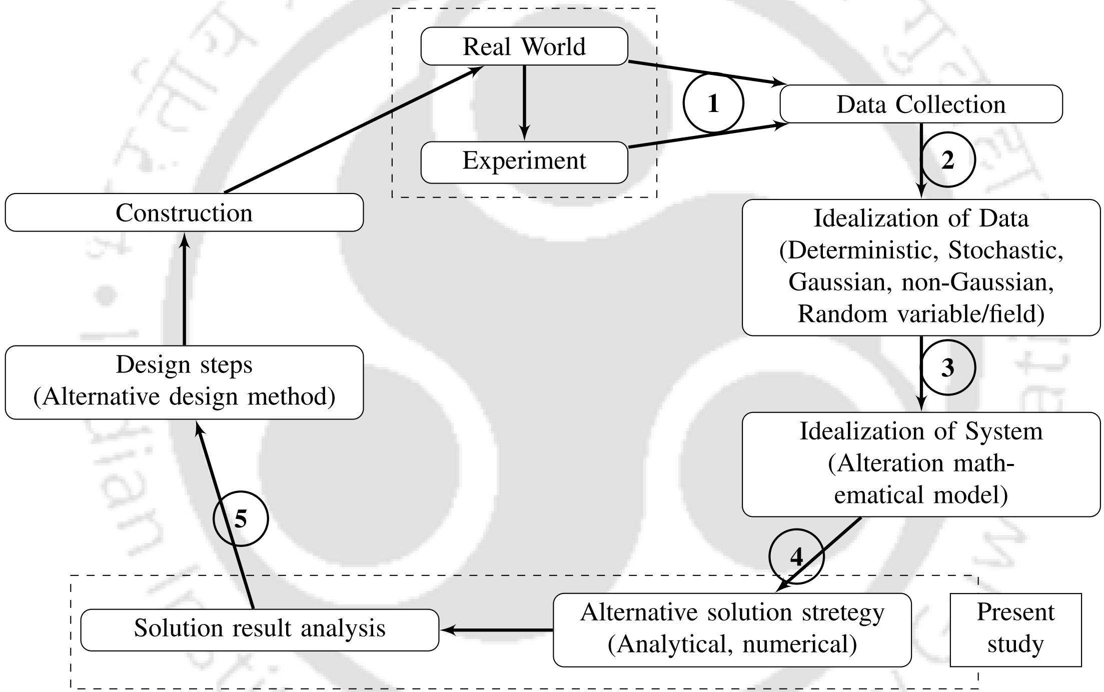

Fig. 1.1: Typical flow chart of various steps in engineering process.

1.3 Problem Statement

It has been observed from previous sections as to how important is the study related to uncertainty to enhance safety and reliability of design of any structure. Random nature of loads and its effect on structures are extensively studied under random vibration (Newland and Newland, 1984), and still an active area of research. However, researchers suggested that the engineering material also have a significant variability (Shinozuka, 1972, Shinozuka and Lenoe, 1976) along with loading. Thus, it is also necessary to study the effect of random material properties on the variability of responses, which is an active area of research in the last few decades.

The primary objective of the present study is to conduct a systematic and scientific study related to certain aspects of randomness present in structural mechanics problems and to formulate an efficient numerical strategy to carry out analysis considering these uncertainties. The detailed objectives are discussed in section 1.4. From a long time, researches have been focused on the improvement of modelling of the physical systems for better representation of reality. The solutions of these mathematical models provide variation of the responses. However, the analytical solution of a mathematical model is often limited to simple structural problems.

With the advancement of computer, researcher have focussed on the numerical solution of more involved problems. Finite Element Method (FEM) is one of such methods to obtain an appropriate solution for different classes of physical problems. In case of boundary value problems, the partial differential equations are converted to a set of algebraic equations which are easy to solve. In the case of initial value problems, FEM is combined with other time integration scheme to solve the time-dependent problem. FEM converts the spatial derivatives into algebraic expressions and time integration scheme converts the temporal derivatives into algebraic equations. However, the standard deterministic FEM does not consider the uncertainties present in the system variables in its mathematical model. The system is analysed for its representative sample, which can be mean, maximum or any other characteristic values.

Monte Carlo method or Monte Carlo simulation (MCS) is a brute force method where the deterministic FEM is used to calculate the response of the system for each of the random data generated. In this way, the ensemble of the responses can be calculated. As it uses the deterministic FEM, a large number of times, the computational time/demand of MCS is very high. Stochastic or Probabilistic Finite Element (SFEM or PFEM) is a branch of FEM, where uncertainties are studied by combining uncertainty model with finite element technique to find the stochastic solution of the system where one or more parameters are considered to have uncertainties.

In order to overcome the computational demand of MCS, other approximate methods are proposed by various researchers in the past and are discussed in section 2.4 and these approaches are further evolving. The present study considers further explorations of PC based method for the solution of structural mechanics problems with random material properties.

In the PC based method, the responses are approximated using known random orthogonal polynomials and unknown coefficients. Thus, the evaluation of stochastic responses become equivalent to finding the coefficient. With the increase in the number of random variables and/or order of expansion, the size of PC expansion increases exponentially and is known as the curse of dimensionality. Moreover, in case of time dependent problem, the PC based method losses its efficiency as time progresses. This can be addressed considering Time-Dependent generalized Polynomial Chaos (TDgPC), where PCs are changed as time progress. The present study considers a PC based framework to address the curse of dimensionality in linear structural mechanics problems with random material properties. The detailed objective and scope of research are presented in sections 1.4 and 1.5 respectively.

1.4 Objective of present study

The study of structural mechanics problems with stochastic input parameters is essential for enhancing the reliability of designed structures. Moreover, with the advancement of computer facility, demand for analysis of large structural mechanics problems are also increasing. The present study thus considers an analysis of structural mechanics problems with random material properties in the PC framework. The detailed objectives of the present study are as follows,

I. To develop a PC based framework of computationally efficient approaches for the solution of linear structural mechanics problems with stochastic system parameters.

II. To efficiently implement the proposed strategy for problems with both Gaussian and non-Gaussian system parameters.

III. To explore the efficacy of the proposed strategy for problems under static loading.

IV. To study structural dynamic problems under long duration of loading with random system parameters using Time-Dependent generalized Polynomial Chaos (TDgPC).

V. To address errors associated with the discretization of random fields and to implement an efficient adaptive strategy for discretization.

1.5 Scope of research

As discussed in section 1.3, the PC based method converts the stochastic problem to the evaluation of coefficients of the polynomial. However, as the number of random variables of system input or/and order of expansion increases, the total number of terms increase exponentially. Various authors proposed different schemes to enhance the computational efficiency of the PC based method and are discussed in section 2.4.2. In the present study, the PC based method is further explored to enhance the computational efficacy of the scheme for linear static structural mechanics problems. Generally, material properties and loads are considered as Gaussian, and the applicability of the proposed method is checked for Gaussian input by considering three different problems. A truss with random Young's modulus and sectional areas of members are considered along with random loads. Considering Young's modulus as a 1-D random field, a 3-D beam and settlement of soil below foundation, idealized as plane stress problem are solved. The considered random fields are discretized using KL expansion.

It is always a debatable topic whether one can consider strictly positive physical quantities like Young's modulus, and other elastic moduli as well as sectional areas of members as Gaussian or not. Moreover, from experimental studies, it has been observed that material properties are non-Gaussian in nature. A Gaussian model of random variable/field of Young's modulus may be suitable for a low value of coefficient of variation (c.o.v.), where the assumption that the physical quantity is positive is generally valid. Thus, the proposed method is further explored to consider non-Gaussian material property and loads. Suitable modifications are done to address the non-Gaussian randomness in the input parameters. The numerical examples considered in the case of Gaussian randomness are also considered with non-Gaussian randomness.

The responses evaluated using the proposed method are studied for accuracy and convergence by comparing with responses of MCS. The computational efficacy of the proposed method is checked with respect to MCS and PC based method.

Polynomial dimensional decomposition (PDD) is one of the dimension reduction methods, where the multidimensional stochastic problems are solved using uni-, bi-, tri-variate components. The complete responses are evaluated by considering a linear combination of responses of different variates. The individual variate of responses can be calculated by considering PC for each one. The previously proposed method is combined with PDD to increase the efficacy of PDD-PC approach, where individual variates are evaluated using iterative PC. The responses of MCS, PDD-PC and proposed method of PDD and iterative PC are studied for accuracy and convergence.

The statistical responses of a structure under dynamic loading can be evaluated by considering the numerical scheme like Newmark-β with PC. The responses can be represented using PC, which converts the stochastic problem to an equivalent deterministic problem after Galerkin projection. The converted problem can be solved using a numerical scheme like Newmark-β method. However, initially considered PC might not be suitable to represent responses at a later stage of time instant due to change in the stochastic properties of responses over time. Gerritsma et al. (2010) proposed Time-Dependent generalized Polynomial Chaos (TDgPC) to overcome this difficulty, where polynomials are generated on the fly based on the responses. In the present study, TDgPC is considered to evaluate the responses of structural systems with random material properties and time-varying load.

The present study considered KL expansion for the discretization of random fields. In this process, continuous random fields are approximated using limited random variables. Thus, errors due to discretization are present in the simulated data. The accuracy of the simulated data is studied for various errors due to discretization. An adaptive scheme is implemented for the discretization of random fields using KL expansion by limiting all the possible associated errors.

1.6 Outline of the dissertation

This dissertation is divided into eight chapters. In the first chapter, the general idea of stochasticities present in structural mechanics problems and the importance of its study are discussed. A brief discussion on SFEM including discretization, formulation and solution strategies are discussed. The objective and scope of research are also discussed.

Chapter 2 presents a detailed literature review to illustrate the background on the various solution methodologies available for analysis of structural mechanics problems with random parameters followed by detail discussion on Polynomial Chaos based method. The input parameters and its representation and techniques for the discretization of random fields are also discussed in this chapter.

Chapter 3 presents the theoretical development of a proposed method in the intrusive PC framework. An iterative method for the solution of structural mechanics problems under static loading with Gaussian material property is proposed. Detail discussion of the proposed method is followed by its application to three different types of problems.

Chapter 4 presents the extension of the proposed iterative method for the solution of structural mechanics problems to non-Gaussian material randomness. The discretization and generation of non-Gaussian random field using KL expansion and application of independent component analysis is discussed. From the numerical studies on three different types of problems, the applicability and efficacy of the proposed method in case of non-Gaussian random input are also demonstrated.

Chapter 5 presents the application of the proposed method along with polynomial dimensional decomposition (PDD). A hybrid method of PDD and the previously proposed method is studied in this chapter. The proposed method is applied to problems of stochastic nature where multivariate problems are decomposed to multiple uni-, bi- variate problems. The solutions of these uni-, bi- variate problems are solved using the proposed iterative method. A comparison study has been carried out for PC based PDD and proposed iterative hybrid PDD method.

Chapter 6 presents the solution of structural mechanics problem for long duration of loading using PC and TDgPC. The drawbacks of PC based method for a time-dependent problems are discussed, followed by applications of TDgPC to problems of long duration of loading. Numerical study of structural mechanics problems with both Gaussian and non-Gaussian material properties are carried out.

In case of random field problem, the random fields need to be discretized to incorporate in FEM. A detailed study of various parameter affecting the accuracy of simulated data is discussed in Chapter 7$^{\text{th}}$. Further, an adaptive discretization method has been presented where the elements which are below an assumed accuracy level are further discretized. Numerical studies have been conducted to show the accuracy of the simulated random field due to various parameters.

The final chapter (Chapter 8) of this dissertation presents summary and conclusion based on the research work presented so far in different chapters, followed by a recommendation for future research.

2

Literature Review

Contents

2.1 Introduction

The chapter provides background knowledge of the research conducted, available methodologies and various parameters considered in the present study on stochastic finite element analyses of structural mechanics problems. The chapter is divided into three major parts. In section 2.2, stochastic input variables and their representation as considered by various authors in the past are discussed. Various physical quantities considered as random can be categorised as either Gaussian or non-Gaussian and are discussed. Random input quantities are represented as either variables or field/process. In the case of representation as a random field/process, the random field needs to be discretised to represent as a set of random variables. Various discretization methods are discussed in section 2.3. The literature review of the formulation and available solution strategies of stochastic finite element method are presented in section 2.4.

2.2 Input random quantities

Input parameters for structural mechanics problems are material properties, geometric properties, boundary conditions, loading and initial conditions (in case of dynamic problems).

Primary material properties like Young's modulus are often considered as a random variable and hence varies with different samples only while maintaining a constant value over the spatial domain. On the contrary, researchers suggested that the engineering material and load also have a significant spatial variability (Shinozuka, 1972, Shinozuka and Lenoe, 1976). The nature of randomness may be either Gaussian (Liu et al., 1987, Reusch and Estrin, 1998, Yamazaki et al., 1988, Spanos and Ghanem, 1989, Takada, 1990b,a, Zhu et al., 1992, Chakraborty and Dey, 1995, Adhikari, 2011, Kundu et al., 2014, Kundu and Adhikari, 2014) or non-Gaussian (Blatman and Sudret, 2008, 2010, 2011) and are discussed in details in sections 2.2.1 and 2.2.2 respectively.

The other independent material parameter in case of plane stress/strain, 2-D/3-D problems is Poisson's ration (ν). However, the stiffness matrix is a non-linear function of ν, and hence Young's modulus and Poisson's ratio are often transformed to Lamé's constants as these are related linearly to stiffness matrix. Graham and Deodatis (2001) considered Young's modulus and Poisson's ratio as a 2-D random field for local average approach. However, in the case of weighted integral method, the parameters are transformed to Lamé's constant. Noh (2004) studied the effect of random Poisson's ratio by expanding the denominator of the constitutive matrix using binomial expansion. Graham and Deodatis (2001) observed that the effect of Poisson's ratio on response variability is lesser compared to that of Young's modulus.

Thus, though there are uncertainties of various forms in structural mechanics problem, Young's modulus is considered as primary random quantity, and the same is treated as either Gaussian or non-Gaussian in the present study. These random quantities are modelled either as random field or variable depending upon the problem statement.

2.2.1 Gaussian model for Young's modulus

A Gaussian random variable can be completely described by its first and second order statistics, i.e. its mean and standard deviation or variance. Similarly, a Gaussian random field can be completely described using its first two statistical parameters, i.e. mean and covariance.

The random fields in civil engineering application are assumed to be weakly homogeneous, thus specified using marginal distribution, mean and covariance function (Allaix and Carbone, 2009). If the random field is considered as homogeneous, the covariance function only depends on the distance separated, $x_1 - x_2$, rather than the absolute coordinates.

Generally, the covariance function is of the form $\boldsymbol{C}(x_1,x_2) = f(x_1 - x_2, L_c)$, where L_c is known as correlation length or proportional to correlation length and plays an important role in the representation and accuracy of simulated random fields. If the value of correlation length is very small, it approaches a delta-correlation process known as white noise. On the other hand, for a large value of correlation length compared to the domain under consideration, the process becomes a random variable. Generally, the correlation length is not expressed as absolute, rather expressed as a normalizing factor to the length of the element. Huang et al. (2001) studied the effect of correlation length on the accuracy of the simulated random field. In the present study, the random fields are considered as homogeneous in nature.

Two commonly considered covariance functions are of exponential type with different parameters in its arguments. The first exponential covariance function with the absolute value of separation distance between two points as its argument for 1-D random field is given as,

$$\boldsymbol{C}(x_1,x_2) = \sigma^2 \exp\left(-\frac{|x_1 - x_2|}{L_c}\right) \tag{2.1}$$

where σ is the standard deviation of the random field, x_1, x_2 are the coordinates within the limit $[-a, a]$, where a is known as length of the process and the value is $L/2$, L is the length of the member. A number of researchers used this covariance function for different stochastic problems. Liu et al. (1987) considered this covariance function for uniaxial yield stress and compression load as independent stationary random field with correlation length 18 and 9 for a 12 unit length plate. Takada (1990a) considered correlation length as 2 for a 10 unit length plane stress problem. Spanos and Ghanem (1989) considered L_c as 1. Shinozuka and Deodatis (1988), Chakraborty and Dey (1995), Adhikari (2011), Kundu et al. (2014), Kundu and Adhikari (2014) considered the covariance function (Eq. 2.1) for stochastic representation of material property in both one dimensional as well as two dimensional random field. The 2-D covariance is of the following form,

$$\boldsymbol{C}(x_1,x_2;y_1,y_2) = \sigma^2 \exp\left(\frac{-|x_1 - x_2|}{L_{c_x}} + \frac{-|y_1 - y_2|}{L_{c_y}}\right) \tag{2.2}$$

where L_{c_x} and L_{c_y} are the correlation length in x and y directions respectively.

The second covariance function is a square exponential covariance function whose argument is square of the separation length, $x_1 - x_2$ and square of covariance length L_c and expressed as,

$$\boldsymbol{C}(x_1,x_2) = \sigma^2 \exp\left(-\frac{(x_1-x_2)^2}{L_c^2}\right) \tag{2.3}$$

Reusch and Estrin (1998), Yamazaki et al. (1988), Takada (1990b), Zhu et al. (1992) and others used this covariance function for spatial variation of material property. Similar to the previous covariance function, the 2-D covariance function can be written as

$$\boldsymbol{C}(x_1,x_2;y_1,y_2) = \sigma^2 \exp\left(\frac{-(x_1-x_2)^2}{L_{c_x}^2} + \frac{-(y_1-y_2)^2}{L_{c_y}^2}\right) \tag{2.4}$$

2.2.2 Non-Gaussian model for Young's modulus

A Gaussian model of random field of Young's modulus is suitable for low values of c.o.v., where all the admissible values of physical quantities can be assumed as positive. However, from experimental studies, the material properties are generally observed to be non-Gaussian in nature. Many a times, due to higher values of c.o.v. or due to non-Gaussian property of the physical quantity, it may be required to model the random quantity as non-Gaussian or put some restriction on the idealization as Gaussian random field. Yamazaki et al. (1988) considered such restriction on the Gaussian random field as

$$-1+\delta \leq f(x) \leq 1-\delta, \quad 0<\delta<1 \tag{2.5}$$

The same restriction is also imposed by Wall and Deodatis (1994). The lower limit of the restriction is imposed so that the random quantity is always positive. On the other hand, the upper limit is set such that the data is symmetric about its mean, and the mean value remains unchanged. However, this leads to change in standard deviation of the random field. Thus, modelling of uncertainty in physical quantities by considering other forms of random field would be a better option, where all the admissible values of the random field are always positive.

Researchers are improving numerical model to directly consider non-Gaussian material properties in analysis. Log-normal random variables for variation of material property as well as area of members along with random loading as Gumbel distribution was considered by Blatman and Sudret (2008, 2010) for calculation of reliability of deflection of a truss using SFEM. Similarly, Blatman and Sudret (2011) considered Young's modulus of beam as homogeneous log-normal random field with exponential covariance function (Eq. 2.3).

Rahman (2006) considered Young's modulus, Poissons ratio and mass density as log-normal independent random variables along with stochastic thickness as random field for shell element. Baroth et al. (2007) considered a sphere under internal pressure with random Young's modulus and Poissons ratio modelled as bi-dimensional log-normal random variable.

One of the major challenges in the analysis of non-Gaussian random field problem is the generation of random field. As already discussed in section 2.2.1, a Gaussian random field can be fully characterized by its first and second order statistics, whereas for a non-Gaussian field, the joint pdf of the random field is necessary. However, it is difficult to obtain joint pdf and thus the marginal pdfs as well as correlation functions are generally considered in practice. However, in many cases, only a few of the lower order moments (mean, variance, skewness, kurtosis) are specified with correlation function, which was studied by Gurley et al. (1997). The most significant drawback of the method with only a few of the lower order moments is the possibility to have different admissible realization that have same lower order moments, but different marginal pdfs.

Simulation of non-Gaussian fields (or processes) with prescribed marginal pdf and correlation structure or spectral function are mainly categorised into two types. These are (i) memoryless transformation process to Gaussian random field and (ii) direct simulation of non-Gaussian random field. In the memoryless transformation, the basic principle is to generate a Gaussian random field of some correlation/spectral function so that the non-linear transformation will generate the non-Gaussian random field of target correlation/spectral function and prescribed marginal cumulative distribution function (CDF). The process is known as translation process (Grigoriu, 1984) and can be written as,

$$\gamma(x,\theta) = F^{-1}(\Phi(\alpha(x,\theta))) \tag{2.6}$$

where Φ is the marginal cumulative distribution function of Gaussian random field $\alpha(x,\theta)$ and F is the marginal cumulative distribution function of non-Gaussian random field $\gamma(x,\theta)$. Grigoriu (1998) presented a translation process to generate non-Gaussian random field, whose covariance function and marginal CDF are specified.

An iterative process to simulate non-Gaussian random field of specific spectral density function ($S^T_{\gamma\gamma}(\kappa)$), and marginal CDF was proposed by Yamazaki and Shinozuka (1988).

The method iteratively generates the spectral function ($S^T_{\alpha\alpha}(\kappa)$) for Gaussian random field, which is generated using spectral method. The iteration process is given by

$$S^{i+1}_{\alpha\alpha}(\kappa) = \frac{S^i_{\alpha\alpha}(\kappa)}{S^i_{\gamma\gamma}(\kappa)} S^T_{\gamma\gamma}(\kappa) \tag{2.7}$$

where $S^i_{\alpha\alpha}(\kappa)$ and $S^{i+1}_{\alpha\alpha}(\kappa)$ are the spectral density function of the Gaussian random field at i^{th} and $(i+1)^{\text{th}}$ iterations respectively. $S^i_{\gamma\gamma}(\kappa)$ is the spectral density function of the sample non-Gaussian random field and is generated as,

$$S^i_{\gamma\gamma}(\kappa) = \frac{1}{2\pi L} \int_0^L \gamma(x,\theta) \exp(-j\kappa x) dx, \quad j = \sqrt{-1} \tag{2.8}$$

The method is used to generate slightly skewed marginal distribution. Deodatis and Micaletti (2001) further improved the method by introducing an exponent, β to the iteration process so as to simulate highly skewed marginal distribution. Thus,

$$S^{i+1}_{\alpha\alpha}(\kappa) = S^i_{\alpha\alpha}(\kappa) \left[\frac{S^i_{\gamma\gamma}(\kappa)}{S^T_{\gamma\gamma}(\kappa)} \right]^\beta \tag{2.9}$$

Lagaros et al. (2005) further improved the computational efficiency of the method proposed by Deodatis and Micaletti (2001) by introducing Neural network to simulate the unknown Gaussian field. The method retained the same accuracy of the previous method, while drastically reducing the computational complexity. The method can simulate narrow band field with large skewness.

PC based translation algorithm to generate both stationary and non-stationery non-Gaussian random field was proposed by Sakamoto and Ghanem (2002). The Gaussian random field was generated using KL expansion from covariance function instead of spectral function and PC was considered to generate non-Gaussian field.

Direct simulation of non-Gaussian random field using KL expansion was proposed by Huang et al. (2000) and Phoon et al. (2002), where the target covariance function always matches with the theoretical one for large sample size irrespective of iteration number. Thus, it is required only to match the target marginal CDF. The method is suitable for both stationary and non-stationary process, particularly with low non-Gaussianity as it is unable to match the tail of the distribution for strong non-Gaussian process. Instead of using Latin Hypercube sampling technique (Phoon et al., 2002, Florian, 1992), Phoon et al. (2005) tried to further improve the method by considering Product-moment orthogonalization technique for orthogonalization of random variables. However, the modified method is still unable to simulate highly skewed non-Gaussian marginal distribution. Further, the calculated random variables considered to generate the random field may not be necessarily independent though uncorrelated. Khalil and Sarkar (2008, 2014) considered independent component analysis (ICA) (Comon, 1994, Hyvärinen and Oja, 2000) to ensure that the random variables are independent. ICA replaces the random variables by a linear combination of independent random variables. Khalil and Sarkar (2008) demonstrated how ICA can be used along with KL expansion for generation of non-Gaussian random field, and subsequently Khalil and Sarkar (2014) solved 1-D wave propagation problem with non-Gaussian random field using KL expansion, ICA and MCS. Li and Zhang (2013) studied ground water flow through porous non-Gaussian media and considered KL expansion with ICA to generate random field and solved using PC expansion in finite deference framework. Kernel principal component analysis (KPCA) was considered by Sarma et al. (2008), Li and Zhang (2013) for generation of non-Gaussian random field. KPCA can be considered as an extension of principle component analysis, where a non-linear representation is considered instead of linear one.

The present study considers direct simulation of non-Gaussian random field and the same is discussed in details in section 4.2.1. Similar to Gaussian random field, a non-Gaussian random field is also needed to provide its covariance function and marginal distribution. An exponential covariance function given by Eq. 2.1 (Blatman and Sudret, 2011) with log-normal distribution is considered in the present study.

2.2.3 Discussion

In the previous sections, it has been observed that material properties can be Gaussian or non-Gaussian and different researchers considered different distributions. Whether a random variable model of material is sufficient to describe the uncertainty or a random field model is necessary, which takes into account the spatial randomness in material should be based on engineering knowledge, importance of the structure, available computational facility etc. These studies are however not included in the present exercise. The present study only includes numerical method to study the responses to random material property. The random field of material property is described using mean, standard deviation and covariance functions.

In the present study, exponential covariance function, given by Eq. 2.1 is considered with a value of correlation length as $L/2$ in all the numerical studies for cases with both Gaussian and non-Gaussian (Log-normal) distributions. The effect of different types of covariance functions, values of correlation lengths and discretization on the accuracy of simulated data are studied in details in Chapter 7.

2.3 Discretization of random field

The representation of random material for structural mechanics problem is discussed in the previous section. A random variable model of material can be directly implemented in a FE model. However, as a random field is a continuous function, it has an infinite number of points in the spatial axis, which requires an infinite number of random variables to represent it. Thus, to implement in a FE model, it is required to convert to a countable number of random variables. The process of representation of a continuous function random field with a countable number of random variables is known as stochastic discretization or simply discretization (Stefanou, 2009). Thus, the accuracy of discretization will depend on the ability of representing a continuous random field, $\alpha(x,\theta)$ by $\hat{\alpha}(x,\theta)$. Discretization of a random field provides the essential mathematical framework to convert a continuous random field to a set of random variables forming a random vector which would enable it to be implemented in a FE framework.

KL expansion (Loeve, 1977) is one of the prominent methods for discretization of random fields. KL expansion can be considered for generation and discretization of random field for both Gaussian (Ghanem and Spanos, 1991b) and non-Gaussian (Phoon et al., 2005) random field. The present study considers KL expansion for discretization of random fields. However, few of the other important methods for discretization are discussed below along with their properties.

Spatial Average (SA) discretization, is also known as Local Average discretization, where the field value over an element is represented by the spatial average of the field over the element (Vanmarcke and Grigoriu, 1983). The spatial average of a one dimensional random field $\alpha(x,\theta)$ over the interval X_i centred at x_i defined in spatial coordinate x is given by

(Vanmarcke and Grigoriu, 1983).

$$\alpha_{X_i} \equiv \hat{\alpha}_{X_i}(x_i) = \frac{1}{X_i}\int_{x_i - X_i/2}^{x_i + X_i/2} \alpha(x)dx = \overline{\alpha}_e \tag{2.10}$$

The $\hat{\alpha}_{X_i}$ represents a single value (average value) of the random field for each finite element. The discretized random field forms a discontinuous function at interface of elements and has the same value over an element. The discretized random field is easy to implement in an existing FEM by considering the calculated average values of the random field for each element. However, the major disadvantage of this method is that generally the variability is under-represented (Kiureghian and Ke, 1988). Moreover, in the case of a non-rectangular domain, which is represented using non-overlapping rectangles may lead to a non-positive definite covariance matrix (Matthies et al., 1997). The advantage of local average method is that an accurate result may even be obtained for a coarse mesh (Kiureghian and Ke, 1988)

The second method of discretization is the Interpolation of Nodal Points (INP) method (Liu et al., 1986b). In this method, a random field over an element is represented by the interpolation of the values at the nodal points of the element and was introduced by Liu et al. (1986b). This method is also known as Shape Function Method of discretization. The random field is approximated in each element by the nodal value ($\alpha(x_i)$) of random function and associated shape functions $N_i(x)$. Thus,

$$\hat{\alpha}_{X_i} = \sum_{i=1}^{n} N_i(x)\alpha(x_i) \tag{2.11}$$

where n is the number of nodes. The approximation creates a continuous function over an element rather than single value as in the case of SA or mid-point method. However, as the value is a function of coordinates, it is difficult to implement in existing FE model and needs higher order integration. It is also important to note that the shape function considered can be independently chosen rather than considering FE shape functions (Matthies et al., 1997).

In Mid-point (MP) discretization method, the random field is approximated using the value of the random field at mid-point (or centroid) over the element dimension ($\mathscr{D}^e$) and was considered by Kiureghian and Ke (1988). Thus, the field value within an element is constant and given by $\hat{\alpha}(x,\theta) = \alpha(x_c,\theta)$ for $x_c \in \mathscr{D}^e$, x_c is the mid point of the element. Similar to SA, the discretized random field has a common value within an element can be directly implemented in an existing FE model. However, the method over estimates the variability of the random field (Kiureghian and Ke, 1988).

Weighted Integral (WI) method was introduced by Deodatis (1990, 1991), Deodatis and Shinozuka (1991) and Takada (1990b,a). The method is particularly attractive as it does not require any discretization of the random field. However, it uses a hidden discretization. The random field is projected onto the deterministic FE mesh (Matthies et al., 1997), thus avoids discretization. It considers the element stiffness matrix as basic random quantities. The element stiffness matrix is given by,

$$\boldsymbol{K}^{(e)} = \boldsymbol{K}_0^{(e)} + \sum_{i=1}^{N_{WI}} \Delta\boldsymbol{K}_i^{(e)} \chi_i^{(e)} \tag{2.12}$$

where $\boldsymbol{K}^{(e)}$ is the deterministic, mean stiffness matrix. $\chi_i^{(e)}$ are the weighted integral and random in nature with $\Delta\boldsymbol{K}_i^{(e)}$ as associated deterministic matrix. The number of terms N_{WI} are the number of weighted integral and depends on the type of finite element considered. The formulation of $\Delta\boldsymbol{K}_i^{(e)}$ and $\chi_i^{(e)}$ for beam column was carried out by Deodatis (1991) and that of plane stress and strain were carried out by Wall and Deodatis (1994).

Another category of discretization method is the series expansion method, comprising of Karhunen-Loève (KL) expansion (Loeve, 1977) method and Orthogonal Series expansion (Zhang and Ellingwood, 1994). A zero mean random function can be expressed as a sum of multiplication of a deterministic orthogonal function of coordinates and a random function. KL expansion is a special case of orthogonal series expansion, where the orthogonal functions are considered as the eigenfunctions of the covariance function (Zhang and Ellingwood, 1994, Huang et al., 2001). The main advantage of the KL expansion over other series expansion is that it forms a bi-orthogonal expansion as both random variables and the deterministic functions are orthogonal (Huang et al., 2001).

Series expansion methods take advantage of the orthogonal series. The accuracy can be controlled by the inclusion of number of terms in the truncated series as desired. Thus, it may be considered as a better approximation procedure of random field than other methods discussed so far. The implementation of these methods to finite element is though challenging. The accuracy of KL expansion depends on the number of terms considered in the expansion. It has been observed that the contribution of initial terms are higher than the later. The order of truncation can be evaluated based on expected energy calculation (Huang et al., 2001). However, the expected energy depends on the discretization. Allaix and Carbone (2009) studied truncation of KL expansion considering Genetic algorithm. Further, Allaix and Carbone (2010, 2012) proposed adaptive discretization of random field using KL expansion.

In Optimal linear Estimation (OLE) method (Li and Der Kiureghian, 1993), the random field $\alpha(.)$ in the domain $\mathscr{D}$ is described by the nodal values of the random field by a linear combination as

$$\hat{\alpha}(x) = a(x) + \sum_{i=1}^{N} b_i(x)\alpha(x_i) = a(x) + \boldsymbol{b}^T(x)\boldsymbol{v} \tag{2.13}$$

where N represents nodal points of the domain, $a(x)$ is a scalar function of x, $b(x) = [b_i(x)]$ is vector function of x with its elements $B_i(x)$, $\boldsymbol{v} = \alpha(x_i)$. The vector $a(x)$ and $\boldsymbol{b}(x)$ are calculated by minimizing the variance of the error $\alpha(x) - \widehat{\alpha}(x)$ with the condition that $\widehat{\alpha}(x)$ is an unbiased estimation of $\alpha(x)$ in mean. Writing these condition in equation form as

$$\text{minimize} \quad Var[\alpha(x) - \hat{\alpha}(x)] \tag{2.14}$$

$$\text{with} \ \mathbb{E}[\alpha(x) - \hat{\alpha}(x)] = 0 \tag{2.15}$$

Expansion Optimal Linear Estimation (EOLE) method is proposed by Li and Der Kiureghian (1993) and is an expansion and improvement of OLE method, which can be achieved by spectral decomposition of nodal variables.

Integration point method was proposed by Brenner and Bucher (1995). In this method, the random field is represented by the values of the random field at its integration (Gauss Points) points rather than mid point or node of element. This method has particular advantage over mid point and nodal point representation of random field. If the random field is considered at Gauss points, it can be directly implemented in finite element during numerical integration using Gauss quadrature method.

Stefanou (2009) categorized these methods into two categories. The first category is the point discretization methods where the discretized random fields are specified at specific points of the system domain. Midpoint, nodal point, integration point and interpolation methods are included in this category. The second category of discretization method considers the random field as a weighted integral of the original stochastic field over each finite element. Local average and weighted integral methods are included in this category.

2.3.1 Discussion

The present study considers KL expansion for discretization of random fields. The method is applicable to discretization of Gaussian random field (Ghanem and Spanos, 1991b) and can be applied for non-Gaussian random field using an iterative process (Huang et al., 2000, Phoon et al., 2002, 2005). The advantage of KL expansion is that it is a bi-orthogonal expansion. Both the random functions and the deterministic functions are orthogonal function. This property is used in PC based method to represent responses using orthogonal function of KL expansion (input variables). The numerical details of KL expansion for Gaussian random field is discussed in section 3.2.1 and that of non-Gaussian is discussed in section 4.2

The accuracy of simulated data also depend on correlation length, type of covariance function, number of element along with number of terms considered in the expansion. A detailed study has been conducted to appreciate the effect of these parameters on the accuracy of simulated data in Chapter 7. Further, an adaptive discretization scheme is also proposed, where the elements having a variance lesser than a prescribe value are further discretized. The proposed method has been illustrated using numerical examples in Chapter 7. The random fields are represented at Gauss point rather than mid point or nodes. The advantages of Gauss point representation over other two are discussed and elaborated using numerical study.

2.4 Formulation and solution of Stochastic Finite Element Method

2.4.1 Overview

After the discretization of random field, the next step in SFEM is to formulate the stochastic finite element equation followed by its solution. The formulation methodologies are same as those available for deterministic finite element methods, like minimization of potential energy, virtual work principle, variational principle etc. The main difference in the formulation is the consideration of quantities as stochastic instead of deterministic. For example, if stiffness matrix is given by $\boldsymbol{K} = \int_V \boldsymbol{B}^T \widetilde{\boldsymbol{D}} \boldsymbol{B} dV$ for deterministic case, for a stochastic case of

$\widetilde{\boldsymbol{D}} = \widetilde{\boldsymbol{D}}_0(1 + f(x,y,z))$, the same would be given by,

$$\boldsymbol{K} = \int_V \boldsymbol{B}^T \widetilde{\boldsymbol{D}}_0 \boldsymbol{B} dV + \int_V \boldsymbol{B}^T \widetilde{\boldsymbol{D}}_{\boldsymbol{0}} \boldsymbol{B} f(x,y,z) dV \tag{2.16}$$

where $f(x,y,z)$ is a stochastic field. The formulation of SFE under dynamic loading is similar to the standard procedure used in deterministic FE formulation.

In the present study KL expansion is considered for the discretization of random field and Young's modulus is considered as primary random quantity. The formulation of stiffness matrix is discussed in section 3.2.2 for Gaussian Young's modulus and appropriate modification for non-Gaussian Young's modulus in discussed in section 4.2.3. The formulation of SFE under dynamic loading is discussed in Chapter 6.

One of the most commonly used methods for solution of SFEM is Monte Carlo Sampling/Simulation (MCS) or one of its variants. In MCS, random samples for the random quantities are generated based on the assumed distributions of the physical quantities. For a particular realization of the generated random sample, the problem is deterministic and can be solved using any deterministic analysis method. Once the system is solved for all the realizations of input samples, the ensembles for the responses are obtained. Thus, the MCS process can be shown as in Fig. 2.1, where R is the deterministic relationship between inputs and responses. From these ensembles of responses, statistical information (e.g., mean, variance etc.) are evaluated. Thus, MCS is straightforward to apply, while only requires repetitive analysis using deterministic method. However, typically a large number of samples are needed as convergence is relatively slow. Moreover, with large number of DOF, the computational burden is too high.

- Generate random sample $\theta_1, \theta_2, \ldots, \theta_n$
- for $i = 1$ to n
    - Evaluate response $R(i) = f(\theta(i))$
- end for
- Evaluate statistical properties from R

Fig. 2.1: Symmetric diagram of MCS.

Researcher are improving the computational efficiency of MCS by proposing alternative MCS procedure like important sampling (Melchers, 1989), quasi Monte Carlo sampling (Sobol, 1998), directional sampling (Bjerager, 1988). However, the computational demand of these methods are higher compared to other approximate methods (Rahman and Xu, 2004), and thus alternative approximate methods are generally considered for evaluation of statistical responses. MCS methods are generally considered when alternative approaches are not applicable or inaccurate and/or alternative methods are required to be verified (Rahman and Xu, 2004). In the present study, MCS is considered to verify the accuracy of responses evaluated using different methods.

Some of the methods for approximate solution of stochastic equations are Perturbation method, Neumann expansion, Weighted integral method, reduced basis method and PC based method. In the present study, PC based method is considered for the analysis and further improvement are proposed in terms of computational complexity and the same is demonstrated through the solution of stochastic structural mechanics problem. PC is discussed in details in the next subsection.

The principle of perturbation method is to expand all the input random variables about their individual mean using Taylor series expansion w.r.t. to stochastic parameter. The unknown variables are also expanded using Taylor expansion and the same orders are equated (each order is equated to zero) to obtain the derivatives of the responses. Thus, the expansion of stiffness matrix ($\boldsymbol{K}$), load vector ($\boldsymbol{q}$) and response vector ($\boldsymbol{u}$) can be written as (Liu et al., 1986b)

$$\boldsymbol{K} = \boldsymbol{K}^0 + \sum_k \boldsymbol{K}_k^I \vartheta_k + \frac{1}{2}\sum_k \sum_l \boldsymbol{K}_{kl}^{II} \vartheta_k \vartheta_l + \ldots \tag{2.17}$$

$$\boldsymbol{q} = \boldsymbol{q}^0 + \sum_k \boldsymbol{q}_k^I \vartheta_k + \frac{1}{2}\sum_k \sum_l \vartheta \boldsymbol{q}_{kl}^{II} \vartheta_k \vartheta_l + \ldots \tag{2.18}$$

$$\boldsymbol{u} = \boldsymbol{u}^0 + \sum_k \boldsymbol{u}_k^I \vartheta_k + \frac{1}{2}\sum_k \sum_l \boldsymbol{u}_{kl}^{II} \vartheta_k \vartheta_l + \ldots \tag{2.19}$$

The zeroth-, first-, second order terms can be calculated by substituting these equation in finite element equation $\boldsymbol{Ku} = \boldsymbol{q}$ and equating these. The response derivatives can be calculated in a recursive pattern. The method is considered by various researcher for calculation stochastic responses of both linear and non-linear problems with static and dynamic loading (Liu et al., 1986b,a, 1987). The variation assumed is small (Liu et al., 1986b). As the Taylor series expansion is used in Perturbation approach, with the increase in c.o.v. of input the random variables, more and more number of terms are needed to be included in the series. Thus, the computation becomes too costly and some times may becomes inefficient. Yamazaki et al. (1988) studied computational demand of perturbation method and compared with MCS and Neumann expansion and observed that second order perturbation is too high and becomes uneconomical.

Shinozuka and Deodatis (1988) studied the response variability of one dimensional axially loaded prismatic bar under deterministic static load using first Neumann Expansion of stiffness matrix for homogeneous elastic modulus. The stochastic stiffness matrix was derived by minimization of the potential energy of the system. The Neumann Expansion for stochastic stiffness matrix can be written as (Yamazaki et al., 1988)

$$\boldsymbol{K}^{-1} = (\boldsymbol{K}_0 + \Delta\boldsymbol{K})^{-1} = (\boldsymbol{I} - \boldsymbol{A} + \boldsymbol{A}^2 - \boldsymbol{A}^3 + \dots)\boldsymbol{K}_0^{-1} \tag{2.20}$$

where $\boldsymbol{K}_0$ is the deterministic stiffness matrix, $\Delta\boldsymbol{K}$ is the fluctuation of stiffness matrix due to randomness, and $\boldsymbol{A} = \boldsymbol{K}_0^{-1}\Delta\boldsymbol{K}$. The displacement is given by,

$$\boldsymbol{u} = \boldsymbol{u}_0 - \boldsymbol{A}\boldsymbol{u}_0 + \boldsymbol{A}^2\boldsymbol{u}_0 - \boldsymbol{A}^3\boldsymbol{u}_0 + \dots \tag{2.21}$$

$$\boldsymbol{u} = \boldsymbol{u}_0 - \boldsymbol{u}_1 + \boldsymbol{u}_2 - \boldsymbol{u}_3 + \dots \tag{2.22}$$

$\boldsymbol{u}_i$ can be found from $\boldsymbol{K}_0\boldsymbol{u}_i = \Delta\boldsymbol{K}\boldsymbol{u}_{i-1}$. The advantage of Neumann Expansion is that the deterministic part of the stiffness matrix is required to be inverted only once to find $\boldsymbol{A}$ and the $\boldsymbol{u}_i$ are evaluated as recurring process. Yamazaki et al. (1988) studied structural mechanics problem with Gaussian material properties using Neumann expansion. Shinozuka and Deodatis (1988) carried out numerical study using Neumann expansion on both statically determinate and indeterminate rod with four different autocorrelation functions with four different correlation distances and two different loading conditions. Chakraborty and Dey (1995) also study SFEM using Neumann expansion where both material and loading are considered as random.

Weighted integral method is one of the formulations and solution methods considered in SFEM. As discussed in section 2.3, weighted integral method does not consider a discretization, rather uses a hidden discretization. The method often combined with Perturbation method or Neumann expansion for evaluation of responses.

Reduced basis method (Nair, 2001, Nair and Keane., 2002) is another method of evaluation of stochastic responses. The method is known as reduced basis method as the number of unknowns to be evaluated is lesser than DOF. The responses are approximated using a linear combination of stochastic basis vector with unknown coefficients. The method uses Bavnov-Galerkin scheme to evaluate the unknown coefficient.

Based on the work of Wiener (1938), Ghanem and Spanos (1990, 1991b) introduced PC to solve structural mechanics problem with Gaussian randomness in the input variables. The method approximates the response using known random orthogonal function and unknown coefficients. Thus, evaluations of statistical responses become equivalent to evaluation of the coefficients of the expansion. PC based method has gained lot of attention from research community and has been used in different fields of engineering. However, the method has some drawback like the curse of dimensionality, which has been discussed briefly in Chapter 1. In the present study, PC based method is further explored to address the curse of dimensionality leading to improved computational efficiency. A detailed literature review of PC based method is presented in section 2.4.2.

2.4.2 Polynomial Chaos based method

Ghanem and Spanos (1990, 1991b) approximated responses of structural mechanics problem using PC, which is based on the work of Wiener (1938). As discussed earlier, approximation of responses using PC converts the stochastic problem to an equivalent problem of finding the coefficients of PC expansion. The responses are approximated as

$$\boldsymbol{u}(\theta) = \boldsymbol{a}_0 H_0 + \sum_{i_1=0}^{\infty} \boldsymbol{a}_{i_1} H_1(\xi_{i_1}(\theta)) + \sum_{i_1=0}^{\infty} \sum_{i_2=0}^{i_1} \boldsymbol{a}_{i_1 i_2} H_2(\xi_{i_1}(\theta), \xi_{i_2}(\theta) + \dots \tag{2.23}$$

where $\boldsymbol{a}_0, \boldsymbol{a}_{i_1}, \boldsymbol{a}_{i_1,i_2}$ are the unknown coefficients and $H_1(\xi(\theta), H_2(\xi_1(\theta), \xi_2(\theta)$ are random orthogonal function with one and two random variable $(\xi_1(\theta), \xi_2(\theta))$. The zeroth order polynomial, H_0 is $\{1\}$. The expression can be written in a simplified form as,

$$\boldsymbol{u} = \sum_{i=0}^{\infty} \boldsymbol{c}_i \Psi_i[\{\boldsymbol{\xi}_r(\theta)\}] \tag{2.24}$$

where $\boldsymbol{c}_i$ are unknown coefficient and can be related to the unknown coefficient $\boldsymbol{a}_i$. Further, $\Psi_i[\{\boldsymbol{\xi}_r(\theta)\}]$ can be related to $H_i(\xi_1(\theta), \xi_2(\theta)))$ of Eq. 2.23. Ghanem and Spanos (1990, 1991b) considered Hermite polynomial for Gaussian random variable. Thus, $\Psi_i[\{\boldsymbol{\xi}_r(\theta)\}]$ are Hermite polynomial of input random variables $\xi_i(\theta)$, r is the number of random variables. The multidimensional PCs are generated using tensor product of univariate PCs. The basic property of PC is that Polynomial of different orders are orthogonal to each other and also true for same order with different argument. The mean of PC higher than zeroth order is zero, and mean of zeroth order polynomial is one. Thus,

$$\langle \Psi_i[\{\boldsymbol{\xi}_r(\theta)\}]\Psi_j[\{\boldsymbol{\xi}_r(\theta)\}]\rangle = \delta_{ij}\left\langle \Psi_i^2[\{\boldsymbol{\xi}_r(\theta)\}]\right\rangle \tag{2.25}$$

$$\langle \Psi_i[\{\boldsymbol{\xi}_r(\theta)\}]\rangle = 0, \quad i > 0 \tag{2.26}$$

$$\langle \Psi_0[\{\boldsymbol{\xi}_r(\theta)\}]\rangle = 1 \tag{2.27}$$

There are two procedures for the evaluation of the coefficient (c_i) of Eq. 2.24, known as *Intrusive* and *non-intrusive* method. In case of intrusive method, the basic stochastic equation (Eq. 2.16) is converted to a set of equivalent deterministic simultaneous equations using Galerkin projection and this procedures was considered by many researcher (Ghanem and Spanos, 1990, 1991b, Doostan et al., 2007, Gerritsma et al., 2010, Pascual and Adhikari, 2012, Ozen and Bal, 2016). These deterministic equations can be solved using a standard deterministic solver. The second approach is known as non-intrusive method, where a countable number of input-output relationships from the sample input data are solved using MCS. From these available data, the coefficients are evaluated using regression method and was considered by Blatman and Sudret (2008, 2010). The basic stochastic equation (Eq. 2.16) does not change in case of non-intrusive method. The present study considers further studies on PC based method in the intrusive framework.

Initially the proposed PC based method was used to approximate responses for Gaussian input quantities where the responses were approximated using Hermite PC assuming that the responses are also Gaussian in nature. Xiu and Karniadakis (2002) extended PC approximation to non-Gaussian random quantities by considering different types of polynomials for different types of random variables. These polynomials are taken from Askey-family and known as Winer-Askey polynomial chaos expansion or generalized polynomial chaos (gPC) (Xiu and Karniadakis, 2002). The polynomial given for each type of random variables are optimal for that particular type of random variable. The basic idea for selection of appropriate polynomials are that when the random variables are considered as weight function to the polynomial, these are orthogonal. The various polynomials proposed by Xiu and Karniadakis (2002) are shown in Table 2.1. Hermite polynomial is a subset of gPC.

Table 2.1: Different type of Wiener-Askey polynomial with underlying random variables (Xiu and Karniadakis, 2002).

	Random Variable ξ	Wiener-Askey chaos	Support
Continuous	Gaussian	Hermite-Chaos	$(-\infty,\infty)$
	Gamma	Laguerre-chaos	$[0,\infty)$
	Beta	Jacobi-chaos	$[a,b]$
	Uniform	Legendre-chaos	$[a,b]$
Discrete	Poisson	Charline-chaos	$\{0,1,2,\dots\}$
	Binomial	Krawtchouk-chaos	$\{0,1,2,\dots,N\}$
	Negative binomial	Meixner-chaos	$\{0,1,2,\dots\}$
	Hyper-geometric	Hahn-chaos	$\{0,1,\dots,N\}$

PC expansion is an infinite series and often truncated at a suitable term. Thus Eq. 2.24 becomes

$$\boldsymbol{u} = \sum_{i=0}^{P} \boldsymbol{c}_i \Psi_i[\{\boldsymbol{\xi}_r(\theta)\}] \tag{2.28}$$

where $(P+1)$ is the total number of terms in the expansion. The total number of terms can be calculated using

$$(P+1) = \frac{(Q+p)!}{Q!p!} \tag{2.29}$$

where p is the order of expansion and Q is the number of random variables considered. Few calculated values of total number of terms, $(P+1)$ are shown in Table 2.2.

As discussed in Chapter 1, one major drawback of the PC based method is the curse of dimensionality. As the order of expansion and/or the number of variables increase, the size of expansion increases exponentially, which can be seen from Table 2.2. Thus, for each DOF, $P+1$ number of unknown coefficients are required to be evaluated. A system with N DOFs will thus have total number of unknowns as $N(P+1)$.

Table 2.2: Total number of terms $(P+1)$ in PC for p order of expansion and Q number of random variables

Q	p					
	0	1	2	3	4	5
1	1	2	3	4	5	6
2	1	3	6	10	15	21
3	1	4	10	20	35	56
4	1	5	15	35	70	126
5	1	6	21	56	126	252
6	1	7	28	84	210	462
10	1	11	66	286	1001	3003

Another drawback of PC based method in case of time-dependent problem is that the accuracy of the PC based method reduces as time duration increases. In the case of time-dependent problem, PC based method is combined with a time integration scheme to evaluate stochastic responses along time. The responses are approximated using PC expansion and application of Galerkin projection converts the stochastic equation to a set of simultaneous deterministic equations, which can be solved using standard time integration scheme. However, as the time progresses, the PC expansion losses its efficiency. There may be two possibilities for the deviation of gPC as (1) singularity in the random space and (2) long time integration problem (Wan and Karniadakis, 2006b). The former is studied by Wan and Karniadakis (2005, 2006c) using ME-gPC. The later is also considered by different authors and is also considered in this study. The reason for failure of gPC in long time integration is the loss of optimality of the initially considered gPC expansion. As time progresses, the statistical properties of responses also undergo changes. However, responses are approximated using initial considered gPC and hence, gPC expansion loses its efficiency (Gerritsma et al., 2010).

PC based method has gained a lot of attention among researcher and has been considered in many of the engineering fields like fluid flow along with structural mechanics in both time-invariant and time-dependent response calculation. With time, PC based method has further evolved for accurate and efficient calculation of stochastic responses and are discussed below.

Xiu and Karniadakis (2002) studied PC expansion and showed that the convergence of responses for different types of random input can be achieved by considering different polynomial. The authors proposed generalized form of PC expansion by considering different polynomials for different types of input random variables and these are shown in Table 2.1. The authors showed that a particular polynomial is more appropriate than the others for attaining an exponential convergence. In case of random variables, which do not belong to any of the listed category as shown in Table 2.1, the authors recommended to project the input random process onto the Wiener-Askey polynomial chaos directly in order to solve the differential equation.

Wan and Karniadakis (2005) proposed a methodology known as multi-element generalized polynomial chaos (ME-gPC) to deal with the long-term integration and discontinuities in stochastic differential equation. Generally gPC shows exponential convergence. However, for long-term integration, the absolute error increases gradually with time. In this method, the random input space was discretized to non overlapping spaces when the relative error in variance was more than the permissible limit. A new random variable and a gPC scheme was used in each element. A lower order of gPC could be used in each element as the degree of randomness was proportionally reduced. The responses were evaluated locally for each element and statistical results from each element were used to calculate the global statistical moments of responses for the entire domain by using Bayes's theorem of total probability. Wan and Karniadakis (2006a) further extended their work to arbitrary probability description. Wan and Karniadakis (2006b) studied long time behaviour of gPC and ME-gPC in stochastic flow and found that while gPC failed for long time integration problem, ME-gPC could capture the long time random behaviour correctly.

Witteveen et al. (2007) constructed PC for one dimension using Gram-Schmidt orthogonalization based on the statistical input of the arbitrary probability. The multidimensional PC was constructed using tensor product of one dimensional PCs. For generation of multidimensional PCs from one dimensional PC using tensor product, the random variable should be uncorrelated, $\mathbb{E}[\xi_i(\theta)\xi_j(\theta)] = \delta_{ij}$, which is difficult to construct. In order to overcome the difficulties, Navarro et al. (2014) constructed PC expansion considering tensor product of random variable before orthogonalization, thus avoiding the requirement of uncorrelation.

Doostan et al. (2007) carried out analysis in the intrusive framework using different meshes starting with a coarse mesh. Based on the analysis using coarse mesh, optimal order of PC expansion to achieve an acceptable level of accuracy was evaluated and analyses were carried out considering fine meshes with PC generated from responses of initial course mesh. Hermite PC of Gaussian random variables were used to evaluate the responses. The Gaussian random variables were constructed using linear transformation of random variables from KL expansion of responses. Further, Soize and Ghanem (2009) and Arnst et al. (2014) extended the work to consider vector valued time dependent problems and coupled problems respectively. Many researcher were also working on non-intrusive framework and proposed a sparse PC expansion.

Blatman and Sudret (2008, 2010, 2011) studied structural mechanics problem in non-institutive framework for both Gaussian and non-Gaussian input parameters. Blatman and Sudret (2011) considered hyperbolic PC expansion, where higher order cross terms among random variables were not considered in the expansion. Blatman and Sudret (2011), Shao et al. (2017) considered a sensitivity analysis by allowing a tolerance limit to evaluate the dominant terms of PC expansion and obtain a global sparsity. Doostan and Owhadi (2011) studied sparse solution of stochastic PDF in non-intrusive non-adaptive framework based on comprehensive sampling formalism. Jakeman et al. (2015, 2017), considered l^1 minimization to find the dominant modes of PC expansion. Thus, construction of sparse PC is not a straight forward procedure and requires additional post processing. Moreover, the accuracy of solution depends on the chosen initial order of expansion, which depends on the randomness of the problem.

Gerritsma et al. (2010) proposed Time-Dependent generalized Polynomial Chaos (TDgPC) to over come the loss of optimality of PC expansion for time dependent problem. The authors proposed to consider an updation of PC expansion, when the expansion is no more suitable to evaluate the responses within an assumed accuracy limit. The updated PCs are generated based on the responses. The authors studied first-order ODE and Kraichnan-Orszag's three mode ODF problem with uniformly distributed random decay rate and random initial conditions respectively. Ozen and Bal (2016) studied long-time evaluation of responses to complex stochastic force in fluid dynamics, the Brownian motion considered as Markov process. The PC is updated at predefined time location and the PC is generated from random variables of Brownian motion and moments of responses. Ozen and Bal (2017) extended further to consider higher-dimensional problems with Markovian forces, where the dominant components of responses are evaluated using KL expansion.

In most of these methods, it is assumed that the input random variables are statistically independent in nature. However, there may be some amount of dependency or correlation among the input random variables and generally some transformation like Cholesky decomposition is used for dependent random Gaussian variables. Navarro et al. (2014) constructed PC using Gram-Schmidt orthogonalization for correlated variables by considering tensor product before orthogonalization process. The same is considered in this study for generation of PC and is termed as modified PC (mPC) as discussed in section 3.4.3

The accuracy of representation of simulated random field depends on the ratio of length of the process (domain of the random field) to the correlation length. A higher correlation length compared to domain of the problem requires lesser number of terms. Based on this properties, Chen et al. (2015) decomposed the physical domain to non-overlapping domain so that the higher correlation length can be achieved. The problem is solved for each domain, thus reducing the curse of dimensionality of PC expansion. This was further studied by Pranesh and Ghosh (2016), where it was generalized to any covariance function with domain shape independence and used finite element tearing and interconnecting solver.

Rahman (2017) introduced a transformation-free, generalized polynomial chaos expansion comprising multivariate Hermite orthogonal polynomials in dependent Gaussian random variables. The method employs non-polynomial basis unamenable to producing analytical formulae for response statistics and focuses strictly on Gaussian variables. Further, in order to innovate beyond tensor-product PCEs and capable of tackling non-product-type probability measures, Rahman (2018b) introduced a truly generalized PCE that accounts for arbitrary yet dependent probability distributions.

Pranesh and Ghosh (2018) studied the curse of dimensionality of PC expansion for elliptical equation by adaptively selecting the PC bases. The unknown coefficient of PC expansion are evaluated from the set of algebraic deterministic equations which are obtained after stochastic Galerkin projection. The curse of dimensionality is addressed by considering an adaptive scheme for selection of dominant chaos bases. The adaptive selection is done during the iterative process of preconditioned conjugate gradient (PCG) for solution of the algebraic equations. During initial few PCG iterations, all the terms of PC expansion are considered and later only dominant terms are considered. The authors further increased the computational efficiency by considering a reformulation of stochastic Galerkin method as generalized Sylvester equation.

Cheng and Lu (2018) studied the curse of dimensionality of PC expansion by proposing an adaptive sparse PC expansion. A full PC model is established using support vector regression. Based on the contribution to variance of the model output, non-significant terms are deleted and significant terms are retained. Further, an iterative algorithm of forward adding and backward deleting of PC bases were considered to obtain a desired level of accuracy. The major strength of the proposed method is that it could detect a group of basis functions simultaneously, thus making it as efficient for high dimensional problems. Moreover, support vector regression is better than least square regression as least square regression is more prone to over-fitting for higher order polynomials with non-linear approximation.

Another prominent approach to address the curse of dimensionality is Polynomial Dimension Decomposition (PDD) method (Rahman and Xu, 2004, Xu and Rahman, 2004, Rahman, 2008, Yadav and Rahman, 2014, Rahman, 2018a), which is based on a hierarchical decomposition of a multivariate response function in terms of variables with increasing dimensions. PDD deflates the curse of dimensionality to some extent by developing an input-output behaviour of complex systems with low effective dimensions, which are highly non-linear. PDD arranges terms of the expansion considering degree of interaction among the finite number of random variables rather than order of polynomial, which is generally considered in PC. The method is observed to be accurate, convergent and computationally efficient for probabilistic estimation of random mathematical functions and mechanical systems. Yadav and Rahman (2014) presented two novel adaptive-sparse PDD methods for solving practical science and engineering high-dimensional quantification problems. While the full PDD contains an infinite number of orthonormal polynomials, the number must be finite for practical application. The truncation parameters are automatically chosen and can achieve desired level of accuracy with significantly lesser number of coefficients as compared to the existing PDD approximation. Rahman (2018a) examined important mathematical properties of PDD for arbitrary but independent probability measures of input random variables.

2.4.3 Discussion

PC based methods are discussed in details, highlighting its drawback in terms of dimensionality and loss of optimality in the evaluation of stochastic responses. In the subsequence chapters, PC based methods are studied in details to address the curse of dimensionality and loss of optimality. The method proposed by Navarro et al. (2014) can generate PC with correlated random variables and the same is considered in the present study. Further, PDD, which can somewhat reduce the curse of dimensionality is also considered for further studies. Kundu and Adhikari (2014) observed that the dynamic responses of linear structural system evaluated using PC based method deviates from MCS as time progresses. TDgPC is considered to study long time analysis of linear structural dynamics problem with random material and geometric properties. Further, the computational demand of SFEM also depends on the representation of random field and its discretization. A detailed study on this regard is considered necessary for accurate representation of random field so that the size of the system matrix can be kept under control. An adaptive discretization of random field is proposed for this purpose.

3

Iterative PC for problems with Gaussian randomness

Contents

3.1 Introduction

In the previous two chapters, randomness in system parameters of structural elements are discussed along with different existing numerical techniques for analysis. Specifically, the PC based method is discussed in details along with its drawback like dimensional curse. In this chapter, the solution of linear structural mechanics problems with random coefficients is explored in the framework of PC expansion to enhance the computational efficacy of the scheme. The materials and loadings are considered as either Gaussian variables or fields.

An iterative type PC based method in the intrusive framework is presented. The method solves the problem using low dimensional PC expansion, thus reduces the curse of dimensionality of PC. The iterative method is based on the orthogonal expansion of stochastic responses of the system. The PC expansion is generated based on the responses of the previous iteration. The number of random variables in the expansion is reduced by considering the dominant component of the responses and are evaluated using KL expansion.

It is observed that the responses of structure with random material are generally non-Gaussian in nature even though the inputs are Gaussian in nature. In the present method, the non-Gaussian responses are thus approximated using proper PC expansion of non-Gaussian random variables. In the case of random field problem, the material randomness is discretized using the KL expansion. The proposed iterative method is observed to be more efficient than the conventional PC based method in terms of both accuracy and computational demand.

The usefulness of the proposed method is evaluated using three different problems. A truss problem with multiple random properties in material, geometry and loading is considered, where each of the random quantities is modelled as Gaussian random variables. A 3-D beam and a plane stress problem, where the material is modelled as a 1-D random field are also considered to demonstrate the efficacy of the proposed method. The proposed iterative scheme may be seen as an effective strategy for addressing a large class of structural mechanics problem with random material properties.

The chapter is organised as follows. In section 3.2, the discretization of random field and formulation of SFE is discussed. Section 3.3 discusses the solution of SFE using PC. The proposed iterative method is discussed in section 3.4, followed by the numerical study in section 3.5 along with a comparison with MCS and PC based method. The conclusion of the study is elaborated in section 3.6.

3.2 Discretization of random field and formulation of SFEM

Discretization of random field using KL expansion and formulation of SFE equation is described next in section 3.2.1 and 3.2.2 respectively. The combination of KL expansion with PC is widely used in SFEM and brief account of these procedure are presented in subsequent section.

3.2.1 Discretization of random field using KL expansion

KL expansion (Loeve, 1977) is considered for discretization of the input random field. It is also considered for the calculation of dominant components and random variables of the response covariance, which is used to evaluate the proposed iterative PC. A zero mean random function can be expressed as a sum of multiplication of a deterministic orthogonal function of coordinate and a random function. KL expansion is a special case of orthogonal series expansion, where the orthogonal functions are considered as the eigenfunctions of the covariance function (Zhang and Ellingwood, 1994, Huang et al., 2001). The main advantage of the the KL expansion over other series expansion is that it forms a bi-orthogonal expansion as both random variables and the deterministic functions are orthogonal (Huang et al., 2001). A zero mean random field $\alpha(x,\theta)$ with finite variance and covariance function $\boldsymbol{C}(x_1,x_2)$ is a function of position vector x defined over domain $\mathscr{D}$, with θ belonging to space of random event Ω. The random field is expressed using KL expansion as (Loeve, 1977),

$$\alpha(x,\theta) = \sum_{n=1}^{\infty} \xi_n(\theta)\sqrt{\lambda_n} f_n(x) \tag{3.1}$$

where, λ_n and $f_n(x)$ are eigenvalues and eigenvectors of the covariance function and $\xi_n(\theta)$ is given by

$$\xi_n(\theta) = \frac{1}{\sqrt{\lambda_n}} \int_{\mathscr{D}} \alpha(x,\theta) f_n(x) dx \tag{3.2}$$

$\xi_n(\theta)$ are uncorrelated random variables with

$$\mathbb{E}[\xi_n(\theta)] = 0 \tag{3.3a}$$

$$\mathbb{E}[\xi_n(\theta)\xi_m(\theta)] = \delta_{nm} \tag{3.3b}$$

where $\mathbb{E}[.]$ indicates the expectation operator.

Specifically, for Gaussian random field, the random variables ($\xi_n(\theta)$) are standard Gaussian random variables. The covariance function can be calculated as

$$\boldsymbol{C}(x_1,x_2) = \mathbb{E}[\alpha(x_1,\theta)\alpha(x_2,\theta)] \tag{3.4a}$$

$$= \sum_{n=1}^{\infty}\sum_{m=1}^{\infty} \mathbb{E}[\xi_n(\theta)\xi_m(\theta)]\sqrt{\lambda_n\lambda_m} f_n(x_1) f_m(x_2) \tag{3.4b}$$

$$= \sum_{n=1}^{\infty} \lambda_n f_n(x_1) f_n(x_2) \tag{3.4c}$$

Multiplying Eq. 3.4 by $f_n(x_1)$ and taking integral over the domain gives an integral equation as (Homogeneous Fredholm integral equation of the second kind)

$$\int_{\mathscr{D}} \boldsymbol{C}(x_1,x_2) f_n(x_1) dx_1 = \lambda_n f_n(x_2) \tag{3.5}$$

and solution of this integral equation gives the eigenvalue and eigenvector of the covariance function. The KL expansion can be truncated at a optimal number of terms, Q can be obtained by considering the expected energy criteria of the covariance function (Huang et al., 2001).

The analytical solution of the integral equation is however limited to only few of the covariance function and often numerical solution needs to be considered. The accuracy of simulated data is more in case of analytical method of calculation of eigenpairs (Huang et al., 2001). There are numerous methods for the numerical solution, few of these were reviewed by Betz et al. (2014). However in the present study, the eigenpairs are calculated from covariance matrices numerically as a general procedure for both material and responses as it is not easier to calculate the eigenpairs analytically for the response covariance.

3.2.2 Formulation of SFEM

The formulation of stochastic finite element is similar to that of deterministic counterpart, like minimization of potential energy, Galerkin formulation etc. The stochastic finite element equation can be written as (Ghanem and Spanos, 1990, 1991b),

$$\left[\overline{\boldsymbol{K}}_{(N\times N)} + \sum_{n=1}^{Q} \xi_n(\theta)\boldsymbol{K}_{n_{(N\times N)}}\right]\boldsymbol{u}_{(N\times 1)} = \boldsymbol{q}_{(N\times 1)} \tag{3.6}$$

$\overline{\boldsymbol{K}}$ and $\boldsymbol{K}_n$ are the deterministic and stochastic parts of the stiffness matrix. The subscript N indicates the size of the matrix, equal to the number of degrees of freedom. The stochastic Eq. 3.6 is solved to find the response statistics. Generally it can be solved using MCS for each of the realization of $\xi_n(\theta)$. However, MCS is computationally intensive and in order to overcome this, Ghanem and Spanos (1990, 1991b) considered PC expansion (Wiener, 1938) to approximate the responses, which is discussed in brief in next section. With PC approximation of responses, the stochastic equation can be converted to a set of deterministic equations following Galerkin projection, which can be solved using deterministic solver.

3.3 Solution using Polynomial Chaos: Generalized PC (gPC)

The KL expansion can be used when the eigenvalues and eigenpairs of the covariance function of the random field are known. Thus, it is used to represent the random material property, where random behaviour of the material is depicted by covariance function. However, while dealing with responses, the mean and covariance function are not known *apriori* and hence can not be approximated using KL expansion. Ghanem and Spanos (1990, 1991b) used the concept of homogeneous chaos proposed by Wiener (1938) to overcome such constraint, and proposed spectral stochastic finite element method, where Hermite polynomial of Gaussian process was used to approximate the response processes. A second-order random variable can be represented by a mean square convergent series using PC expansion (Ghanem and Spanos, 1991b). The response processes are approximated as

$$\boldsymbol{u} = \sum_{i=0}^{P} \boldsymbol{c}_i \Psi_i[\{\boldsymbol{\xi}_r(\theta)\}] \tag{3.7}$$

$(P+1)$ is the total number of terms of Polynomial Chaos used in the expansion and r is the number of random variables. The basic property of PC is that Polynomial of different orders are orthogonal to each other and also true for same order with different argument. Thus,

$$\langle \Psi_i[\{\boldsymbol{\xi}_r(\theta)\}]\Psi_j[\{\boldsymbol{\xi}_r(\theta)\}] \rangle = \delta_{ij} \left\langle \Psi_i^2[\{\boldsymbol{\xi}_r(\theta)\}] \right\rangle \tag{3.8}$$

The mean of PC higher than zeroth order is zero,

$$\langle \Psi_i[\{\boldsymbol{\xi}_r(\theta)\}] \rangle = 0, \quad i > 0 \tag{3.9}$$

and mean of zeroth order polynomial is one,

$$\langle \Psi_0[\{\boldsymbol{\xi}_r(\theta)\}] \rangle = 1 \tag{3.10}$$

Due to this orthogonality property, using Galerkin projection the stochastic algebraic equation can be converted to set of deterministic equations as

$$\overline{\boldsymbol{K}}\left\langle \Psi_m^2 \right\rangle \boldsymbol{c}_m + \sum_{i=0}^{P} \boldsymbol{Y}_{im}\boldsymbol{c}_i = \langle \boldsymbol{q}\Psi_m \rangle \tag{3.11}$$

where $\boldsymbol{Y}_{im} = \sum_{n=1}^{Q} \boldsymbol{K}_n \boldsymbol{X}_{nim}$ and $\boldsymbol{X}_{nim} = \left\langle \xi_n(\theta)\Psi_i\Psi_m \right\rangle$, $m = 0,1,2,\ldots P$. The above equation can be solved using any standard deterministic solver. However, the size of the matrix increases exponential with the order of polynomial chaos, p and the matrix size becomes $N(P+1) \times N(P+1)$. A few of the calculated values of $(P+1)$ for different p and Q, shown in Table 2.2, are evaluated using Eq. 3.12 (Xiu and Karniadakis, 2002). The matrix size increases exponentially, if order of expansion or/and number of random variables increases.

$$(P+1) = \frac{(Q+p)!}{Q!p!} \tag{3.12}$$

In Eq. 3.7, $\Psi_i[\{\boldsymbol{\xi}_r(\theta)\}]$ are known quantities and random in nature and $\boldsymbol{c}_i$ are unknown and can be obtained by solving Eq. 3.11. $\Psi_i[\{\boldsymbol{\xi}_r\}]$ are functions of random variables $\{\boldsymbol{\xi}_r(\theta)\}$ and form a orthogonal polynomial base. In case of Gaussian $\boldsymbol{\xi}_r(\theta)$, these polynomial are Hermite polynomial. The Hermite polynomial are optimal for Gaussian random field.

Xiu and Karniadakis (2002) generalized the concept of PC to other forms of random processes by considering different sets of orthogonal polynomials for different types of random processes and are known as generalized PC (gPC). These polynomials are from the Askey scheme. Different optimal polynomials were suggested for different random processes. In case of structural mechanics problem, as the standard deviation (SD) of the input random field/variable is increased, the responses become more and more non-Gaussian. Thus, to represent the response accurately using Hermite Polynomial, a higher order expansion is required. In this context, it may be appropriate to approximate the responses gPC. However, in order to consider an appropriate variant of gPC, the distributions of responses are not available *apriori*. Wan and Karniadakis (2006a) and Witteveen et al. (2007) proposed PC expansion for an arbitrary probability input. The former proposed Multi-Element generalized Polynomial Chaos (ME-gPC), where the stochastic space was discretized into mutually exclusive space and numerically generated orthogonal polynomials in each space with corresponding conditional probability density function. However, the later author constructed PC for one dimension using Gram-Schmidt orthogonalization based on the statistical input of the arbitrary probability. The multidimensional PC was constructed using tensor product of one dimensional PCs. Further, Yin et al. (2018) proposed a strategy for improving computational accuracy of responses, while using arbitrary probability input.

3.4 Solution using Proposed Approach

3.4.1 Basic idea

The problem related to an exponential increase in matrix size was discussed by various authors, and different strategies were proposed for the generation of sparse PC expansion as discussed in section 2.4.2. In the present study, an iterative PC based method in the intrusive framework is proposed to overcome such problems of large dimension of system matrices. As the SD of the input random field increases, the responses become non-Gaussian. However, it is represented by Hermite polynomial of Gaussian random variables in the traditional PC. Thus, it requires a higher order of expansion for improving the accuracy of the solution.

In the present method, responses are evaluated using a PC of non-Gaussian random variables, which are calculated using an iterative scheme from the previous iteration. The initial responses are calculated using a first-order PC, and subsequently, these responses are used to formulate the iterative PC of different orders. A method to generate PC for non-Gaussian random variables is discussed in section 3.4.3. The numbers of random variables are also reduced in the iteration process by considering only the dominant components of the response evaluated using KL expansion. Thus, while the numbers of random variables are reduced, PC is also formed using non-Gaussian random variables, which requires a lesser order of expansion than conventional PC.

In case of random field problem, the input random field is also discretized using KL expansion. The size of stiffness matrix can be reduced by considering the random field at Gauss points of each element instead of the generally considered midpoints and are discussed in detail in section 3.4.2. Moreover, the system matrix size can be further reduced following Pascual and Adhikari (2012) as discussed in section 3.4.5.

3.4.2 Discretization of input random field

The input random field is discretized using KL expansion. It is, however, important to represent the covariance function of the random field in its best possible manner, which can be achieved by increasing the number of points in the covariance function. The general procedure to represent the covariance function and thus, the random field is to consider the value of the random field at the midpoint of an element. Thus, to increase the number of points in the covariance function for better representation, the number of elements should be increased while discretizing the structure in FE method. However, in this process, the size of the stiffness matrix of the system also increases. Brenner and Bucher (1995) proposed to consider the random field at Gauss points so that more information can be accessed. This way, the number of points to represent the random field can be increased without increasing the size of the problem. Moreover, if Gauss point values are considered, it can be directly utilized in the numerical integration process using Gauss quadrature. In the present study, the random field is considered at Gauss points by defining the eigenvector of covariance function at Gauss point rather than at midpoint of elements. A comparative study of the accuracy of the eigenvector of the covariance for midpoint and Gauss point representation for a 1-D random field problem is carried out in section. 3.5.2

3.4.3 Generation of PC for arbitrary probability: A modified PC (mPC)

A PC expansion for arbitrary probability distribution is presented. The orthogonal expansion is carried out using Gram-Schmidt orthogonalization process inline with Navarro et al. (2014). Generally, the multi-dimensional PC expansion are evaluated by considering tensor product of the one-dimensional PC expansions. However, for this process the considered random variables should be uncorrelated *i.e* $\mathbb{E}[\xi_i \xi_j] = \delta_{ij}$, which is difficult to construct. Thus, it is proposed to consider the tensor product before the orthogonalization process. The basis vectors for the Gram-Schmidt process are formulated by considering the tensor product of each of the random variables. Thus the basis vectors for Gram-Schmidt process for a two random variables problem are $V(\boldsymbol{\xi}) = G(\xi_i) \otimes G(\xi_j)$, where, $G(\xi_i) = \{1,\ \xi_i,\ \xi_i^2,\ \xi_i^3,\ \ldots,\ \xi_i^p\}$, where p is the order of expansion. For example, for two random variables ξ_1, ξ_2 and order of PC=3, the basis vectors for Gram-Schmidt orthogonalization process are $V(\xi_1,\xi_2)_{j=0}^{9} = \{1,\ \xi_1,\ \xi_2,\ \xi_1^2, \xi_2^2,\ \xi_1\xi_2,\ \xi_1^3,\ \xi_2^3,\ \xi_1^2\xi_2, \xi_1\xi_2^2\}$. The Gram-Schmidt process is carried out as (Golub and Van Loan, 1983)

$$\Psi_k(\xi) = V_k(\xi) - \sum_{l=0}^{k-1} \frac{\langle V_k(\xi), \Psi_l(\xi)\rangle}{\langle \Psi_l(\xi), \Psi_l(\xi)\rangle} \Psi_l(\xi),\ \ \Psi_0(\xi) = 1, \quad k = 1,2,3,\ldots,P \tag{3.13}$$

where the dimension $(P+1)$ is given by the dimension of $V(\boldsymbol{\xi})$. The advantage of the modified PC (mPC) formulated using Gram-Schmidt process over gPC is that it can form a orthogonal polynomial even for arbitrary random variables.

3.4.4 Proposed iterative scheme (ImPC)

The first step of the proposed iterative method is to solve the stochastic problem using first-order mPC with the desired number of random variables from KL expansion of the input random field. Depending on the SD of the random field, the responses are likely to be of different probability distributions. However, these evaluated responses are not accurate as only first-order expansion is considered initially and the proposed iterative process is presented as,

$$\left[\overline{\boldsymbol{K}}_{(N\times N)} + \sum_{n=1}^{Q} \xi_n(\theta)\boldsymbol{K}_{n_{(N\times N)}}\right] \boldsymbol{u}_{(N\times 1)} = \boldsymbol{q}_{(N\times 1)}$$

Approximate $\boldsymbol{u}$ using first order PC

$$\boldsymbol{u} = \sum_{i=0}^{P} \boldsymbol{c}_i \Psi_i[\{\boldsymbol{\xi}_r(\theta)\}]$$

Solve for $\boldsymbol{c}$ using Galerkin projection and iteratively approximate $\boldsymbol{u}$ using higher order PC as

$$\boldsymbol{u}^{(j+1)} = \sum_{i=0}^{P} \boldsymbol{c}_i \Psi_i[\boldsymbol{u}^{(j)}[\{\boldsymbol{\xi}_r(\theta)\}]]$$

Iterate till $\boldsymbol{u}$ shows convergence.

The dominant components of the responses are then evaluated using KL expansion of the covariance function ($\boldsymbol{C_{uu}}$) of the responses.

The polynomial is updated based on the new random variable ($\xi_i(\theta)_{\text{new}}$) using the proposed mPC based method of the desired order. The optimal number of random variables in the new PC expansion can be evaluated from the expected energy consideration of the random field of the responses. The formation of new random variables and new PC expansion can be performed iteratively until the desired convergence is obtained. It may be noted that $\xi(\theta)$ used in the KL expansion of input random field of Young's modulus will not change as it describes the material property alone. The new $\xi_i(\theta)_{\text{new}}$ is considered only in the updation of polynomial bases for the orthogonalization process to generate mPC. It may be noted that, Xiu and Karniadakis (2002) observed that orthogonal polynomial are optimal for representation of a random process when the weight functions for some orthogonal polynomials are identical to the probability functions. Thus, in the proposed approach as the PCs are generated using random variables obtained from responses, the updated PCs are optimal for the response to be calculated.

The proposed method differs from previous work of Doostan et al. (2007) in some ways. A discretized spatial domain is obtained by considering both randomness in material and deterministic finite element mesh size requirement, which is generally from stress consideration. The dominant components of responses based on first order PC are evaluated from responses using KL expansion, which is further used to formulate next higher-order PC expansion using Gram-Schmidt orthogonalization. Generally, for uncorrelated random variables, the multidimensional PC are formulated from univariate PC using the tensor product. However, it is difficult to generate fully uncorrelated random variables, and hence, Cholesky decomposition is used in the conventional approach. Navarro et al. (2014) constructed PC using Gram-Schmidt orthogonalization for correlated variables by considering tensor product before the orthogonalization process. The same is considered in this study for generation of PC and is termed as modified PC (mPC) as discussed in section 3.4.3. Further, in the proposed method, the improved responses can be evaluated using iterative PC, wherein the same order of PCs are used, and the responses are observed to converge. Moreover, since the initial order of PC to evaluate responses are of the first order, it significantly reduces computational cost. Order of PCs is increased only if the errors are not within the acceptable limit. In the method proposed by Doostan et al. (2007), the order of PC is first decided, and then finite element discretization is carried out till the solution converges. On the other hand, the proposed strategy considers an appropriately discretized mesh based on both finite element and material characteristic and order of PC expansion is continuously updated with an additional iterative process in each order of expansion till an accurately converged solution is obtained.

Stepwise Algorithm of ImPC:

A1-1 Calculate stiffness matrix using KL expansion

{

Discretize the covariance function of random field considering the random field at Gauss point of each element.

$$E(x,\theta) = E_0 \left(1 + \sum_{n=1}^{Q} \xi_n(\theta) \sqrt{\lambda_n} f_n(x) \right)$$

Calculate the number of random variables (Q) based on expected energy consideration.

{

while energy $\leq$threshold

$Q = Q + 1$

energy=energy+$\lambda_Q / sum(\lambda)$

end while

}

Formulation of SFEM as discussed in section 3.2.2.

}

A1-2 Construct first order PC using the random variables calculated in step A1-1.

$$\mathrm{PC}_{\text{1st Order}} = f(\xi_Q(\theta))$$

A1-3 Solve stochastic equation using Galerkin projection as discussed in section 3.3.

A1-4 Calculate ensemble of responses by multiplying the coefficient evaluated in step A1-3 with corresponding PC as per Eq. 3.7

A1-5 { Consider order of PC expansion $p > 1$

(a) Perform KL expansion on the covariance function ($\boldsymbol{C_{u_1 u_2}}$) of responses and new random variables $\xi_i(\theta)_{\text{new}}$ are calculated as,

$$\xi_i(\theta)_{\text{new}} = \frac{1}{\sqrt{\lambda_{\text{new}_i}}} \boldsymbol{u}_{\text{mean}} E_{\text{vector new}_i}$$

where λ_{new_i} and $E_{\text{vector new}_i}$ are the eigenvalue and eigenvector of the covariance function of the responses. $\boldsymbol{u}_{\text{mean}}$ is the matrix of zero mean responses. The covariance function of responses is calculated as,

$$\boldsymbol{C}_{u_1 u_2} = \mathbb{E}[(u_1 - \text{mean}(u_1))(u_2 - \text{mean}(u_2))]$$

(b) Calculate the optimal number of $\xi_i(\theta)_{\text{new}}$ based on expected energy consideration.

(c) Formulate the basis for Gram-Schmidt orthogonalization as discussed in section 3.4.3

e.g. for 2 random variables (ξ_1, ξ_2)

$V = \{1,\ \xi_1,\ \xi_2,\ \xi_1^2,\ \xi_2^2,\ \xi_1\xi_2,\ \ldots\}$

(d) Formulate PC using Gram-Schmidt orthogonalization process using $\xi_i(\theta)_{\text{new}}$ and Eq. 3.13.

{

$U(:,1) = V(:,1);$

for $i = 2 : k$

$U(:,i) = V(:,i);$

for $j = 1 : i-1$

$$U(:,i) = U(:,i) - \frac{\left\langle (U(:,i)^T * U(:,j)) \right\rangle}{\left\langle (U(:,j)^T * U(:,j)) \right\rangle} U(:,j);$$

end for

$PC(:,i) = U(:,i);$

end for

}

(e) Solve using new PC. Calculate ensemble of response and response statistics.

(f) Check for convergence using error measure as discussed in section 3.4.6.

If converged (i.e. errors are not changing any more)

then go to step A1-6

Else go to A1-5a for next iteration.

}

A1-6 If errors (as per section 3.4.6) > Permissible limit

New order of PC, $p = p + 1$

Go to step A1-4

Else

Finish

Step A1-1 is to be considered only for random field problems. In case of problems with random variables, the proposed method can start directly from step A1-2.

3.4.5 Reduction of size of stiffness matrix

The matrix size and computational time can further be reduced by considering the reduction of size of the stiffness matrix. Pascual and Adhikari (2012) proposed a reduced polynomial chaos expansion method, where eigenvalue decomposition of stiffness matrix was carried out to reduce the size of the stiffness matrix. Considering the deterministic part of the stiffness matrix, the eigenvalue decomposition of Eq. 3.6 is carried out as detailed below.

$$\overline{\boldsymbol{K}}\boldsymbol{u} = \boldsymbol{q} \tag{3.14}$$

The eigenvalue problem is written as

$$\overline{\boldsymbol{K}}\{\phi\}_k = \lambda_{0_k}\{\phi\}_k; \quad k = 1,2,3,\dots N \tag{3.15}$$

and the eigenvalue and eigenvector matrices are

$$[\Lambda_0] = \text{diag}[\lambda_{0_1}, \lambda_{0_2}, \lambda_{0_3}, \dots \lambda_{0_N}], \quad [\Phi]_N = [\{\phi\}_1, \{\phi\}_2, \{\phi\}_3, \dots \{\phi\}_N] \tag{3.16}$$

Now, the response can be approximated as,

$$\boldsymbol{u} = \overline{\boldsymbol{K}}^{-1}\boldsymbol{q} = [\Phi]\Lambda_0^{-1}([\Phi]^T\boldsymbol{q}) = \sum_{k=1}^{N} \frac{\{\phi\}_k^T\{q\}}{\lambda_{0_k}}\{\phi\}_k \tag{3.17}$$

However, depending upon the magnitude of the eigenvalues, it is possible to truncate this series expansion at a suitable term S, where $\lambda_{0_1}/\lambda_{0_S} \leq \varepsilon$, ε is a small positive value. Thus,

$$\boldsymbol{u} \approx \sum_{k=1}^{S} \frac{\{\phi\}_k^T \boldsymbol{q}}{\lambda_{0_k}} \{\phi\}_k \tag{3.18}$$

The reduced eigenpairs become

$$[\Lambda_0]_S = \text{diag}[\lambda_{0_1}, \lambda_{0_2}, \lambda_{0_3}, \ldots \lambda_{0_S}], \quad [\Phi]_S = [\{\phi\}_1, \{\phi\}_2, \{\phi\}_3, \ldots \{\phi\}_S] \tag{3.19}$$

Considering the $[\Phi]_S$ as coordinate transformation, Eq.3.6 can be converted to a equation of smaller size

$$\left[\overline{\boldsymbol{K}}_{(S\times S)} + \sum_{n=1}^{Q} \xi_n(\theta) \boldsymbol{K}_{n_{(S\times S)}}\right] \boldsymbol{u}_{(S\times 1)} = \boldsymbol{q}_{(S\times 1)} \tag{3.20}$$

where $\overline{\boldsymbol{K}}_{(S\times S)} = [\Phi]_S^T \overline{\boldsymbol{K}}_{(N\times N)} [\Phi]_S$, $\boldsymbol{u}_{(N\times 1)} = [\Phi]_S \boldsymbol{u}_{(S\times 1)}$, $\boldsymbol{K}_{n_{(S\times S)}} = [\Phi]_S^T \boldsymbol{K}_{n_{(N\times N)}} [\Phi]_S$ and $\boldsymbol{q}_{(S\times 1)} = [\Phi]_S^T \boldsymbol{q}_{(N\times 1)}$. Eq. 3.20 is solved using PC, similar to the strategy adopted for full matrix. The size of the final deterministic equation (Eq. 3.11) for reduced stiffness approach is $S(P+1)\times S(P+1)$, whereas for original stiffness, the size is $N(P+1)\times N(P+1)$ leading to reduction in computational cost for solution of the problem.

3.4.6 Convergence and accuracy of the proposed approach

The performance of the proposed iterative strategy is assessed by considering the goodness of the calculated response. Since the problem is statistical in nature, the responses are checked for accuracy at individual response level, overall response level and statistical response level. The responses are compared with MCS responses for the evaluation of different error measures.

The individual responses are checked against corresponding responses of MCS. The normalized absolute maximum error is calculated as

$$\text{Err}_{\text{Abs}} = \frac{\text{Max}\left|u_i^{\text{MCS}} - u_i^{\text{PC}}\right|}{\left|\mathbb{E}[u^{\text{MCS}}]\right|}, \qquad i = 1,2,3,\ldots,\text{Sample Size} \tag{3.21}$$

where u_i^{MCS} are the responses from MCS and u_i^{PC} are corresponding responses from PC solution and $\mathbb{E}[.]$ denotes the expectation operator. The error is normalized with respect to the mean of the MCS responses. It gives a measure of the maximum of the error between corresponding responses of MCS and PC.

The accuracy of responses are also checked by evaluating RMS error. The RMS error gives overall measure of correctness of a response vector. It is defined as the square root of mean of square of error in responses between MCS and PC. The error is normalized with respect to mean value of MCS responses.

$$\text{RMS Error,} \quad \text{Err}_{\text{RMS}} = \frac{\sqrt{\text{Mean}((u_i^{\text{MCS}} - u_i^{PC})^2)}}{\left|\mathbb{E}[u^{\text{MCS}}]\right|}, \quad i = 1, 2, 3, \ldots, \text{Sample Size} \tag{3.22}$$

The statistical response parameters are further utilized for assessment of accuracy of responses. The % error in mean, SD, skewness and Kurtosis are calculated for responses of proposed iterative scheme with respect to MCS responses. Different statistical error measures are defined as shown in Table 3.1.

Table 3.1: Various statistical error measure considered to check accuracy of responses.

Sl. No.	% Error in	Formula
1	Mean	$\frac{\left\|\mathbb{E}[u^{\text{MCS}}] - \mathbb{E}[u^{\text{PC}}]\right\|}{\left\|\mathbb{E}[u^{\text{MCS}}]\right\|} \times 100\%$
2	SD	$\frac{\left\|\text{SD}(u^{\text{MCS}}) - \text{SD}(u^{\text{PC}})\right\|}{\text{SD}(u^{\text{MCS}})} \times 100\%$
3	Skewness	$\frac{\left\|\text{Skewness}(u^{\text{MCS}}) - \text{Skewness}(u^{\text{PC}})\right\|}{\left\|\text{Skewness}(u^{\text{MCS}})\right\|} \times 100\%$
4	Kurtosis	$\frac{\left\|\text{Kurtosis}(u^{\text{MCS}}) - \text{Kurtosis}(u^{\text{PC}})\right\|}{\text{Kurtosis}(u^{\text{MCS}})} \times 100\%$

The statistical response parameters are further utilized for assessment of accuracy of responses. The % error in mean, SD, skewness and Kurtosis are calculated for responses of proposed iterative scheme with respect to MCS responses. The SD, skewness, kurtosis are calculated with bias-correction using formulae for skewness and kurtosis as,

$$\text{Skewness,} \quad s_0 = \frac{\sqrt{S(S-1)}}{S-2} s_1, \tag{3.23}$$

where

$$s_1 = \frac{\frac{1}{S}\sum_{i=1}^{S}(u_i - \overline{u})^3}{\left(\sqrt{\frac{1}{S}\sum_{i=1}^{S}(u_i - \overline{u})^2}\right)^3} \tag{3.24}$$

$$\text{Kurtosis,}\;\; k_0 = \frac{S-1}{(S-2)(S-3)}((S+1)k_1 - 3(S-1)) + 3 \tag{3.25}$$

where

$$k_1 = \frac{\frac{1}{S}\sum_{i=1}^{S}(u_i - \overline{u})^4}{\left(\frac{1}{S}\sum_{i=1}^{S}(u_i - \overline{u})^2\right)^2} \tag{3.26}$$

These statistical moments can be evaluated using MATLAB® command ”skewness” and ”kurtosis” with bias-correction. Different statistical error measures are defined as shown in Table 3.1.

An acceptable limit of different error measures may be chosen for stopping of iterations and the solution is deemed to have converged. In the present study, the responses are compared with MCS for ascertaining accuracy and convergence. However, similar convergence as well as accuracy of solution can also be evaluated by considering responses corresponding to two consecutive iterations and orders, if MCS results are not available.

3.5 Numerical Examples

To demonstrate the applicability, accuracy, and efficacy of the proposed scheme for the solution of stochastic mechanics problem, three examples are considered as (i) 2-D truss problem (ii) Euler-Bernoulli cantilever beam and (iii) settlement analysis of foundation resting on a random soil media. The materials and sectional areas for the members of the truss are modelled as independent Gaussian random variables. The loadings are also considered as independent Gaussian random variables. In the case of beam and foundation problem, the materials are modelled as a 1-D random field. Monte Carlo Simulation (MCS) using deterministic FE method are performed to generate benchmark results for comparison of the accuracy of the proposed strategy. The same seeds of uncorrelated random variables are considered in all the methods so that there is no anomaly in the data while comparing results from different approaches. A sample size of 5×10^5 for the truss problem and 3×10^4 for all beam and foundation problems are considered.

3.5.1 Truss problem : A random variable problem with multiple randomness in material, geometry and loading

The first problem considered is a truss structure of 23 members as shown in Fig.3.1. The structure is subjected to six vertical loads as shown, which are random in nature. The material and area of the truss members are also considered as random. The problem was studied by different researchers in the past (Blatman and Sudret, 2008, 2010). In the present study, Young's modulus, area and loading are considered as independent Gaussian random variables and are shown in Table 3.2. Total ten random variables are considered as

$$\boldsymbol{Z} = \{E_1, E_2, A_1, A_2, q_1, q_2, q_3, q_4, q_5, q_6\}^T \tag{3.27}$$

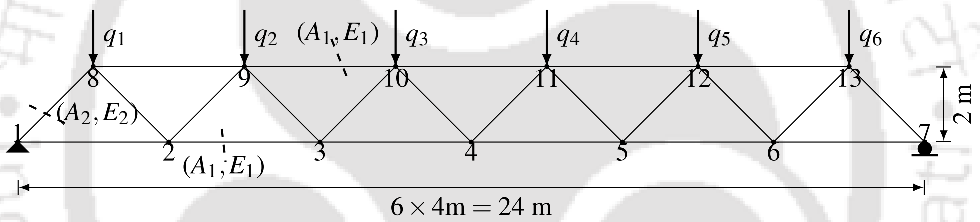

Fig. 3.1: 23 member truss structure with loading.

Table 3.2: Input random variable for truss problem.

Variable	Unit	Mean	SD
A_1	m^2	2.0×10^{-3}	2.0×10^{-4}
A_2	m^2	1.0×10^{-3}	1.0×10^{-4}
E_1	Pa	2.1×10^{11}	2.1×10^{10}
E_2	Pa	2.1×10^{11}	2.1×10^{10}
q_1 to q_6	N	5×10^4	7.5×10^3

Thus, with axial rigidity $EA = E(\theta)A(\theta)$, the finite element equation can be written as,

$$\sum_{i=1}^{R} \boldsymbol{K}_i(E_i(\theta)A_i(\theta))\boldsymbol{u} = \sum_{j=1}^{S} \boldsymbol{q}_j(\theta) \tag{3.28}$$

where, $\boldsymbol{K}_i$ is formulated considering the members of the truss with axial rigidity $E_i(\theta)A_i(\theta)$. R and S are the number of pairs of $E(\theta)A(\theta)$ and number of random load vectors respectively.

The response of the structure is calculated using modified PC and the proposed ImPC method and compared with that of MCS responses. Though the input random variables are Gaussian in nature, these variables have different mean as well as SD. Hence, these are recast as standard normal random variables with zero mean and unit SD by subtracting the mean and dividing by the SD of the corresponding random variables (X_i). The transformed random variables are considered only for generation of PC, the input random variables considered in Eq. 3.28 remain same as they represent the input random data. Thus the displacement $\boldsymbol{u}$ is approximated as,

$$\boldsymbol{u} = \sum_{i=0}^{P} \boldsymbol{a}_i \Phi_i(\boldsymbol{X}) \tag{3.29}$$

where Φ_i are the PC evaluated as discussed in section 3.4 depending upon the considered method mPC or ImPC.

3.5.1.1 Response of truss

The vertical displacement of node 4 (Fig.3.1) is considered for the detail study. The pdfs of transformed random variables (X_i) considered to generate PC are shown in Fig. 3.2 and the statistical parameters of the random variables are shown in Tables 3.3 and 3.4. It can be observed that the random variables are identically distributed Gaussian but they are not perfectly uncorrelated as may be observed from off-diagonal terms in Table 3.4. In case of Hermite polynomial chaos the random variables need to be Gaussian and uncorrelated to form an orthogonal basis vector. However, the proposed polynomial chaos generated considering Gram-Schmidt orthogonalization process as described in section 3.4 is orthogonal.

The problem is solved using mPC generated as described in section 3.4.3. The pdfs of the vertical displacement of node 4 are shown in Fig. 3.3. It can be observed that the pdf responses of first order mPC based method does not match with MCS. However, as the order increases, the pdf converges towards MCS. The size of polynomial also increases as the order of the mPC increases.

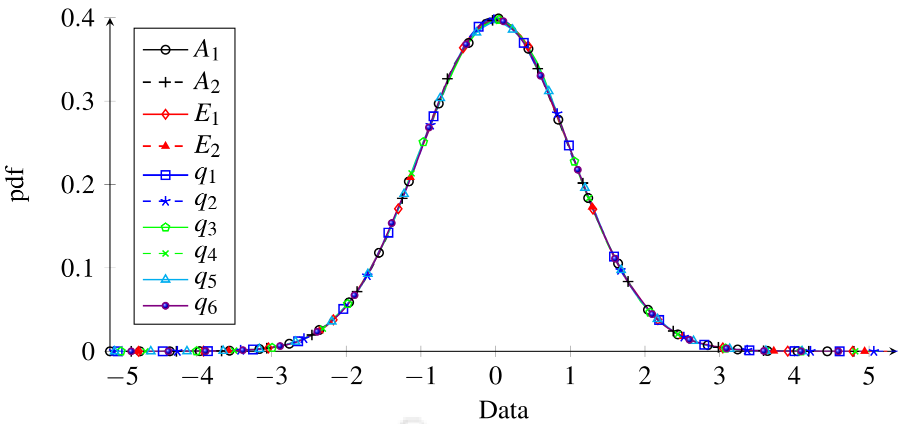

Fig. 3.2: pdfs of transformed random variables for truss problem.

Table 3.3: Statistical parameters of the transformed random variables of truss problem.

Variable	Mean	SD	Skewness	Kurtosis
q_1	-7.889×10^{-12}	1	-5.318×10^{-04}	3.0004
q_2	-3.670×10^{-11}	1	-6.365×10^{-04}	3.0077
q_3	-1.050×10^{-11}	1	-5.728×10^{-03}	2.9965
q_4	5.885×10^{-12}	1	-2.406×10^{-03}	3.0082
q_5	2.647×10^{-11}	1	-2.261×10^{-03}	2.9894
q_6	-1.813×10^{-11}	1	2.296×10^{-04}	3.0054
A_1	3.220×10^{-11}	1	4.977×10^{-04}	3.0069
E_1	1.016×10^{-11}	1	-2.543×10^{-03}	3.0021
A_2	1.198×10^{-11}	1	5.296×10^{-03}	3.0035
E_2	-3.464×10^{-13}	1	4.756×10^{-03}	2.9931

Table 3.4: Value of $\mathbb{E}[X_i, X_j]$ for transformed random variables of truss.

	q_1	q_2	q_3	q_4	q_5	q_6	A_1	E_1	A_2	E_2
q_1	1	0.0015	0.0014	0.0003	-0.0008	-0.0013	-0.0020	-0.0014	0.0008	0.0019
q_2	0.0015	1	0.0011	0.0006	-0.0028	-0.0017	-0.0009	0.0017	-0.0010	-0.0013
q_3	0.0014	0.0011	1	-0.0025	0.0003	-0.0015	-0.0022	-0.0006	-0.0002	-0.0008
q_4	0.0003	0.0006	-0.0025	1	-0.0012	-0.0004	0.0014	-0.0001	-0.0003	-0.0005
q_5	-0.0008	-0.0028	0.0003	-0.0012	1	0.0008	0.0017	-0.0010	-0.0012	0.0001
q_6	-0.0013	-0.0017	-0.0015	-0.0004	0.0008	1	-0.0002	0.0000	0.0001	0.0016
A_1	-0.0020	-0.0009	-0.0022	0.0014	0.0017	-0.0002	1	-0.0006	0.0004	0.0017
E_1	-0.0014	0.0017	-0.0006	-0.0001	-0.0010	0.0000	-0.0006	1	0.0011	0.0003
A_2	0.0008	-0.0010	-0.0002	-0.0003	-0.0012	0.0001	0.0004	0.0011	1	0.0005
E_2	0.0019	-0.0013	-0.0008	-0.0005	0.0001	0.0016	0.0017	0.0003	0.0005	1

In order to reduce the dimension of mPC expansion, the problem is solved using proposed iterative method. The ImPC expansion is generated iteratively after solving the problem using first order mPC expansion, and subsequently the responses are considered to generate mPC expansion of desired order. It is observed that the most of the expected energy is concentrated within the first few modes, and only three random variables corresponding to first three modes are considered for the iteration process. The iteration processes of 2$^{\text{nd}}$ order with 3 random variables for first and second iterations are designated as "EV3PC2I1", "EV3PC2I2" respectively. Similarly, for 3$^{\text{rd}}$ order PC, it is designated as "EV3PC3I1", "EV3PC3I2". The pdfs of the vertical displacement of node 4 for third order ImPC with different iterations are shown in Fig.3.4. It is observed that the pdf of first order mPC does not match with MCS. However, as iteration increases, pdfs are observed to converge towards MCS. Various errors associated with the responses are shown in Fig. 3.5. For comparison with mPC based method, the error associated with different orders of mPC are also plotted along y axis vs number of orders along x axis. The errors in absolute maximum error, RMS error and various statistical errors are observed to reduce as iterations and orders are increased. The accuracy of the results can further be increased by increasing the number of random variables considered in the iteration process. It can be observed that the error in 3$^{\text{rd}}$ order mPC is comparable to 3$^{\text{rd}}$ order proposed ImPC. However, the number of random variables in case of mPC is ten, while it is only three in case of the proposed scheme.

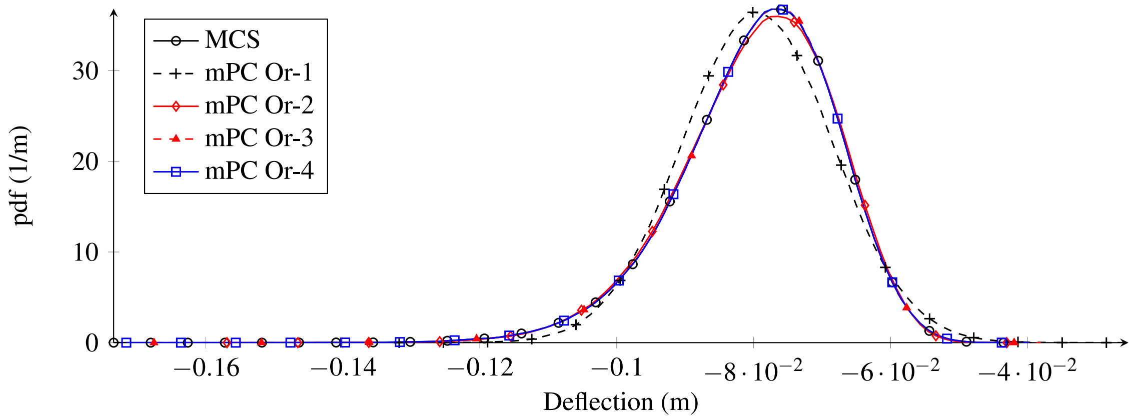

Fig. 3.3: pdfs of vertical displacement of node 4 of truss (Fig. 3.1)for different orders of mPC and comparison with MCS.

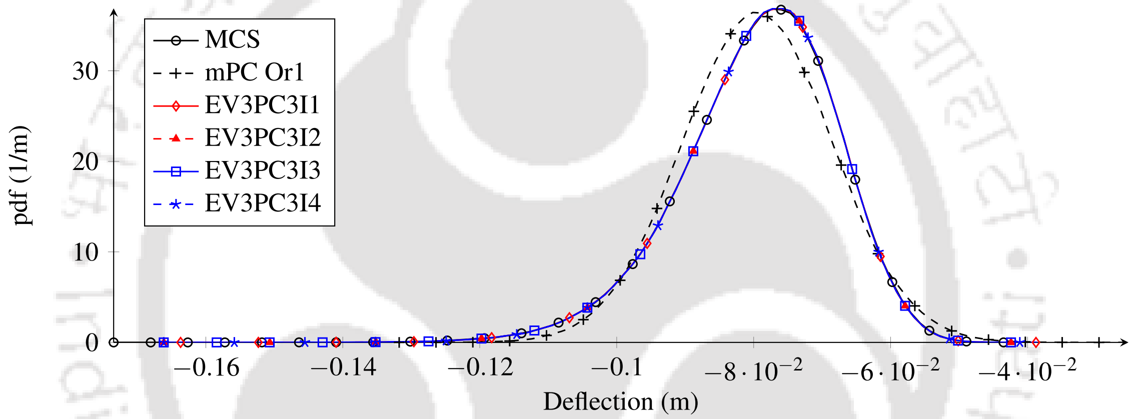

Fig. 3.4: pdfs of vertical displacement at node 4 of truss (Fig.3.1) solved using iterative PC with different orders and iterations and comparison with MCS and mPC1.

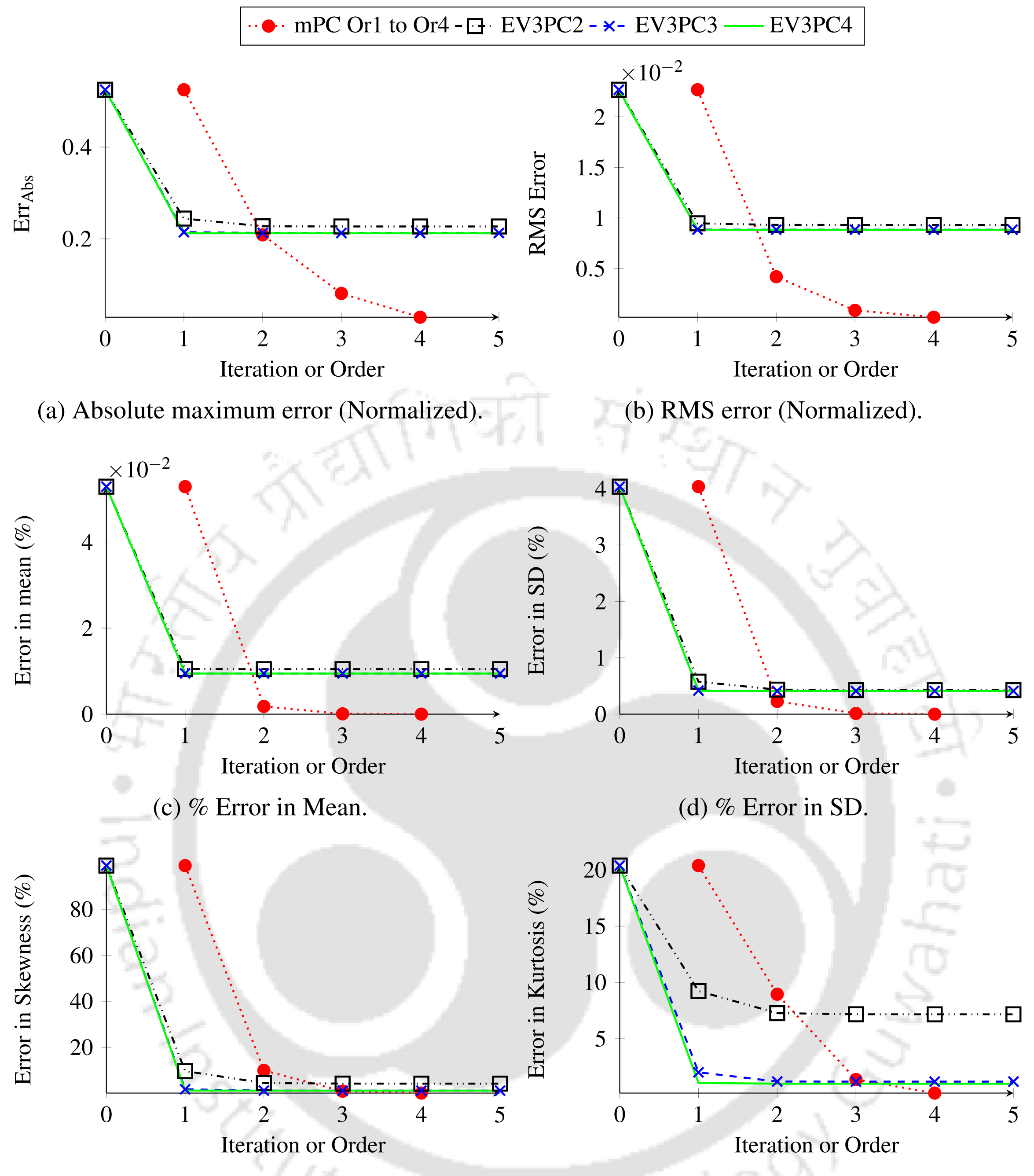

(a) Absolute maximum error (Normalized). (b) RMS error (Normalized).

(c) % Error in Mean. (d) % Error in SD.

(e) % Error in Skewness. (f) % Error in Kurtosis.

Fig. 3.5: Various error quantities in evaluated vertical deflection at node 4 (Fig. 3.1) using Proposed iterative method for different orders of PC with three random variables in the iteration process.

3.5.1.2 Reliability of response

The serviceability of the truss structure with respect to some allowable maximum deflection ($v_{max}^{(4)}$) at midpoint of the bottom cord is studied. The limit state function associated with vertical displacement of node four is,

$$g(x) = v_{\max}^{(4)} - |v^{(4)}| \leq 0 \tag{3.30}$$

The probability of failure P_f^{MCS} evaluated from MCS responses of 5×10^5 samples is considered as reference result. The associated generalized reliability index is given as $\beta^{\text{MCS}} = -\Phi^{-1}(P_f^{\text{MCS}})$. The reliability indices for different methods of analysis are shown in Table 3.5 for different values of threshold $v_{\max}^{(4)}$. It is observed that the error in reliability index evaluated based on the proposed ImPC method is very less and are well within the acceptable limit, though marginally higher than those based on mPC. It may be noted that the error in the evaluated reliability indices using 3rd order mPC are very small for all the considered threshold values of vertical deflection (Table 3.5). Thus, the modified PC is highly reliable, though the computational complexity is higher compared to the proposed ImPC.

Table 3.5: Reliability index of truss problem due to random material and loading and % error compared to MCS.

$v_{\max}^{(4)}$	MCS	mPC3		EV3PC3I3	
(cm)	β^{MCS}	β^{PC}	% Error	β^{PM}	% Error
10	1.66	1.65	-0.6	1.66	0
11	2.26	2.26	0	2.27	0.44
12	2.78	2.79	0.36	2.81	1.08
14	3.63	3.68	1.38	3.71	2.2
16	4.61	4.61	0	4.61	0

3.5.1.3 Computational aspect

It is observed that the responses of the proposed iterative scheme for 3$^{\text{rd}}$ order of PC and iteration with three random variable are comparable with responses of mPC of 3$^{\text{rd}}$ order. However, the polynomial sizes are different. The total number of terms in mPC for three and ten random variables are shown in Table 2.2. Thus, the computational complexities of matrix inversion for MCS, 3$^{\text{rd}}$ order mPC and proposed iterative method (ImPC) of 3$^{\text{rd}}$ order with three random variables and three iterations are $5 \times 10^5 \times 23^3 : (286 \times 23)^3 : (11 \times 23)^3 + 3(20 \times 23)^3 = 19.74 : 923.5 : 1$.

3.5.2 Beam problem : 3-D Euler-Bernoulli beam with 1-D random field for Young's modulus

The second example considered is a cantilever beam as shown in Fig. 3.6. The Young's modulus (E) is considered as one dimensional spatially varying Gaussian random field of the form

$$E(x,\theta) = E_0[1+\alpha(x,\theta)] \tag{3.31}$$

where E_0 is the mean of the random field and $\alpha(x,\theta)$ is a homogeneous zero mean Gaussian random field with an exponential covariance function

$$\boldsymbol{C}(x_1,x_2) = \sigma^2 \exp\left(\frac{-|x_1-x_2|}{L_c}\right) \tag{3.32}$$

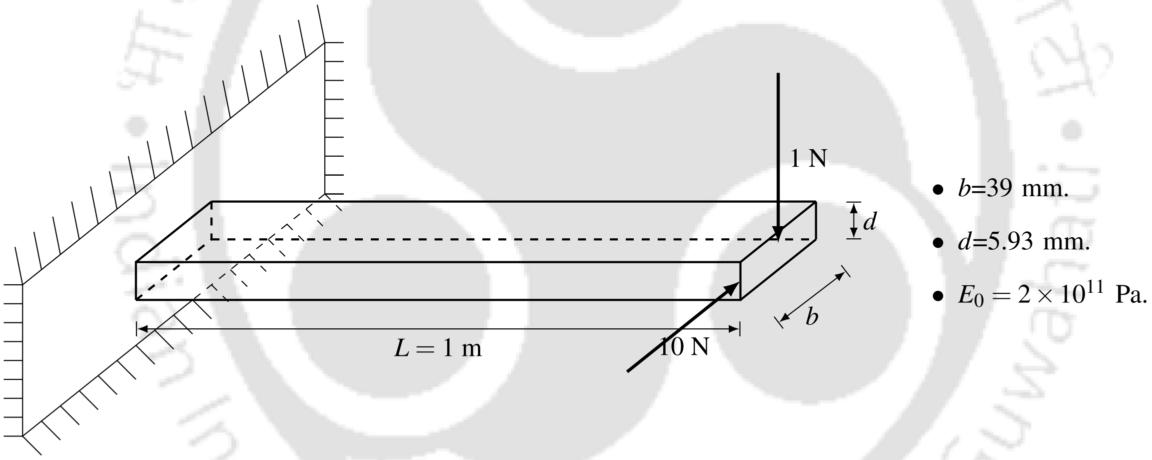

Fig. 3.6: Cantilever beam with point loads at free end.

where σ is the SD of the random field, L_c is correlation length. x_1, x_2 are the coordinates within the limit $[-a,a]$, known as length of the process. In the present study, the length of the process is $L/2$ for exponential covariance function, while the correlation lengths are considered as $L/2$.

3.5.2.1 Requirement of discretization of random field

The input random field is discretized using KL expansion. Fig. 3.7 shows a typical finite element model of a discretized beam showing mid points and Gauss points. The sixth eigenvector of the covariance function considering mid point and Gauss point representation with number of elements as 10, 20 and 30 are shown in Fig 3.8. It can be observed that the Gauss point representation is better than the mid point representation of the random field. The decay of eigenvalues and cumulative % expected energy associated with different modes are shown in Figs. 3.9.a and 3.9.b respectively. The total expected energy is calculated by summing up the eigenvalues upto first 30 numbers. It is observed that the most of the expected energy is associated with first few modes. In the present numerical analysis, first six eigenvectors are considered.

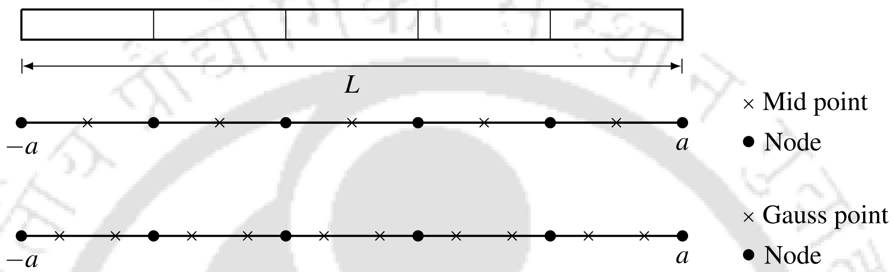

Fig. 3.7: Finite element model of beam showing mid points and Gauss points.

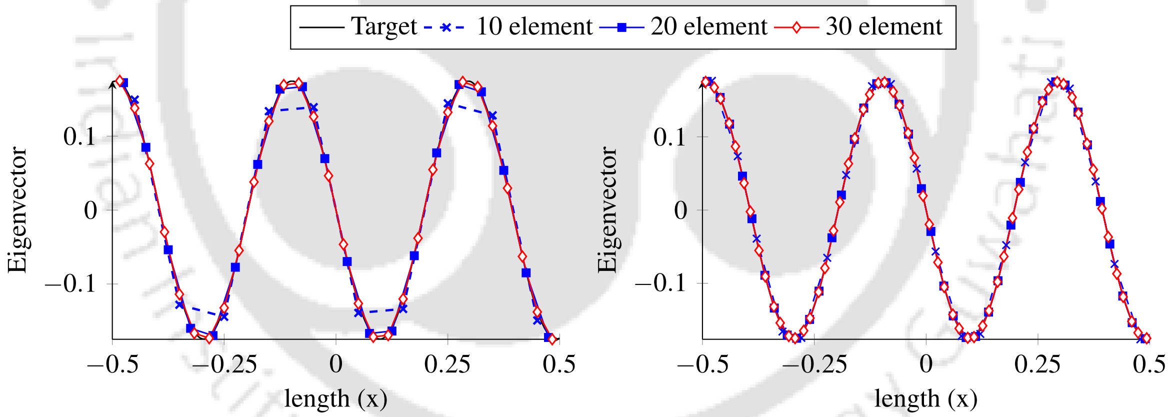

(a) Mid point (b) Gauss Point

Fig. 3.8: Sixth eigenvector of exponential covariance function with Mid point and Gauss point representation for different number of elements.

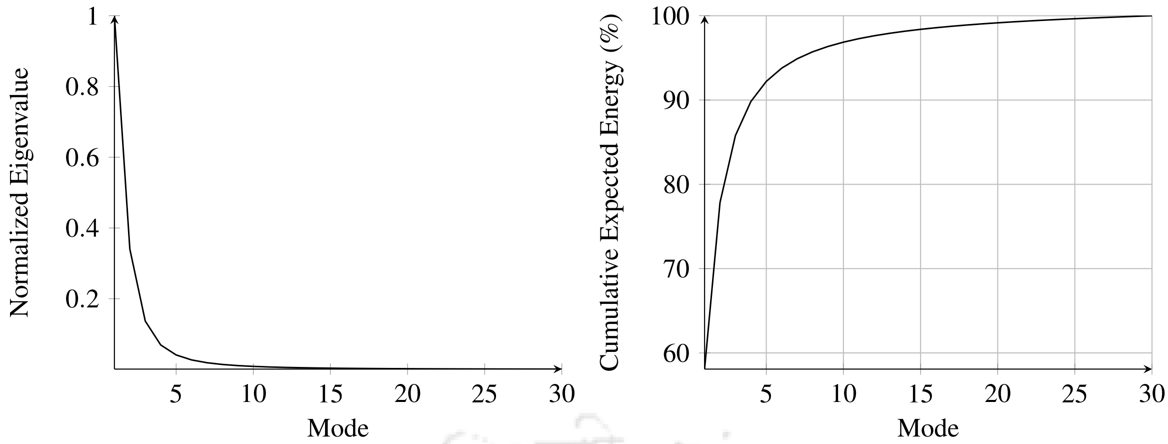

(a) Decay of eigenvalues. (b) Cumulative expected energy *vs* modes.

Fig. 3.9: Relative properties of the eigenvalues of the covariance function.

3.5.2.2 Responses for beam problem

The cantilever beam is divided into 30 elements of equal sizes and modelled using 2 noded 3-D Euler Bernoulli beam elements. Boundary conditions are applied by restraining both rotational and translational degrees of freedom at one of its ends. A transverse vertical load of 1 N and a horizontal load of 10 N are applied at the free end. The problem is first analysed deterministically with 10, 20, 30 and 40 elements and 30 elements are chosen to satisfy both the requirement of appropriate representation of covariance as well as FE analysis. The problem is analysed for different values of SD, $\sigma = \{0.05\ \ 0.10\ \ 0.15\ \ 0.20\}$ of the input random field. The statistical parameters of deflection at the free end are shown in Table 3.6. The value of the tip deflection considering deterministic mean value of Young's modulus $(PL^3 = 3E_0I)$ is 2.4592 mm and from deterministic FEM is 2.4592 mm. It can be observed that responses tend to become non-Gaussian with the increase in SD of Young's modulus. The mean deflection is observed to increase with the increase in SD, though the mean values of Young's modulus are same for all SDs. The mean, SD, skewness and kurtosis of deflection at free end are observed to increase as SD of the random field increases.

Table 3.6: Statistical parameter of deflection at the free end of cantilever beam for different values of SD of input random field E.

SD of Random Field (E)	Mean (m) $\times 10^{-3}$	SD (m) $\times 10^{-3}$	Skewness	Kurtosis
0.05	-2.465	0.103	-0.280	3.158
0.10	-2.483	0.212	-0.566	3.666
0.15	-2.514	0.335	-0.934	4.910
0.20	-2.564	0.490	-1.622	10.037

The problem is first analysed using mPC of different orders generated using Gram-Schmidt process as discussed in section 3.4.3 with six random variables from KL expansion. The stiffness matrix size is further reduced using eigenvalue decomposition as discussed in section 3.4.5 (Pascual and Adhikari, 2012). The ratio $\lambda_{0_1}/\lambda_{0_S}$ is considered to be less than 10^{-3}, which yields the value of S as 18. Thus the 120×120 matrix is reduced to 18×18 matrix. The pdfs of vertical deflection at the free end for different orders of mPC are shown in Fig. 3.10. Different order mPC expansions are designated as KL6mPC1, KL6mPC2 and so on for first order and second order mPC respectively. The corresponding responses from mPC with reduced stiffness matrix are termed as RKL6mPC1, RKL6mPC2 respectively. It can be observed that the pdf of first order mPC does not match with pdf of MCS, which however converges to MCS as order increases. It is also observed that for higher SD, a higher order PC expansion is required. Similar trends are observed for PC with reduced stiffness matrix.

Various errors calculated with respect to MCS are plotted in Fig. 3.11. It is observed that as the order of mPC expansion increases, the error reduces. The error is more in case of higher SD for same order of expansion, meaning that for same level of accuracy it is required to have a higher order of expansion for higher values of SD. Errors in case of mPC with reduced stiffness matrix are same as those of full stiffness except error in mean, where it is marginally higher. Thus, the errors in general are observed to reduce with the increase in the order of expansion. However, the size of system matrix also increases and the polynomial sizes for different order and number of random variables as discussed in section 3.3 may be seen in Table 2.2.

To overcome the difficulty of such increase in dimension of system matrix, the problem is solved using the proposed iterative scheme, where it is first solved using first order mPC and subsequently, the responses are used to generate an iterative PC. After the initial solution using first order mPC, the dominant modes of the responses are calculated using KL expansion. It is observed that most of the expected energy of the response covariance function is attained within the first two modes (>99%). Thus, two random variables calculated from the response are considered in the iteration process. It reduces the number of random variables to be considered in PC expansion from six to two. The new random variables are non-Gaussian in nature as SD of the random field increases. It rather makes the new PC a function of non-Gaussian random variables for a non-Gaussian response. The iteration processes of 2^{nd} order with 2 random variables for 1^{st} and 2^{nd} iterations are designated as ”KL6EV2PC2I1”, ”KL6EV2PC2I2” respectively. Similarly for 3^{rd} order, it is designated as ”KL6EV2PC3I1”, ”KL6EV2PC3I2”. The same for reduced stiffness is designated as ”RKL6EV2PC3I1”, ”RKL6EV2PC3I2” respectively.

The pdfs for vertical deflection at the free end of the cantilever beam for SD=0.05 is shown in Fig. 3.12. Various error quantities in the evaluated vertical deflection of the free end using the proposed method for SD=0.05 are shown in Fig. 3.13. Similarly, the pdfs and error measures for SD=0.2 are shown shown in Figs. 3.14 and 3.15 respectively. It is observed that the pdf of first order PC (KL6mPC1) does not match with MCS even for low SD, however as the iteration process continues with the proposed iterative method, the pdf converges towards MCS. The error in the responses are observed to reduce as the orders and iterations are increased. However, it is also observed that for a higher value of SD of Young’s modulus, a higher order of updated PC is required. For the present example, low value of SD ($\sigma = 0.05$), third order mPC and third order ImPC give comparable response. However, the size of third order mPC is 84 whereas third order PC with proposed ImPC scheme is only 10. Thus, size of matrix is considerably reduced. For high value of SD ($\sigma = 0.2$), fourth order mPC responses are comparable with third order ImPC, where the expansion sizes are 210 and 15 respectively. The error in mean is however very small and the observed changes with increase in order of mPC and iterations in the proposed scheme are found to be insignificant. The differences in error between PC based method with reduced stiffness matrix and full stiffness matrix are marginal and thus PC with reduced stiffness matrix is recommended to be used to further reduce the size of the final system matrix.

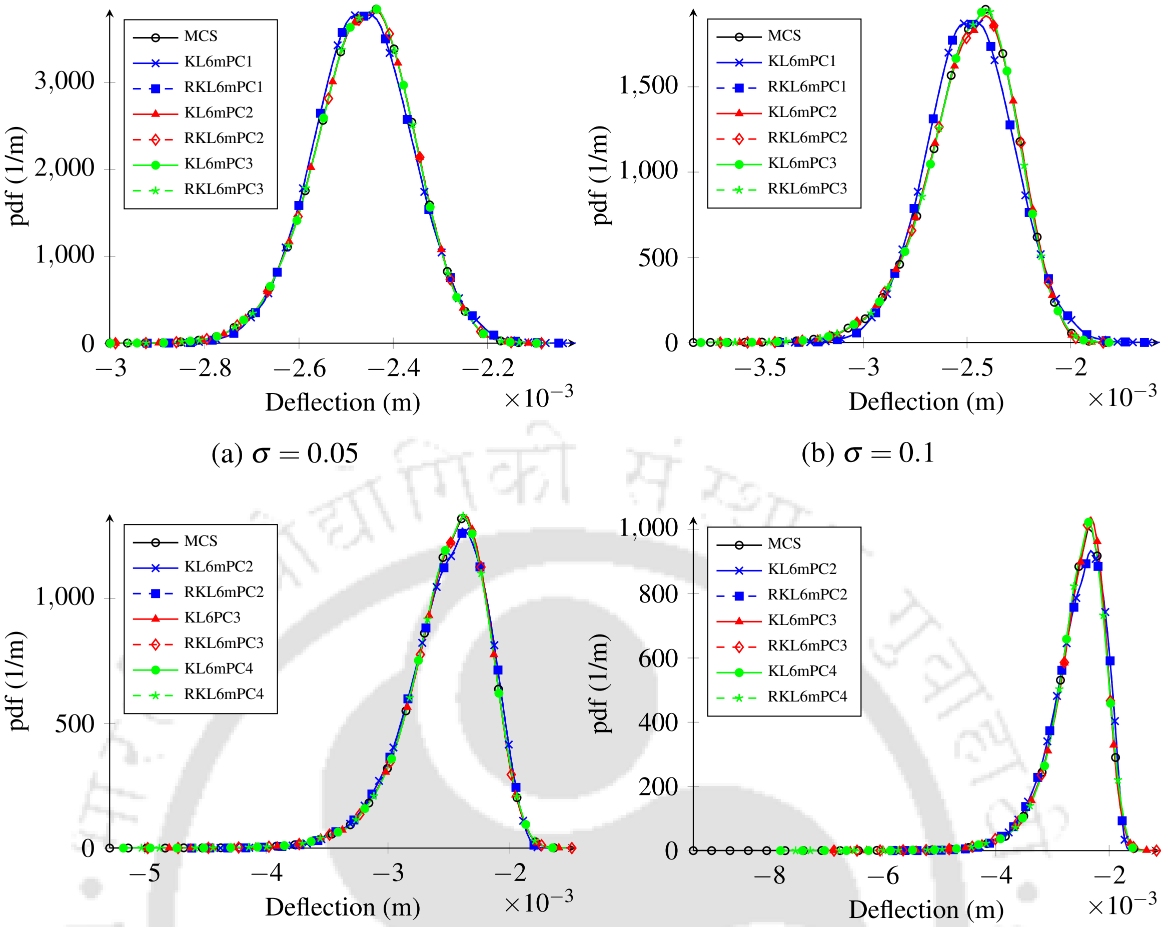

(a) $\sigma = 0.05$ (b) $\sigma = 0.1$

(c) $\sigma = 0.15$ (d) $\sigma = 0.2$

Fig. 3.10: pdfs of tip deflection of cantilever beam for different orders of PC expansion compared with MCS ($\sigma = \{0.05\ \ 0.1\ \ 0.15\ \ 0.2\}$).

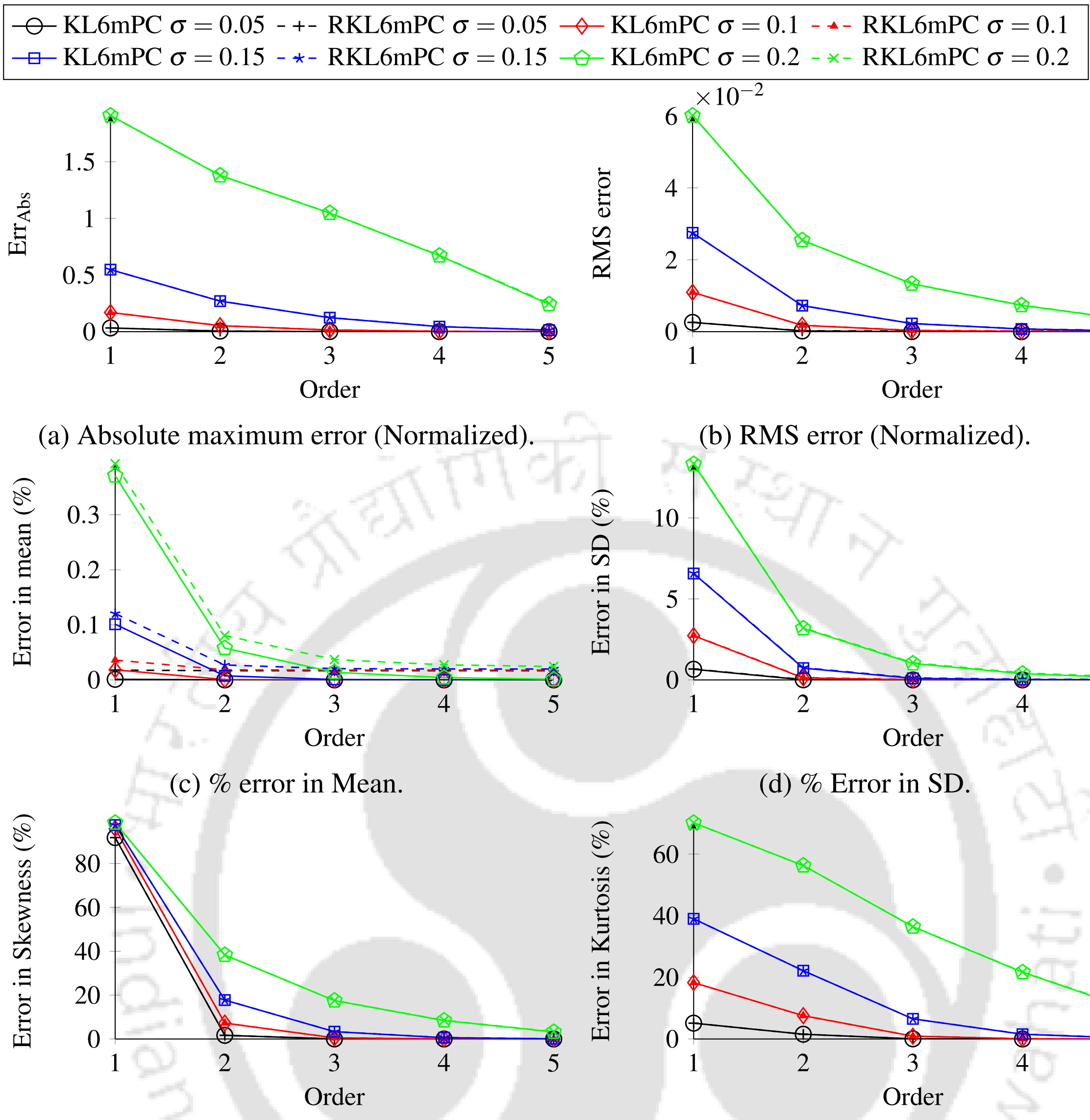

(a) Absolute maximum error (Normalized).

(b) RMS error (Normalized).

(c) % error in Mean.

(d) % Error in SD.

(e) % Error in Skewness.

(f) % Error in Skewness.

Fig. 3.11: Various error quantities in evaluated tip deflection of cantilever beam using PC based method and PC based method with reduces stiffness matrix for different orders of PC.

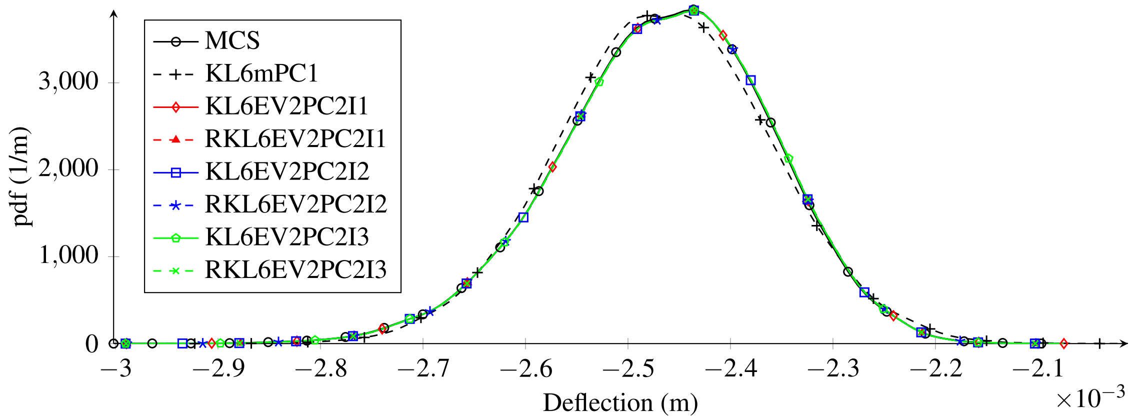

(a) Second order.

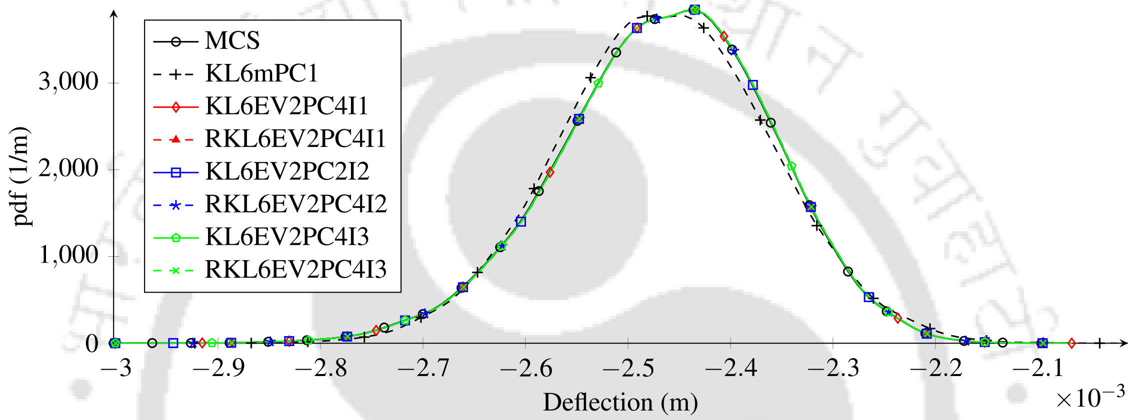

(b) Fourth order.

Fig. 3.12: pdfs of tip deflection of the cantilever beam solve using propose method with different orders and iterations compare with MCS and KL6PC1 ($\sigma = 0.05$).

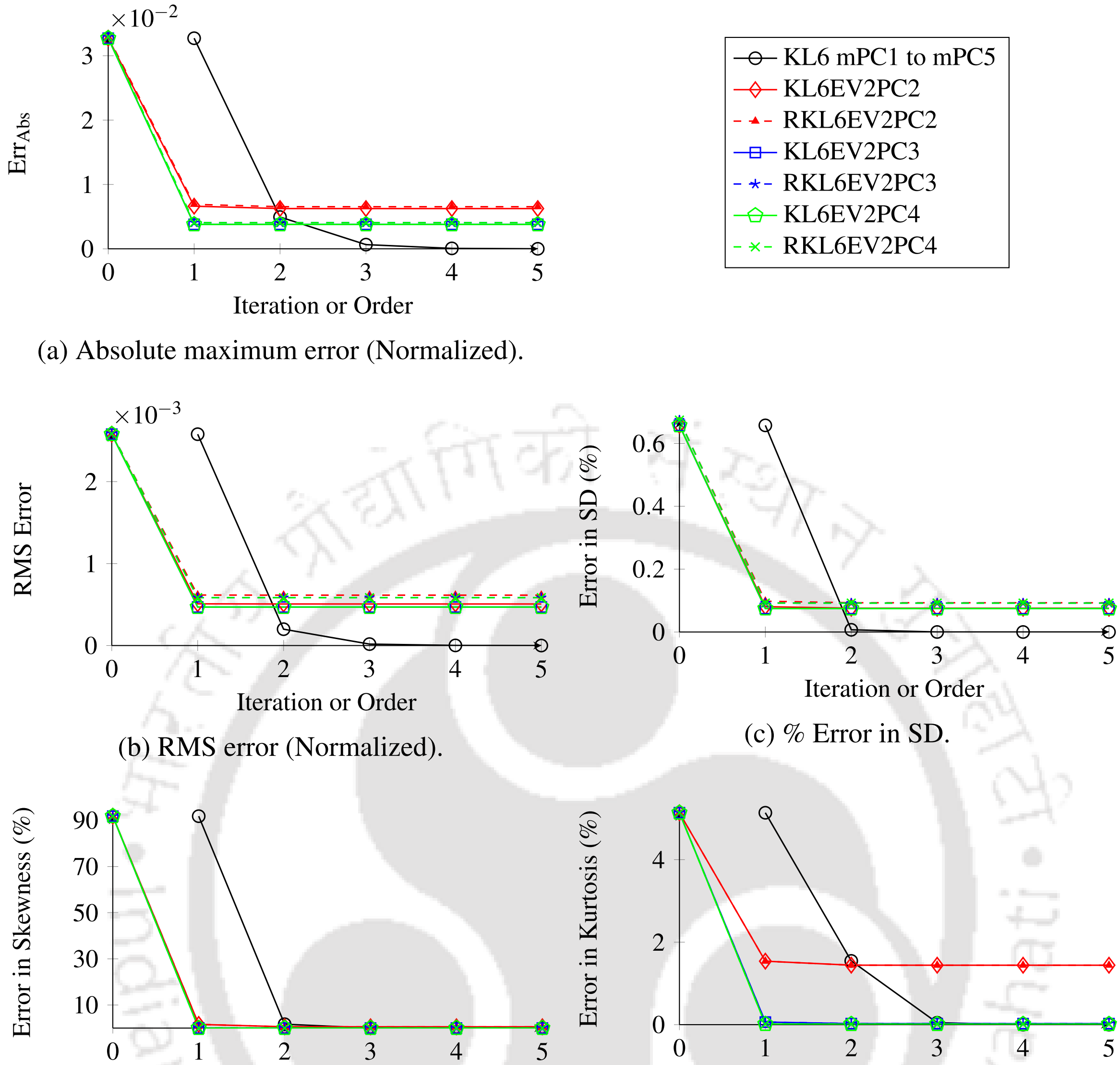

(a) Absolute maximum error (Normalized).

(b) RMS error (Normalized).

(c) % Error in SD.

(d) % Error in Skewness.

(e) % Error in Kurtosis.

Fig. 3.13: Various error quantities in evaluated tip deflection of cantilever using Proposed iterative method and Proposed iterative method with reduces stiffness matrix for different orders of PC with two random variables in the iteration process ($\sigma = 0.05$).

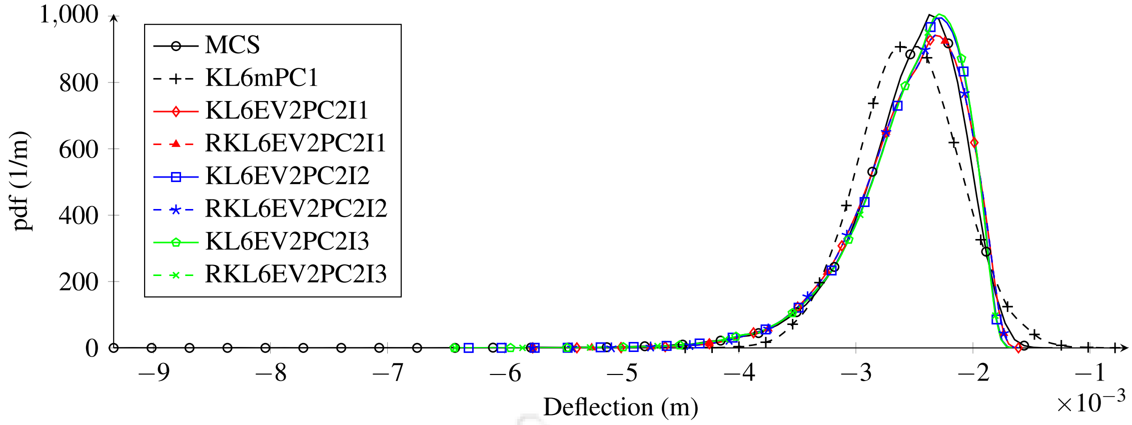

(a) Second order.

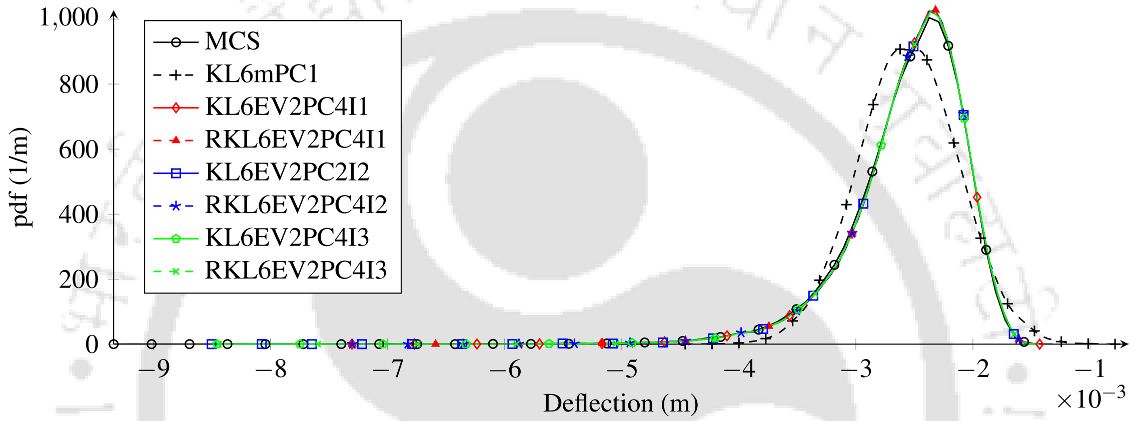

(b) Fourth order.

Fig. 3.14: pdfs of tip deflection of the cantilever beam solve using propose method with different orders and iteration compare with MCS and KL6PC1 ($\sigma = 0.2$).

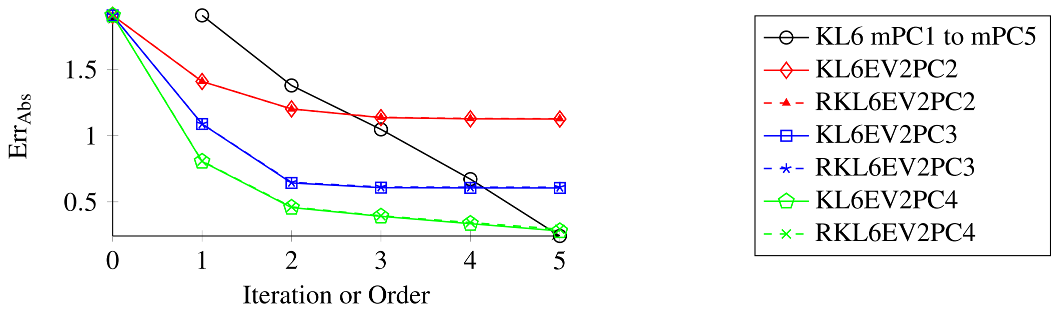

(a) Absolute maximum error (Normalized).

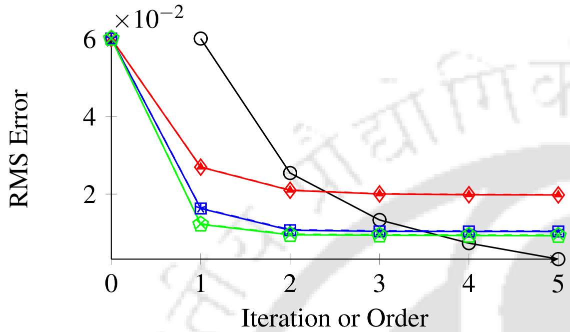

(b) RMS error (Normalized).

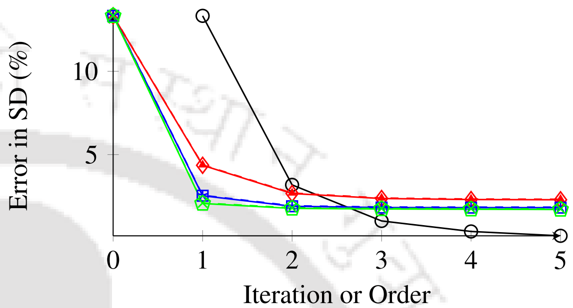

(c) % Error in SD.

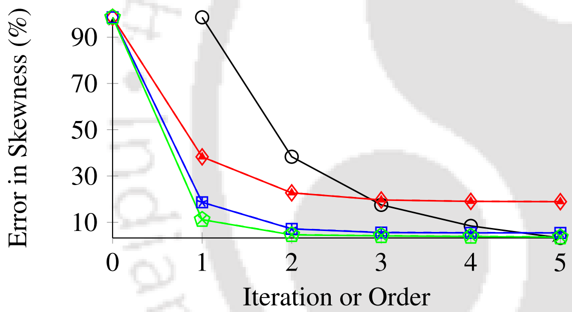

(d) % Error in Skewness.

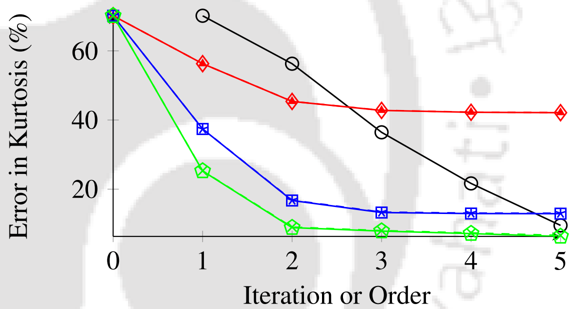

(e) % Error in Kurtosis.

Fig. 3.15: Various error quantities in evaluated tip deflection of cantilever using Proposed iterative method and Proposed iterative method with reduces stiffness matrix for different orders of PC with two random variables in the iteration process ($\sigma = 0.2$).

3.5.2.3 Computational aspect

It is observed that the responses of the proposed scheme for an order of PC and iteration are comparable with responses of mPC of some higher order. The matrix size in the proposed approach is thus smaller than conventional PC, which will enable to perform analysis with lesser computational resources. However, for attaining accuracy in the proposed method, it is required to carry out analysis in iterative manner. In case of MCS, the computational cost for inversion is 3×10^4 times N^3. The results of fourth order mPC and third order

ImPC are comparable and computational complexity is also compared. In case of mPC based method computational complexity is $[N \times (P+1)]^3 = (N \times 210)^3$, on the other hand the computational complexity of the proposed method is the cumulative contribution from PC solution of first order and third order proposed method with number of iterations. If 3 iterations are considered, the total complexity is $(N \times 7)^3 + 3(N \times 15)^3$. In case of reduced stiffness method the computational complexity can be calculated by replacing N with S. For the present beam problem $N = 120$ and $S = 18$ and the ratio of computation complexities for matrix inversion for MCS, fourth order mPC and third order ImPC with 3 iterations and ImPC of same order with reduced stiffness matrix are $849.15 : 2.62 \times 10^5 : 296.3 : 1$. In case of mPC based and proposed ImPC method additional time is required for calculation of ensembles of responses, which however is marginal. Further, additional time is required in the proposed method for solution of eigenvalue problem required to calculate the random variables to be used in each iteration.

3.5.3 Foundation on a random soil layer : A plane stress problem

The third example considered is a problem on settlement of foundation resting on a random heterogeneous soil media as shown in Fig. 3.16. The problem was solved by Sachdeva et al. (2006) and Sudret and Kiureghian (2002) for random soil media considering randomness of soil in vertical direction. The present problem also considers Young's modulus as 1-D spatially varying random field expressed as

$$E(y,\theta) = E_0[1+\alpha(y,\theta)] \tag{3.33}$$

where E_0 $(= 50 \times 10^6$ Pa) is the mean of the random field and $\alpha(y,\theta)$ is a homogeneous zero mean Gaussian random field with an exponential covariance function

$$\boldsymbol{C}(y_1,y_2) = \sigma^2 \exp\left(\frac{-|y_1-y_2|}{L_c}\right) \tag{3.34}$$

σ is the SD of the random field, and L_c is correlation length. The value of length of the process is $t_h/2$ and the correlation length is considered as $t_h/2$.

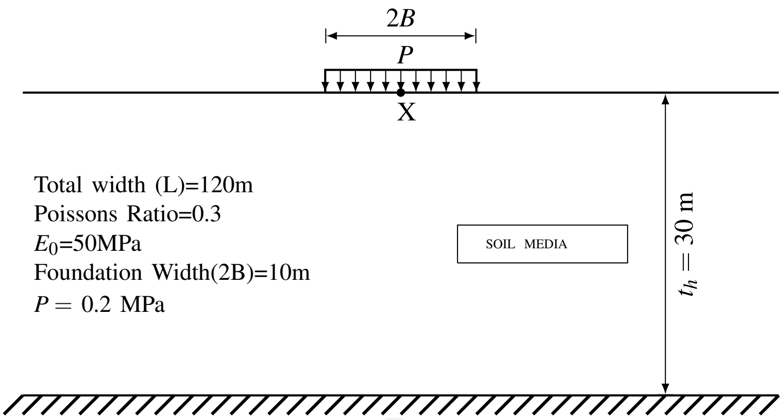

Fig. 3.16: Foundation resting on soil strata.

3.5.3.1 Requirement of discretization

The problem is idealized as plane stress problem and modelled using 4 noded isoparametric elements. Since the material, loading and boundary conditions are symmetric in horizontal direction about the vertical central line, the problem is analysed for only symmetric half of the domain. Boundary conditions are imposed by restraining both the degrees of freedom along the bottom fixed end and horizontal degrees of freedom along the vertical symmetric line. In order to obtain an acceptable mesh size for stochastic analysis, the problem is first solved deterministically considering mean Young's modulus of the soil with fine mesh of 0.5 m×0.5 m and 1 m×1 m. The deflection at mid point of foundation (point X in Fig. 3.16) is found to be 5.9474 cm and 5.9435 cm respectively. However, these two mesh sizes require large computational time and hence an optimum mesh size is needed. From the consideration of stress gradient, a finer mesh is desirable below the loading and relatively coarser mesh can be considered away from the loaded point. Further, from stochastic analysis consideration, it is observed from the earlier considered beam analysis that a minimum number of 30 elements is required for proper representation of eigenvectors when Gauss point based discretization is considered. Thus, the maximum size of an element for a uniformly discretized domain in vertical direction may be 30/30=1 m, while in horizontal direction it can be considered from FE analysis consideration. Considering these, an optimal mesh size is obtained as shown in Fig.3.17 along with the deflected shape as indicated by dotted lines. The maximum deflection at point X (Fig. 3.16) is found to be 5.9437 cm, which is only 0.06% lesser than the value obtained earlier with very fine mesh throughout. The maximum aspect ratio is kept as 5, considering the sensitivity of isoparametric elements. Similar to the beam problem, the random field is discretized using KL expansion and six eigenvectors are considered in the analysis.

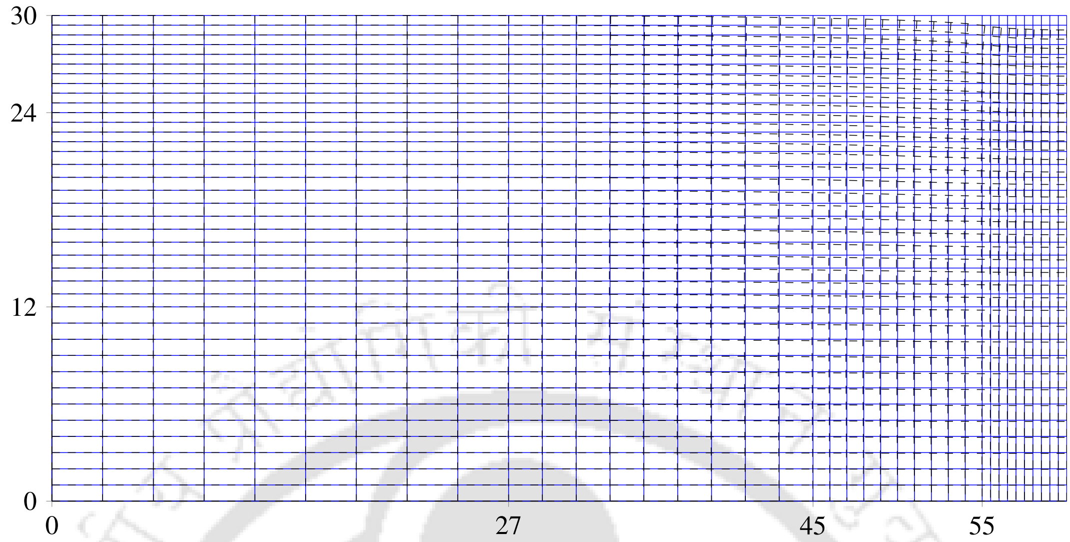

Fig. 3.17: Deflected shape of the soil domain below foundation (Not to scale. Only symmetric left half is shown. Dotted lines are typical deflected shape).

3.5.3.2 Settlement of foundation

Similar to the beam problem, the settlement of foundation (Fig. 3.16) is also analysed using mPC of different orders and the proposed method for SD of random field $\sigma = \{0.1 \;\; 0.2\}$ and results are compared with the results of MCS. Using the proposed scheme, the plane stress problem is initially solved using first order mPC expansion and subsequently responses are used to generate an iterative PC. It is observed that the cumulative expected energy of the response covariance function considering first three modes is more than 99%. Thus, using first order mPC response, three random variables are considered for the iteration process. As the number of DOFs are very high and higher order mPC expansion is required for improving accuracy, the problem is solved using reduced stiffness matrix. The ratio, $\lambda_{0_1}/\lambda_{0_S}$ is considered to be less than 10^{-3} for reduction of size of stiffness matrix, which yields the value of S as 1089. Thus, 2926×2926 matrix size reduces to 1089×1089. The pdfs of the vertical deflection of the mid point of foundation (point X in Figs. 3.16) for SD equal to 0.1 and 0.2 are shown in Fig. 3.18 and 3.19 respectively. It is observed that the pdf of first order PC based method (KL6mPC1) does not match with MCS results. It is further observed that the pdf of vertical deflection at point X converges towards MCS as the order or/and iteration increases, while evaluating using the proposed ImPC. Various errors associated with the response for SD equal to 0.1 and 0.2, are shown in Figs. 3.20 and 3.21 respectively. For comparison with mPC based method, the errors associated with different orders of mPC with reduced stiffness are also plotted along y axis *vs* number of orders along x axis. It can be observed that the error in 3rd order mPC is comparable to 3rd order proposed ImPC with 2 iterations. However, the number of random variables in case of PC is six, while it is only three in case of the proposed scheme.

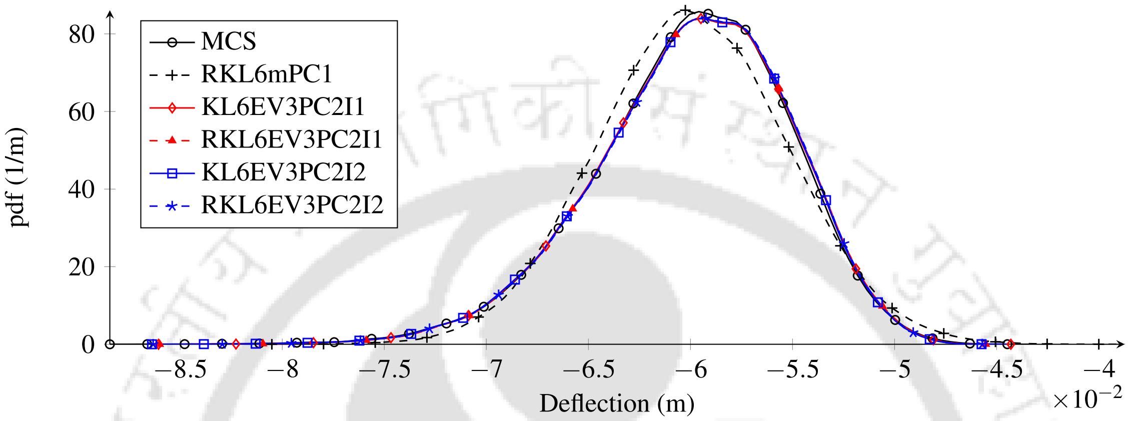

(a) Second order.

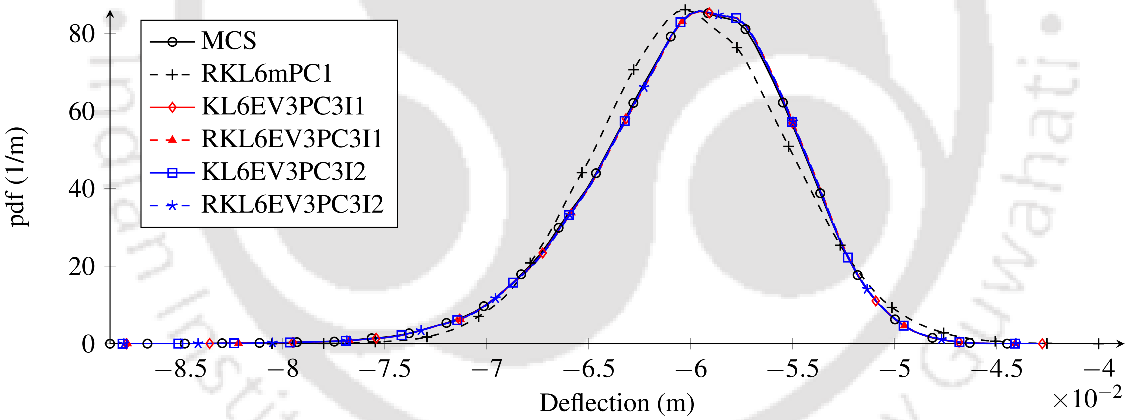

(b) Third order

Fig. 3.18: pdfs of vertical displacement at mid point of foundation solve using proposed method with different orders and iteration compare with MCS and KL6mPC1 ($\sigma = 0.1$).

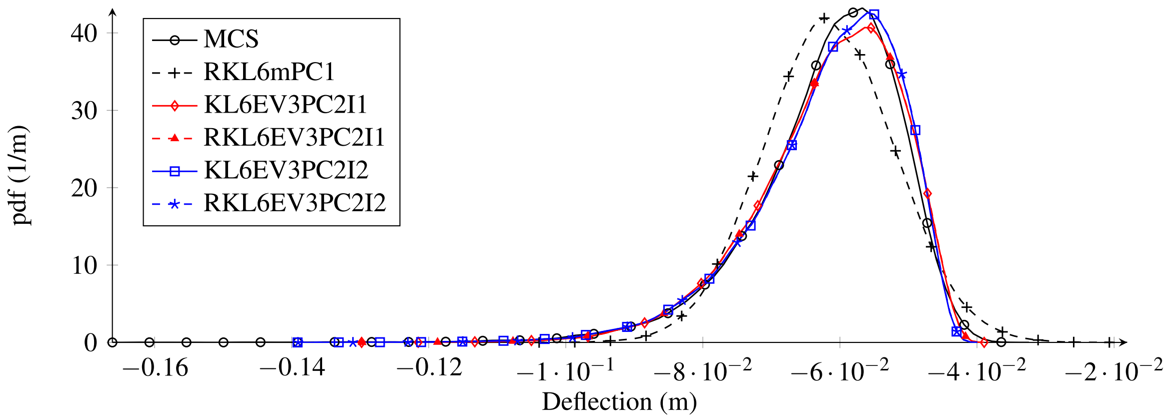

(a) Second order.

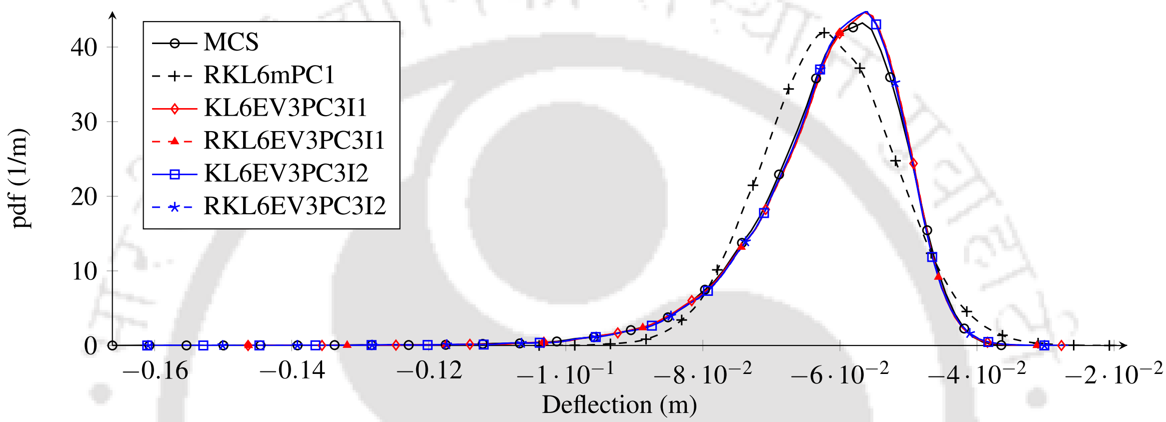

(b) Third order

Fig. 3.19: pdfs of vertical displacement at mid point of foundation solve using proposed method with different orders and iteration compare with MCS and KL6mPC1 ($\sigma = 0.2$).

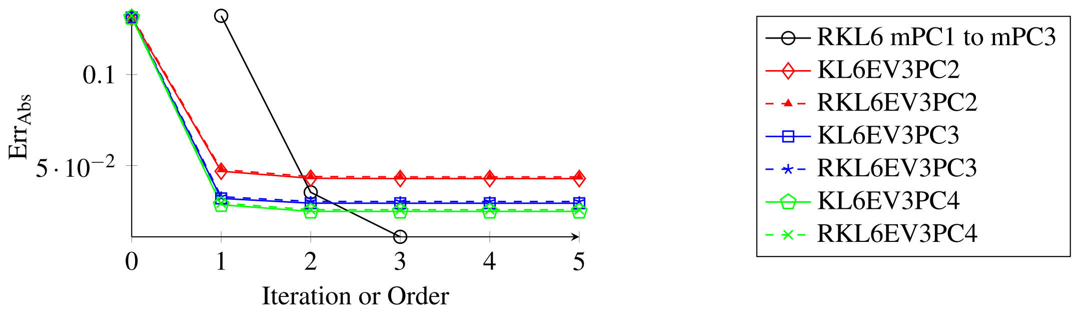

(a) Absolute maximum error (Normalized).

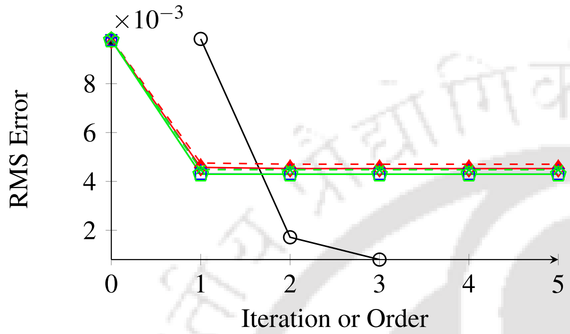

(b) RMS error (Normalized).

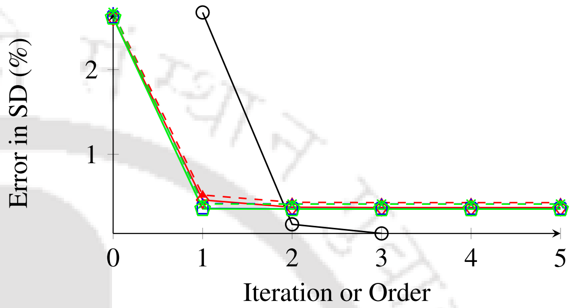

(c) % Error in SD.

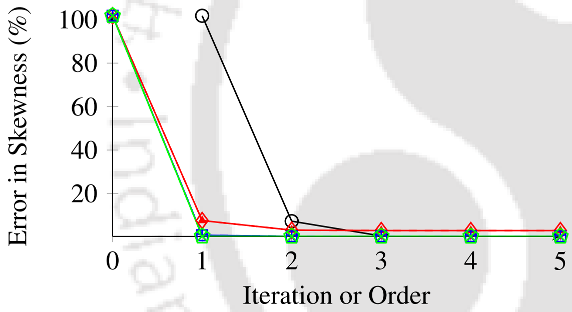

(d) % Error in Skewness.

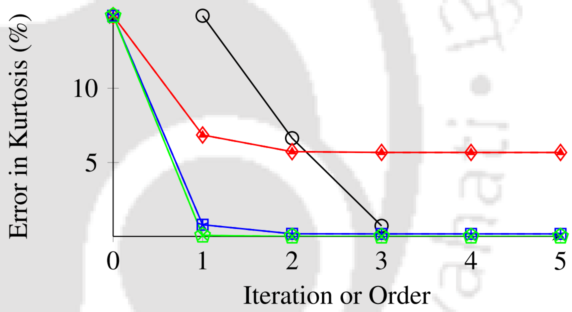

(e) % Error in Kurtosis.

Fig. 3.20: Various error quantities in evaluated vertical deflection at mid point of foundation (point X) using Proposed iterative method and Proposed iterative method with reduced stiffness matrix for different orders of PC with three random variables in the iteration process ($\sigma = 0.1$).

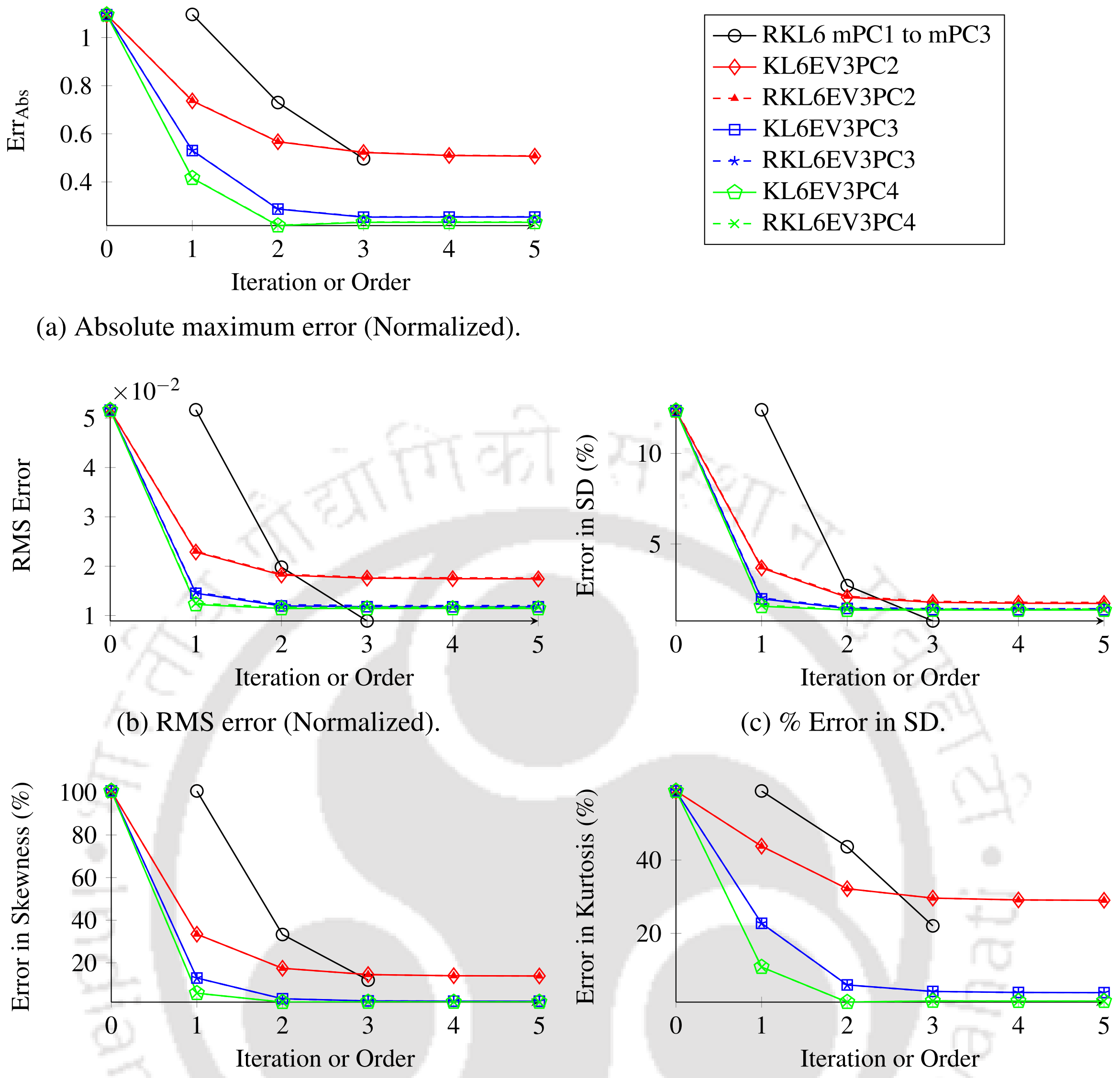

(a) Absolute maximum error (Normalized).

(b) RMS error (Normalized).

(c) % Error in SD.

(d) % Error in Skewness.

(e) % Error in Kurtosis.

Fig. 3.21: Various error quantities in evaluated vertical deflection at mid point of foundation (point X) using Proposed iterative method and Proposed iterative method with reduced stiffness matrix for different orders of PC with three random variables in the iteration process ($\sigma = 0.2$).

3.5.3.3 Computational aspect

The size of the matrix is significantly large even with adopted reduced stiffness scheme in case of mPC. The proposed ImPC scheme however employs much smaller sizes of matrices as compared to mPC. Computational complexities for matrix inversion in case of MCS, 3rd order mPC with reduced stiffness, 3rd order ImPC with 3 random variables and 2 iterations and 3rd order ImPC with 3 random variables and 2 iterations with reduced stiffness are $30 \times 10^3 \times 2926^3 : (84 \times 1089)^3 : (7 \times 2926)^3 + 2(20 \times 2926)^3 : (7 \times 1089)^3 + 2(20 \times 1089)^3 = 35.607 : 36.267 : 19.3972 : 1$. Thus, huge computational efficiency can be observed in ImPC, which would be really advantageous for solving any real time problem with large degrees of freedom. Moreover, in the context of the present problem, mPC could be used only for system with reduced stiffness matrix as degree of freedom for the problem with full stiffness matrix is very high and could not be solved due to the constraint in the available computational facility. The solution of 3rd order mPC with full stiffness will exhibit a much higher ratio of computational complexity of matrix inversion when compared with ImPC with similar full system matrix and thus will demand computational facility of even higher specification. Thus, while ImPC could be successfully used to solve the problem with acceptable error limit, the same problem however, could not be solved using mPC. The system matrix sizes in case of 3rd order mPC and 3rd order mPC with reduced stiffness are $(84 \times 2926) \times (84 \times 2926)$ and $(84 \times 1089) \times (84 \times 1089)$ respectively. However, in case of ImPC with full and reduced stiffness matrix, the maximum system matrix sizes are $(20 \times 2926) \times (20 \times 2926)$ and $(20 \times 1089) \times (20 \times 1089)$ respectively. Thus, ImPC demands much lesser RAM, which is evident from the fact that even the mPC with even reduced system could not be executed beyond third order as presented in Fig. 3.20 and 3.21.

3.5.3.4 Convergence study of responses

The convergence and accuracy of the evaluated responses using the proposed ImPC are assessed with respect to MCS as demonstrated in the earlier section. However, in the absence of any such reference results, the responses can be checked for convergence to accurate values by utilizing the responses from successive higher orders and iterations. The rate of convergence of responses is studied by considering two successive iterations for a particular order and calculating their differences in absolute maximum, RMS, and statistical moments. The responses are considered to have converged when the rate is near to zero. The error in different statistical parameters for a particular order of expansion varying with different iterations for SD=$\{0.1, 0.2\}$ are shown in Figs. 3.22 and 3.23 respectively. It can be observed that the rate of convergence is near to zero after 4th iteration for all the three orders considered (2nd, 3rd, 4th). Thus, 4 iterations are sufficient to achieve a converged response in a particular order for the problem considered and can be treated as a stopping criteria. Further, convergence to the accurately estimated responses are assessed by considering converged responses (e.g. corresponding to 4th iteration) of successive orders and calculating the difference in all the earlier adopted statistical parameters between two such responses. Figs. 3.24 and 3.25 show the error between two successive orders upto 4th for SD 0.1 and 0.2 respectively. It can be clearly observed from Figs. 3.22 - 3.25 that as the orders and iterations of ImPC increase, the responses converge and the error associated with the converged response for the expansion with highest number of orders considered is practically zero. Thus the responses corresponding to 4th and 5th order and 4th iteration are very accurate, which is further substantiated from Figs. 3.20 - 3.21, where the evaluated errors with respect to MCS also lead to a similar conclusion.

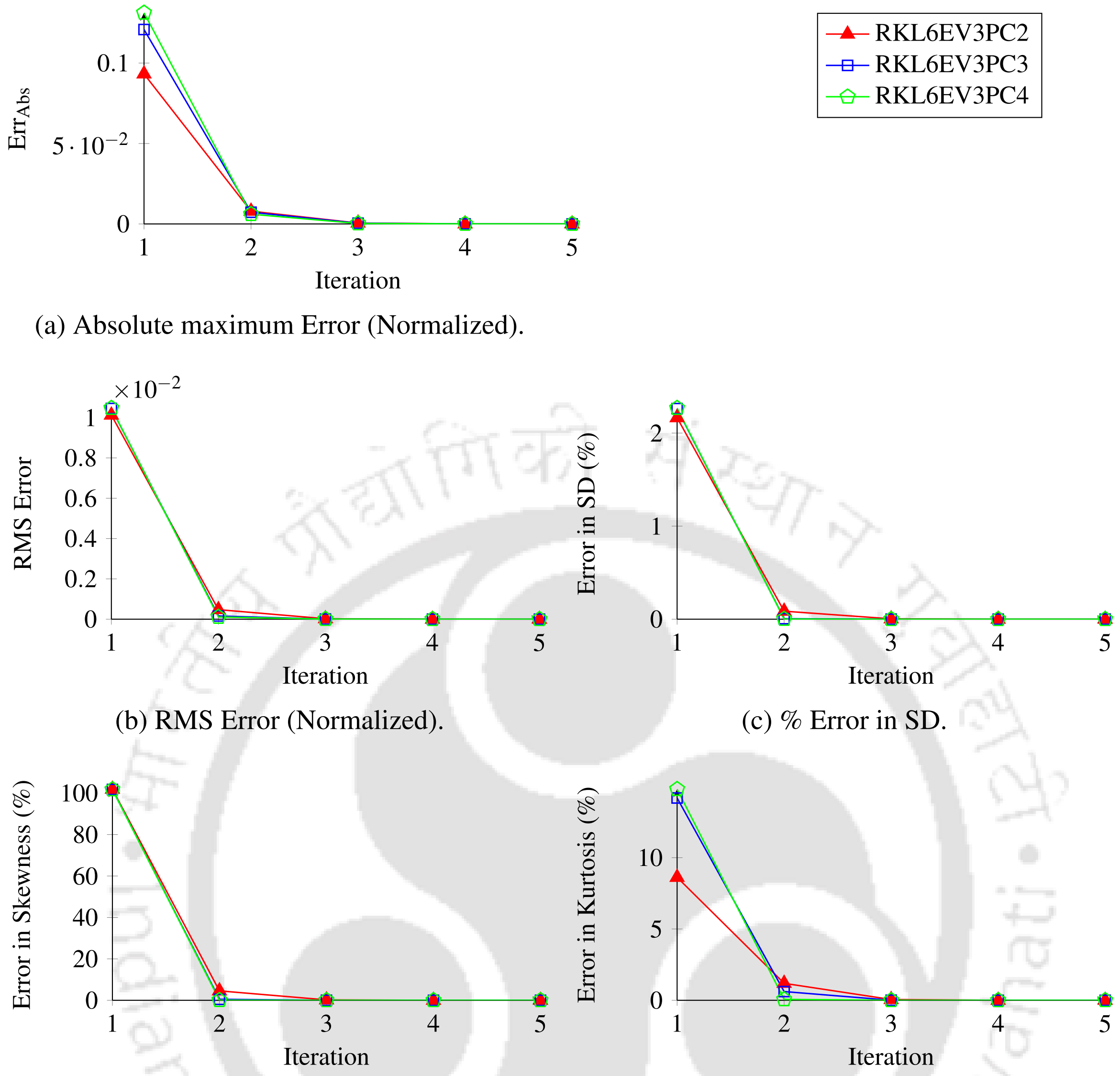

(a) Absolute maximum Error (Normalized).

(b) RMS Error (Normalized).

(c) % Error in SD.

(d) % Error in Skewness.

(e) % Error in Kurtosis.

Fig. 3.22: Convergence of error in vertical deflection at mid point of foundation (point X) in different error measures with iteration for different orders in ImPC ($\sigma = 0.1$).

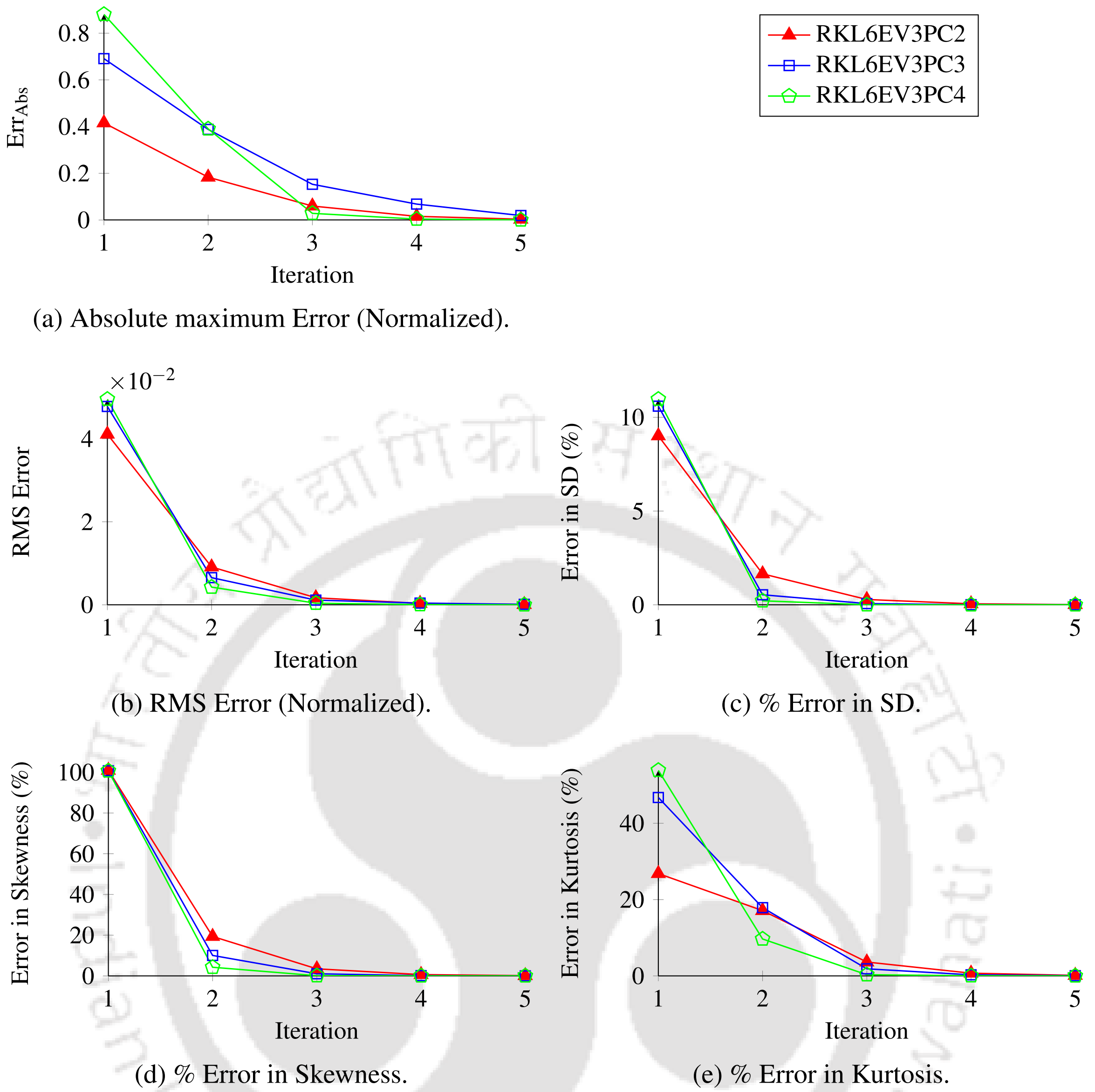

(a) Absolute maximum Error (Normalized).

(b) RMS Error (Normalized).

(c) % Error in SD.

(d) % Error in Skewness.

(e) % Error in Kurtosis.

Fig. 3.23: Convergence of error in vertical deflection at mid point of foundation (point X) in different error measures with iteration for different orders in ImPC ($\sigma = 0.2$).

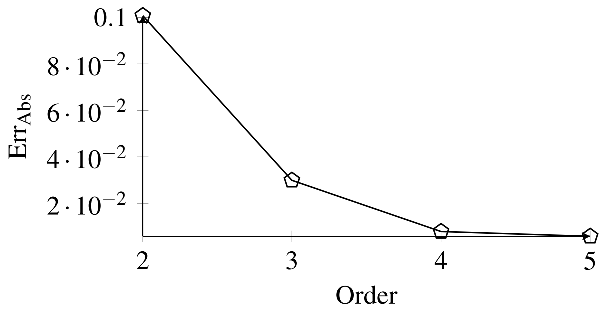

(a) Absolute maximum Error (Normalized).

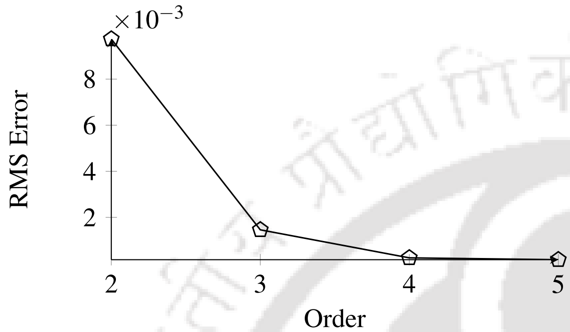

(b) RMS Error (Normalized).

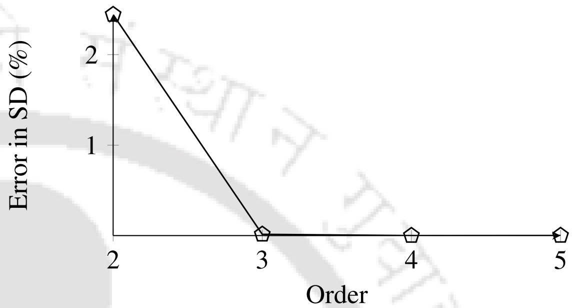

(c) % Error in SD.

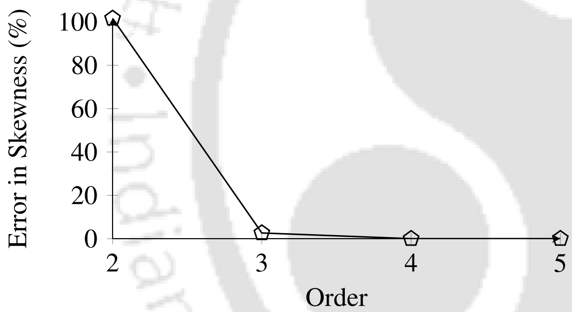

(d) % Error in Skewness.

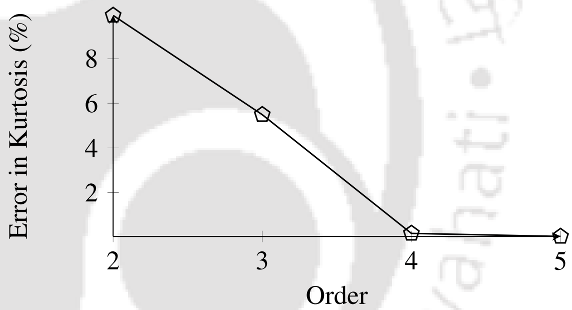

(e) % Error in Kurtosis.

Fig. 3.24: Convergence of error in different error measures for converged solution (corresponding to 4$^{\text{th}}$ iteration) at mid point of foundation (point X) for different orders of ImPC ($\sigma = 0.1$).

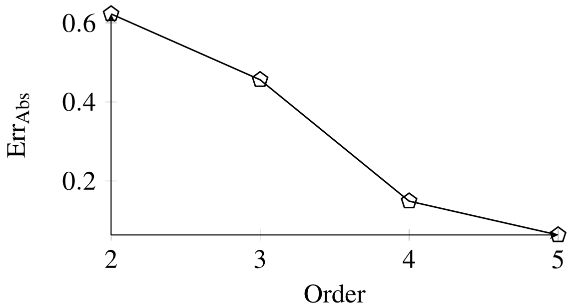

(a) Absolute maximum Error (Normalized).

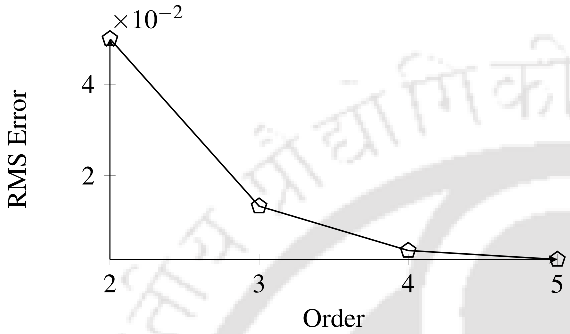

(b) RMS Error (Normalized).

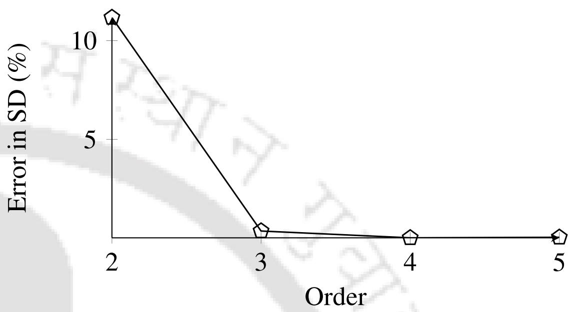

(c) % Error in SD.

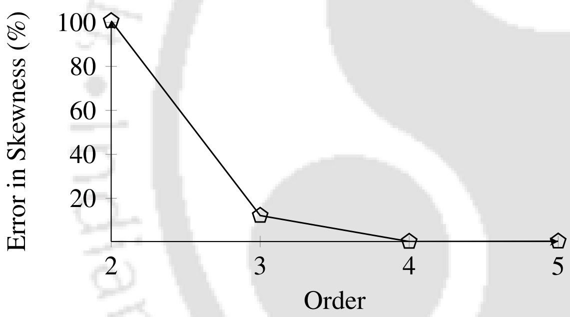

(d) % Error in Skewness.

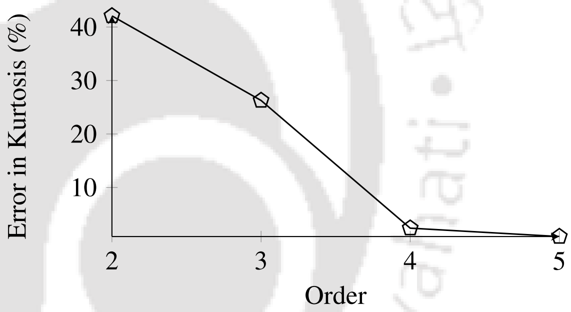

(e) % Error in Kurtosis.

Fig. 3.25: Convergence of error in different error measures for converged solution (corresponding to 4^{th} iteration) at mid point of foundation (point X) for different orders of ImPC ($\sigma = 0.2$).

3.6 Conclusions

A PC framework based numerical strategy to solve linear stochastic mechanics problem with random coefficient is presented, which is observed to be more efficient than conventional PC based method in terms of computational demand and accuracy. A method to construct PC for arbitrary pdf is also presented, which is based on Gram-Schmidt orthogonalization process. The proposed iterative method generates PC, based on responses of previous iteration.

The proposed method addresses the issue of computational demand and accuracy at multiple level. First, it reduces the computational demand as well as increases the accuracy by representing the eigenvector of KL expansion at Gauss points instead of mid points of elements. The numbers of random variables to represent the response in PC expansion are reduced by considering the dominant components of the response using KL expansion after the first order solution using PC expansion. The reduction of size of stiffness matrix by considering eigen decomposition (Pascual and Adhikari, 2012) further reduces the computational requirement without compromising the accuracy of results. The proposed iteration scheme leads to improvement of responses and very good agreement with MCS results are observed for multiple example solved. Higher order expansion is used in the proposed ImPC for obtaining accurate response, which however could not be used in mPC due to constraint in RAM of the available computational facilities. Thus, ImPC can be effectively implemented to obtained accuracy even with limited computational facilities. From the convergence studies with successive orders and iterations, it can be observed that the proposed ImpC can be effectively used for the evaluation of response parameter for linear structural mechanics problem types considered in the present study with random modulus of elasticity, where MCS responses are not necessarily required for comparison.

4

Iterative PC for problems with non-Gaussian randomness

Contents

4.1 Introduction

In the previous chapter (Chapter 3), stochastic linear structural mechanics problem with Gaussian material properties are discussed along with a proposed method for its solution. As discussed in Chapter 2, it may be appropriate to model material as some non-Gaussian distribution as Gaussian model may not always provide a positive value of the physical quantity as in case of a higher value of c.o.v. However, one of the major difficulties in considering a non-Gaussian model of a physical quantity is the generation of non-Gaussian field. There are two major categories of methods for generation of non-Gaussian random fields, and these are discussed in section 2.2.2. It has also been discussed in section 2.2.3 that KL expansion can be considered for discretization and generation of random fields for both Gaussian (Ghanem and Spanos, 1991b) and non-Gaussian (Phoon et al., 2005) random field. The random variables of KL expansion for a non-Gaussian random field may not however be independent. Thus, ICA is considered to obtain a set of independent random variables. ICA has been considered before by different authors and has been discussed in section 2.2.2.

In this chapter, the proposed iterative method discussed in Chapter 3 for the solution of stochastic linear mechanics problems is further explored to consider non-Gaussian randomness. The proposed iterative method is observed to be more efficient than the conventional PC based method in terms of both accuracy and computational demand requirement. Numerical example considered in Chapter 3 are considered again with non-Gaussian randomness.

The chapter is organized as follows. Section 4.2 discusses the discretization and simulation of non-Gaussian random field and formulation of SFE equations. The proposed method for non-Gaussian randomness is discussed in section 4.3. Numerical examples are included in section 4.4 with the final conclusion and discussion in section 4.5.

4.2 Discretization using KL expansion and formulation of SFEM

Discretization of the random field to a set of random variables is performed using KL expansion. The general principle of KL expansion is already discussed in section 3.2.1. However, in case of a non-Gaussian random field, the field is generated by iterative methods and are discussed in section 4.2.1. The improvement of KL expansion using ICA and formulation of SFEM are discussed in section 4.2.2 and 4.2.3, respectively.

Random variables, $\xi_n(\theta)$ of Eq. 3.1 are standard Gaussian uncorrelated random variables for Gaussian random field. However, for a non-Gaussian random field, random variables are needed to be calculated, and two different approaches of calculation of these random variables exist. In the first method, the non-Gaussian random field is generated first followed by the generation of random variables, $\xi_n(\theta)$ using Eq. 3.2. The second method directly utilizes KL expansion for the generation of random variables for the non-Gaussian field. However, the first method is not advisable as there may be loss of information due to successive transformations and possible truncations. The present study considers the direct generation of random field using KL expansion and is discussed in the next section.

4.2.1 Direct generation of non-Gaussian random field using KL expansion

Direct simulation of non-Gaussian field can be carried out by considering KL expansion as proposed by Huang et al. (2000) and Phoon et al. (2002, 2005) applicable to both stationary and non-stationary non-Gaussian processes. The philosophy of the method is to update $\xi_n(\theta)$ of KL expansion (Eq. 3.1) iteratively, so that the generated random field would match with the target marginal CDF satisfying the relationship given by Eq. 3.3 at each iteration. Since the random vector $(\xi_n(\theta))$ at each iteration satisfy Eq. 3.3, the simulated covariance function is observed to agree with the theoretical covariance function for a reasonably large samples. It can be observed from the Eq. 3.1 and 3.2 that $\alpha(x,\theta)$ and $\xi_n(\theta)$ are to be generated iteratively to match with the desired properties. The generation of non-Gaussian random field using KL expansion can be described as below (Phoon et al., 2005),

1. Consider S samples of Q numbers of random variables $\xi_n(\theta)$, $n = 1,2,\ldots,Q$ (initial assumption).

2. Generate random field following Eq. 3.1 for the considered random variables as

$$\alpha_Q^{(k)}(x,\theta_m) = \sum_{n=1}^{Q} \xi_n^{(k)}(\theta_m)\sqrt{\lambda_n} f_n(x), \quad m = 1,2\ldots S \tag{4.1}$$

   where k is the iteration number. λ_n and $f_n(x)$ are the eigenpairs of the target covariance function.

3. Calculate empirical cumulative marginal distribution, $\overline{F}^{(k)}(y|x)$ of the simulated random field and simulate covariance function $\overline{\boldsymbol{C}}_Q(x_1,x_2)$ as,

$$\overline{F}^{(k)}(y|x) = \frac{1}{S}\sum_{i=1}^{S} I(\alpha^{(k)}(x,\theta) \leq y) \tag{4.2}$$

$$\overline{\boldsymbol{C}}_Q(x_1,x_2) = \frac{1}{S}\sum_{m=1}^{S} \left[\alpha_Q^k(x_1,\theta_m)\right] \times \left[\alpha_Q^k(x_2,\theta_m)\right] \tag{4.3}$$

   where $I()$ is equal to one if true and zero otherwise.

4. Each of the calculated $\overline{F}^{(k)}(y|x)$ is transformed to match target marginal distribution F

$$\gamma^{(k)}(x,\theta) = F^{-1}\overline{F}^{(k)}[\alpha^{(k)}(x,\theta)] \tag{4.4}$$

5. The new random variables ξ_n for the iteration process are calculated using KL expansion (Eq. 3.2) as

$$\xi_n^{(k+1)}(\theta_m) = \frac{1}{\sqrt{\lambda_n}}\int_D [\gamma_Q^{(k)}(x,\theta_m) - \overline{\gamma}_Q^{(k)}(x)] f_n(x)dx \tag{4.5}$$

   where $\overline{\gamma}_Q^{(k)}(x)$ mean of $\gamma_Q^{(k)}(x,\theta_m)$

6. Calculated $\xi_n^{(k+1)}(\theta_m)$ is standardize to unit variance.

7. Repeat step 2 to 6 until the sample function achieve the target marginal distribution.

The initial random variables are generally considered as that of the target marginal distribution of the random field satisfying Eq. 3.3. The simulated and theoretical covariance function match at each step for a large sample size. However, there is a difference in theoretical and target covariance function as the theoretical one depends on the number of eigenvectors considered. It may be observed from Eq. 4.1 that updation is required only for the random variables ($\xi_n(\theta)$), while it is evident from Eq. 3.4(c) that the covariance function always matches with the theoretical one. The random variables generated at step 5 however may not remain uncorrelated. Phoon et al. (2005) suggested to consider product moment orthogonalization of the random variables to reduce the correlation, which is implemented in the present study.

4.2.2 Independent component analysis

ICA (Comon, 1994) is a statistical technique of minimizing statistical dependence between its components by a linear combination of random variables. The random variables generated for non-Gaussian random field are uncorrelated and follow Eq. 3.3. However, these are not necessarily statistically independent for non-Gaussian random field. Khalil and Sarkar (2008, 2014), Li and Zhang (2013) considered ICA along with KL expansion so that the random variables are also statistically independent. The uncorrelated random variables can be transformed to independent one by using ICA as [1]

$$\boldsymbol{\xi}(\theta) = \boldsymbol{H}_{\text{mixing}} \boldsymbol{\eta}(\theta) \tag{4.6}$$

where $\boldsymbol{H}_{\text{mixing}}$ is an unknown mixing matrix, which mapped the independent random variables $\boldsymbol{\eta}$ to $\boldsymbol{\xi}$. For the further study, the eigenvalue and eigenvector are considered as one quantity $h_i(x) = \sqrt{\lambda_i} f_i(x)$. Thus KL expansion (Eq. 3.1) for non-Gaussian random field can be written as

$$\alpha(x,\theta) = \sum_{n=1}^{Q} \xi_n(\boldsymbol{\eta}(\theta)) h_n(x) \tag{4.7a}$$

$$= \sum_{n=1}^{M} \eta_n(\theta) H_{\text{mixing}_n}(x) \tag{4.7b}$$

where ICA modes ($H_{\text{mixing}_n}(x)$) are linear combinations of eigenvector ($\boldsymbol{B}h(x)$) of KL expansion.

4.2.3 Formulation of SFEM

The formulation of stochastic finite element for Gaussian randomness is discussed in section 3.2.2. The formulation with non-Gaussian randomness is similar to that of Gaussian, the only difference is that instead of $\xi_i(\theta)$ the $\eta_i(\theta)$ need to be considered. Thus, the stochastic FE equation can be written as

$$\left[\overline{\boldsymbol{K}}_{(N\times N)} + \sum_{n=1}^{Q} \eta_n(\theta) \boldsymbol{K}_{n_{(N\times N)}} \right] \boldsymbol{u}_{(N\times 1)} = \boldsymbol{q}_{(N\times 1)} \tag{4.8}$$

$\overline{\boldsymbol{K}}$ and $\boldsymbol{K}_n$ are as defined as in section 3.2.2. This equation can be solved using PC based method using Galerkin projection as described in section 3.3. However, $\eta_n(\theta)$ are not of same distribution, and thus are generally transformed to same distribution in the generation PC. These transformed random variables are considered only to generate PC, the random variables in Eq. 4.8 remain same.

[1] A MATLAB® implementation ICA using fastICA algorithm is available at WWW address: http://research.ics.aalto.fi/ica/fastica/

4.3 Solution using Proposed Approach

4.3.1 Basic idea

The problem related to exponential increase in matrix size was discussed by different authors and different strategies were proposed for generation of sparse PC expansion as discussed in section 2.4. In Chapter 3, an iterative PC based method in the intrusive framework is proposed to overcome such problem of large dimension of system matrix with Gaussian material properties. In this section, the proposed method is extended to consider non-Gaussian materials properties.

As discussed in section 3.4, the responses are represented using PC of non-Gaussian random variables, which are calculated using an iterative scheme from the previous iteration, while the initial responses are calculated using first order PC. Subsequently these responses are used to formulate the iterative PC of different orders. The same method as described in section 3.4.3 is considered to generate PC for non-Gaussian random variables.

In case of random field problem, the input random field is discretized and generated using KL expansion as discussed in section 4.2.1. The random variables of KL expansion for non-Gaussian random field are not independent and ICA is considered to improve the non-dependency among the random variables and are discussed in section 4.2.2.

As discussed in section 3.4.2, the random field should be represented at its best possible manner. Thus, following the same philosophy, the random field is considered at two Gauss points of each element rather than mid point. Further, the system matrix size can further be reduced following Pascual and Adhikari (2012) as discussed in section 3.4.5.

In case of multiple random quantities with different distributions, the random variables are converted to identical distribution with same mean and variance. Moreover, after performing ICA, the random variables are not of same distribution. Thus, these are also converted to the same distribution with the same mean and variance. It may be noted that all such above-mentioned transformations are limited to the generation of PC, while the original input data remain unaltered. Moreover, though the input random variables to PC are of same distribution, there may be correlation among the random variables. Thus, use of gPC is not considered as method requires uncorrelated and independent random variables in the input. The PCs are generated using Gram-Schmidt orthogonalization as discussed in section

3.4.3. Similarly, in case of iterative process, the random variables are generated using KL expansion and are generally uncorrelated.

The performance of the proposed iterative strategy is assessed by considering the goodness of the calculated response as discussed in section 3.4.6.

4.3.2 Proposed iterative scheme (ImPC)

The first step of the proposed method is to solve the stochastic problem using first order multidimensional PC with the desired number of random variables from KL expansion of the input random field. Depending on the SD of the random field, the responses are likely to be of different probability distribution. However, these evaluated responses are not likely to be accurate as only first-order expansion is considered initially and thus the iterative method proposed in Chapter 3 are considered to evaluate the responses.

Stepwise Algorithm of ImPC:

A2-1 Calculate stiffness matrix using KL expansion

{

Discretize the covariance function of random field considering Gauss point of each element.

$$E(x,\theta) = E_0\left(1+\sum_{n=1}^{Q}\xi_n(\theta)\sqrt{\lambda_n}f_n(x)\right)$$

Calculate the number of random variables (Q) based on expected energy consideration.

{

while energy $\leq$threshold

$Q = Q+1$

energy=energy+$\lambda_Q/sum(\lambda)$

end while

}

Calculate random variables $\xi_n(\theta)$ iteratively as discussed in section 4.2.1

Perform ICA on the random variables of KL expansion.

$$\xi_n(\theta)_{\text{Dependent}} \xrightarrow{\text{using FastICA}} \xi_n(\theta)_{\text{Independent}}$$

Formulation of SFEM as discussed in section 4.2.3.

}

A2-2 The random variables after ICA are converted to random variables with identical probability distribution as (Also for random variables of different distributions.)

$$\xi_n(\theta)_{\text{Independent}} \xrightarrow{\text{Non-linear transformation}} \xi_n(\theta)_{\text{Same disctribution}}$$

A2-3 Construct first order PC using the random variables calculated in step A2-2

$$\text{PC}_{\text{1st Order}} = f(\xi_n(\theta)_{\text{Same disctribution}})$$

A2-4 The algorithm presented in Chapter 3 from A1-3 to A1-6 is followed.

It is also important to note that as the random field is considered at Gauss points, the integration in iterative calculation of random variables ($\xi_n(\theta)$) are spaced unevenly. Algorithm proposed by Gill and Miller (1972) is considered to evaluate the integral in step 5 of section 4.2.1. The random variables obtained after conversion in step A2-2 are to be considered only to generate PC for approximation of responses. In the present study, conversion of random variables after ICA is done to standard Gaussian random variables in all the numerical examples considered.

4.4 Numerical examples

4.4.1 Deflection of a Truss: A multiple non-Gaussian random variable problem

The first problem is the same 23 member truss problem considered in section 3.5.1. However, in the present case, random variables are considered as independent non-Gaussian and moreover, the loadings are considered with different statistical parameters. Thus, the loadings can be considered as unsymmetrical. The truss is shown in Fig. 4.1 for ready reference.

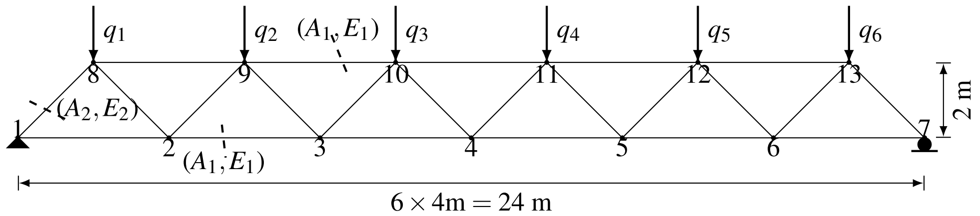

Fig. 4.1: Truss structure comprising of 23 members showing loading.

The ten considered independent random variables are

$$\boldsymbol{Z} = \{E_1, E_2, A_1, A_2, q_1, q_2, q_3, q_4, q_5, q_6\}^T \tag{4.9}$$

where E_1, E_2 represent Young's modulus, A_1, A_2 represent area of truss members and q_i, $i = 1\ldots6$ represents loading as shown in Fig. 4.1. The random input parameters are shown in Table 4.1.

Table 4.1: Input random variable for truss problem.

Variable	Unit	Distribution	Mean	SD
A_1	m^2	Log-normal	2.0×10^{-3}	2.0×10^{-4}
A_2	m^2	Log-normal	1.0×10^{-3}	1.0×10^{-4}
E_1	Pa	Log-normal	2.1×10^{11}	2.1×10^{10}
E_2	Pa	Log-normal	2.1×10^{11}	2.1×10^{10}
q_1, q_2, q_3	N	Gumbel	2.5×10^{4}	3.75×10^{3}
q_4, q_5, q_6	N	Gumbel	7.5×10^{4}	11.25×10^{3}

With axial rigidity $EA = E(\theta)A(\theta)$, the finite element equation can be written as,

$$\sum_{i=1}^{R} \boldsymbol{K}_i(E_i(\theta)A_i(\theta))\boldsymbol{u} = \sum_{j=1}^{S} \boldsymbol{q}_j(\theta) \tag{4.10}$$

where $\boldsymbol{K}_i$ is formulated considering the members of the truss with axial rigidity $E_i(\theta)A_i(\theta)$. R and S are the number of pairs of $E(\theta)A(\theta)$ and number of random load variables respectively.

The responses of the structure are evaluated using the proposed iterative PC based method as well as mPC based method and compared with those of MCS. A sample size of 5×10^5 is considered for all the methods and the same seeds of independent random variables are considered for all the methods as well, so that there would not be any anomaly in input considered for the analysis. The input random variables are statistically different in nature and are recast as standard normal random variables X_i as,

$$X_i = \Phi^{-1}(F_{Z_i}(Z_i)), \quad i = 1,2,\ldots,10 \tag{4.11}$$

where Φ is the standard Gaussian CDF and F_{Z_i} is CDF of Z_i. Thus the displacement $\boldsymbol{u}$, using PC is approximated as,

$$\boldsymbol{u} = \sum_{i=0}^{P} \boldsymbol{a}_i \Psi_i(\boldsymbol{X}) \tag{4.12}$$

The transformed random variables are considered only for generation of PC, the input random variables considered in Eq. 4.10 remain same as these represent the input random data.

Table 4.2: Statistical parameters of the transformed random variables of truss problem.

Variable	Mean	SD	Skewness	Kurtosis
q_1	1.779×10^{-04}	1.001	1.800×10^{-03}	2.991
q_2	3.165×10^{-04}	1.001	5.810×10^{-03}	2.993
q_3	2.367×10^{-04}	1.001	4.068×10^{-03}	2.995
q_4	1.096×10^{-04}	1.000	8.022×10^{-04}	2.995
q_5	-4.960×10^{-05}	1.000	-4.257×10^{-03}	2.991
q_6	1.476×10^{-04}	1.001	1.634×10^{-03}	2.991
A_1	6.471×10^{-05}	0.999	-7.462×10^{-03}	3.004
E_1	9.248×10^{-06}	1.000	2.970×10^{-03}	2.998
A_2	-3.265×10^{-05}	1.000	4.152×10^{-05}	3.009
E_2	-7.893×10^{-06}	1.000	-2.632×10^{-03}	3.004

Table 4.3: Value of $\mathbb{E}[X_i, X_j]$ for transformed random variables of truss

	q_1	q_2	q_3	q_4	q_5	q_6	A_1	E_1	A_2	E_2
q_1	1.0012	0.0000	0.0008	0.0022	-0.0002	0.0009	0.0015	-0.0010	0.0040	-0.0007
q_2	0.0000	1.0025	-0.0014	0.0012	0.0006	-0.0006	0.0008	0.0017	0.0003	-0.0020
q_3	0.0008	-0.0014	1.0018	0.0025	0.0006	0.0005	-0.0032	0.0002	0.0028	-0.0006
q_4	0.0022	0.0012	0.0025	1.0007	0.0004	0.0017	-0.0016	-0.0029	0.0011	0.0008
q_5	-0.0002	0.0006	0.0006	0.0004	0.9991	-0.0001	-0.0022	0.0010	-0.0023	-0.0003
q_6	0.0009	-0.0006	0.0005	0.0017	-0.0001	1.0011	0.0010	-0.0012	0.0026	-0.0001
A_1	0.0015	0.0008	-0.0032	-0.0016	-0.0022	0.0010	0.9989	0.0000	-0.0005	-0.0017
E_1	-0.0010	0.0017	0.0002	-0.0029	0.0010	-0.0012	0.0000	0.9997	0.0006	0.0019
A_2	0.0040	0.0003	0.0028	0.0011	-0.0023	0.0026	-0.0005	0.0006	1.0006	-0.0017
E_2	-0.0007	-0.0020	-0.0006	0.0008	-0.0003	-0.0001	-0.0017	0.0019	-0.0017	1.0002

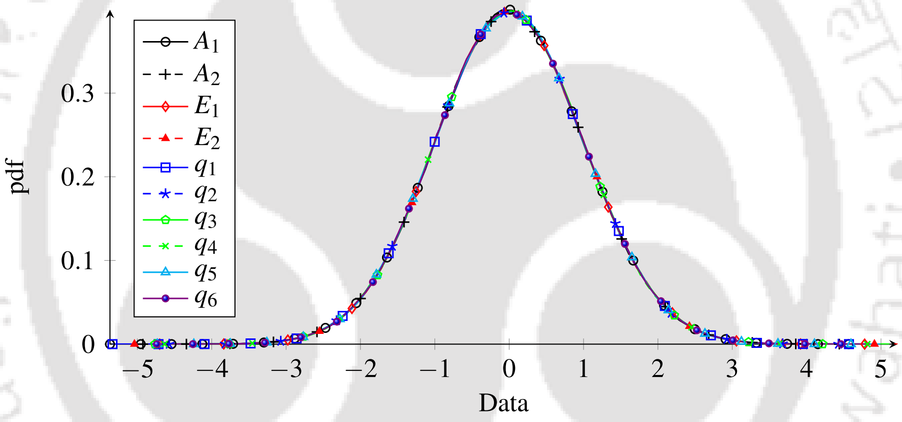

Fig. 4.2: pdf of the transformed random variables (X_i).

4.4.1.1 Response of truss

The vertical displacement at node 4 (Fig.4.1) is considered for the detailed study. The pdf of transformed random variables (X_i) considered to generate PC are shown in Fig. 4.2 and the statistical parameters of the random variables are shown in Table 4.2 and 4.3. It can be observed that the random variables are identically distributed, but are not perfectly uncorrelated as may be observed from off-diagonal terms in Table 4.3. In case of Hermite polynomial chaos, the random variables need to be Gaussian and uncorrelated to form an orthogonal basis vector. However, the proposed polynomial chaos generated considering Gram-Schmidt orthogonalization process as described in section 4.3 are orthogonal.

The problem is solved using polynomial chaos generated as described in section 3.4.3 (named mPC). The pdfs of the vertical displacement at node 4 for different orders of PCs are shown in Fig. 4.3. It can be observed that as the order of PC increases, the pdf converges towards MCS. However, the size of PC expansion increases exponentially from 11 to 1001 as the order increases from 1^{st} to 4^{th} (Table. 2.2).

Similar to the Gaussian problem, in order to reduce the dimension of mPC expansion, the problem is solved using the proposed iterative method. The iterative PC expansion is generated after solving the problem using first order mPC expansion, and subsequently the responses are considered to generate mPC expansion. It is observed that most of the expected energy is concentrated within the first three modes (approximately equal to 1) and corresponding random variables are considered for the iteration process. The iteration process of 2^{nd} order with 3 random variables for first and second iterations are designated as "EV3PC2I1", EV3PC2I2" respectively. Similarly, for 3^{rd} order PC, it is designated as "EV3PC3I1", EV3PC3I2". The pdfs of the vertical displacement of node 4 for third order ImPC with different iterations are shown in Fig. 4.4. It is observed that the pdf of first order mPC does not match with MCS. However, as iteration increases, pdfs are observed to converge towards MCS. Various errors associated with the response corresponding to different orders and iterations are shown in Fig. 4.5. For comparison with mPC based method, the error associated with different orders of mPC are also plotted along y axis *vs* number of orders along x axis. The errors in absolute maximum error, RMS error and various statistical errors are observed to reduce as iterations and orders are increased. It can be observed that the error in 3^{rd} order mPC is comparable to 3^{rd} order proposed scheme. However, the number of random vectors in case of mPC is ten, while it is only three in case of the proposed scheme. The accuracy of the results using the proposed method can further be increased by increasing the number of random variables considered in the iteration process.

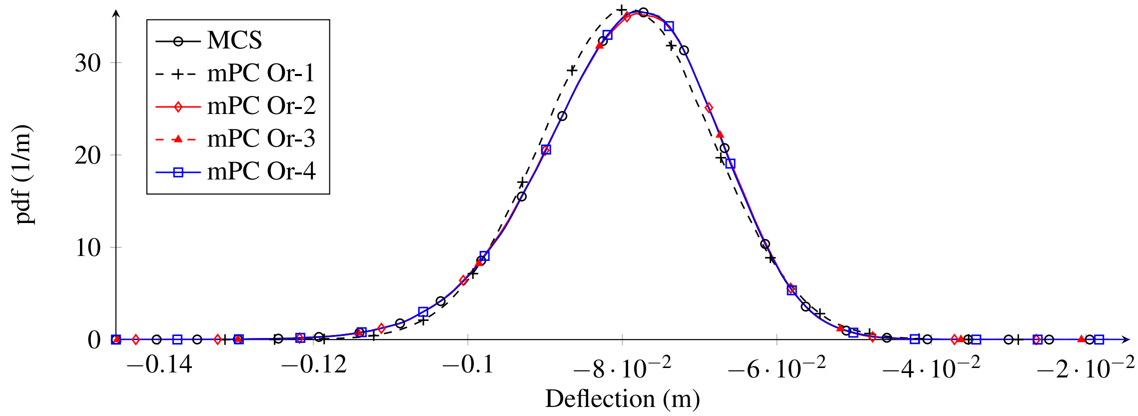

Fig. 4.3: pdf of vertical displacement of node 4 of truss (Fig. 4.1)for different orders of mPC and comparison with MCS.

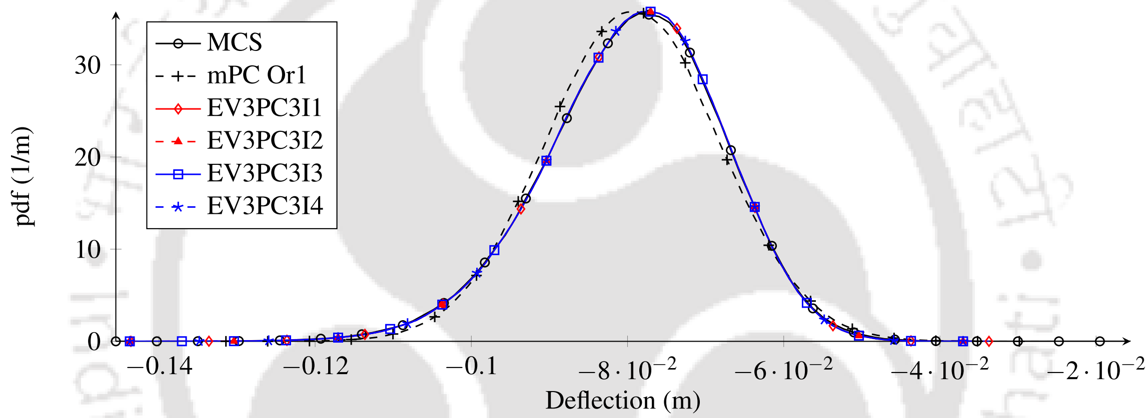

Fig. 4.4: pdf of vertical displacement at node 4 of truss (Fig.4.1) solved using iterative PC with different orders and iterations and comparison with MCS and mPC Or 1.

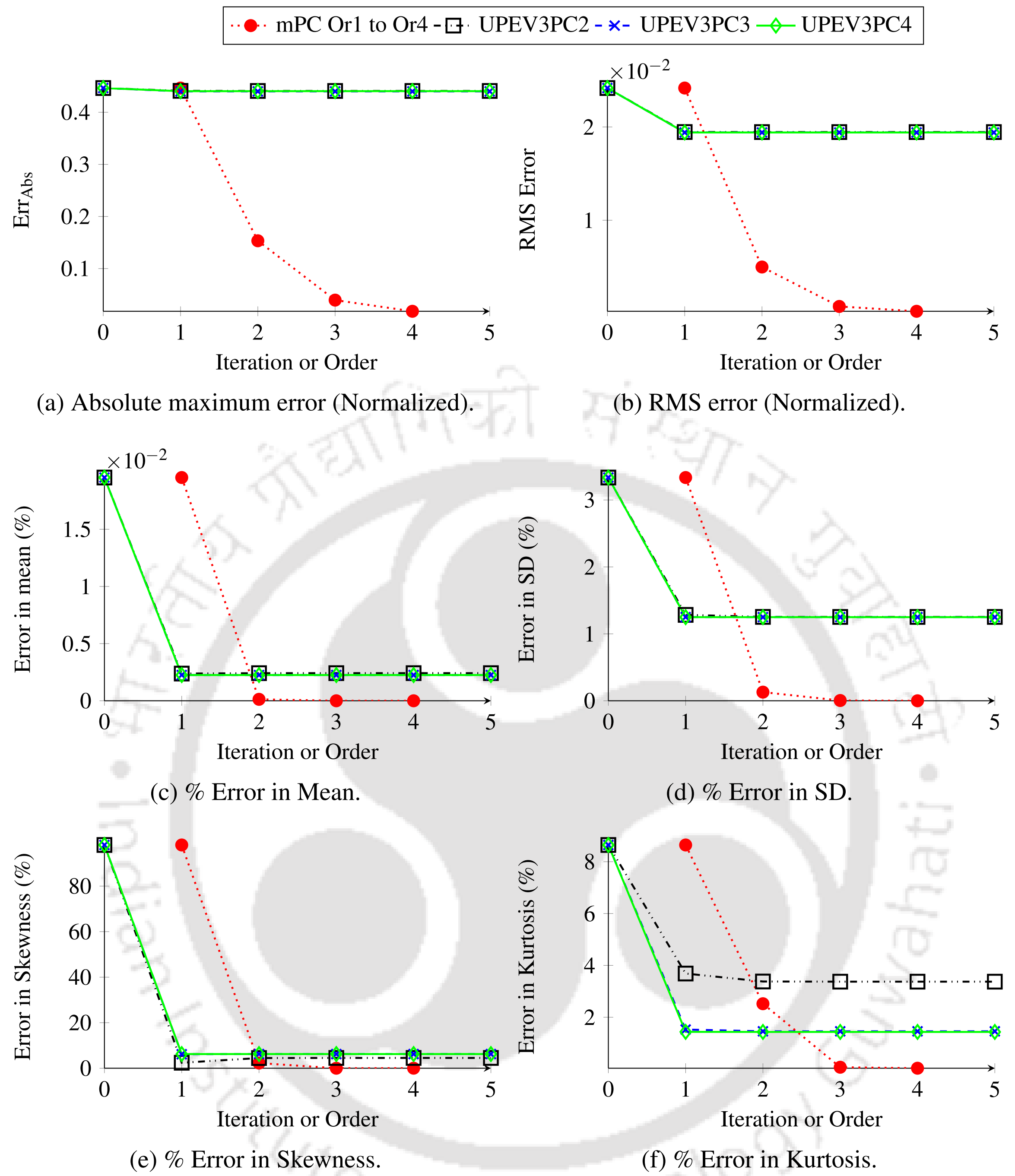

Fig. 4.5: Various error quantities in vertical deflection at node 4 (Fig. 4.1) using Proposed iterative method for different orders of PC with three random variables in the iteration process.

4.4.1.2 Reliability of response

Similar to the Gaussian problem in section 4.4.1.2, the serviceability of the truss structure with respect to some allowable maximum vertical deflection ($v_{\max}^{(4)}$) at midpoint of bottom cord (node 4) is studied. The limit state function associated with vertical displacement of node four is,

$$g(x) = v_{\max}^{(4)} - |v^{(4)}| \leq 0 \tag{4.13}$$

The probability of failure P_f^{MCS} evaluated from MCS responses of 5×10^5 samples is considered as reference result. The associated generalized reliability index is given as $\beta^{\text{MCS}} = -\Phi^{-1}(P_f^{\text{MCS}})$. The reliability index for different methods of analysis are shown in Table 4.4 for different values of threshold $v_{\max}^{(4)}$. It is observed that the error in reliability indices based on the proposed method is very less, though marginally higher than those based on mPC. It may be noted that the error in the evaluated reliability index using 3rd order mPC are very small for all the considered threshold values of vertical deflection (Table 4.4). Thus, while the modified PC is highly reliable, the computational complexity is however much higher compared to the proposed ImPC.

Table 4.4: Reliability index of truss problem due to random material and loading and % error compared to MCS.

$v_{\max}^{(4)}$ (cm)	MCS β^{MCS}	mPC3 β^{PC}	mPC3 % Error	EV3PC3I3 β^{PM}	EV3PC3I3 % Error
8	0.11	0.11	0	0.11	0
10	1.71	1.71	0	1.72	0.58
12	3.03	3.04	0.33	3.08	1.65
13	3.7	3.7	0	3.69	-0.27
14	4.22	4.26	0.95	4.47	5.92

4.4.1.3 Computational aspect

It is observed that the responses of the proposed iterative scheme for 3$^{\text{rd}}$ order of PC and 3 iteration with three random variables are comparable with responses of mPC of 3$^{\text{rd}}$ order. However, the polynomial sizes are different. The total number of terms in mPC for three and ten random variables are shown in Table 2.2. Thus, the computational complexity of matrix inversion for MCS, mPC and proposed iterative method (ImPC) of 3$^{\text{rd}}$ order with three random variable is $5 \times 10^5 \times 23^3 : (286 \times 23)^3 : (11 \times 23)^3 + 3(20 \times 23)^3 = 19.74 : 923.5 : 1$. Thus, a higher computational gain can be achieved in case of proposed ImPC method.

4.4.2 Deflection of Beam: 3-D Euler-Bernoulli beam with 1-D random field for Young's modulus

The second example considered is the same three dimensional cantilever beam considered in section 3.5.2 with Gaussian Young's modulus. However, in the present study, the Young's modulus (E) is considered as one dimensional non-Gaussian spatially varying random field of the form

$$E(x,\theta) = E_0[1+\alpha(x,\theta)] \tag{4.14}$$

where E_0 is the mean value of the random field and $\alpha(x,\theta)$ is a homogeneous zero mean log-normal random field with an exponential covariance function as

$$\boldsymbol{C}(x_1,x_2) = \sigma^2 \exp\left(\frac{-|x_1-x_2|}{L_c}\right) \tag{4.15}$$

where σ is the SD of the random field, L_c is the correlation length, which acts as a normalizing factor to the length of the process considered. The mean of the random field is 2.1×10^{11} Pa. The beam is shown in Fig. 4.6 for ready references. In the present study, the length of the process is taken as $L/2$ for exponential covariance function, while the correlation length is considered as $L/2$. The problem is analysed for SD, $\sigma = \{0.05, 0.1, 0.15, 0.2\}$. However, the generation of random field is shown only for SD=0.2 and convergence is demonstrated for SD 0.05 and 0.2.

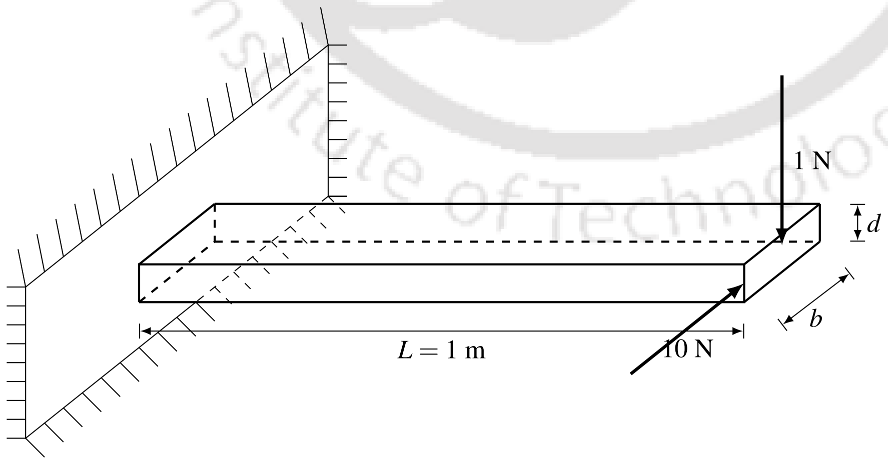

- b=39 mm.
- d=5.93 mm.
- $E_0 = 2\times10^{11}$ Pa.

Fig. 4.6: Cantilever beam with a point load at free end.

4.4.2.1 Generation and discretization of random field using KL expansion

The random field is generated and discretized using KL expansion as discussed in section 4.2. The discretization and number of random variables requirement are studied in section 3.5.2.1 for Gaussian random field. As the eigenpairs are independent of type of distribution, the same discretization and number of random variables as considered in the case of Gaussian field (in section 3.5.2) are considered in the present case also. Thus, in this case also first six eigenvectors with 30 element of equal sizes are considered in the numerical analysis with random field represented at two Gauss points of each element.

The target covariance function and target marginal CDFs are shown in Fig.4.7(a) and 4.7(b) respectively. The target log-normal distribution is considered as $(1+\alpha(x,\theta))$ instead of considering only zero mean random field, $\alpha(x,\theta)$. The theoretical covariance is calculated using Eq. 3.4c. It can be observed that the covariance function calculated using Eq. 3.4c is independent of random variables and only depends on eigenpairs. The difference in the considered target and theoretical covariance functions is due to the fact that only the first six eigenpairs are considered in evaluating the covariance function. Further, the theoretical covariance will be considered as benchmark for measuring the accuracy of the simulated random field.

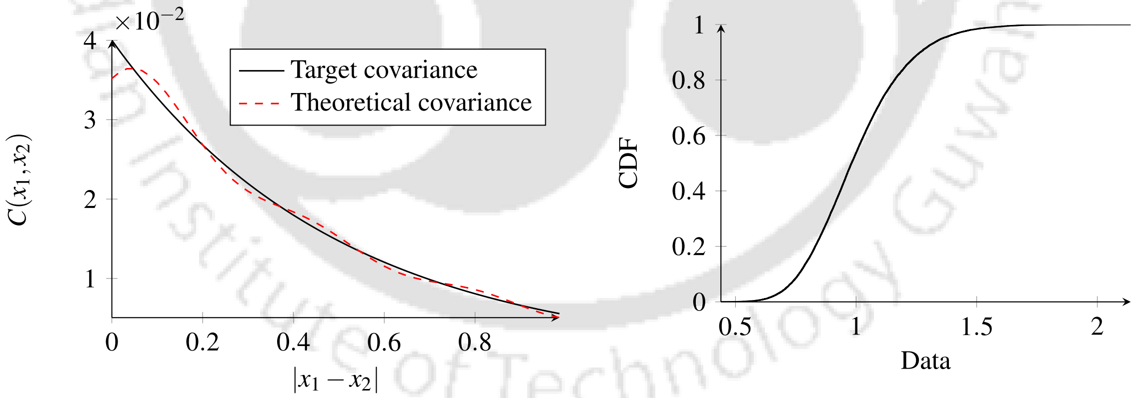

(a) Target covariance function. (b) Target log-normal CDF.

Fig. 4.7: Target properties of the random field (a) Target Covariance function (b) Target marginal CDF.

The covariance function and CDF of simulated log-normal distribution after first, third and sixth iterations are shown in Figs.4.8 and 4.9 respectively. It can be observed that the simulated results are close to theoretical covariance and target CDF. The random variables generated after the sixth iteration are considered for the analysis.

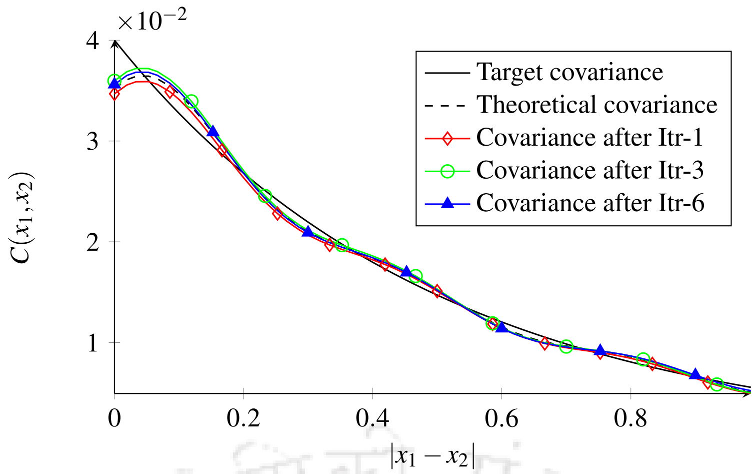

Fig. 4.8: Calculated Covariance function.

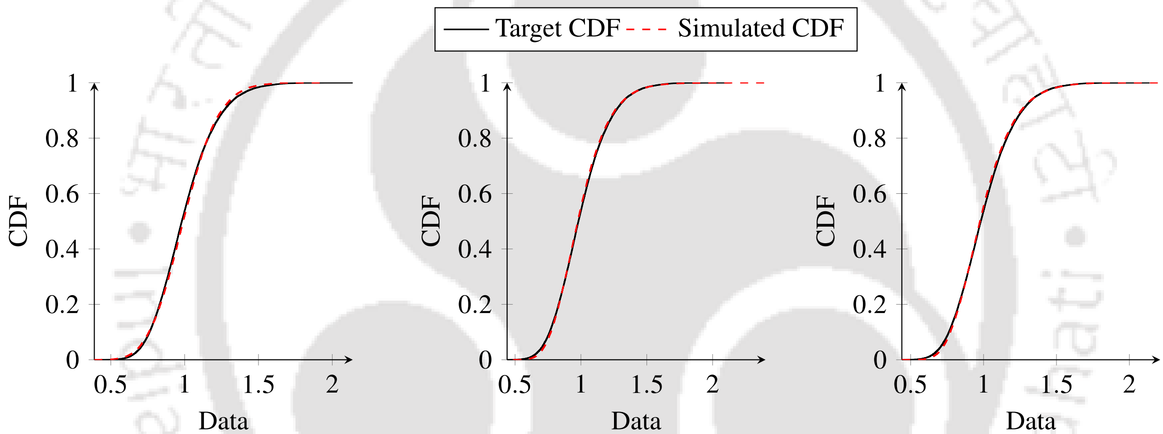

(a) CDF after first iteration (b) CDF after third iteration (c) CDF after sixth iteration

Fig. 4.9: Representative simulated CDF after (a) first (b) third (c) sixth iteration along with target CDF.

ICA is performed on the random variables after generation of a random field using KL expansion. The ICA modes obtained by linear combination of mixing matrix and eigenvectors of KL expansion for 10, 20 and 30 element are shown in Fig. 4.10 along with the eigenvectors of KL expansion for 30 elements. It is observed that ICA modes corresponding to 10 elements do not show smooth curves for all the modes. However, as the number is increased to 20 and 30, the smoothness in curves are achieved. It can further be observed that the shape of these eigenvectors do not match with the corresponding eigenvector with different numbers of elements. These is because of the ambiguities of ICA, which states that it is not possible to determine the order of the independent component (Hyvärinen and Oja, 2000). The mixing matrix of ICA may change in each execution and thus the order as well as shape of generated ICA modes. The present study considers 30 finite elements in discretization and once the mixing matrix and independent components are evaluated, the same is used for all the analyse methods considered. The mixing matrix for 30 elements is shown in Eq. 4.16.

$$\text{Mixing Matrix}, \boldsymbol{H}_{\text{mixing}} = \begin{bmatrix} 0.121 & -0.001 & -0.501 & -0.054 & -0.022 & 0.855 \\ 0.005 & -0.999 & -0.027 & 0.004 & -0.028 & -0.017 \\ 0.006 & 0.028 & -0.862 & 0.033 & 0.051 & -0.502 \\ -0.001 & -0.010 & -0.006 & -0.998 & -0.007 & -0.065 \\ 0.004 & 0.046 & -0.037 & -0.005 & -0.997 & -0.048 \\ 0.992 & 0.000 & 0.050 & -0.015 & -0.001 & -0.111 \end{bmatrix} \tag{4.16}$$

The pdf of the random variables before orthogonalization and after orthogonalization in KL expansion along with pdf of random variables after ICA are shown in Figs.4.11(a), 4.11(b) and 4.11(c) respectively. The covariance matrices of the random variables of KL expansion before and after orthogonalization are shown in Table 4.5 and 4.6 respectively and that of ICA is shown in Table 4.7. It can be clearly observed that the ICA random variables have shown best uncorrelation as the off diagonal terms are very low. Examination of Fig. 4.11(a)-(c) and Tables 4.5 - 4.6 further reveals that while random variables of KL expansion before and after orthogonalization are identically distributed and uncorrelated, random variables after ICA are not identically distributed though show more decorrelation. Khalil and Sarkar (2014) mentioned that the extent of decorrelation in the random variables can be reasonably related to the statistical independence of the random variables after transformation with ICA.

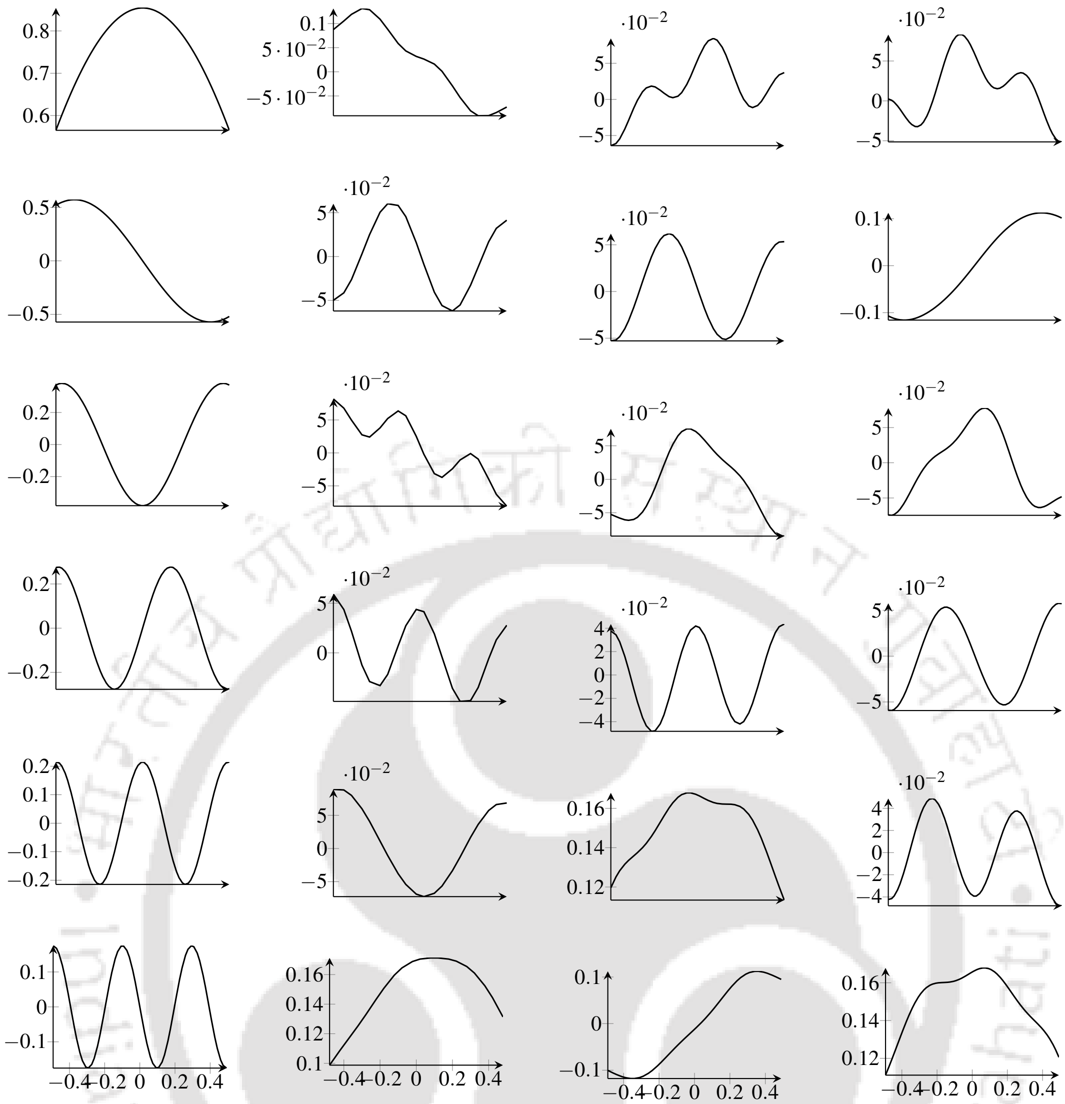

(a) (b) (c) (d)

Fig. 4.10: First six eigenvectors of KL expansion and ICA modes for different element number (a) KL expansion with 30 element (b) ICA, 10 elements (c) ICA, 20 elements (d) ICA, 30 elements.

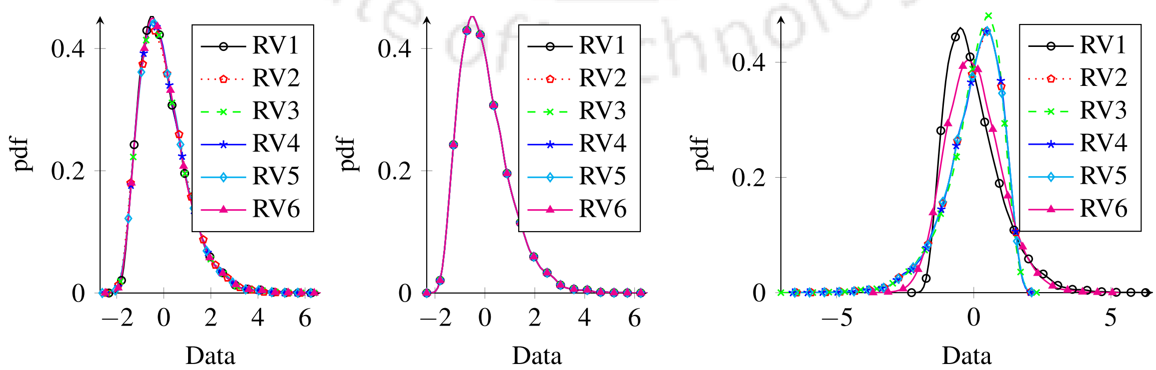

(a) before orthogonalization. (b) after orthogonalization. (c) after ICA.

Fig. 4.11: pdf of random variable.

Table 4.5: Covariance matrix of the random variables of KL expansion before orthogonalization

RV	RV1	RV2	RV3	RV4	RV5	RV6
RV1	1	-7.292×10^{-03}	-2.881×10^{-02}	-1.673×10^{-02}	-7.778×10^{-02}	6.075×10^{-03}
RV2	-7.292×10^{-03}	1	2.338×10^{-02}	-8.574×10^{-02}	3.638×10^{-03}	-8.800×10^{-02}
RV3	-2.881×10^{-02}	2.338×10^{-02}	1	-8.065×10^{-03}	-4.608×10^{-02}	3.894×10^{-03}
RV4	-1.673×10^{-02}	-8.574×10^{-02}	-8.065×10^{-03}	1	1.075×10^{-02}	-4.108×10^{-02}
RV5	-7.778×10^{-02}	3.638×10^{-03}	-4.608×10^{-02}	1.075×10^{-02}	1	1.138×10^{-02}
RV6	6.075×10^{-03}	-8.800×10^{-02}	3.894×10^{-03}	-4.108×10^{-02}	1.138×10^{-02}	1

Table 4.6: Covariance matrix of the random variables of KL expansion after orthogonalization

RV	RV1	RV2	RV3	RV4	RV5	RV6
RV1	1	4.506×10^{-04}	6.860×10^{-04}	1.122×10^{-03}	6.258×10^{-04}	9.494×10^{-04}
RV2	4.506×10^{-04}	1	3.333×10^{-03}	7.515×10^{-03}	-1.652×10^{-02}	5.229×10^{-03}
RV3	6.860×10^{-04}	3.333×10^{-03}	1	3.979×10^{-03}	5.778×10^{-03}	1.844×10^{-02}
RV4	1.122×10^{-03}	7.515×10^{-03}	3.979×10^{-03}	1	1.523×10^{-02}	2.087×10^{-02}
RV5	6.258×10^{-04}	-1.652×10^{-02}	5.778×10^{-03}	1.523×10^{-02}	1	8.326×10^{-03}
RV6	9.494×10^{-04}	5.229×10^{-03}	1.844×10^{-02}	2.087×10^{-02}	8.326×10^{-03}	1

Table 4.7: Covariance matrix of the random variables of ICA expansion

RV	RV1	RV2	RV3	RV4	RV5	RV6
RV1	1	1.589×10^{-16}	1.630×10^{-16}	2.686×10^{-16}	-3.771×10^{-16}	8.432×10^{-17}
RV2	1.589×10^{-16}	1	-5.590×10^{-17}	8.053×10^{-18}	4.909×10^{-16}	-6.348×10^{-17}
RV3	1.630×10^{-16}	-5.590×10^{-17}	1	1.857×10^{-16}	1.350×10^{-16}	-1.440×10^{-16}
RV4	2.686×10^{-16}	8.053×10^{-18}	1.857×10^{-16}	1	-2.996×10^{-16}	-1.071×10^{-16}
RV5	-3.771×10^{-16}	4.909×10^{-16}	1.350×10^{-16}	-2.996×10^{-16}	1	8.527×10^{-17}
RV5	8.432×10^{-17}	-6.348×10^{-17}	-1.440×10^{-16}	-1.071×10^{-16}	8.527×10^{-17}	1

4.4.2.2 Response statistics

The cantilever beam is modelled using 30 numbers of equal sized 2 noded 3-D Euler Bernoulli beam elements. Boundary conditions are applied by restraining both rotational and translational degrees of freedom at one of its ends. A vertical load of 1 N and horizontal load of 10 N are applied at the free end. The problem is first analysed deterministically with 10, 20, 30 and 40 elements and 30 elements observed to satisfy both the requirement of appropriate representation of covariance as well as FE analysis. The problem is analysed for different values of SD, $\sigma = \{0.05\ \ 0.10\ \ 0.15\ \ 0.20\}$ of the input random field. The statistical parameters of deflection at the free end are presented in Table 4.8. A tip deflection of 2.4592 mm is observed when solved using deterministic FEM with a meanvalue of Young's modulus. It can be observed that the responses are non-Gaussian and tend to become skewed with an increasing value of kurtosis with the increase in SD of Young's modulus. The mean deflection is observed to increase with an increase in SD, though the mean values of Young's modulus are same for all SDs. The mean, SD, skewness and kurtosis of deflection at free end are observed to increase with the increase in SD of the random field.

Table 4.8: Statistical parameter of deflection at the free end of cantilever beam for different values of SD of input random field E.

SD of Random Field (E)	Mean (m) $\times 10^{-3}$	SD (m) $\times 10^{-3}$	Skewness	Kurtosis
0.05	-2.465	0.102	-0.113	3.010
0.10	-2.482	0.206	-0.253	3.197
0.15	-2.512	0.322	-0.602	4.364
0.20	-2.556	0.439	-0.786	5.028

The problem is first analysed using mPC of different orders generated using Gram-Schmidt process as discussed in section 3.4.3 with six random variables from KL expansion. The stiffness matrix size is further reduced using eigenvalue decomposition as discussed in section 3.4.5 (Pascual and Adhikari, 2012). The ratio, $\lambda_{0_1}/\lambda_{0_S}$ is considered as less than 10^{-3}, which yields the value of S as 18, and thus reduces 120×120 matrix to 18×18. The pdf of vertical deflection at the free end for different orders are shown in Fig. 4.12. Different order PC expansions are designated as KL6mPC1, KL6mPC2 and so on for first order and second order PC respectively. The corresponding responses from mPC based method with reduced stiffness matrix are termed as RKL6mPC1, RKL6mPC2 respectively. It can be observed that the pdf of response of first order PC based method does not match with pdf of MCS, which however converges to MCS as the order increases. It is also observed that for higher SD, a higher order PC expansion is required. Similar trends are observed for mPC with reduced stiffness matrix.

Various errors in mPC calculated with respect to MCS are plotted in Fig. 4.13. It is observed that as the order of PC expansion increases, the error reduces. The error is more in case of higher SD for the same order of expansion, meaning that for the same level of accuracy, it is required to have a higher order of expansion for higher values of SD. Errors in case of PC with reduced stiffness matrix are almost as same as those of full stiffness except error in mean, where it is marginally higher. Thus, the errors in general are observed to reduce with the increase in the order of expansion. However, the size of system matrix also increases and the polynomial sizes for different order and number of random variables as discussed in section 3.3 may be seen in Table 2.2.

To overcome the difficulty of such increase in dimension of the system matrix, the problem is solved using the proposed iterative scheme, where it is first solved using first order mPC and subsequently, responses are used to generate an iterative PC (ImPC). After the initial solution using first order mPC, the dominant modes of the responses are calculated using KL expansion. It is observed that most of the expected energy of the response covariance function is attained within the first two modes ($> 99\%$). Thus, the two random variables calculated from the response are considered in the iteration process. It reduces the number of random variable to be considered in PC expansion from six to two. The iteration process of 2^{nd} order with 2 random variables for first and second iterations are designated as ”KL6EV2PC2I1”, KL6EV2PC2I2” respectively. Similarly, for 3^{rd} order, it is designated as ”KL6EV2PC3I1”, KL6EV2PC3I2”. The same for reduced stiffness is designated as ”RKL6EV2PC3I1”, RKL6EV2PC3I2” respectively.

The pdf for vertical deflection at the free end of the cantilever beam for SD=0.05 and 0.2 are shown in Figs. 4.14 and 4.15 respectively. Various error quantities in ImPC calculated with respect to MCS for the vertical deflection at free end for SD=0.05 are shown in Fig. 4.16. Similarly, the error measures for SD=0.2 are shown in Fig. 4.17. It is observed that the pdf of first order mPC (KL6mPC1) does not match with MCS even for low SD. However, as the iteration process continues with the proposed method, the pdf converges towards MCS. The error in the responses are observed to reduce as the orders and iterations are increased. However, it is also observed that for a higher value of SD of Young’s modulus, a higher order of updated PC is required. In the present example with low value of SD ($\sigma = 0.05$), third order mPC and third order ImPC with 2 iterations give comparable response. However, the size of third order PC is 84, whereas third order PC with the proposed scheme is only 10. Thus, the size of matrix is considerably reduced. For high value of SD ($\sigma = 0.2$), fourth order mPC responses are comparable with fourth order ImPC with 2 iterations, where the expansion sizes are 210 and 15 respectively. The error in mean is actually very small and the observed changes with order of PC and iterations in the proposed scheme are found to be insignificant. The differences in error between PC based method with reduced stiffness matrix and full stiffness matrix are marginal and thus PC with reduced stiffness matrix is recommended to be used to further reduce the size of the final system matrix.

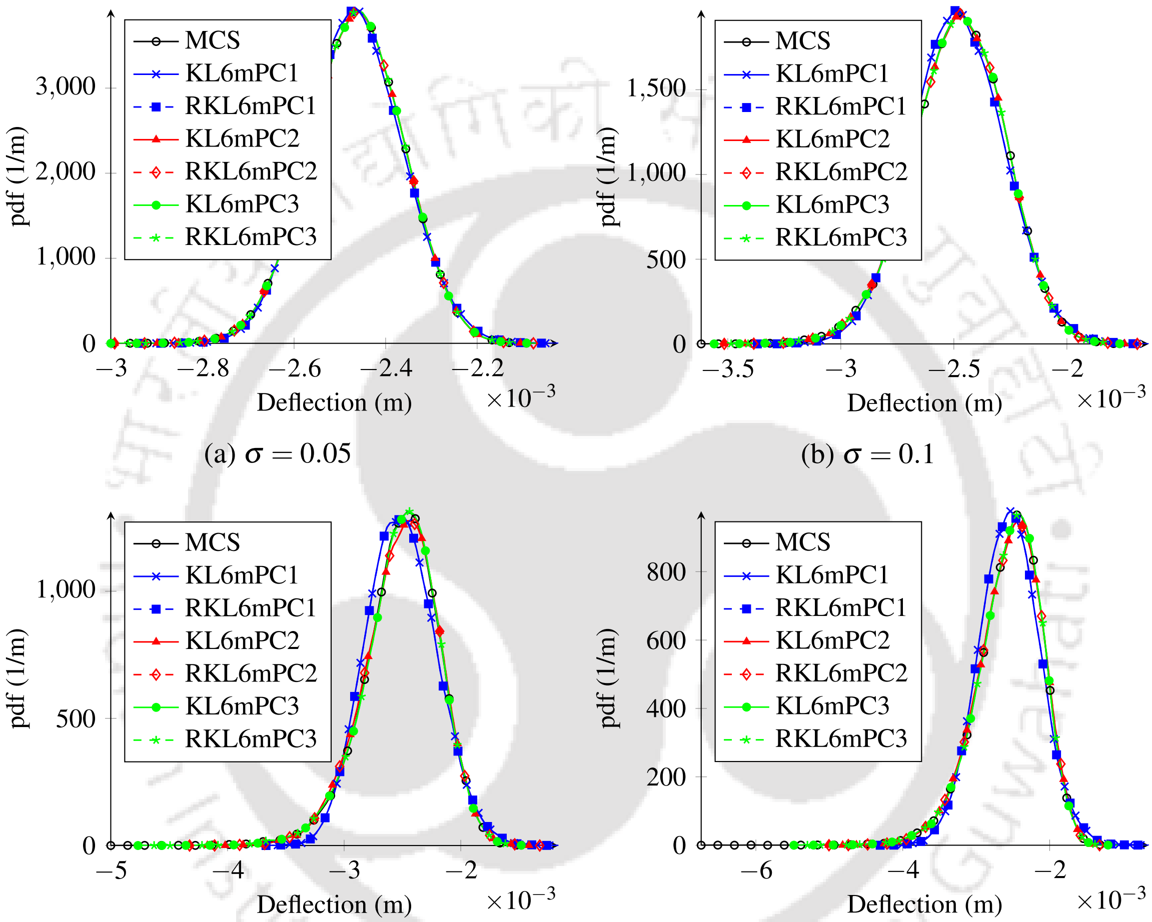

(a) $\sigma = 0.05$ (b) $\sigma = 0.1$

(c) $\sigma = 0.15$ (d) $\sigma = 0.2$

Fig. 4.12: pdf of tip deflection of cantilever beam for different orders of mPC expansion and comparison with MCS ($\sigma = \{0.05\ \ 0.1\ \ 0.15\ \ 0.2\}$).

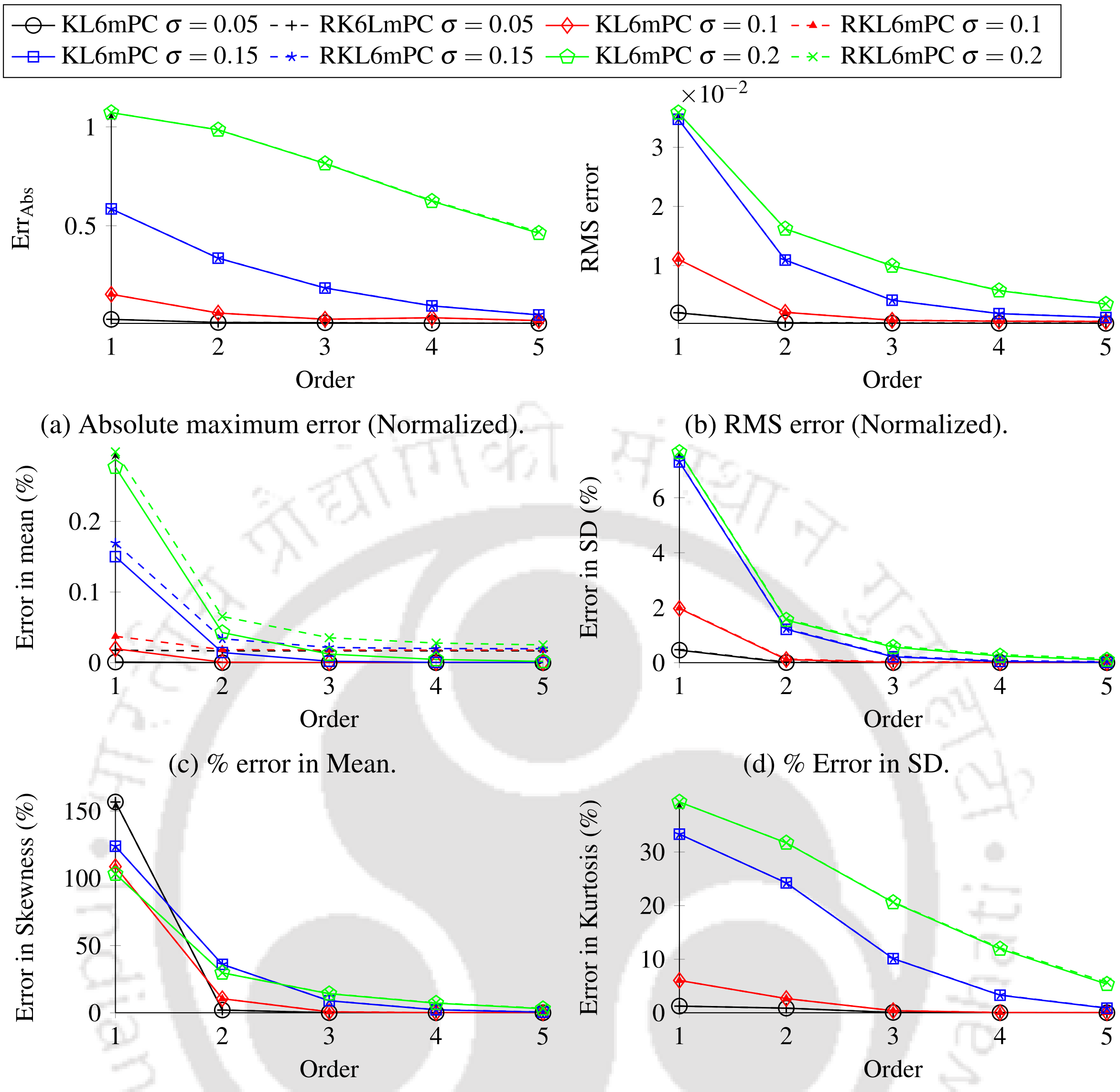

(a) Absolute maximum error (Normalized).

(b) RMS error (Normalized).

(c) % error in Mean.

(d) % Error in SD.

(e) % Error in Skewness.

(f) % Error in Skewness.

Fig. 4.13: Various error quantities in tip deflection of cantilever beam using mPC based method and mPC based method with reduced stiffness matrix for different orders of mPC.

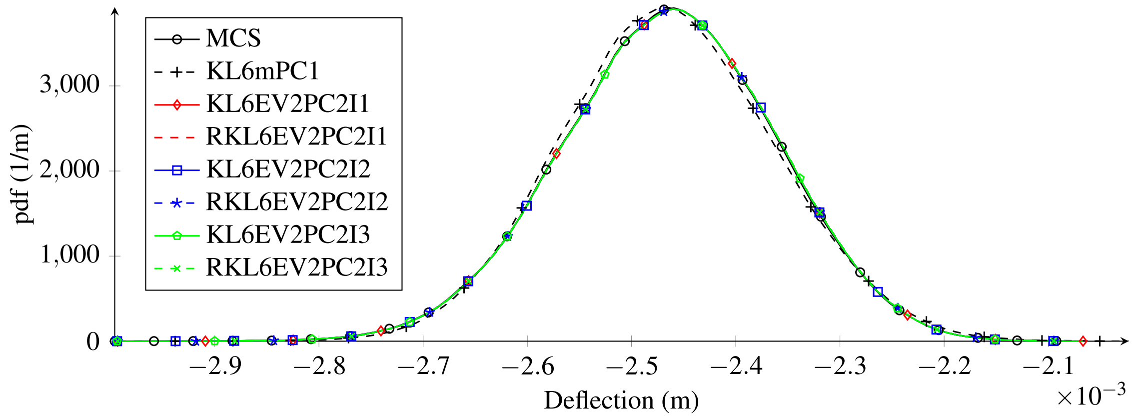

(a) Second order.

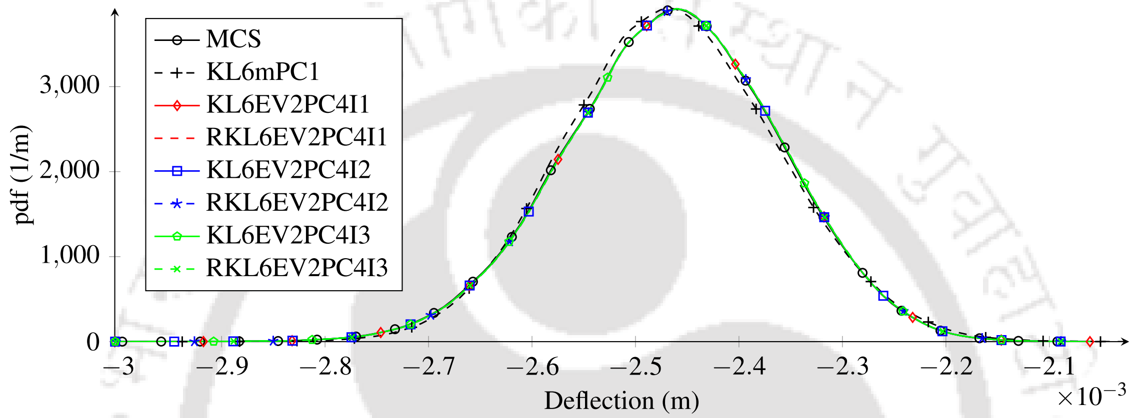

(b) Fourth order.

Fig. 4.14: pdf of tip deflection of the cantilever beam solve using propose method with different orders and iterations and comparison with MCS and KL6PC1 ($\sigma = 0.05$).

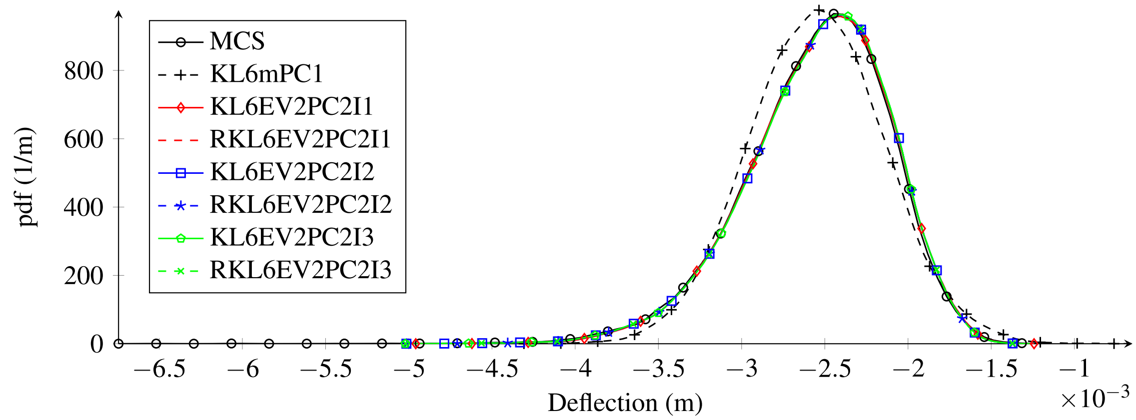

(a) Second order.

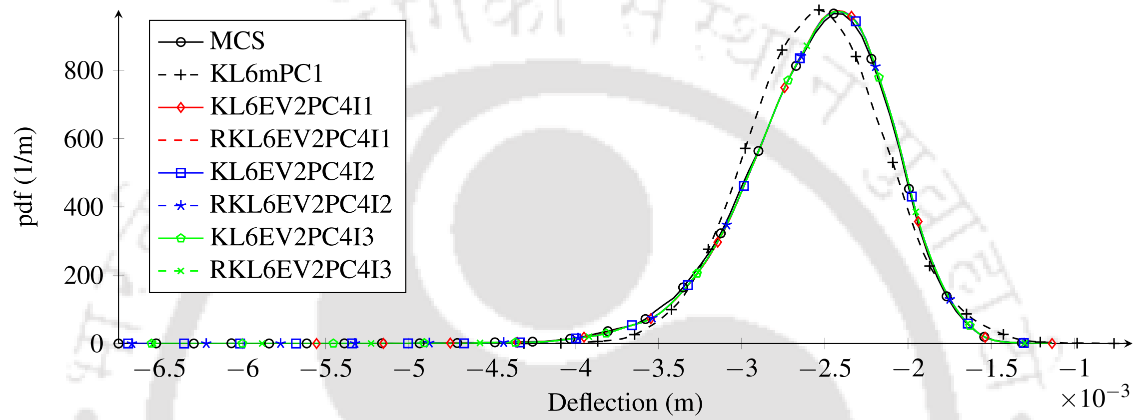

(b) Fourth order.

Fig. 4.15: pdf of tip deflection of the cantilever beam solve using propose method with different orders and iterations and comparison with MCS and KL6PC1 ($\sigma = 0.2$).

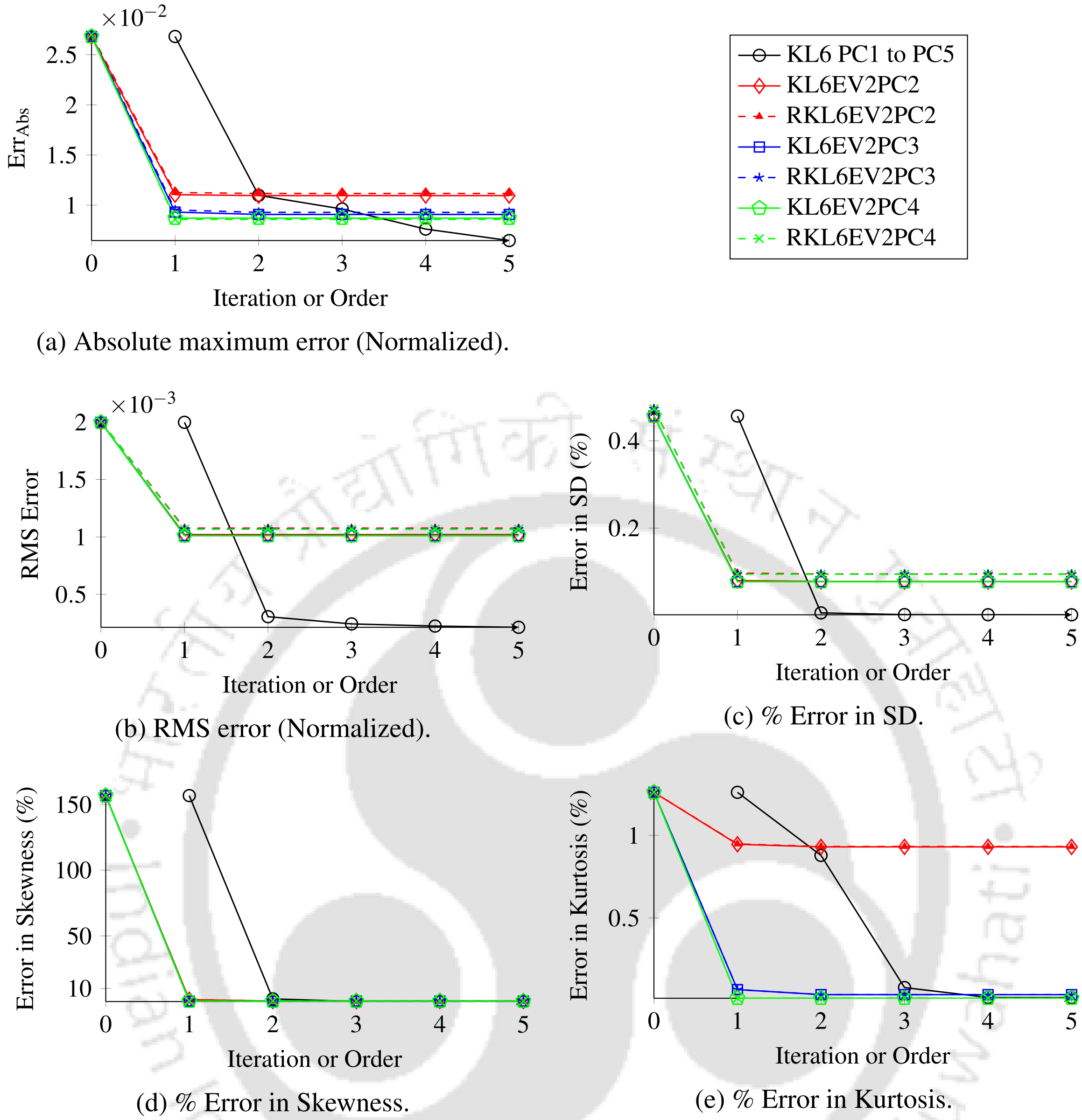

(a) Absolute maximum error (Normalized).

(b) RMS error (Normalized).

(c) % Error in SD.

(d) % Error in Skewness.

(e) % Error in Kurtosis.

Fig. 4.16: Various error quantities in tip deflection of cantilever using Proposed iterative method and Proposed iterative method with reduces stiffness matrix for different orders of PC with two random vectors in the iteration process ($\sigma = 0.05$).

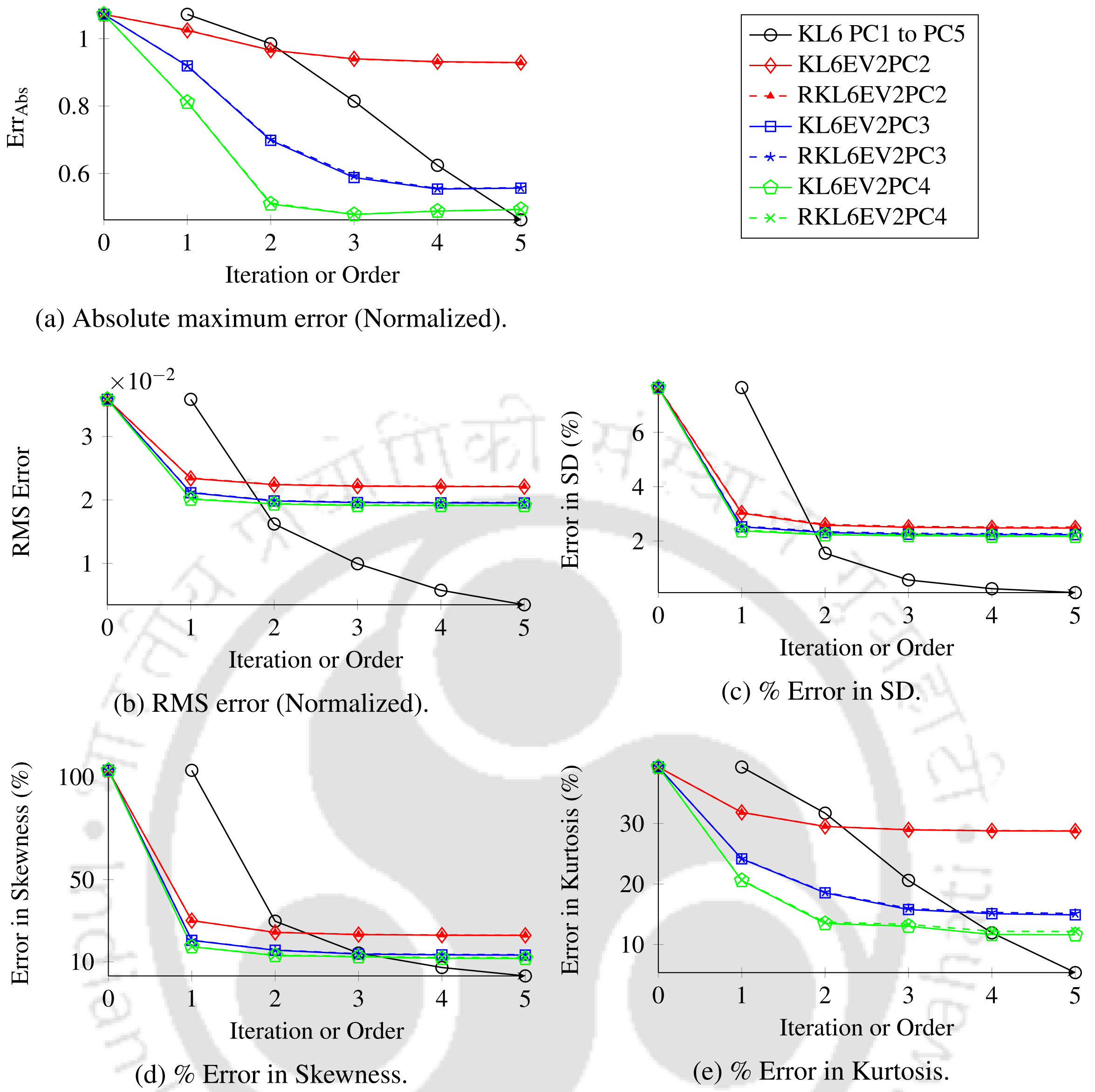

(a) Absolute maximum error (Normalized).

(b) RMS error (Normalized).

(c) % Error in SD.

(d) % Error in Skewness.

(e) % Error in Kurtosis.

Fig. 4.17: Various error quantities in tip deflection of cantilever using Proposed iterative method and Proposed iterative method with reduces stiffness matrix for different orders of PC with two random vectors in the iteration process ($\sigma = 0.2$).

4.4.2.3 Computational aspect

The responses of the proposed scheme for an order of iterative PC (ImPC) are observed to be comparable with responses of mPC of some higher order. In case of the proposed ImPC, the matrix size is smaller than conventional gPC or mPC, which will enable to perform analysis with lesser computational resources. However, for attaining accuracy in the proposed ImPC method, it is required to carry out analysis in an iterative manner. In case of MCS, the computational cost for inversion is 3×10^4 times N^3. The result of fourth order mPC and third order proposed ImPC method are observed to be comparable and computational complexity is compared. The computational complexities of mPC are $[N\times(P+)]^3 = (N\times 210)^3$, whereas in case of proposed ImPC method, the same is calculated from cumulative contribution from PC solution of first order and third order ImPC method with number of iterations. The total complexity in case of 3 iterations are thus observed as $(N\times 7)^3 + 3(N\times 15)^3$. In case of reduced stiffness method the computational complexity can be calculated by replacing N with S. In the present beam problem, $N = 120$ and $S = 18$ and the ratios of computation complexity for matrix inversion for MCS, mPC based and proposed ImPC method and reduced proposed ImPC method are $849.15 : 2.62\times 10^5 : 296.3 : 1$. In case of mPC and ImPC method, some additional time is required for calculation of ensembles of responses, which however is marginal. Further, additional time is required in the ImPC method for solution of eigenvalue problem, which is required to calculate the random variables to be used in each iteration. However, it is marginal as compared to the reduction in computational complexity due to reduced size of system matrix.

4.4.3 Foundation on a random soil layer : A plane stress problem

The third example considered is a problem on settlement of foundation already discussed in section 3.5.3. However, in this case the randomness is considered as non-Gaussian random field instead of Gaussian. The problem is shown in Fig. 4.18 for ready reference. The present problem considers Young's modulus as 1-D spatially varying random field in the vertical direction expressed as

$$E(y,\theta) = E_0[1+\alpha(y,\theta)] \tag{4.17}$$

where E_0 $(=50\times 10^6$ Pa$)$ is the mean of the random field and $\alpha(y,\theta)$ is a homogeneous zero mean log-normal random field with an exponential covariance function

$$\boldsymbol{C}(y_1,y_2) = \sigma^2 \exp\left(\frac{-|y_1-y_2|}{L_c}\right) \tag{4.18}$$

σ is the SD of the random field, and L_c is correlation length. The value of length of the process is $t_h/2$ and the correlation length is considered as $t_h/2$.

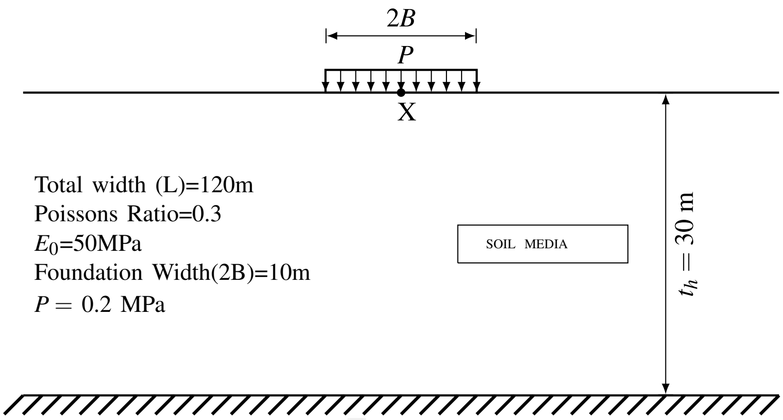

Fig. 4.18: Foundation resting on soil strata.

4.4.3.1 Requirement of discretization

The problem is idealized as a plane stress problem and modelled using 4 noded isoparametric elements. The requirement of discretization in the case of Gaussian randomness is discussed in section 3.5.3.1. Since the discretization depends on the covariance function rather than the type of randomness, the same discretization as shown in Fig. 3.17 is considered in the present case also. Similar to the beam problem, the random field is discretized using KL expansion and six eigenvectors are considered in the analysis. ICA is performed on the random variables generated using iterative KL expansion for the considered covariance function and distribution. Random variables after 6^{th} iteration is considered for performing transformation using ICA. Since the random variables are of different distribution, these are transformed to standard Gaussian distribution for the generation of PC.

4.4.3.2 Settlement of foundation

Similar to the beam problem, the settlement of foundation (Fig. 4.18) is also analysed using mPC of different orders and the proposed method for SD of random field $\sigma = \{0.1 \;\; 0.2\}$ and the results are compared with the results of MCS. Using the proposed iterative scheme, the plane stress problem is initially solved using first order mPC expansion and subsequently the responses are used to generate an iterative PC. It is observed that the cumulative expected energy of the response covariance function considering the first three modes is more than 99%. Thus, using first order mPC response, three random variables are considered for the iteration process. As the number of DOFs are very high and a higher order mPC expansion is required for improving accuracy, the problem is solved using reduced stiffness matrix. The ratio, $\lambda_{0_1}/\lambda_{0_S}$ is considered as less than 10^{-3} for reduction of size of the stiffness matrix, which yields the value of S as 1089. Thus, a matrix size of 2926×2926 reduces to 1089×1089. The pdfs of the vertical deflection of the mid point of foundation (point X in Fig. 4.18) for SD equal to 0.1 and 0.2 are shown in Figs. 4.19 and 4.20 respectively. It is observed that the pdf of first order PC based method (KL6mPC1) does not match with MCS results. It is further observed that the pdf of vertical deflection at point X converges towards MCS as the order or/and iteration increases, while evaluating using the proposed ImPC. Various errors associated with the response for SD equal to 0.1 and 0.2 are shown in Figs. 4.21 and 4.22 respectively. For comparison with mPC based method, the error associated with different orders of mPC with reduced stiffness are also plotted along y axis *vs* number of orders along x axis. It can be observed that the error in 3rd order mPC is comparable to the 3rd order proposed ImPC with 2 iteration. However, the number of random variables in case of PC is six, while it is only three in case of proposed scheme.

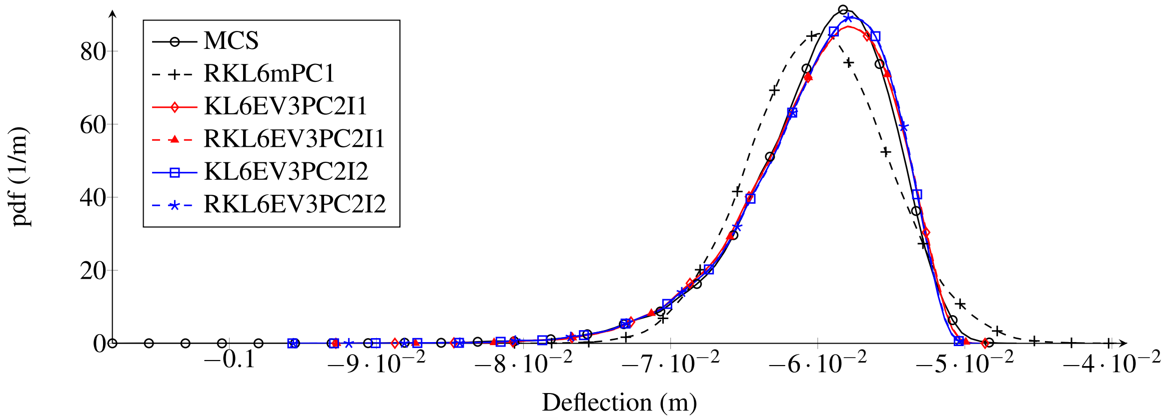

(a) Second order.

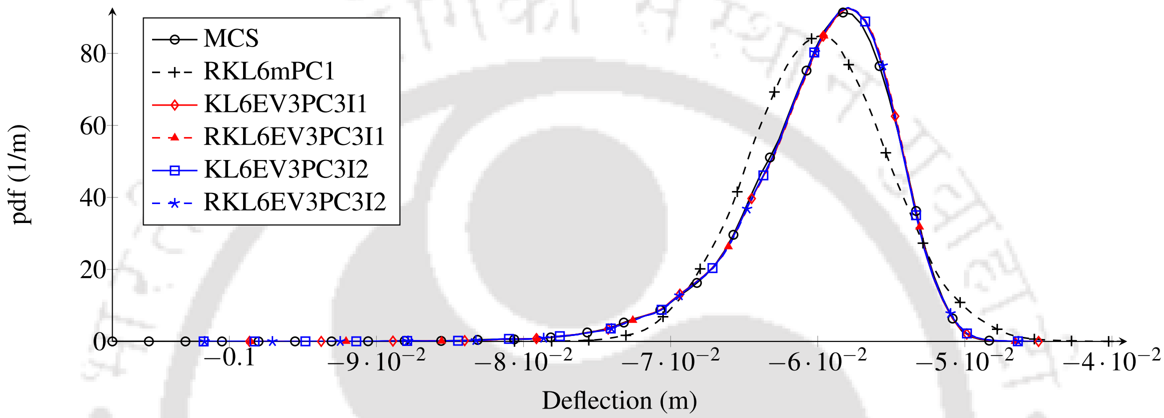

(b) Third order

Fig. 4.19: pdfs of vertical displacement at mid point of foundation solve using proposed method with different orders and iteration compare with MCS and KL6mPC1 ($\sigma = 0.1$).

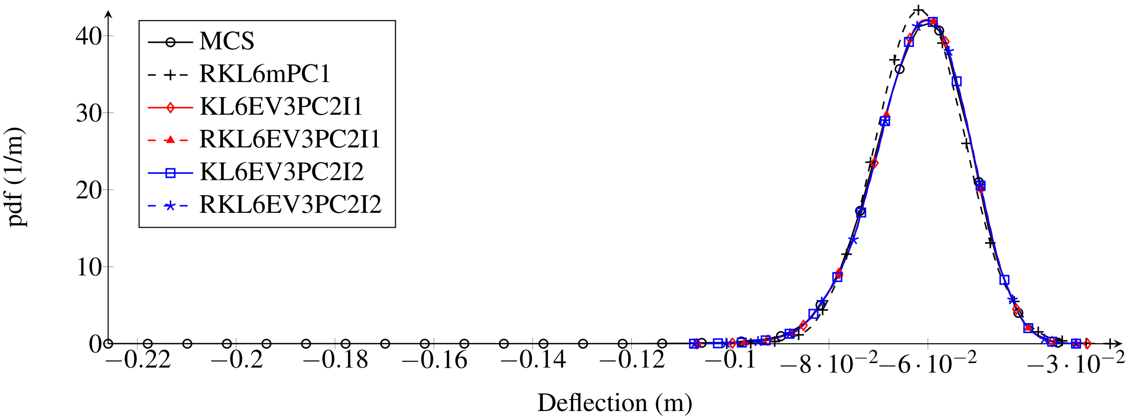

(a) Second order.

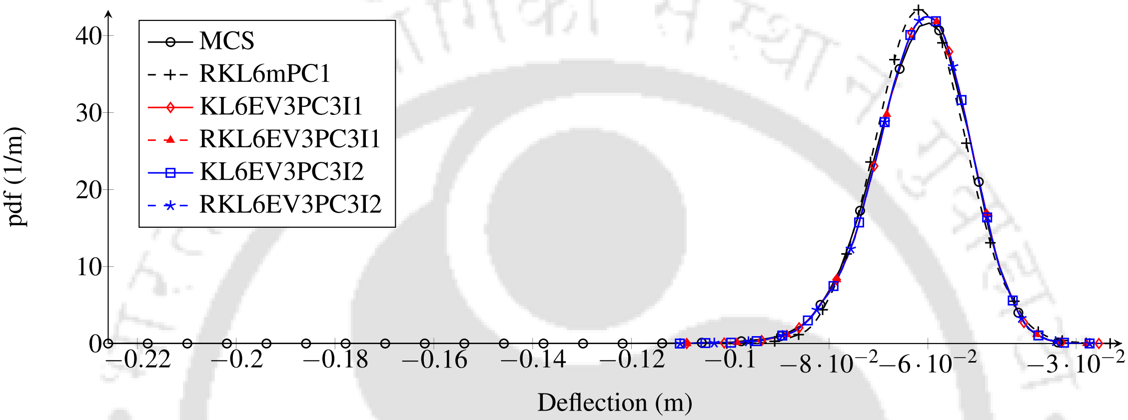

(b) Third order

Fig. 4.20: pdfs of vertical displacement at mid point of foundation solve using proposed method with different orders and iteration compare with MCS and KL6mPC1 ($\sigma = 0.2$).

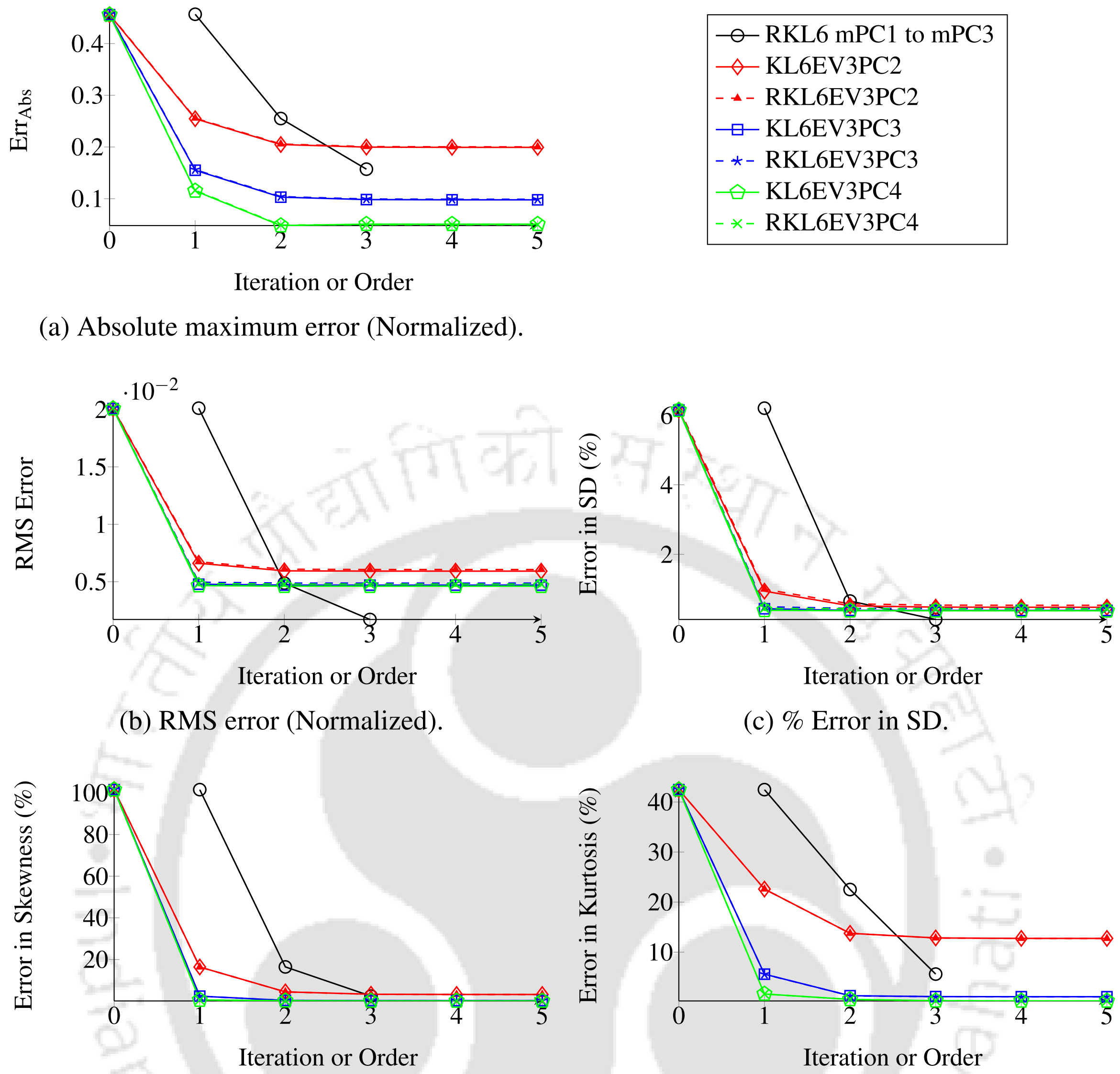

(a) Absolute maximum error (Normalized).

(b) RMS error (Normalized).

(c) % Error in SD.

(d) % Error in Skewness.

(e) % Error in Kurtosis.

Fig. 4.21: Various error quantities in vertical deflection at mid point of foundation (point X) using Proposed iterative method and Proposed iterative method with reduced stiffness matrix for different orders of PC with three random variables in the iteration process ($\sigma = 0.1$).

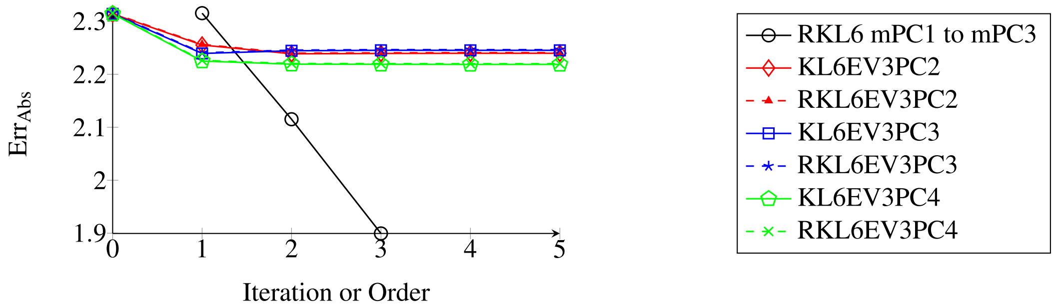

(a) Absolute maximum error (Normalized).

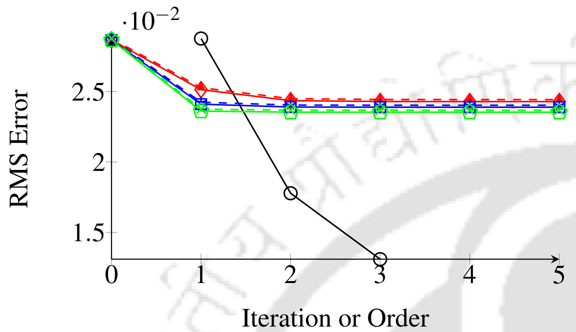

(b) RMS error (Normalized).

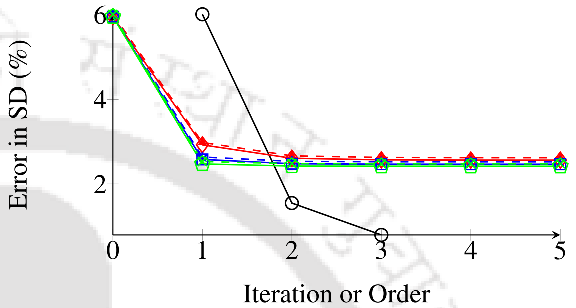

(c) % Error in SD.

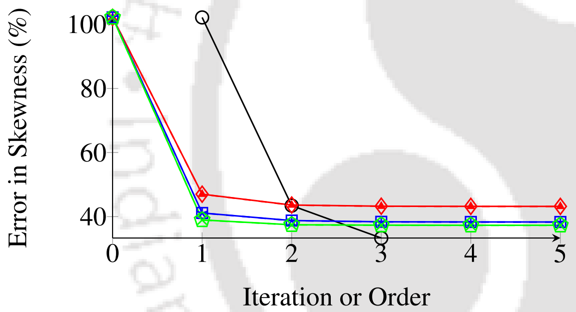

(d) % Error in Skewness.

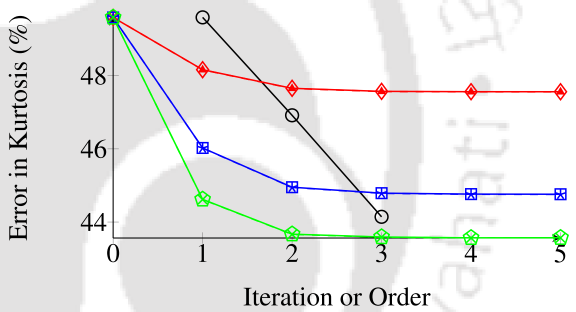

(e) % Error in Kurtosis.

Fig. 4.22: Various error quantities in vertical deflection at mid point of foundation (point X) using Proposed iterative method and Proposed iterative method with reduced stiffness matrix for different orders of PC with three random variables in the iteration process ($\sigma = 0.2$).

4.4.3.3 Computational aspect

The size of the system matrix is significantly large even with the adopted reduced stiffness scheme in case of mPC. The proposed ImPC scheme however employs a much smaller size of matrices as compared to mPC. The size of mPC expansion for 3rd order PC with three and six random variables are 20 and 84 respectively. Thus, the system matrix in ImPC is much smaller as relatively lesser number of random variables are required as compared to mPC. Computational complexity for matrix inversion in case of MCS, 3rd order mPC with reduced stiffness, 3rd order ImPC with 3 random variables and 2 iterations and 3rd order ImPC with 3 random variables and 2 iterations with reduced stiffness are $30 \times 10^3 \times 2926^3 : (84 \times 1089)^3 : (7 \times 2926)^3 + 2(20 \times 2926)^3 : (7 \times 1089)^3 + 2(20 \times 1089)^3 = 35.607 : 36.267 : 19.3972 : 1$. Thus, huge computational efficiency can be observed in ImPC, which would be really advantageous for solving any real time problem with large degrees of freedom. Moreover, in the context of the present problem, mPC could be used only for system with reduced stiffness matrix as degree of freedom for the problem with full stiffness matrix is very high and could not be solved due to the constraint in the available computational facility. The solution of 3rd order mPC with full stiffness will exhibit a much higher ratio of computational complexity of matrix inversion when compared with ImPC with a similar full system matrix and thus will demand computational facility of even higher specification. Thus, while ImPC could be successfully used to solve the problem within acceptable error limit, the same problem however, could not be solved using mPC. The system matrix size in case of 3rd order mPC and 3rd order mPC with reduced stiffness are $(84 \times 2926) \times (84 \times 2926)$ and $(84 \times 1089) \times (84 \times 1089)$ respectively. However, in case of ImPC with full and reduced stiffness matrix, the maximum system matrix sizes are $(20 \times 2926) \times (20 \times 2926)$ and $(20 \times 1089) \times (20 \times 1089)$ respectively. Thus, ImPC demands much lesser RAM, which is evident from the fact that the mPC with even reduced system could not be implemented beyond third order using the available facility as presented in Figs. 4.21 and 4.22. However, in case of mPC and proposed ImPC method, additional time is required for calculation of ensembles of responses, which however is marginal. Further, additional time is required in the proposed method for solution of eigenvalue problem required to calculate the random variables to be used in each iteration, which is also insignificant as compared to overall computational time.

4.4.3.4 Convergence study of responses

The convergence and accuracy of the evaluated responses using the proposed ImPC are assessed with respect to MCS as demonstrated in the earlier section. However, in the absence of any such reference results, the responses can be checked for convergence to accurate values by utilizing the responses from successive higher orders and iterations. The rate of convergence of responses is studied by considering two successive iterations for a particular order and calculating their differences in absolute maximum, RMS, and statistical moments. The responses are considered to have converged when the rate is near to zero. The error in different statistical parameters for a particular order of expansion varying with different iteration for SD={0.1, 0.2} are shown in Figs. 4.23 and 4.24 respectively. It can be observed that the rate of convergence is near to zero after 4^{th} iteration for all the three orders considered (2^{nd}, 3^{rd}, 4^{th}). Thus, 4 iterations are sufficient to achieve a converged response in a particular order for the problem considered and can be treated as a stopping criteria. Further, convergence to the accurately estimated responses are assessed by considering converged responses (e.g. corresponding to 4^{th} iteration) of successive orders and calculating the difference in all the earlier adopted statistical parameters between two such responses. Figs. 4.25 and 4.26 show the error between two successive orders upto 4^{th} for SD 0.1 and 0.2 respectively. It can be clearly observed from Figs. 4.23-4.26 that as the orders and iterations of ImPC increase, the responses converge and the errors associated with the converged response for the expansion with highest number of orders considered are practically zero. Thus the responses corresponding to 4^{th} and 5^{th} order and 4^{th} iteration are very accurate, which is further substantiated from Figs. 4.21 and 4.22, where the evaluated errors with respect to MCS also lead to a similar conclusion.

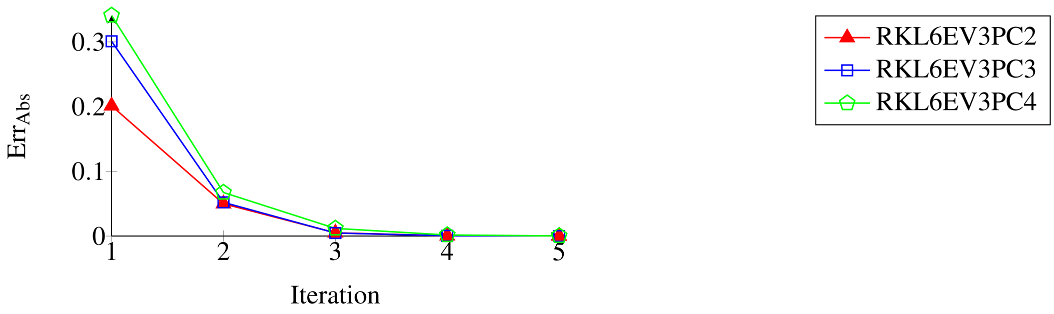

(a) Absolute maximum Error (Normalized).

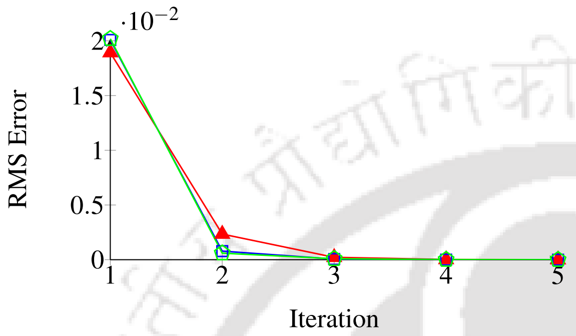

(b) RMS Error (Normalized).

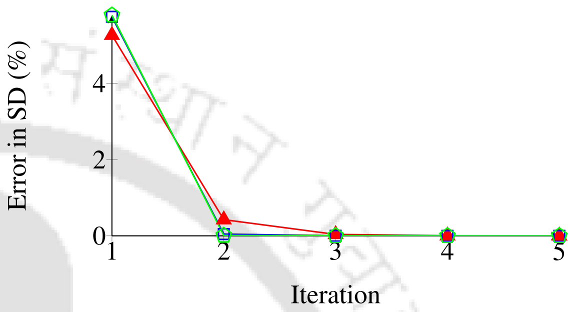

(c) % Error in SD.

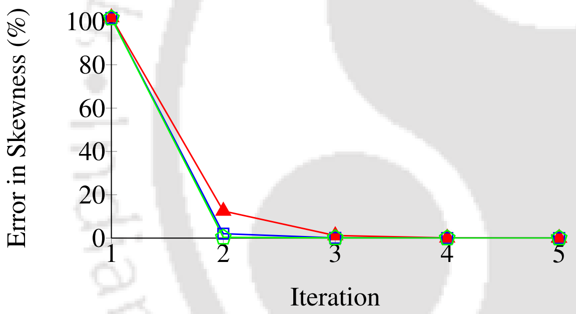

(d) % Error in Skewness.

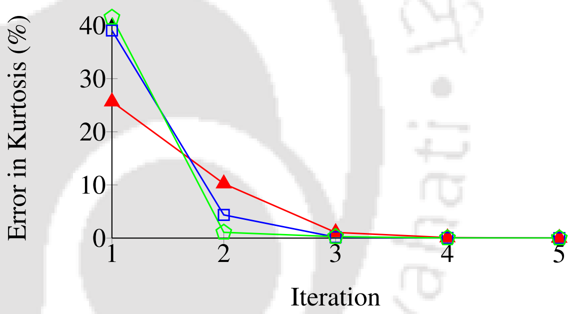

(e) % Error in Kurtosis.

Fig. 4.23: Convergence of error in vertical deflection at mid point of foundation (point X) in different error measures with iteration for different orders in ImPC ($\sigma = 0.1$).

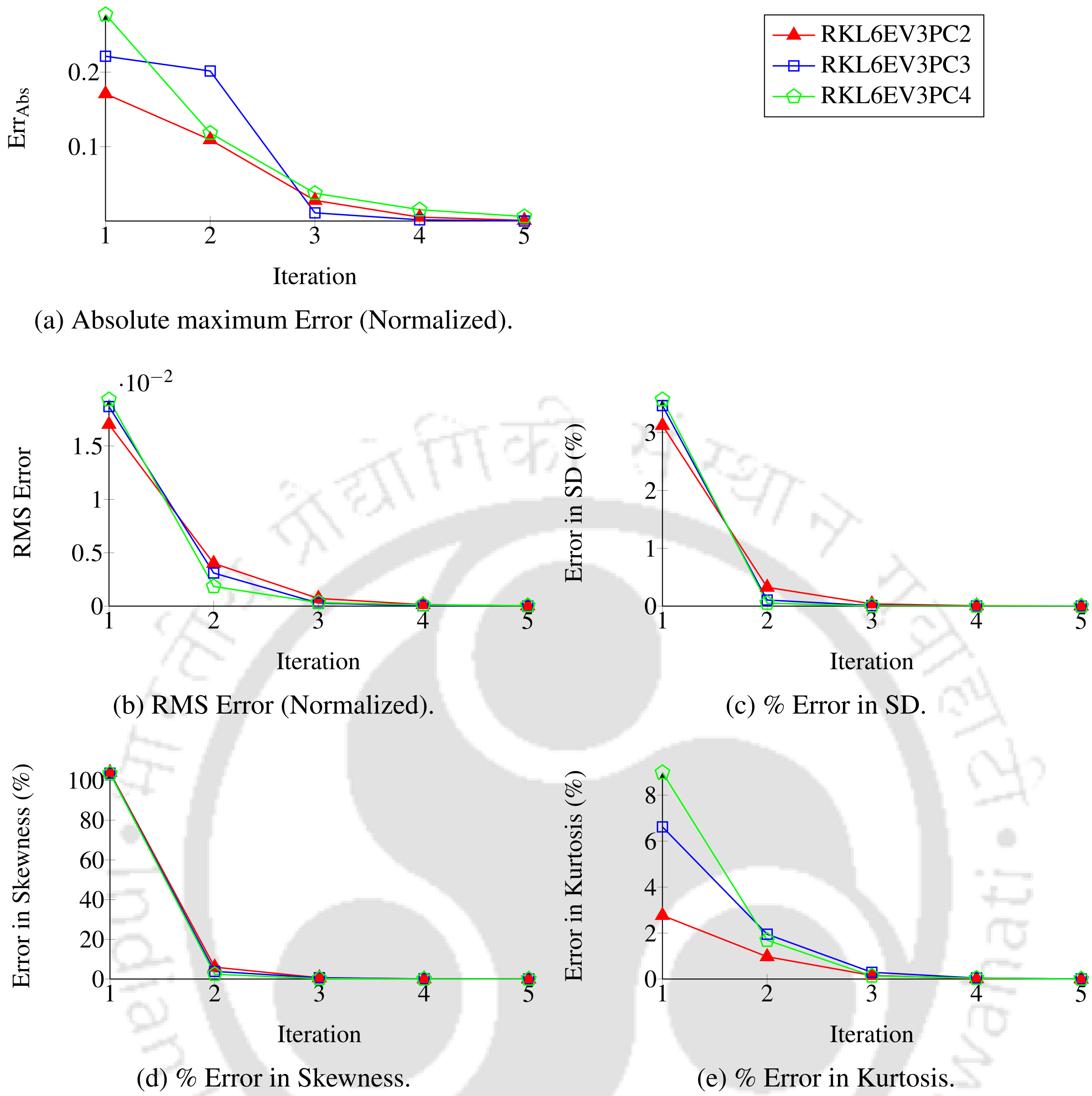

Fig. 4.24: Convergence of error in vertical deflection at mid point of foundation (point X) in different error measures with iteration for different orders in ImPC ($\sigma = 0.2$).

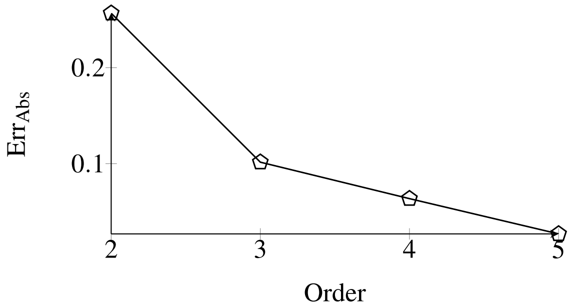

(a) Absolute maximum Error (Normalized).

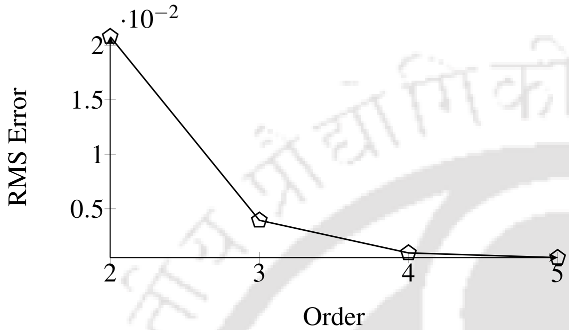

(b) RMS Error (Normalized).

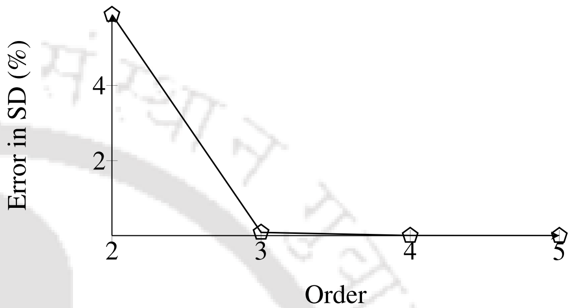

(c) % Error in SD.

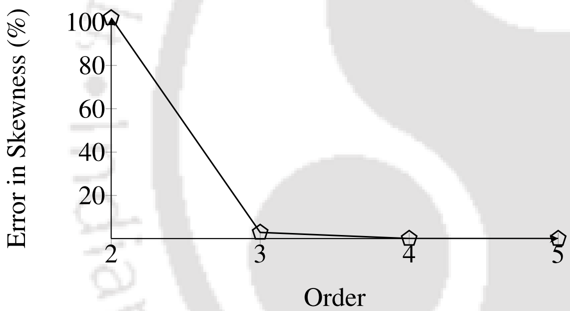

(d) % Error in Skewness.

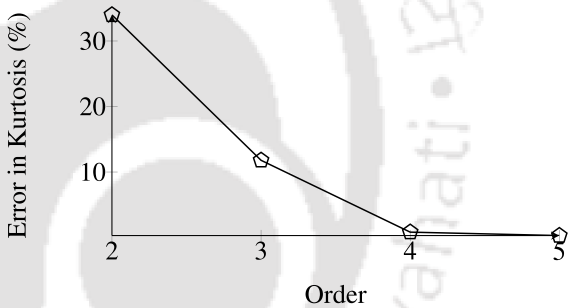

(e) % Error in Kurtosis.

Fig. 4.25: Convergence of error in different error measures for converged solution (corresponding to 4^{th} iteration) at mid point of foundation (point X) for different orders of ImPC ($\sigma = 0.1$).

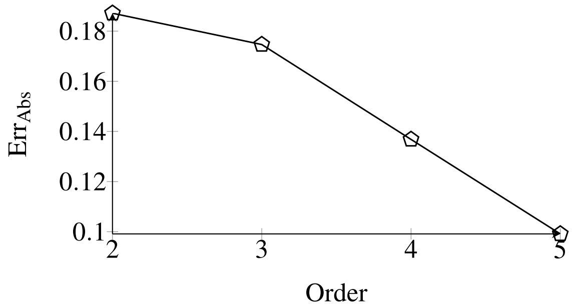

(a) Absolute maximum Error (Normalized).

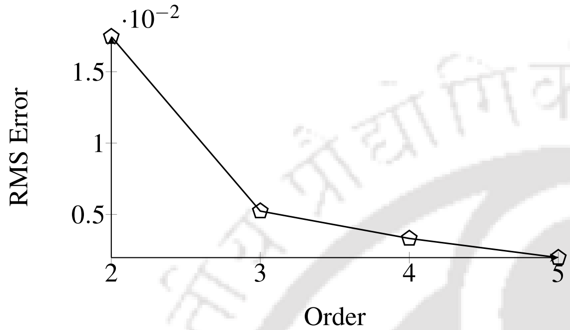

(b) RMS Error (Normalized).

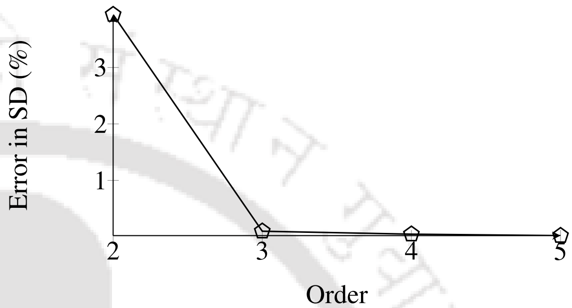

(c) % Error in SD.

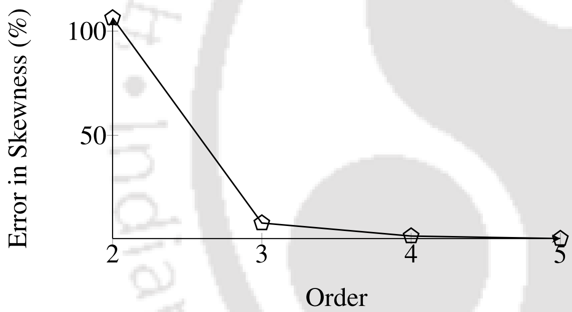

(d) % Error in Skewness.

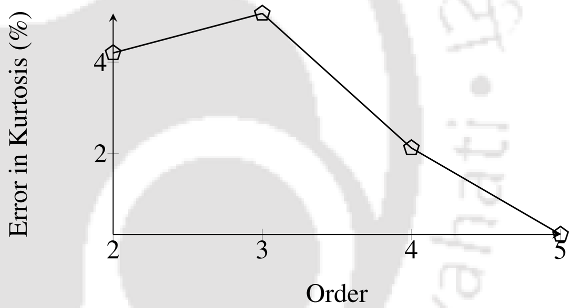

(e) % Error in Kurtosis.

Fig. 4.26: Convergence of error in different error measures for converged solution (corresponding to 4^{th} iteration) at mid point of foundation (point X) for different orders of ImPC ($\sigma = 0.2$).

4.5 Conclusions

A PC framework based numerical strategy to solve stochastic linear elastostatic mechanics problems with random coefficients is presented, which is observed to be more efficient in terms of computational demand and accuracy than generalized PC based method for the problem types considered. The proposed method iteratively generates PC, based on the responses of previous iteration. A method to construct PC for arbitrary pdf is also presented, which is based on Gram-Schmidt orthogonalization process. The proposed iterative method can efficiently solve non-Gaussian structural mechanics problem. Iterative KL expansion is considered for the generation of non-Gaussian random fields. However, the random variables for non-Gaussian random field in KL expansion are statistically. Thus, ICA is introduced to minimize statistical dependency of the random variables. The proposed method addresses at multiple levels, the issue related to the increase in size of the system matrix with increase in the order of expansion in mPC. First, it reduces the discretization requirement by representing the eigenvector of KL expansion at Gauss points instead of mid points of elements. The numbers of random variables to represent the response in PC expansion are reduced by considering only the dominant components of the response using KL expansion after the first order solution using PC expansion. The reduction in size of stiffness matrix by considering eigen decomposition (Pascual and Adhikari, 2012) further reduces the system matrix without compromising the accuracy of the results. The proposed iteration scheme is successfully used to solve multiple examples, where very good agreement is observed with MCS. Higher order expansion is used in ImPC for obtaining accurate response, which however could not be used in mPC due to constraint in RAM of the available computational facilities. Thus, ImPC can be effectively implemented to obtained accuracy even with limited computational facilities. The convergence studies with successive orders and iterations also show that the proposed ImpC can be effectively used for the evaluation of response parameter for linear elastostaitc structural mechanics problem types considered in the present study with random modulus of elasticity, where MCS responses are not necessarily required for comparison.

5

Hybrid method of PDD and ImPC

Contents

5.1 Introduction

Iterative method for the solution of stochastic mechanics problem with random material properties is discussed in the previous two Chapters. The method is shown as a suitable alternative for computationally demanding MCS and an improved version of conventional PC based method, wherein the curse of dimensionality is appropriately addressed. Moreover, the ImPC method are mostly observed to provide more accurate results than conventional PC based method, while adopting same order of expansion. It has also been shown that the proposed method is able to solve a comparatively large stochastic system, where conventional PC may fail due to relatively large size of the system matrix.

PDD is one of the dimension reduction techniques, where the multidimensional (multivariate) function is represented using multiple smaller dimensional functions. PDD can represent the responses with a lesser number of random variables, thus reduces the size of the system matrix. Complete responses are expressed by the weighted sum of individual reduced dimension components calculated using standard gPC based method or some other methods. Thus, PDD is seen as a further improvement in the process of reduction of dimensional curse in approximate estimation of the stochastic responses. In the present study, it is proposed to consider a hybrid method comprising of PDD and previously proposed ImPC to evaluate structural responses. PDD is considered to reduce the dimension of the problem, and each component responses are evaluated using ImPC. Adoption of ImPC in place of conventional PC is expected to further enhance the computational efficacy of the PDD based approach.

The chapter is organized as follows. In section 5.2, the basic philosophy of PDD is discussed. The detailed discussion on hybrid PDD and ImPC method is discussed in section 5.3 followed by numerical examples in section 5.4. The formulation of SFEM for Gaussian and non-Gaussian material is discussed in Chapter 3 and 4 respectively. In case of random field problem, the discretization and simulation of random field are carried out as discussed in section 3.4.2 and 4.2.1 respectively for Gaussian and non-Gaussian random field. Numerical studies are carried out involving both Gaussian and non-Gaussian randomness. Similar to the previous chapters, the PCs are generated using Gram-Schmidt orthogonalization process as formulated in section 3.4.3.

5.2 Polynomial dimensional decomposition (PDD)

PDD is one of the dimension reduction techniques where a multidimensional (multivariate) function is represented using multiple smaller dimensional functions. Rahman and Xu (2004) proposed univariate dimension reduction for stochastic mechanics problem. The method was further improved by Xu and Rahman (2004) using multidimensional dimension reduction technique. PDD addresses the curse of dimensionality using a hierarchical decomposition of a multivariate response function in terms of variables with increasing dimensions. PDD deflates the curse of dimensionality to some extent by developing an input-output behaviour of complex systems with low effective dimensions, which are highly non-linear. PDD arranges terms of the expansion considering degree of interaction among the finite number of random variables rather than order of polynomial, which is generally considered in PC. The method is observed to be accurate, convergent and computationally efficient for probabilistic estimation of random mathematical functions and mechanical systems.

Complete responses are given by a weighted sum of individual reduced dimension components calculated using standard gPC based method or other methods. A random function y is considered with Q random input quantities with prescribed pdfs. $\{\mu_1, \mu_2, \mu_3, \dots \mu_Q\}$ are the mean of the random variables $\{x_1, x_2, x_3, \dots \mu_Q\}$. The approximation of y using bivariate PDD is given by,

$$\begin{aligned}\hat{y}(x) = &\sum_{i_1<i_2}^{Q} y_2(\mu_1, \mu_2, \dots, x_{i_1}, \dots \mu_{Q-r-1}, \mu_{Q-r} \dots, x_{i_2}, \dots, \mu_{Q-1}, \mu_Q) \\ &- (Q-2)\sum_{i=1}^{Q} y_1(\mu_1, \mu_2, \dots, x_{i_1}, \dots, \mu_{Q-1}, \mu_Q) \\ &+ \frac{(Q-1)(Q-2)}{2} y_0(\mu_1, \mu_2, \mu_3, \dots \mu_Q)\end{aligned} \tag{5.1}$$

where y_2, y_1 and y_0 are the bivariate, univariate and component with all mean value respectively. The individual components are evaluated using any PC based or any other methods. The generalized form of a S variate PDD is given by,

$$\hat{y} = \sum_{i=0}^{S} (-1)^i \binom{Q-S+i-1}{i} y_{S-i} \ , \quad S \leq Q \tag{5.2}$$

5.3 Hybrid method combining PDD and ImPC

5.3.1 Basic philosophy

As discussed in previous chapters (Chapters 3 and 4), random field for material (Young's modulus) is discretized and generated using KL expansion. In the case of Gaussian random fields, the discretization using KL expansion is discussed in section 3.2.1, and the case of non-Gaussian random fields is discussed in section 4.2.1. Moreover, in the case of non-Gaussian random fields, ICA is carried out on the random variables generated in iterative KL expansion as discussed in section 4.2.2. The number of random variables in stochastic FEM is decided based on the expected energy criteria of the covariance function considered. The formulation of SFEM is discussed in section 3.2.2 and 4.2.3 for Gaussian and non-Gaussian random field respectively. The multivariate SFE equation (Eq. 3.6 or Eq. 4.8) are transformed to mean and multiple uni-, bi- and higher variate components using PDD as discussed in section 5.2. Each component of PDD can be solved using PC as discussed in section 3.3. In the current study, it is proposed to consider the previously developed ImPC (Chapters 3 and 4) to be used for the solution of each component of PDD. The stepwise procedure for the hybrid method is discussed in the next section.

5.3.2 Hybrid PDD-ImPC method

Once the SFE equations are formulated (Eq. 3.6 or Eq. 4.8), the responses are required to be evaluated. PDD considers the responses as a linear combination of univariate and higher variate components. Thus,

$$\boldsymbol{u} = a_0\boldsymbol{u}_0 + a_1\boldsymbol{u}_1 + a_2\boldsymbol{u}_2 + \dots \tag{5.3}$$

where $\boldsymbol{u}_0$ is the mean component of responses when SFE equations (Eq. 3.6 or Eq. 4.8) are solved for all the $\xi_i(\theta)$ at mean value. This can be done by taking expectation of Eq. 3.6 or Eq. 4.8 and solving for $\boldsymbol{u}$. However, in the present study as KL expansion is considered to discretize the random field, all the $\xi_i(\theta)$ have a zero mean. Thus $\boldsymbol{u}_0$ can be calculated from deterministic equations at mean value of the random field. $\boldsymbol{u}_1$ is the univariate components of responses and can be calculated by considering only one of the $\xi_i(\theta)$ at a time and other components as mean value. For Q terms in the KL expansion, there would be a total Q univariate components. Thus,

$$\boldsymbol{u}_1 = \sum_{i=1}^{Q} \boldsymbol{u}_1^{(i)}(\xi_i(\theta)), \quad \text{with } \xi_{j\neq i_1}(\theta) = \langle \xi_{j\neq i_1}(\theta) \rangle \tag{5.4}$$

Similarly, responses corresponding to bivariate components, $\boldsymbol{u}_2$ can be calculated by considering two of the $\{\xi_{i_1}(\theta), \xi_{i_2}(\theta)\}$ at a time and other $\xi_i(\theta)$ as their mean values. Similar procedure is followed for higher variate components.

Each component of uni-, bi-, and higher variate components can be solved to obtain the responses corresponding to each component using ImPC, rather than PC. For Q terms in the KL expansion, number of terms in each variate can be calculated as $\binom{Q}{S}$, where S is the variate of PDD. The bi-variate component is

$$\boldsymbol{u}_2 = \sum_{i_1<i_2}^{Q} \boldsymbol{u}_2^{(i_1 i_2)}(\xi_{i_1}(\theta), \xi_{i_2}(\theta)), \quad \text{with } \xi_{j\neq i_1}(\theta) = \langle \xi_{j\neq i_1}(\theta) \rangle, \ \xi_{j\neq i_2}(\theta) = \langle \xi_{j\neq i_2}(\theta) \rangle \tag{5.5}$$

The coefficient a_0, a_1, a_2 etc. can be calculated from Eq. 5.2. Thus

$$a_i = (-1)^i \binom{Q-S+i-1}{i} \tag{5.6}$$

In particular for structural mechanics problem with random field discretized using KL expansion, the mean value of random variables $\xi_i(\theta)$ are zero. Thus, Eqs. 5.4 and 5.5 become

$$\boldsymbol{u}_1 = \sum_{i=1}^{Q} \boldsymbol{u}_1^{(i)}(\xi_i(\theta)) \tag{5.7}$$

$$\boldsymbol{u}_2 = \sum_{i_1<i_2}^{Q} \boldsymbol{u}_2^{(i_1 i_2)}(\xi_{i_1}(\theta), \xi_{i_2}(\theta)) \tag{5.8}$$

respectively.

Stepwise algorithm:

A3-1 Perform KL expansion on the random field of Young's modulus

{

Discretize the covariance function of random field considering Gauss point of each element.

$$E(x,\theta) = E_0\left(1 + \sum_{n=1}^{Q} \xi_n(\theta)\sqrt{\lambda_n} f_n(x)\right)$$

Calculate the number of random variables (Q) based on expected energy consideration.

{

while energy $\leq$threshold

$Q = Q + 1$

energy=energy+$\lambda_Q/sum(\lambda)$

end while

}

}

A3-2 In case of non-Gaussian random field,

(a) Calculate random variables $\xi_n(\theta)$ iteratively as discussed in section 4.2.1

(b) Perform ICA on the random variables of KL expansion.

$$\xi_n(\theta)_{\text{Dependent}} \xrightarrow{\text{using FastICA}} \xi_n(\theta)_{\text{Independent}}$$

(c) The random variables after ICA are converted to random variables with identical probability distribution as (Also in case of random variables of different distribution)

$$\xi_n(\theta)_{\text{Independent}} \xrightarrow{\text{Non-linear transformation}} \xi_n(\theta)_{\text{Same disctribution}}$$

A3-3 Formulation of SFEM as discussed in section 3.2.2 or 4.2.3.

A3-4 Apply PDD on the SFE equations and generate the individual components to be solved.

A3-5 Chose a order of PC expansion (p) for the solution of each component of PDD.

A3-6 Solution for mean component

(a) Solve the mean equation considering mean values of the random variables (mean value of random variables are 0 in the case of KL random variables) in Eq. 3.6 or 4.8.

(b) Calculate the coefficient of PDD for mean component Eq. 5.2 or 5.6.

A3-7 Solution for each component of uni-variate and higher variate components adopting ImPC.

(a) Construct mPC of desired order (considered in step A3-5) using Gram-Schmidt orthogonalization process as discussed in section 3.4.3 using the random variables calculated in step A3-1 or A3-2c.

(b) Solve each component of PDD using Galerkin projection as discussed in section 3.3.

(c) Calculate ensemble of responses by multiplying the coefficients evaluated in step A3-7b with corresponding PC as per Eq. 3.7

(d) i. Perform KL expansion on the covariance function ($\boldsymbol{C}_{\boldsymbol{u}_1\boldsymbol{u}_2}$) of responses and new random variables $\xi_i(\theta)_{\text{new}}$ are calculated as,

$$\xi_i(\theta)_{\text{new}} = \frac{1}{\sqrt{\lambda_{\text{new}_i}}}\boldsymbol{u}_{\text{mean}}E_{\text{vector new}_i}$$

where λ_{new_i} and $E_{\text{vector new}_i}$ are the eigenvalue and eigenvector of the covariance function of the responses. $\boldsymbol{u}_{\text{mean}}$ is the matrix of zero mean responses.

The covariance function of responses is calculated as,

$$\boldsymbol{C}_{u_1u_2} = \mathbb{E}[(u_1 - \text{mean}(u_1))(u_2 - \text{mean}(u_2))]$$

ii. Calculate the optimal number of $\xi_i(\theta)_{\text{new}}$ based on expected energy consideration.

iii. Formulate the basis for Gram-Schmidt orthogonalization as discussed in section 3.4.3.

iv. Formulate PC using Gram-Schmidt orthogonalization process using $\xi_i(\theta)_{\text{new}}$ and as discussed in section 3.4.3.

v. Solve using new PC. Calculate ensemble of responses.

vi. Go to step A3-7d for next iteration.

A3-8 Calculate the coefficients of PDD expansion for each components (a_i) using Eq. 5.2 or 5.6.

A3-9 Calculate the complete responses by combining individual component responses from same iteration using linear combination as given Eq. 5.3.

A3-10 Calculate response statistics.

As mentioned in previous chapters, the random variables after ICA represent material property. The random variables after ICA is again transformed to same distribution (in step A3-2c) only to generate PC, not to represent material randomness.

5.4 Numerical study

The applicability of the proposed hybrid scheme for the solution of linear structural mechanics problems is demonstrated using two numerical examples. Settlement analysis of a foundation resting on a Gaussian random soil media and a 3-D Euler-Bernoulli cantilever beam with non-Gaussian random material are considered for this purpose. The materials are modelled as 1-D random field. MCS using deterministic FE method are performed to generate benchmark results in terms of statistical parameters for comparison of the accuracy of the proposed strategy. The same seeds of uncorrelated random variables are considered in all the methods so that there is no anomaly in the data while comparing results from different approaches. A sample size of 3×10^4 is considered for both the problems.

5.4.1 Foundation on a random soil layer : A plane stress problem

The first example considered is the same settlement of a foundation resting on random soil media problem considered in Chapter 3 (section 3.5.3). The problem is shown in Fig. 5.1 for ready reference. The present problem also considers randomness in Young's modulus as 1-D spatially varying random field in the vertical direction and expressed as

$$E(y,\theta) = E_0[1+\alpha(y,\theta)] \tag{5.9}$$

where E_0 $(=50\times10^6$ Pa) is the mean of the random field and $\alpha(y,\theta)$ is a homogeneous zero mean Gaussian random field with an exponential covariance function

$$\boldsymbol{C}(y_1,y_2) = \sigma^2 \exp\left(\frac{-|y_1-y_2|}{L_c}\right) \tag{5.10}$$

σ is the SD of the random field, and L_c is correlation length. The value of length of the process is $t_h/2$ and the correlation length is considered as $t_h/2$. The problem is solved for standard deviation $\sigma=\{0.1,\ 0.2\}$.

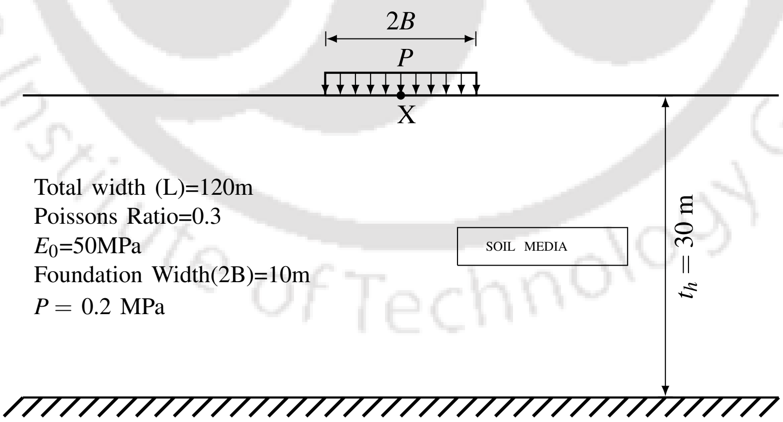

Fig. 5.1: Foundation resting on soil strata

5.4.1.1 Requirement of discretization

The problem is idealized as a plane stress problem and modelled using 4 noded isoparametric elements. The requirement of discretization in the case of Gaussian randomness is discussed in section 3.5.3.1 and the same is considered in the present case also and is shown in Fig. 3.17. Thus, 6 eigenvectors in KL expansion are considered to represent the discretized random field.

5.4.1.2 Settlement of foundation

The problem is first studied using a combined PDD and PC based method. The problem is analysed using different order of PC expansion when the responses are represented using bivariate and trivariate PDD. PCs are generated using Gram-Schmidt orthogonalization process as discussed in section 3.4.3. First and second order PC with bivariate PDD are designated as ”PDD2-PC1” and ”PDD2-PC2” respectively. Similarly first and second order PC with trivariate PDD are designated as ”PDD3-PC1” and ”PDD3-PC2” respectively. Figs. 5.2 and 5.3 show the pdfs of vertical deflection at mid point below foundation (point X in Fig. 5.1) evaluated using different orders of PC expansion when solved using mPC scheme with PDD for $\sigma = 0.1$ and 0.2 respectively. It can be observed that as the order increases, the pdf converges towards MCS. The % error in statistical parameters (mean, SD, skewness, kurtosis) with respect to MCS are shown in Tables 5.1 and 5.2 respectively for $\sigma = 0.1$ and 0.2. It can be observed that as the order of PC increase, the errors are reduced with for same variate of PDD.

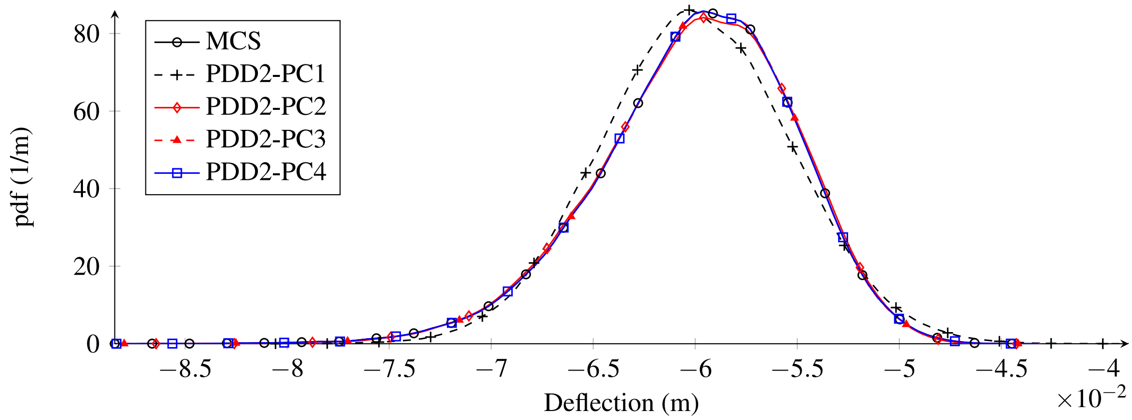

(a) Bivariate PDD.

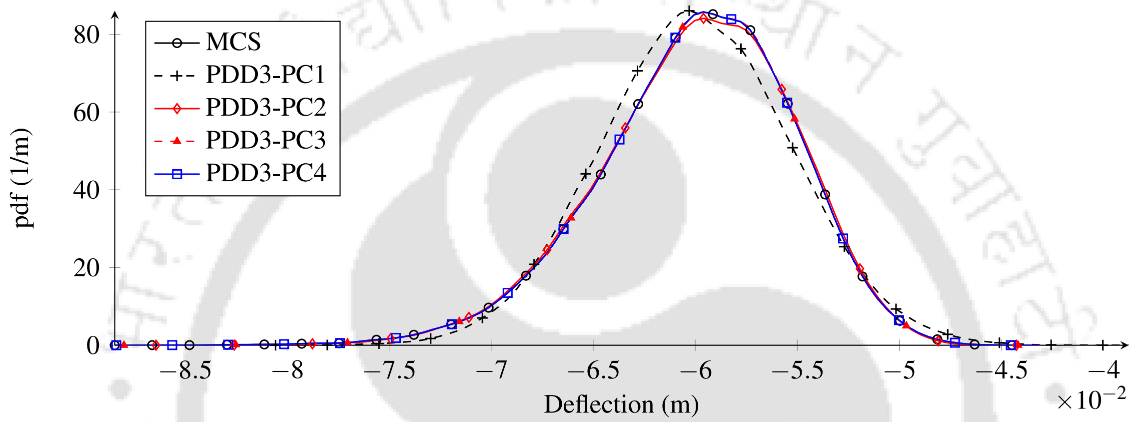

(b) Trivariate PDD.

Fig. 5.2: pdf of vertical deflection at mid point below foundation (point X in Fig. 5.1) evaluated using different order of PC with PDD ($\sigma = 0.1$)

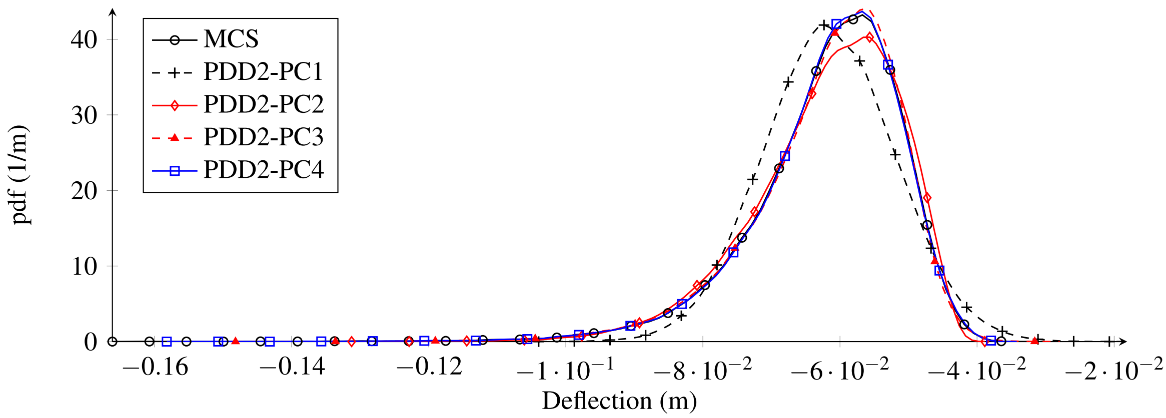

(a) Bivariate PDD.

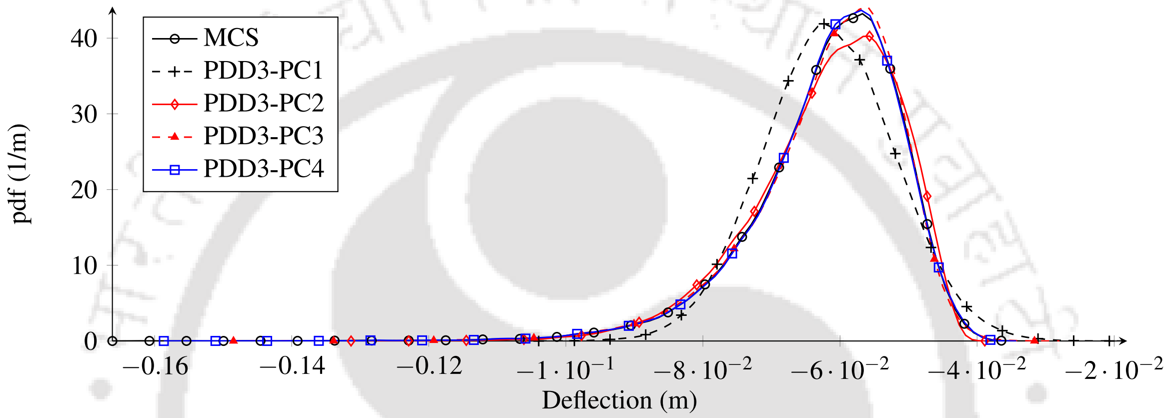

(b) Trivariate PDD.

Fig. 5.3: pdf of vertical deflection at mid point below foundation (point X in Fig. 5.1) evaluated using different orders of PC with PDD ($\sigma = 0.2$)

Table 5.1: % error in various statistical parameters of vertical deflection at mid point below foundation for different order of PC expansion with PDD ($\sigma = 0.1$)

Method	Mean		SD		Skewness		Kurtosis	
	Value (m) $\times 10^{-3}$	% error	Value (m) $\times 10^{-3}$	% error	Value	% error	Value	% error
MCS	-59.99	0.00	4.78	0.00	-0.50	0.00	3.54	0.00
PDD1-PC1	-59.98	0.02	4.64	2.88	0.01	101.79	3.01	14.88
PDD1-PC2	-59.98	0.01	4.72	1.10	-0.44	12.72	3.28	7.42
PDD1-PC3	-59.98	0.01	4.73	1.04	-0.46	7.70	3.46	2.40
PDD1-PC4	-59.98	0.01	4.73	1.04	-0.46	7.44	3.47	1.92
PDD1-PC5	-59.98	0.01	4.73	1.04	-0.46	7.42	3.47	1.89
PDD2-PC1	-59.98	0.02	4.65	2.61	0.01	101.78	3.01	14.88
PDD2-PC2	-59.99	0.00	4.77	0.12	-0.46	7.29	3.31	6.65
PDD2-PC3	-59.99	0.00	4.78	0.02	-0.50	0.59	3.51	0.80
PDD2-PC4	-59.99	0.00	4.78	0.01	-0.50	0.17	3.54	0.14
PDD2-PC5	-59.99	0.00	4.78	0.01	-0.50	0.14	3.54	0.09
PDD2-PC6	-59.99	0.00	4.78	0.01	-0.50	0.14	3.54	0.08
PDD3-PC1	-59.98	0.02	4.65	2.61	0.01	101.78	3.01	14.88
PDD3-PC2	-59.99	0.00	4.77	0.11	-0.46	7.28	3.31	6.64
PDD3-PC3	-59.99	0.00	4.78	0.01	-0.50	0.49	3.51	0.74
PDD3-PC4	-59.99	0.00	4.78	0.00	-0.50	0.04	3.54	0.07

Table 5.2: % error in various statistical parameters of vertical deflection at mid point below foundation for different order of PC expansion with PDD ($\sigma = 0.2$)

Method	Mean		SD		Skewness		Kurtosis	
	Value (m) $\times 10^{-3}$	% error	Value (m) $\times 10^{-3}$	% error	Value	% error	Value	% error
MCS	-61.87	0.00	10.90	0.00	-1.36	0.00	7.33	0.00
PDD1-PC1	-61.62	0.40	9.44	13.41	0.01	100.66	3.01	58.86
PDD1-PC2	-61.71	0.26	10.17	6.68	-0.86	36.71	4.03	44.93
PDD1-PC3	-61.71	0.25	10.28	5.72	-1.07	21.04	5.28	27.98
PDD1-PC4	-61.71	0.25	10.30	5.56	-1.13	16.86	5.84	20.32
PDD1-PC5	-61.71	0.25	10.30	5.53	-1.14	15.80	6.03	17.65
PDD2-PC1	-61.66	0.34	9.56	12.35	0.01	100.65	3.01	58.86
PDD2-PC2	-61.83	0.06	10.60	2.74	-0.90	33.39	4.13	43.67
PDD2-PC3	-61.85	0.02	10.80	0.95	-1.19	12.56	5.67	22.62
PDD2-PC4	-61.86	0.02	10.84	0.55	-1.28	5.60	6.52	11.07
PDD2-PC5	-61.86	0.02	10.85	0.46	-1.31	3.46	6.86	6.33
PDD2-PC6	-61.86	0.02	10.85	0.44	-1.32	2.90	6.97	4.85
PDD3-PC1	-61.66	0.34	9.56	12.35	0.01	100.65	3.01	58.86
PDD3-PC2	-61.84	0.05	10.61	2.66	-0.91	33.32	4.13	43.63
PDD3-PC3	-61.86	0.01	10.82	0.73	-1.19	12.03	5.71	22.13
PDD3-PC4	-61.87	0.00	10.88	0.25	-1.30	4.39	6.62	9.58

The problem is solved again using the combination of PDD and ImPC as discussed in section 5.3, where the responses of each components of PDD are evaluated using ImPC. In the iteration process of ImPC, the number of random variables considered are one and two respectively for the univariate and bivariate components as decided based on expected energy consideration. The solutions are evaluated for different orders of PC expansion with number of iterations. First and second order PC with bivariate PDD and zeroth iteration are designated as ”PDD2-PC1-I0” and ”PDD2-PC2-I0” respectively. Similarly first and second order PC with univariate PDD with first iteration are designated as ”PDD1-PC1-I1” and ”PDD1-PC2-I1” respectively. The PCs are generated using the strategy as discussed in section 3.4.3. The pdfs of vertical displacement at midpoint below foundation when solved using ImPC scheme with PDD for $\sigma = 0.1$ and 0.2 are shown in Figs. 5.4 and 5.5 respectively. The corresponding % errors in statistical parameters with respect to MCS are shown in Tables 5.3 and 5.4 respectively. It can be observed that as the number of iteration increases, % errors in different statistical parameters are reduced. It may be clearly seen from Table 5.2 and 5.4 that the errors in different statistical parameters corresponding to PDD2-PC3 (Table 5.4) with iteration more than 1 are all lesser than PDD2-PC3 and PC4 (Table 5.2). Thus, it is observed that in most of the cases the % error in responses after iteration in the case of combined PDD and ImPC method are lesser than those from combined PDD and PC based method of even higher orders. Thus without increasing the order of expansion, the accuracy of responses can be improved through iteration. However, the computational advantage depends on the convergence rate and the number of iteration required. In the next section, the computational efficiency of the proposed scheme is examined.

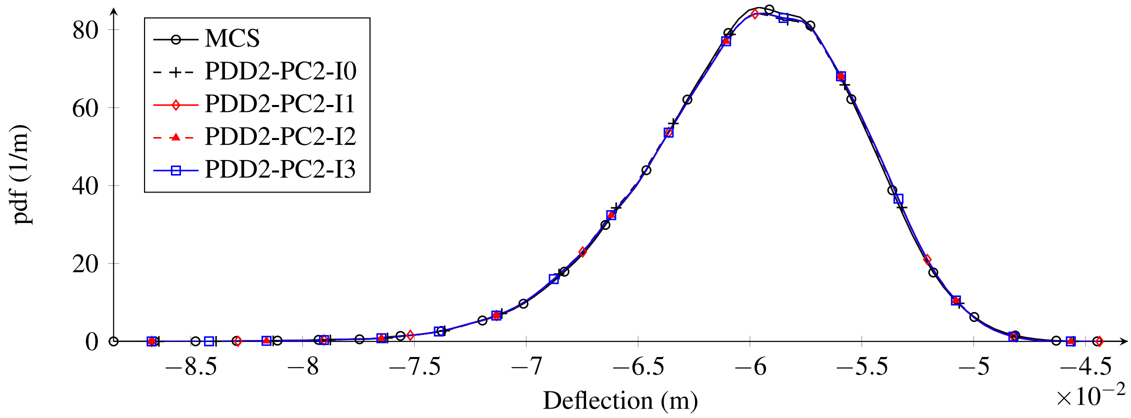

(a) Second order.

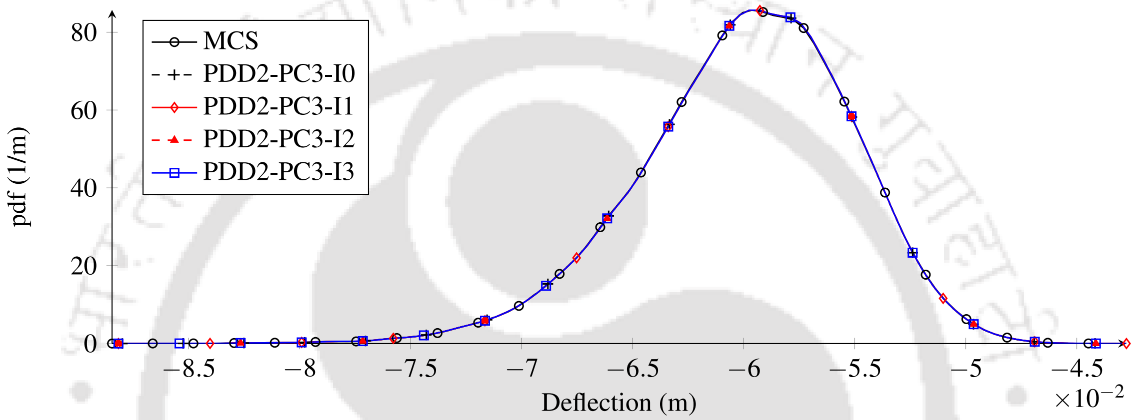

(b) Third order.

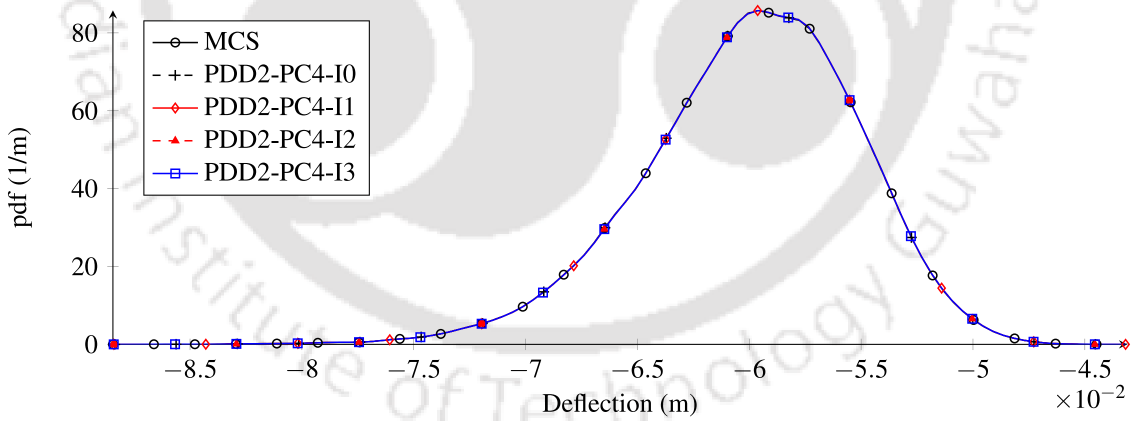

(c) Fourth order.

Fig. 5.4: pdf of vertical deflection at mid point below foundation (point X in Fig. 5.1) evaluated using hybrid method of PDD-ImPC ($\sigma = 0.1$)

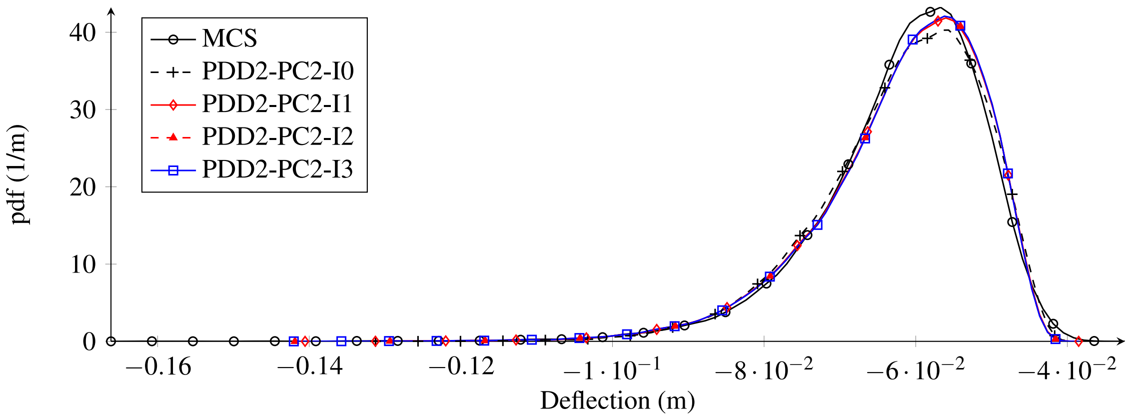

(a) Second order.

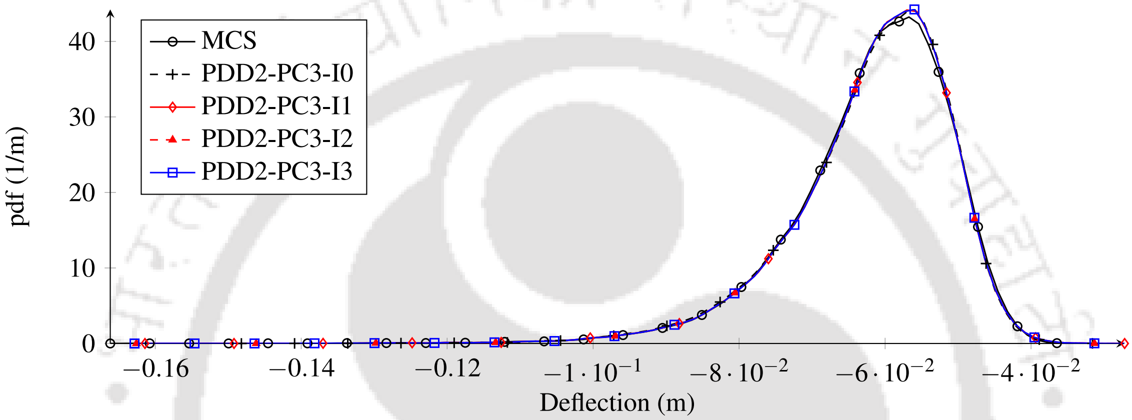

(b) Third order.

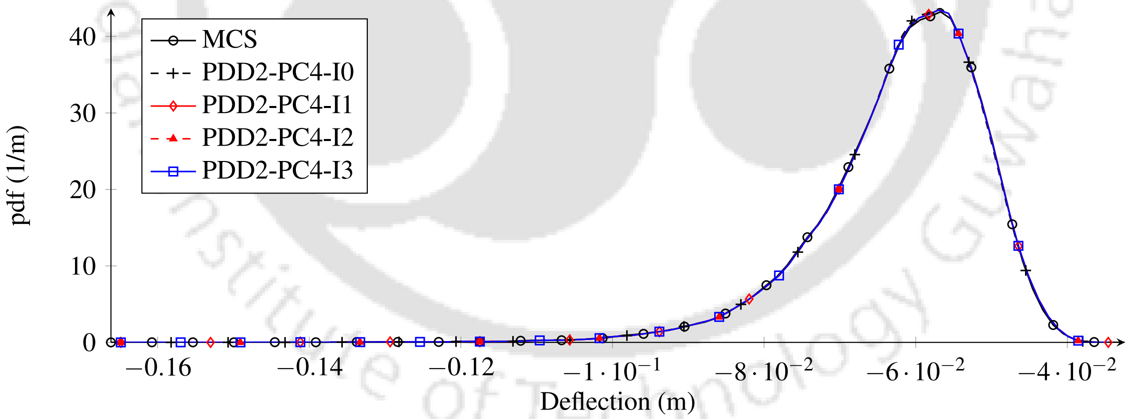

(c) Fourth order.

Fig. 5.5: pdf of vertical deflection at mid point below foundation (point X in Fig. 5.1) evaluated using hybrid method of PDD-ImPC ($\sigma = 0.2$)

Table 5.3: % error in various statistical parameters of vertical deflection at mid point under foundation for different order and iteration ImPC when solve using hybrid method of bivariate PDD ($\sigma = 0.1$)

Method	Mean		SD		Skewness		Kurtosis	
	Value (m) $\times 10^{-3}$	% error	Value (m) $\times 10^{-3}$	% error	Value	% error	Value	% error
MCS	-59.99	0.00	4.78	0.00	-0.50	0.00	3.54	0.00
PDD2-PC2-I0	-59.99	0.00	4.77	0.12	-0.46	7.29	3.31	6.65
PDD2-PC2-I1	-59.98	0.01	4.78	0.02	-0.49	2.85	3.35	5.39
PDD2-PC2-I2	-59.98	0.01	4.78	0.02	-0.49	2.67	3.35	5.33
PDD2-PC2-I3	-59.98	0.01	4.78	0.02	-0.49	2.66	3.35	5.33
PDD2-PC2-I4	-59.98	0.01	4.78	0.02	-0.49	2.66	3.35	5.33
PDD2-PC3-I0	-59.99	0.00	4.78	0.02	-0.50	0.59	3.51	0.80
PDD2-PC3-I1	-59.98	0.01	4.78	0.02	-0.50	0.10	3.53	0.25
PDD2-PC3-I2	-59.98	0.01	4.78	0.02	-0.50	0.09	3.53	0.25
PDD2-PC3-I3	-59.98	0.01	4.78	0.02	-0.50	0.09	3.53	0.25
PDD2-PC3-I4	-59.98	0.01	4.78	0.02	-0.50	0.09	3.53	0.25
PDD2-PC4-I0	-59.99	0.00	4.78	0.01	-0.50	0.17	3.54	0.14
PDD2-PC4-I1	-59.98	0.01	4.78	0.02	-0.50	0.09	3.54	0.08
PDD2-PC4-I2	-59.98	0.01	4.78	0.02	-0.50	0.09	3.54	0.09
PDD2-PC4-I3	-59.98	0.01	4.78	0.02	-0.50	0.09	3.54	0.09
PDD2-PC4-I4	-59.98	0.01	4.78	0.02	-0.50	0.09	3.54	0.09

Table 5.4: % error in various statistical parameters of vertical deflection at mid point under foundation for different order and iteration ImPC when solve using hybrid method of bivariate PDD ($\sigma = 0.2$)

Method	Mean		SD		Skewness		Kurtosis	
	Value (m) $\times 10^{-3}$	% error	Value (m) $\times 10^{-3}$	% error	Value	% error	Value	% error
MCS	-61.87	0.00	10.90	0.00	-1.36	0.00	7.33	0.00
PDD2-PC2-I0	-61.83	0.06	10.60	2.74	-0.90	33.39	4.13	43.67
PDD2-PC2-I1	-61.78	0.14	10.85	0.50	-1.13	16.72	5.04	31.26
PDD2-PC2-I2	-61.78	0.14	10.89	0.15	-1.17	13.89	5.23	28.61
PDD2-PC2-I3	-61.78	0.14	10.89	0.10	-1.18	13.41	5.26	28.15
PDD2-PC2-I4	-61.78	0.14	10.89	0.09	-1.18	13.33	5.27	28.07
PDD2-PC3-I0	-61.85	0.02	10.80	0.95	-1.19	12.56	5.67	22.62
PDD2-PC3-I1	-61.80	0.11	10.85	0.46	-1.31	3.42	6.79	7.34
PDD2-PC3-I2	-61.80	0.11	10.86	0.43	-1.32	2.82	6.86	6.34
PDD2-PC3-I3	-61.80	0.11	10.86	0.43	-1.32	2.80	6.87	6.29
PDD2-PC3-I4	-61.80	0.11	10.86	0.43	-1.32	2.80	6.87	6.29
PDD2-PC4-I0	-61.86	0.02	10.84	0.55	-1.28	5.60	6.52	11.07
PDD2-PC4-I1	-61.80	0.10	10.85	0.45	-1.32	2.64	7.01	4.25
PDD2-PC4-I2	-61.80	0.10	10.85	0.45	-1.32	2.71	7.00	4.43
PDD2-PC4-I3	-61.80	0.10	10.85	0.45	-1.32	2.71	7.00	4.42
PDD2-PC4-I4	-61.80	0.10	10.85	0.45	-1.32	2.71	7.00	4.42

5.4.1.3 Computational aspect

The responses of the proposed hybrid scheme with PDD and ImPC are checked for computational efficacy by comparing the computational complexity of matrix inversion and memory requirement. Thus, in order to compare results, a maximum permissible error of 0.1% and 10% are chosen for $\sigma = 0.1$ and 0.2 respectively. Based on this criterion, it is observed from Table 5.1 and 5.3 that PDD3-PC4 and PDD2-PC4-I1 are comparable for $\sigma = 0.1$. The computational complexity of matrix inversion depends on the numbers of degrees of freedom, which is 2926 in the present case and the total number of terms, $(P+1)$ in the PC expansion. The computational complexity of matrix inversion for PDD3-PC4 is $2926^3 + 6(5 \times 2926)^3 +$

$15(15\times2926)^3+20(35\times2926)^3 = 2.27\times10^{16}$. Similarly, computational complexity for matrix inversion in case of PDD2-PC4-I1 is $2[2926^3+6(5\times2926)^3+15(15\times2926)^3] = 2.5740\times10^{15}$ considering two iterations in the analysis. The ratio of computational complexity PDD3-PC4 : PDD2-PC4-I1=8.85 : 1. Similarly, in the case of $\sigma = 0.2$, (Table 5.2 and 5.4) errors in PDD3-PC4 or PDD2-PC5 and PDD2-PC3-I1 are comparable. Computational complexity of PDD2-PC5 is $2926^3+6(6\times2926)^3+15(21\times2926)^3 = 3.51\times10^{15}$ Thus complexity of PDD2-PC5 is lesser than PDD3-PC4. The computational complexity for PDD2-PC3-I1 is $2[2926^3+6(4\times2926)^3+15(10\times2926)^3] = 7.7082\times10^{14}$. Thus the ratio of the computational complexity of matrix inversion is PDD2-PC5 : PDD2-PC3-I1=4.56 : 1. Further, additional time is required for calculation of ensemble and eigenvalue problem in case of hybrid PDD-ImPC method, which is required to evaluate random variables for the iterative process, though these can be considered as marginal compared to computational gain. The computer memory requirement is studied further, which can be calculated by the largest size of stiffness matrices. In the case of PDD-PC scheme, the maximum size of the system matrices are $(35\times2926)\times(35\times2926)$ and $(21\times2926)\times(21\times2926)$ for SD equal to 0.1 and 0.2 respectively. However, in the case of PDD-ImPC scheme, the maximum size of system matrices are $(15\times2926)\times(15\times2926)$ and $(10\times2926)\times(10\times2926)$ respectively for SD equal to 0.1 and 0.2. Thus the problem can be solved with much lesser computational facilities.

5.4.2 Beam problem : 3-D Euler-Bernoulli beam with 1-D random field for Young's modulus

The second example studied is the same three dimensional cantilever beam considered in section 4.4.2. The problem is shown in Fig. 5.6 for ready reference. The Young's modulus (E) is considered as one dimensional spatially varying random field of the form

$$E(x,\theta) = E_0[1+\alpha(x,\theta)] \tag{5.11}$$

where E_0 is the mean value of the random field and $\alpha(x,\theta)$ is a homogeneous zero mean log-normal random field with an exponential covariance function as

$$\boldsymbol{C}(x_1,x_2) = \sigma^2 \exp\left(\frac{-|x_1-x_2|}{L_c}\right) \tag{5.12}$$

where σ is the SD of the random field, L_c is the correlation length and is considered as $L/2$. The problem is solved for standard deviation $\sigma = \{0.1,\ 0.2\}$.

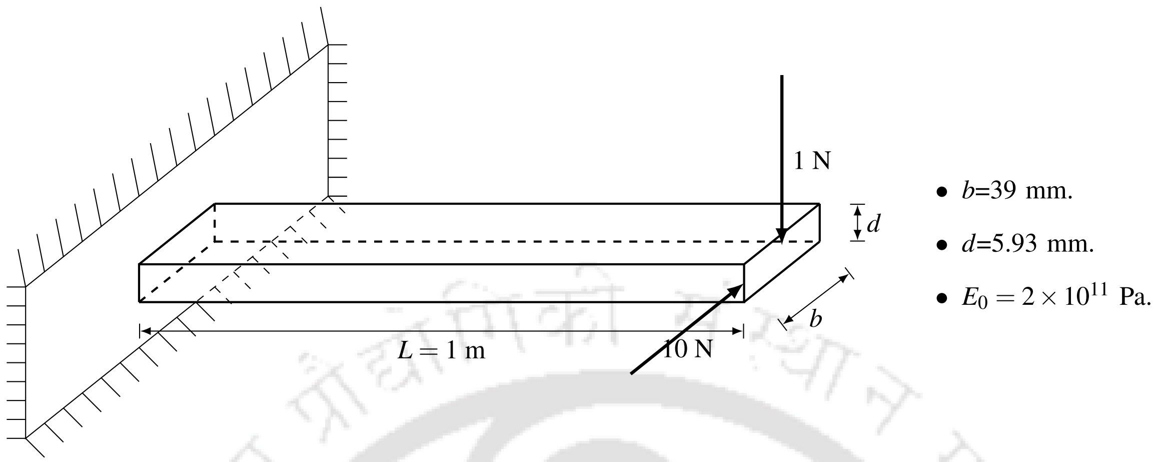

Fig. 5.6: Cantilever beam with a point load at free end.

5.4.2.1 Requirement of discretization of beam

As the same non-Gaussian beam as discussed in section 4.4.2 is considered here, discretized domain and random variables generated in section 4.4.2.1 are considered in this study. Thus, the cantilever beam is modelled using 30 numbers of equal-sized 2 noded 3-D Euler Bernoulli beam elements. Six number of random variables are considered in the discretized random field. The procedure followed in section 4.4.2 to generate PCs after generation of random variables is considered in the present example also.

5.4.2.2 Responses of beam

Similar to the foundation problem, the problem is decomposed into different variates using PDD and subsequently solved using both PC and ImPC scheme. The problems are first solved using different order of PC when responses are decomposed using PDD. The pdfs of vertical deflection at the free end for different orders of PC in mPC scheme for different variates of PDD are shown in Figs. 5.7 and 5.7 respectively for $\sigma = 0.1$ and 0.2. It can be observed that with first order of PC expansion, the pdf does not match with that of MCS. However, as the order of PC expansion increases, the pdfs converge towards MCS. The % error in statistical parameters of vertical deflection at free end are shown in Table Tables 5.5 and 5.6. It can be observed that as the order as the order of PC increases, the error reduces.

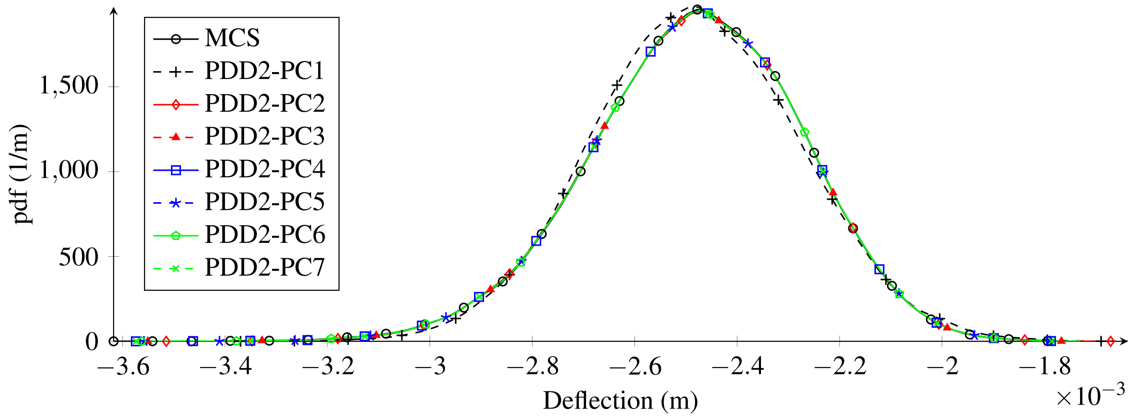

(a) Bivariate PDD.

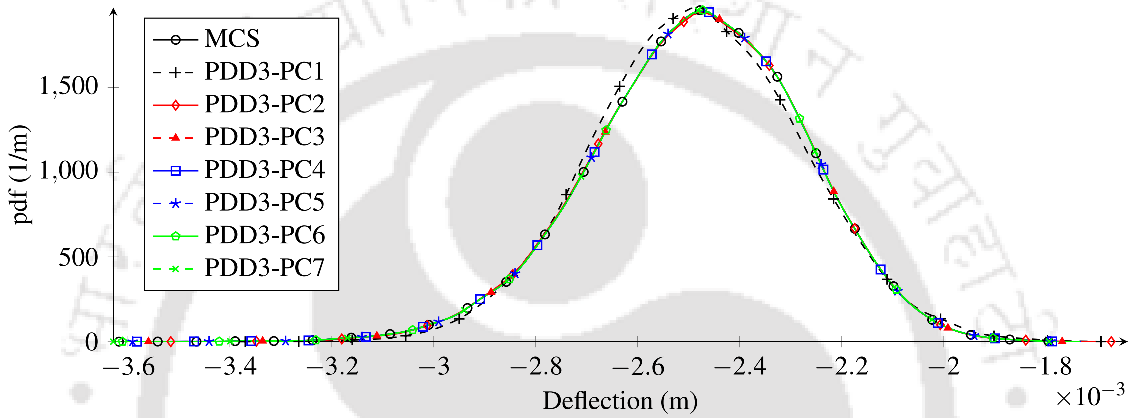

(b) Trivariate PDD.

Fig. 5.7: pdf of vertical displacement at free end for different order of PC and different variate of PDD when solved using PC ($\sigma = 0.1$)

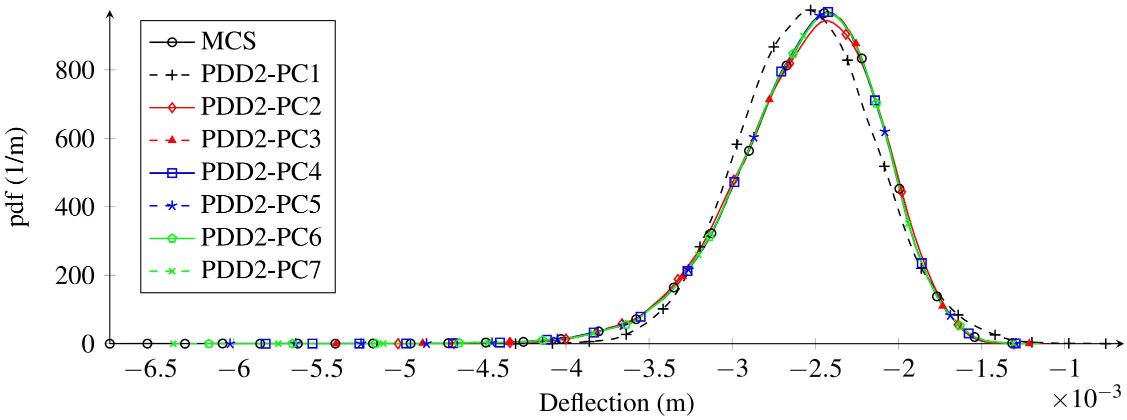

(a) Bivariate PDD.

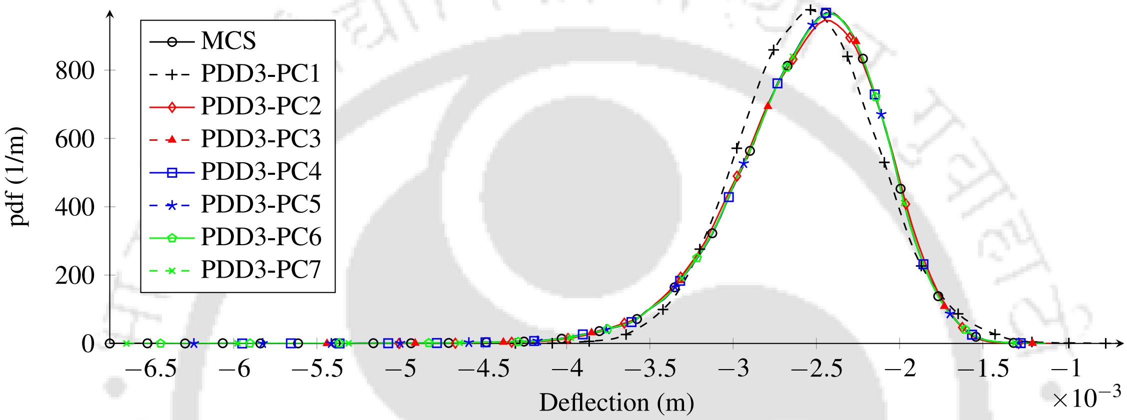

(b) Trivariate PDD.

Fig. 5.8: pdf of vertical displacement at free end for different order of PC and different variate of PDD when solved using PC ($\sigma = 0.2$)

Table 5.5: % error in various statistical parameters of vertical deflection at free end for different order of PC expansion with PDD ($\sigma = 0.1$)

Method	Mean		SD		Skewness		Kurtosis	
	Value (m) $\times 10^{-3}$	% error	Value (m) $\times 10^{-3}$	% error	Value	% error	Value	% error
MCS	-2.482	0.000	0.206	0.000	-0.253	0.000	3.197	0.000
PDD2-PC1	-2.482	0.020	0.202	1.949	0.023	108.952	3.003	6.041
PDD2-PC2	-2.482	0.001	0.206	0.124	-0.226	10.828	3.111	2.684
PDD2-PC3	-2.482	0.000	0.206	0.053	-0.242	4.705	3.148	1.507
PDD2-PC4	-2.482	0.000	0.206	0.049	-0.242	4.364	3.153	1.361
PDD2-PC5	-2.482	0.000	0.206	0.048	-0.242	4.434	3.152	1.400
PDD2-PC6	-2.482	0.000	0.206	0.049	-0.242	4.427	3.151	1.425
PDD2-PC7	-2.482	0.000	0.206	0.049	-0.242	4.383	3.152	1.388
PDD2-PC8	-2.482	0.000	0.206	0.047	-0.243	4.262	3.154	1.342
PDD2-PC9	-2.482	0.000	0.206	0.046	-0.243	4.228	3.154	1.316
PDD2-PC10	-2.482	0.000	0.206	0.045	-0.243	4.209	3.156	1.281
PDD3-PC1	-2.482	0.020	0.202	1.973	0.022	108.698	3.003	6.050
PDD3-PC2	-2.482	0.001	0.206	0.115	-0.227	10.630	3.111	2.680
PDD3-PC3	-2.482	0.000	0.206	0.010	-0.252	0.757	3.183	0.420
PDD3-PC4	-2.482	0.000	0.206	0.004	-0.253	0.179	3.194	0.082
PDD3-PC5	-2.482	0.000	0.206	0.003	-0.253	0.126	3.194	0.070
PDD3-PC6	-2.482	0.000	0.206	0.001	-0.253	0.048	3.196	0.023
PDD3-PC7	-2.482	0.000	0.206	0.001	-0.253	0.009	3.197	0.005
PDD3-PC8	-2.482	0.000	0.206	0.000	-0.254	0.037	3.197	0.028

Table 5.6: % error in various statistical parameters of vertical deflection at free end for different order of PC expansion with PDD ($\sigma = 0.2$)

Method	Mean		SD		Skewness		Kurtosis	
	Value (m) $\times 10^{-3}$	% error	Value (m) $\times 10^{-3}$	% error	Value	% error	Value	% error
MCS	-2.56	0.00	0.44	0.00	-0.79	0.00	5.03	0.00
PDD2-PC1	-2.55	0.27	0.41	7.56	0.04	104.45	3.05	39.29
PDD2-PC2	-2.56	0.04	0.43	1.50	-0.55	29.52	3.41	32.11
PDD2-PC3	-2.56	0.02	0.44	0.72	-0.67	14.42	3.99	20.57
PDD2-PC4	-2.56	0.02	0.44	0.53	-0.71	9.84	4.30	14.53
PDD2-PC5	-2.56	0.02	0.44	0.47	-0.72	7.91	4.45	11.46
PDD2-PC6	-2.56	0.02	0.44	0.44	-0.73	7.03	4.53	9.96
PDD2-PC7	-2.56	0.02	0.44	0.43	-0.74	6.46	4.58	8.89
PDD2-PC8	-2.56	0.02	0.44	0.41	-0.74	6.08	4.62	8.14
PDD2-PC9	-2.56	0.02	0.44	0.41	-0.74	5.93	4.64	7.78
PDD2-PC10	-2.56	0.02	0.44	0.41	-0.74	5.83	4.65	7.54
PDD3-PC1	-2.55	0.28	0.41	7.65	0.03	103.24	3.05	39.34
PDD3-PC2	-2.56	0.04	0.43	1.54	-0.55	29.72	3.43	31.73
PDD3-PC3	-2.56	0.01	0.44	0.57	-0.67	14.48	3.98	20.83
PDD3-PC4	-2.56	0.01	0.44	0.30	-0.72	8.30	4.36	13.32
PDD3-PC5	-2.56	0.00	0.44	0.20	-0.74	5.26	4.60	8.49
PDD3-PC6	-2.56	0.00	0.44	0.16	-0.75	4.06	4.71	6.40
PDD3-PC7	-2.56	0.00	0.44	0.15	-0.76	3.67	4.74	5.68
PDD3-PC8	-2.56	0.00	0.44	0.15	-0.76	3.69	4.74	5.70
PDD3-PC9	-2.56	0.00	0.44	0.15	-0.76	3.76	4.73	5.89
PDD3-PC10	-2.56	0.00	0.44	0.15	-0.76	3.74	4.73	5.88

Similar to the foundation problem, the problem is solved using the proposed hybrid method comprising of PDD and ImPC as discussed in section 5.3. In the iteration process, the PCs are generated using one, two and three random variables for the univariate, bivariate and trivariate components respectively. The responses are generated using linear combination of responses of each component for the same order of PC and iterations as discussed in section 5.3.2. The pdfs for vertical deflection at free end for different orders of PC expansion and iterations when solved using the proposed method for $\sigma = 0.1$ are shown in Fig. 5.9. The corresponding % error in various statistical parameters for bivariate PDD are shown in Table 5.7. Similarly, the pdfs for vertical deflection at free end for different orders of PC expansion and iterations when solved using the proposed method for $\sigma = 0.2$ are shown in Fig. 5.10. The corresponding % error in various statistical parameters for bivariate and trivariate PDD are shown in Tables 5.8 and 5.9 respectively. It is observed that as the number of iteration increases, the % error in statistical parameters are observed to reduce.

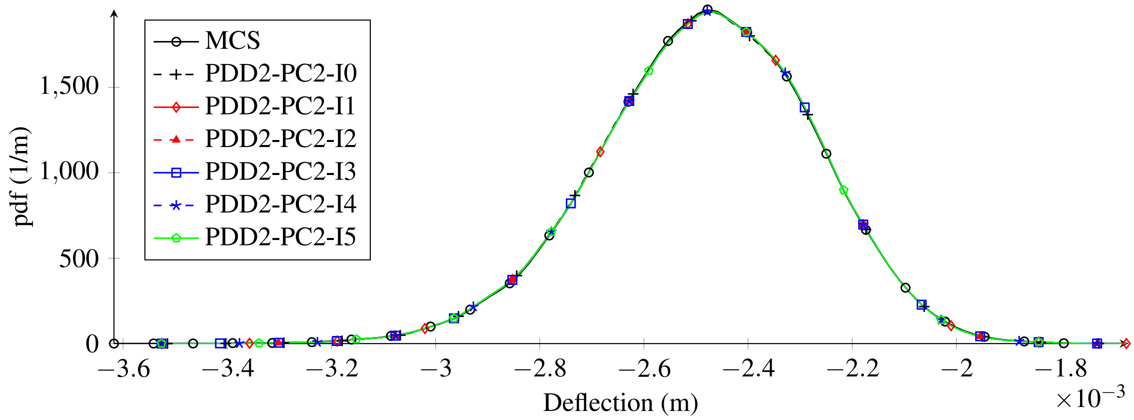

(a) Second order.

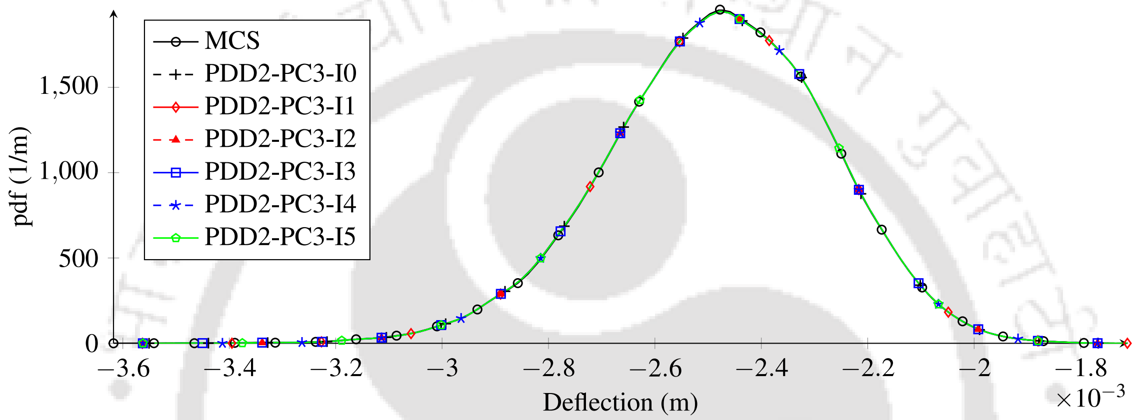

(b) Third order.

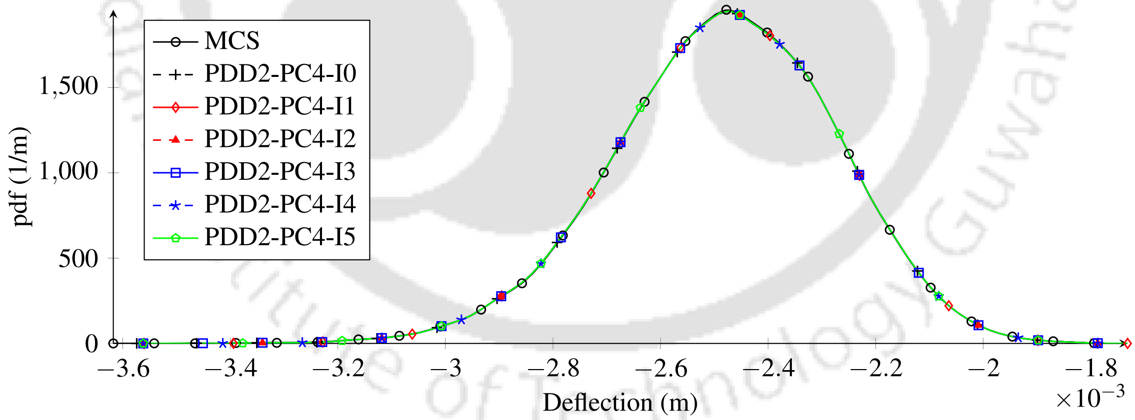

(c) Fourth order.

Fig. 5.9: pdf of vertical displacement at free end for different orders of PC expansion when solve using PDD-ImPC method ($\sigma = 0.1$)

Table 5.7: % error in various statistical parameters of vertical deflection at free end for different order and iteration ImPC when solve using hybrid method of bivariate PDD ($\sigma = 0.1$)

Method	Mean		SD		Skewness		Kurtosis	
	Value (m) $\times 10^{-3}$	% error	Value (m) $\times 10^{-3}$	% error	Value	% error	Value	% error
MCS	-2.48	0.00	0.21	0.00	-0.25	0.00	3.20	0.00
PDD2-PC2-I0	-2.48	0.00	0.21	0.12	-0.23	10.83	3.11	2.68
PDD2-PC2-I1	-2.48	0.00	0.21	0.07	-0.24	3.86	3.13	1.96
PDD2-PC2-I2	-2.48	0.00	0.21	0.07	-0.24	3.48	3.14	1.92
PDD2-PC2-I3	-2.48	0.00	0.21	0.07	-0.24	3.46	3.14	1.92
PDD2-PC2-I4	-2.48	0.00	0.21	0.07	-0.24	3.46	3.14	1.92
PDD2-PC2-I5	-2.48	0.00	0.21	0.07	-0.24	3.46	3.14	1.92
PDD2-PC3-I0	-2.48	0.00	0.21	0.05	-0.24	4.71	3.15	1.51
PDD2-PC3-I1	-2.48	0.00	0.21	0.05	-0.24	4.43	3.15	1.43
PDD2-PC3-I2	-2.48	0.00	0.21	0.05	-0.24	4.43	3.15	1.43
PDD2-PC3-I3	-2.48	0.00	0.21	0.05	-0.24	4.43	3.15	1.43
PDD2-PC3-I4	-2.48	0.00	0.21	0.05	-0.24	4.43	3.15	1.43
PDD2-PC3-I5	-2.48	0.00	0.21	0.05	-0.24	4.43	3.15	1.43
PDD2-PC4-I0	-2.48	0.00	0.21	0.05	-0.24	4.36	3.15	1.36
PDD2-PC4-I1	-2.48	0.00	0.21	0.05	-0.24	4.41	3.15	1.41
PDD2-PC4-I2	-2.48	0.00	0.21	0.05	-0.24	4.39	3.15	1.40
PDD2-PC4-I3	-2.48	0.00	0.21	0.05	-0.24	4.39	3.15	1.40
PDD2-PC4-I4	-2.48	0.00	0.21	0.05	-0.24	4.39	3.15	1.40
PDD2-PC4-I5	-2.48	0.00	0.21	0.05	-0.24	4.39	3.15	1.40

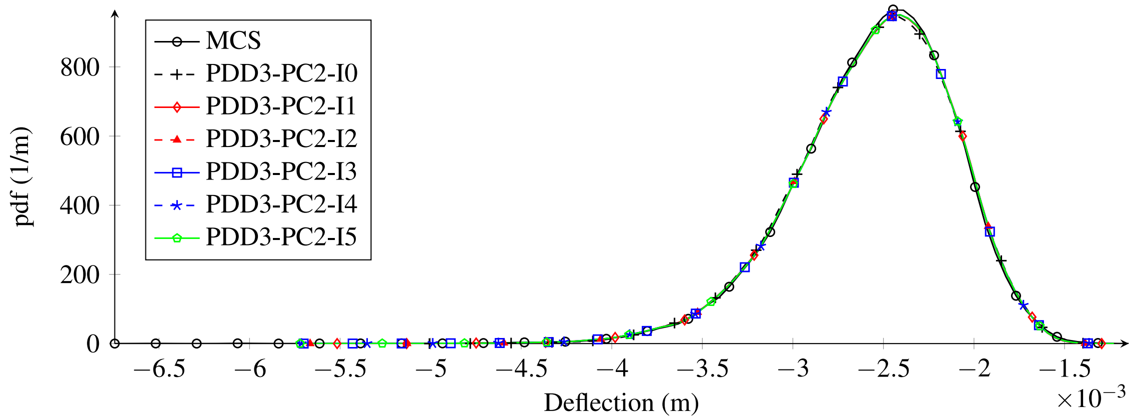

(a) Second order.

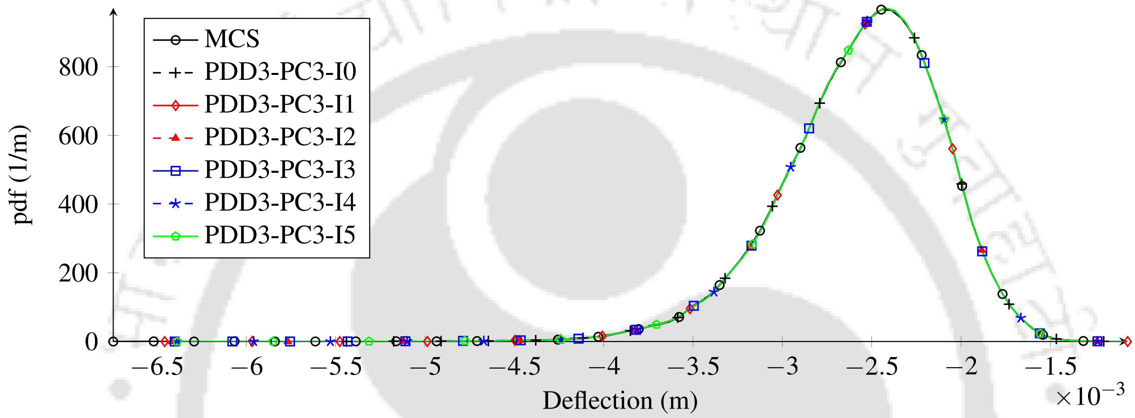

(b) Third order.

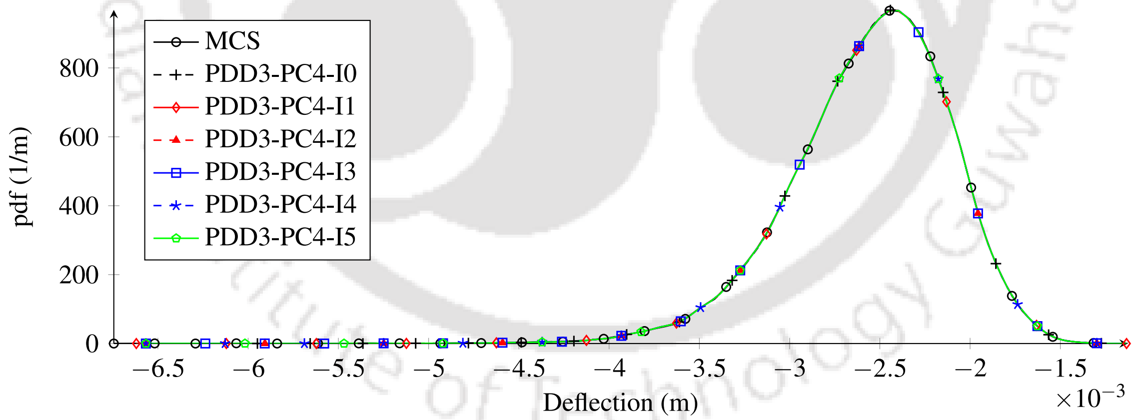

(c) Fourth order.

Fig. 5.10: pdf of vertical displacement at free end for different orders of PC expansion when solve using PDD-ImPC method ($\sigma = 0.2$)

Table 5.8: % error in various statistical parameters of vertical deflection at free end for different order and iteration ImPC when solve using hybrid method of bivariate PDD ($\sigma = 0.2$)

Method	Mean		SD		Skewness		Kurtosis	
	Value (m) $\times 10^{-3}$	% error	Value (m) $\times 10^{-3}$	% error	Value	% error	Value	% error
MCS	-2.56	0.00	0.44	0.00	-0.79	0.00	5.03	0.00
PDD2-PC2-I0	-2.56	0.04	0.43	1.50	-0.55	29.52	3.41	32.11
PDD2-PC2-I1	-2.56	0.04	0.44	0.69	-0.64	18.28	3.75	25.49
PDD2-PC2-I2	-2.56	0.04	0.44	0.55	-0.66	16.19	3.84	23.60
PDD2-PC2-I3	-2.56	0.04	0.44	0.52	-0.66	15.64	3.87	23.05
PDD2-PC2-I4	-2.56	0.04	0.44	0.51	-0.66	15.45	3.88	22.87
PDD2-PC2-I5	-2.56	0.04	0.44	0.51	-0.66	15.39	3.88	22.80
PDD2-PC3-I0	-2.56	0.02	0.44	0.72	-0.67	14.42	3.99	20.57
PDD2-PC3-I1	-2.56	0.02	0.44	0.46	-0.73	7.24	4.49	10.76
PDD2-PC3-I2	-2.56	0.02	0.44	0.43	-0.74	6.19	4.58	8.90
PDD2-PC3-I3	-2.56	0.02	0.44	0.42	-0.74	6.05	4.60	8.59
PDD2-PC3-I4	-2.56	0.02	0.44	0.42	-0.74	6.03	4.60	8.54
PDD2-PC3-I5	-2.56	0.02	0.44	0.42	-0.74	6.02	4.60	8.53
PDD2-PC4-I0	-2.56	0.02	0.44	0.53	-0.71	9.84	4.30	14.53
PDD2-PC4-I1	-2.56	0.02	0.44	0.43	-0.74	6.15	4.63	7.93
PDD2-PC4-I2	-2.56	0.02	0.44	0.42	-0.74	6.09	4.64	7.80
PDD2-PC4-I3	-2.56	0.02	0.44	0.42	-0.74	6.08	4.64	7.78
PDD2-PC4-I4	-2.56	0.02	0.44	0.42	-0.74	6.08	4.64	7.78
PDD2-PC4-I5	-2.56	0.02	0.44	0.42	-0.74	6.08	4.64	7.78
PDD2-PC5-I0	-2.56	0.02	0.44	0.47	-0.72	7.91	4.45	11.46
PDD2-PC5-I1	-2.56	0.02	0.44	0.42	-0.74	5.96	4.65	7.54
PDD2-PC5-I2	-2.56	0.02	0.44	0.42	-0.74	5.98	4.65	7.58
PDD2-PC5-I3	-2.56	0.02	0.44	0.42	-0.74	5.98	4.65	7.57
PDD2-PC5-I4	-2.56	0.02	0.44	0.42	-0.74	5.98	4.65	7.57
PDD2-PC5-I5	-2.56	0.02	0.44	0.42	-0.74	5.98	4.65	7.57
PDD2-PC6-I0	-2.56	0.02	0.44	0.44	-0.73	7.03	4.53	9.96
PDD2-PC6-I1	-2.56	0.02	0.44	0.42	-0.74	6.09	4.63	7.90
PDD2-PC6-I2	-2.56	0.02	0.44	0.42	-0.74	6.05	4.64	7.80
PDD2-PC6-I3	-2.56	0.02	0.44	0.42	-0.74	6.06	4.64	7.82
PDD2-PC6-I4	-2.56	0.02	0.44	0.42	-0.74	6.06	4.64	7.81
PDD2-PC6-I5	-2.56	0.02	0.44	0.42	-0.74	6.06	4.64	7.81
PDD2-PC7-I0	-2.56	0.02	0.44	0.43	-0.74	6.46	4.58	8.89
PDD2-PC7-I1	-2.56	0.02	0.44	0.42	-0.74	6.02	4.64	7.74
PDD2-PC7-I2	-2.56	0.02	0.44	0.42	-0.74	6.03	4.64	7.75
PDD2-PC7-I3	-2.56	0.02	0.44	0.42	-0.74	6.03	4.64	7.75
PDD2-PC7-I4	-2.56	0.02	0.44	0.42	-0.74	6.03	4.64	7.75
PDD2-PC7-I5	-2.56	0.02	0.44	0.42	-0.74	6.03	4.64	7.75

Table 5.9: % error in various statistical parameters of vertical deflection at free end for different order and iteration ImPC when solve using hybrid method of trivariate PDD ($\sigma = 0.2$)

Method	Mean		SD		Skewness		Kurtosis	
	Value (m) $\times 10^{-3}$	% error	Value (m) $\times 10^{-3}$	% error	Value	% error	Value	% error
MCS	-2.56	0.00	0.44	0.00	-0.79	0.00	5.03	0.00
PDD3-PC1-I0	-2.55	0.28	0.41	7.65	0.03	103.24	3.05	39.34
PDD3-PC2-I0	-2.56	0.04	0.43	1.54	-0.55	29.72	3.43	31.73
PDD3-PC2-I1	-2.56	0.02	0.44	0.58	-0.65	17.79	3.77	25.07
PDD3-PC2-I2	-2.56	0.02	0.44	0.40	-0.66	15.44	3.89	22.61
PDD3-PC2-I3	-2.56	0.02	0.44	0.35	-0.67	14.64	3.94	21.64
PDD3-PC2-I4	-2.56	0.02	0.44	0.34	-0.67	14.33	3.96	21.25
PDD3-PC2-I5	-2.56	0.02	0.44	0.33	-0.67	14.19	3.97	21.07
PDD3-PC3-I0	-2.56	0.01	0.44	0.57	-0.67	14.48	3.98	20.83
PDD3-PC3-I1	-2.56	0.01	0.44	0.15	-0.75	3.95	4.68	6.99
PDD3-PC3-I2	-2.56	0.01	0.44	0.13	-0.76	3.54	4.70	6.45
PDD3-PC3-I3	-2.56	0.01	0.44	0.13	-0.76	3.54	4.70	6.50
PDD3-PC3-I4	-2.56	0.01	0.44	0.13	-0.76	3.55	4.70	6.53
PDD3-PC3-I5	-2.56	0.01	0.44	0.13	-0.76	3.55	4.70	6.53
PDD3-PC4-I0	-2.56	0.01	0.44	0.30	-0.72	8.30	4.36	13.32
PDD3-PC4-I1	-2.56	0.01	0.44	0.11	-0.76	2.84	4.80	4.51
PDD3-PC4-I2	-2.56	0.01	0.44	0.11	-0.76	2.81	4.80	4.48
PDD3-PC4-I3	-2.56	0.01	0.44	0.11	-0.76	2.81	4.80	4.47
PDD3-PC4-I4	-2.56	0.01	0.44	0.11	-0.76	2.81	4.80	4.47
PDD3-PC4-I5	-2.56	0.01	0.44	0.11	-0.76	2.81	4.80	4.47
PDD3-PC5-I0	-2.56	0.00	0.44	0.20	-0.74	5.26	4.60	8.49
PDD3-PC5-I1	-2.56	0.01	0.44	0.10	-0.76	2.68	4.81	4.27
PDD3-PC5-I2	-2.56	0.01	0.44	0.11	-0.76	2.66	4.81	4.28
PDD3-PC5-I3	-2.56	0.01	0.44	0.11	-0.76	2.66	4.81	4.26
PDD3-PC5-I4	-2.56	0.01	0.44	0.11	-0.76	2.66	4.81	4.27
PDD3-PC5-I5	-2.56	0.01	0.44	0.11	-0.76	2.66	4.81	4.27

5.4.2.3 Computational aspect

The responses of the proposed hybrid scheme with PDD and ImPC are checked for computational efficacy by comparing the computational complexity of matrix inversion and memory requirement. Thus, in order to compare results, a maximum permissible error of 5% is chosen for all the considered statistical parameters. Based on this criterion, it is observed from Table 5.5 and 5.7 that PDD2-PC3 and PDD2-PC2-I1 are comparable for $\sigma = 0.1$. The computational complexity of matrix inversion depends on the numbers of degrees of freedom, which is 120 in the present case and the total number of terms, $(P+1)$ in the PC expansion. The computational complexity of matrix inversion for PDD2-PC3 is $120^3 + 6(4\times120)^3 + 15(10\times120)^3 = 2.66\times10^{10}$. Similarly, computational complexity for matrix inversion in case of PDD2-PC2-I1 is $2[120^3 + 6(3\times120)^3 + 15(6\times120)^3] = 1.18\times10^{10}$ considering two iterations in the analysis. The ratio of computational complexity PDD2-PC3:PDD2-PC2-I1=2.26:1. Similarly, in the case of $\sigma = 0.2$, error in PDD3-PC7 and PDD3-PC4-I1 are comparable (Table 5.6 and 5.9). The computational complexity for PDD3-PC7 is $120^3+6(8\times120)^3+15(36\times120)^3+20(120\times120)^3 = 6.09\times10^{13}$. The computational complexity for PDD3-PC4-I1 is $2[120^3+6(5\times120)^3+15(15\times120)^3+20(35\times120)^3] = 3.14\times10^{12}$. Thus the ratio of the computational complexity of matrix inversion is PDD3-PC7:PDD3-PC4-I1=19.399:1. Further, additional time is required for calculation of ensemble and eigenvalue problem in case of hybrid PDD-ImPC method, which is required to evaluate random variables for the iterative process, though these can be considered as marginal compared to computational gain. The computer memory requirement is studied further, which can be calculated by the largest size of stiffness matrices. In the case of PDD-PC scheme, the maximum size of the system matrices are $(10\times120)\times(10\times120)$ and $(120\times120)\times(120\times120)$ for SD equal to 0.1 and 0.2 respectively. However, in the case of PDD-ImPC scheme, the maximum size of system matrices are $(6\times120)\times(6\times120)$ and $(35\times120)\times(35\times120)$ respectively for SD equal to 0.1 and 0.2 respectively. Thus the problem can be solved with much lesser computational facilities.

5.5 Conclusions

In continuation to the effort for reduction in dimensional curse of system matrix for problem with stochastic parameters, PDD is introduced in this chapter. Further enhancement in computational efficacy is tried by combining ImPC with PDD. A hybrid method comprising of PDD and ImPC for analysis of linear structural mechanics problem with random material property is utilized. PDD is considered to represent multi variate response as a weighted sum of responses of smaller dimensional problems, where each of these is solved using ImPC. The problem can also be solved by considering mPC based method instead of ImPC. It is observed that for a considered order of PC, the proposed method reduces the error in statistical parameters of responses with iterations. Moreover, it is also observed that the proposed scheme is more efficient in terms of computational demand and accuracy than PDD-PC scheme for the problem types considered. It is also observed that for same level of accuracy, a lesser order of PC expansion can satisfy the requirement as compared to PDD-PC based scheme. Thus, the system matrix sizes are reduced and even higher level of accuracy is possible by increasing the order in the proposed PDD-ImPC method. Thus, the proposed scheme can be implemented effectively, where PDD-PC may fail due to constraint on computer RAM availability.

6

Analysis under dynamic loading using TDgPC

Contents

6.1 Introduction

In the previous chapters, the effect on responses due to randomness in material properties are studied under static loading. In the case of structural analysis under dynamic loading, the uncertainties in external loading are extensively considered in random vibration and are well-documented (Newland and Newland, 1984), though still an active area of study. However, as discussed in previous chapters, the material properties are also random in nature and may affect the dynamic responses significantly. The present study considers structural analysis under deterministic dynamic loading with both Gaussian and non-Gaussian randomness of the system parameters.

As discussed in previous chapters, PC approximation is considered in many fields of engineering. The method can be extended to time-dependent problems by combining PC approximation with appropriate available time integration scheme. In particular, in the case of structural mechanics problems, the method can be extended by considering available time integration scheme like Newmark-β along with PC expansion to approximate the statistical responses. However, as discussed in section 2.4.2, the PC approximation fails to approximate responses for a long duration of time integration. Generally, the PC expansion is formulated considering the initial random variables in the input, assuming the responses are of the same statistical distribution. However, as time progresses, the response statistics change. Thus the initially considered PC expansion losses its efficiency. In order to overcome this drawback, TDgPC was proposed by Gerritsma et al. (2010) and others, and these are discussed in section 2.4.2. In this chapter, studies are conducted to examine the responses of structural dynamics problem under dynamic loading with random system properties using PC and TDgPC.

The chapter is arranged as follows. In section 6.2, the discretization of random field and formulation of the stochastic dynamic equation are discussed. Section 6.3 discusses the approximation of statistical response using PC and solution using Newmark-β method followed by approximation using TDgPC and solution using Newmark-β method in section 6.4. Numerical examples are solved in section 6.5, considering random material properties and sectional properties. However, for simplicity, the damping matrix is not considered as random in nature.

6.2 Discretization using KL expansion and formulation of SFEM

Discretization of the random field to a set of random variables is performed using KL expansion. The discretization of the Gaussian random field using KL expansion is discussed in section 3.2.1 along with the basic principle of KL expansion. The discretization and simulation of non-Gaussian random field using KL expansion with an iterative procedure is discussed in section 4.2.1 and ICA in section 4.2.2 for reducing the interdependency among random variables. The formulation of SFEM for dynamic loading is discussed in the next section.

6.2.1 Formulation of SFEM for dynamic loading

The formulation of stochastic finite element is similar to that of its deterministic counterpart, like minimization of potential energy, Galerkin formulation etc. The discretized structural dynamic equation for linear dynamic system can be written as,

$$\boldsymbol{M}\ddot{\boldsymbol{u}} + \boldsymbol{D}\dot{\boldsymbol{u}} + \boldsymbol{K}\boldsymbol{u} = \boldsymbol{q}(t) \tag{6.1}$$

where $\boldsymbol{M}$, $\boldsymbol{D}$ and $\boldsymbol{K}$ are mass, damping and stiffness matrices of the system, $\boldsymbol{u}$, $\dot{\boldsymbol{u}}$, $\ddot{\boldsymbol{u}}$ and $\boldsymbol{q}(t)$ are displacement, velocity, acceleration and the applied force vector respectively.

The present study considers physical parameters like Young's modulus, sectional dimensions as random. However, for simplicity, damping is not considered as random quantity. In case of random field problem, the field is discretized using KL expansion as discussed in section 6.2. Thus, mass and stiffness matrices can be written in a general form as,

$$\boldsymbol{M} = \overline{\boldsymbol{M}} + \sum_{i=1}^{Q_M} \xi_i^{(M)}(\theta)\boldsymbol{M}_i \tag{6.2}$$

and

$$\boldsymbol{K} = \overline{\boldsymbol{K}} + \sum_{i=1}^{Q_K} \xi_i^{(K)}(\theta)\boldsymbol{K}_i \tag{6.3}$$

respectively, where $\overline{\boldsymbol{M}}$ and $\overline{\boldsymbol{K}}$ are the deterministic parts of the mass and stiffness matrices and $\boldsymbol{M}_i$ and $\boldsymbol{K}_i$ are the stochastic parts of mass and stiffness matrices respectively. Q_K and Q_M are the number of terms considered in KL expansion of Young's modulus and area (a parameter responsible for stochastic component of mass) respectively. In case of material with a non-Gaussian random field, the random variables generated using iterative KL expansion are not independent. Thus, ICA is performed on $\xi_i^{(M)}(\theta)$ and $\xi_i^{(K)}(\theta)$ as discussed in section 4.2.2. $\xi_i(\theta)$ will be replaced by $\boldsymbol{\eta}(\theta)$ and mixing matrix ($\boldsymbol{H}_{\text{mixing}}$) will be multiplied with eigenvectors of KL expansion. A detailed study on the application of ICA on the random variables of KL expansion is discussed in the numerical study of a static beam problem in section 4.4.2.1. The damping matrix, $\boldsymbol{D}$ is calculated from the deterministic part of stiffness and mass matrices. Thus, the stochastic dynamic equation (Eq. 6.1) with random mass and stiffness matrices can be written as,

$$\left(\overline{\boldsymbol{M}} + \sum_{i=1}^{Q_M} \xi_i^{(M)}(\theta)\boldsymbol{M}_i\right)\ddot{\boldsymbol{u}} + \boldsymbol{D}\dot{\boldsymbol{u}} + \left(\overline{\boldsymbol{K}} + \sum_{i=1}^{Q_K} \xi_i^{(K)}(\theta)\boldsymbol{K}_i\right)\boldsymbol{u} = \boldsymbol{q}(t) \tag{6.4}$$

Generally, the stochastic dynamic equation (Eq. 6.4) can be solved using MCS for each of the realizations of $\xi_n(\theta)$. Similar to static problems, PC expansions are also considered to approximate responses. Wan and Karniadakis (2006b) approximated fluid responses using PC expansion and studied its long time behaviour. However, the authors observed that PC failed to approximate response statistics for long duration. Kundu and Adhikari (2014) also made similar observation for long duration of analysis involving structural mechanics problem.

With PC approximation of responses, the stochastic equation (Eq. 6.4) can be converted to a set of deterministic equations following Galerkin projection. These deterministic equations can be solved using time integration scheme like Newmark-β method. In the case of non-Gaussian random field, the random variables generated after ICA ($\eta(\theta)$) are not of the same distribution. Similar to static problem (Chapter 4), the random variables are transformed to standard Gaussian using non-linear transformation for the generation of PC. The transformation is applicable for generation of PC only, while the random variables after ICA ($\eta(\theta)$) considered to represent material properties remain unchanged.

6.3 Solution using PC expansion and Newmark-β method

6.3.1 Approximation of responses using PC

Responses ($\boldsymbol{u}$, $\dot{\boldsymbol{u}}$, $\ddot{\boldsymbol{u}}$) of a structure (Eq. 6.4) are also random in nature as the input quantities are random in nature. The responses can be approximated using PC as

$$\boldsymbol{u} = \sum_{j=0}^{P} \boldsymbol{c}_j \Psi_j[\xi_r(\theta)] \tag{6.5}$$

$$\dot{\boldsymbol{u}} = \sum_{j=0}^{P} \boldsymbol{d}_j \Psi_j[\xi_r(\theta)] \tag{6.6}$$

$$\ddot{\boldsymbol{u}} = \sum_{j=0}^{P} \boldsymbol{e}_j \Psi_j[\xi_r(\theta)] \tag{6.7}$$

where r is the number of random variables comprising of random variables from both mass and stiffness matrices $\{\xi_i^{(M)}(\theta),\ \xi_i^{(K)}(\theta)\}$ and $r = 0, 1, 2, \ldots (Q_M + Q_K)$. Thus, the evaluation of stochastic responses become equivalent to calculation of $\boldsymbol{c}$, $\boldsymbol{d}$ and $\boldsymbol{e}$. The PCs, $\Psi_j[\xi_r(\theta)$ are evaluated using Gram-Schmidt orthogonalization process as discussed in section 3.4.3. Eq. 6.4 is stochastic in nature and can be converted to an equivalent deterministic equation using Galerkin projection as

$$\overline{\boldsymbol{M}}\left\langle\Psi_m^2\right\rangle \boldsymbol{e}_m+\sum_{i=0}^{P} \boldsymbol{Y}_{im}^{(M)} \boldsymbol{e}_i+\boldsymbol{D}\left\langle\Psi_m^2\right\rangle \boldsymbol{d}_m+\overline{\boldsymbol{K}}\left\langle\Psi_m^2\right\rangle \boldsymbol{c}_m+\sum_{i=0}^{P} \boldsymbol{Y}_{im}^{(K)} \boldsymbol{c}_i=\left\langle\boldsymbol{q}(t) \Psi_m\right\rangle \tag{6.8}$$

where

$$\boldsymbol{Y}_{im}^{(M)}=\sum_{n=1}^{Q_M} \boldsymbol{M}_n \boldsymbol{X}_{nim}^{(M)} \tag{6.9}$$

$$\boldsymbol{X}_{nim}^{(M)}=\left\langle\xi_n^{(M)}(\theta) \Psi_i \Psi_m\right\rangle \tag{6.10}$$

$$\boldsymbol{Y}_{im}^{(K)}=\sum_{n=1}^{Q_K} \boldsymbol{K}_n \boldsymbol{X}_{nim}^{(K)} \tag{6.11}$$

$$\boldsymbol{X}_{nim}^{(K)}=\left\langle\xi_n^{(K)}(\theta) \Psi_i \Psi_m\right\rangle \tag{6.12}$$

$m=0,1,2,\ldots P$. It is also important to note that $\boldsymbol{d}$ and $\boldsymbol{e}$ are the first and second derivative of $\boldsymbol{c}$ with respect to time. Eq. 6.8 is deterministic in nature and total $N(P+1)$ deterministic simultaneous equation are formed, which need to be solved to obtain statistical responses of a structural system.

6.3.2 Solution using Newmark-β method

Eq. 6.8 is a deterministic equation describing the evaluation of the coefficients of PC expansion with time. This equation is similar to that of the linear structural dynamic equation in time domain. The time history of the coefficient $(\boldsymbol{c},\boldsymbol{d},\boldsymbol{e})$ of PC expansion can be calculated using different time stepping algorithm. In the present study, Newmark-β (Bathe, 1996) method of time integration is considered for the evaluation of the coefficient and is discussed below.

Eq. 6.8 can be written in a simplified form as

$$\widehat{\boldsymbol{M}}\ddot{\boldsymbol{r}}+\widehat{\boldsymbol{D}}\dot{\boldsymbol{r}}+\widehat{\boldsymbol{K}}\boldsymbol{r}=\widehat{\boldsymbol{q}}(\boldsymbol{t}) \tag{6.13}$$

where

$$\widehat{\boldsymbol{M}} = \begin{bmatrix} \overline{\boldsymbol{M}}\left\langle \Psi_0^2 \right\rangle & 0 & \dots & 0 \\ 0 & \overline{\boldsymbol{M}}\left\langle \Psi_1^2 \right\rangle & \dots & 0 \\ \vdots & \vdots & \ddots & \vdots \\ 0 & 0 & 0 & \overline{\boldsymbol{M}}\left\langle \Psi_P^2 \right\rangle \end{bmatrix} + \begin{bmatrix} \boldsymbol{Y}_{00}^{(M)} & \boldsymbol{Y}_{10}^{(M)} & \dots & \boldsymbol{Y}_{P0}^{(M)} \\ \boldsymbol{Y}_{01}^{(M)} & \boldsymbol{Y}_{11}^{(M)} & \dots & \boldsymbol{Y}_{P1}^{(M)} \\ \vdots & \vdots & \ddots & \vdots \\ \boldsymbol{Y}_{0P}^{(M)} & \boldsymbol{Y}_{1P}^{(M)} & \dots & \boldsymbol{Y}_{PP}^{(M)} \end{bmatrix} \tag{6.14}$$

$$\widehat{\boldsymbol{D}} = \begin{bmatrix} \boldsymbol{D}\left\langle \Psi_0^2 \right\rangle & 0 & \dots & 0 \\ 0 & \boldsymbol{D}\left\langle \Psi_1^2 \right\rangle & \dots & 0 \\ \vdots & \vdots & \ddots & \vdots \\ 0 & 0 & 0 & \boldsymbol{D}\left\langle \Psi_P^2 \right\rangle \end{bmatrix} \tag{6.15}$$

$$\widehat{\boldsymbol{K}} = \begin{bmatrix} \overline{\boldsymbol{K}}\left\langle \Psi_0^2 \right\rangle & 0 & \dots & 0 \\ 0 & \overline{\boldsymbol{K}}\left\langle \Psi_1^2 \right\rangle & \dots & 0 \\ \vdots & \vdots & \ddots & \vdots \\ 0 & 0 & 0 & \overline{\boldsymbol{K}}\left\langle \Psi_P^2 \right\rangle \end{bmatrix} + \begin{bmatrix} \boldsymbol{Y}_{00}^{(K)} & \boldsymbol{Y}_{10}^{(K)} & \dots & \boldsymbol{Y}_{P0}^{(K)} \\ \boldsymbol{Y}_{01}^{(K)} & \boldsymbol{Y}_{11}^{(K)} & \dots & \boldsymbol{Y}_{P1}^{(K)} \\ \vdots & \vdots & \ddots & \vdots \\ \boldsymbol{Y}_{0P}^{(K)} & \boldsymbol{Y}_{1P}^{(K)} & \dots & \boldsymbol{Y}_{PP}^{(K)} \end{bmatrix} \tag{6.16}$$

$$\widehat{\boldsymbol{q}}(\boldsymbol{t}) = \begin{Bmatrix} \left\langle \boldsymbol{q}(t)\Psi_0^2 \right\rangle \\ \left\langle \boldsymbol{q}(t)\Psi_1^2 \right\rangle \\ \vdots \\ \left\langle \boldsymbol{q}(t)\Psi_P^2 \right\rangle \end{Bmatrix} \tag{6.17}$$

and $\ddot{\boldsymbol{r}} = \{\boldsymbol{e}_m\}$, $\dot{\boldsymbol{r}} = \{\boldsymbol{d}_m\}$, $\boldsymbol{r} = \{\boldsymbol{c}_m\}$. The dimension of $\widehat{\boldsymbol{M}}$, $\widehat{\boldsymbol{D}}$ and $\widehat{\boldsymbol{K}}$ matrices are $N(P+1) \times N(P+1)$ and size of vector $\widehat{\boldsymbol{q}}(\boldsymbol{t})$, $\ddot{\boldsymbol{r}}$, $\dot{\boldsymbol{r}}$ and r are $N(P+1) \times 1$, where $N \times N$ is the size of stiffness matrix of the stochastic system (Eq. 6.1). The displacement, velocity and acceleration components can be calculated using time integration scheme. Considering well known Newmark-β method, the equation at time $(n+1)\Delta t$ can be written as

$$[a_0\widehat{\boldsymbol{M}} + a_1\widehat{\boldsymbol{D}} + \widehat{\boldsymbol{K}}]\boldsymbol{r}_{n+1} = \boldsymbol{q}_{n+1}^{eqv} \tag{6.18}$$

$$\boldsymbol{q}_{n+1}^{eqv} = \widehat{\boldsymbol{q}}(\boldsymbol{t})_{n+1} + [a_0\widehat{\boldsymbol{M}} + a_1\widehat{\boldsymbol{D}}]\boldsymbol{r}_n + [a_2\widehat{\boldsymbol{M}} + a_4\widehat{\boldsymbol{D}}]\dot{\boldsymbol{r}}_n + [a_3\widehat{\boldsymbol{M}} + a_5\widehat{\boldsymbol{D}}]\ddot{\boldsymbol{r}}_n \tag{6.19}$$

where

$$a_0 = \frac{1}{\beta \Delta t^2}, \quad a_1 = \frac{\gamma}{\beta \Delta t} \quad a_2 = \frac{1}{\beta \Delta t}, \\ a_3 = \frac{1}{2\beta} - 1, \quad a_4 = \frac{\gamma}{\beta} - 1, \quad a_5 = \left(\frac{\gamma}{2\beta} - 1\right)\Delta t \tag{6.20}$$

where $\gamma = 0.5$ and $\beta = 1/4$, considering average acceleration method of Newmark-β method. It can also be noted that though the matrices $\widehat{\boldsymbol{M}}$, $\widehat{\boldsymbol{D}}$ and $\widehat{\boldsymbol{K}}$ are deterministic in nature, these matrices represent the randomness in the material and geometric properties of the system. The unknown $\ddot{\boldsymbol{r}}$, $\dot{\boldsymbol{r}}$ and $\boldsymbol{r}$ are related to the stochasticity of responses. Similarly, $\boldsymbol{q}_{n+1}^{eqv}$ though deterministic can be related to random forces at time instant $(n+1)\Delta t$. The ensemble of these forces can be calculated using

$$\boldsymbol{q}_{n+1(\text{random})}^{eqv} = \boldsymbol{M}(a_0\boldsymbol{u}_n + a_2\dot{\boldsymbol{u}}_n + a_3\ddot{\boldsymbol{u}}_n) + \boldsymbol{D}(a_1\boldsymbol{u}_n + a_4\dot{\boldsymbol{u}}_n + a_5\ddot{\boldsymbol{u}}_n) \tag{6.21}$$

If mass is also considered as random, which may be due to random geometric properties Eq. 6.21 becomes

$$\boldsymbol{q}_{n+1(\text{random})}^{eqv} = \left(\overline{\boldsymbol{M}} + \sum_{i=1}^{Q_M} \xi_i^{(M)}(\theta)\boldsymbol{M}_i\right)(a_0\boldsymbol{u}_n + a_2\dot{\boldsymbol{u}}_n + a_3\ddot{\boldsymbol{u}}_n) + \boldsymbol{D}(a_1\boldsymbol{u}_n + a_4\dot{\boldsymbol{u}}_n + a_5\ddot{\boldsymbol{u}}_n) \tag{6.22}$$

Values of $\ddot{\boldsymbol{r}}_n$, $\dot{\boldsymbol{r}}_n$ and $\boldsymbol{r}_n$ are required to calculate $\boldsymbol{r}_{n+1}$. Value of $\boldsymbol{r}_n$ is obtained from the solution of the above equation at previous time step. $\dot{\boldsymbol{r}}_n$ and $\ddot{\boldsymbol{r}}_n$ are calculated from the approximation of acceleration and velocity as

$$\ddot{\boldsymbol{r}}_n = a_0\boldsymbol{r}_n - a_0\boldsymbol{r}_{n-1} - a_2\dot{\boldsymbol{r}}_{n-1} - a_3\ddot{\boldsymbol{r}}_{n-1} \tag{6.23}$$

$$\dot{\boldsymbol{r}}_n = a_1\boldsymbol{r}_n - a_1\boldsymbol{r}_{n-1} - a_4\dot{\boldsymbol{r}}_{n-1} - a_5\ddot{\boldsymbol{r}}_{n-1} \tag{6.24}$$

The responses at $n, n+1, \ldots$ represent the responses at time $n\Delta t, (n+1)\Delta t, \ldots$.

In the present study, the Newmark's method with operators corresponding to the assumption of average variation in acceleration (Bathe, 1996) is used, which gives an unconditionally stable time-integration scheme. Other such methods include the Wilson averaging operator and the Houbolt operator (Nickel, 1971), both of which provide unconditional stability to the evaluated dynamic response. The parameters β and γ, guided by the consideration of unconditional stability are taken as 0.25 and 0.5 respectively. For multiple DOF systems, magnitude of T will be guided by the time period of the highest significant vibration mode of the system. Hence, larger the dimension of the system matrix, the value of T is likely to be lower (associated with the highest significant vibration mode) and hence the time-step size, Δt. This can lead to some computational burden on any conventional PC based method as the dimension of the linear system increases exponentially with the increase in order or/and number of random variables used in the solution basis. It may however be noted that the size of system matrix is relatively reduced in TDgPC after any updation of PC basis function.

6.3.3 Initial condition

To solve the dynamic equilibrium equation, initial conditions of the system are required to be applied. Since the system is random in nature, the initial conditions are also needed to be specified in terms of its ensembles, i.e. for each realization, the initial conditions are required to be specified. Thus, the random field of displacement and velocity at time $t = 0$ need to be specified. There may be two possibilities for specifying the initial conditions. The first one is to specify the complete random field for the ensemble, while the second approach is to specify the coefficients ($\boldsymbol{c}^{(0)}$ and $\boldsymbol{d}^{(0)}$ for initial displacement and velocity respectively) of PC expansions as in Eq. 6.5 and 6.6 at time $t = 0$. However, if the initial conditions are specified using the first approach, the coefficients $\boldsymbol{c}^{(0)}$ and $\boldsymbol{d}^{(0)}$ for initial displacement and velocity are needed to be evaluated using Eqs. 6.5 and 6.6. These two sets of coefficients can be related to displacement ($\boldsymbol{r}_0$) and velocity ($\dot{\boldsymbol{r}}_0$) to be used as initial conditions. In the present study, the systems are considered at rest at time $t = 0$. Hence, all the ensemble of displacements and velocities are assumed to be zero, leading to the value of the coefficients $\boldsymbol{c}^{(0)}$ and $\boldsymbol{d}^{(0)}$ as zero. The initial acceleration ($\boldsymbol{e}^{(0)}$) can be calculated from Eq. 6.8 as

$$\overline{\boldsymbol{M}}\left\langle \Psi_m^2 \right\rangle \boldsymbol{e}_m^{(0)} + \sum_{i=0}^{P} \boldsymbol{Y}_{im}^{(M)} \boldsymbol{e}_i^{(0)} = \left\langle \boldsymbol{p}^{(0)}(t)\Psi_m \right\rangle \tag{6.25}$$

This equation is a deterministic equation and can be solved for the coefficients of PC expansion for acceleration at time $t = 0$.

6.4 Solution using Time-Dependent generalized Polynomial Chaos (TDgPC)

6.4.1 Basic idea

The solution strategy, as discussed in the previous section using a combination of PC and Newmark-β method, can provide a reasonably accurate approximation of responses up-to a certain time duration, where responses of a structural system with random material properties are approximated using PC expansion. The stochastic equations are transformed to a set of simultaneous deterministic equations using Galerkin projection, which are solved using Nemarks-β method. Similar to the observation made by Gerritsma et al. (2010), in the case of structural dynamics problem as well, responses deviate as time progresses. The deviation of responses from MCS is delayed as the order of PC expansion increases. Gerritsma et al. (2010) observed that the mean responses of stochastic ordinary differential equation deviate from the deterministic solution as time progresses. In the early stage, the responses do agree, however, as time progresses, the deviation is observed to increase, which is known as stochastic drift. Thus the authors (Gerritsma et al., 2010) concluded that the responses could be approximated as a linear combination of the random input only for early times. Kundu and Adhikari (2014) also made similar observation in case of structural dynamics problem with impact loading, the mean responses deviate from deterministic responses with an effect which can be considered as equivalent to that of a damping on the mean responses. As time progresses, increasing order of PC expansion is required as the non-linear development becomes more and more dominant (Gerritsma et al., 2010). The initially considered PC losses its optimality as the statistic (pdf) of responses changes over time. A similar observation is made in the present study, as time progresses, the pdf of responses changes losing optimality of PC expansion. Thus, the responses deviate from MCS as time progresses. A higher order of PC expansion only delays the deviation of responses. However, with the increase in the order of PC expansion, the computational cost further increases. Time-Dependent Generalized Polynomial Chaos (TDgPC) was proposed by Gerritsma et al. (2010) to address the loss of optimality of PC expansion.

The basic idea of TDgPC is to change the PC expansion where it fails to represent the response with proper approximation. The initially considered PC expansion may provide a reasonably good accuracy up-to a time duration $t = n_1 \Delta t$, which may however fail to provide good accuracy at time $t = (n_1 + 1)\Delta t$. This is because the initially considered PCs are optimal only up-to time $t = n_1 \Delta t$. Due to change of statistical parameters of responses, the initial PCs may not be optimal at time $t = (n_1 + 1)\Delta t$. The responses of a structure under dynamic loading possess Markov property, and thus the responses are dependent only on the responses of the previous time step and not on the history of responses. Hence, the responses at time $t = (n_1 + 1)\Delta t$ can be approximated using a PC expansion generated based on the responses at time $t = n_1 \Delta t$. The PCs are updated at time instant $t = (n + 1)\Delta t$ based on the evaluated accurate response at time $t = n_1 \Delta t$.

Gerritsma et al. (2010) studied ordinary (first-order) differential equation with random decay rate and Kraichnan-Orszag three modes problem using TDgPC. The responses at time $t = n_1 \Delta t$ was used to generate PC using Gram-Schmidt orthogonalization. Ozen and Bal (2016) updated PC at predefined time locations and the PCs were generated using modified Gram-Schmidt orthogonalization process considering the moment of responses rather than considering the ensemble of responses. This type of orthogonalization process from only moments may be suitable for random variables, which can be represented using lower-order moments. Moreover, for a degree of polynomial $m-1$, a total of $2m-1$ moments are needed. However, the calculation of moments without calculating ensembles is computationally demanding. Ozen and Bal (2017) further extended the method to higher-dimensional problems with Markovian forcing, where the orthogonal polynomials are generated using the modified Gram-Schmidt orthogonalization process. The number of random variables for the orthogonalization process was reduced by considering only the dominant component of responses and were evaluated using KL expansion.

In the present study, structural dynamics problems with random material and geometric properties are studied using TDgPC. The PCs are updated at a suitable location based on an assumed accuracy criterion. The updation is based on the responses.

The optimality of PC expansion and updation criteria is discussed in section 6.4.2. PCs are generated at updation time instant using the Gram-Schmidt orthogonalization process, as discussed in section 3.4.3. As the polynomial is updated at some discrete locations, the initial conditions are also needed to be updated, and the same is discussed in section 6.4.3. The algorithm of TDgPC is discussed in section 6.4.4.

6.4.2 Optimality of PC expansion and Updation criteria

As discussed in the previous section, the initially considered PC loses its optimality over time. The PC expansion is assumed to be optimal depending on the relative values of the coefficients of expansion. It is assumed that a particular PC expansion is optimal as long as the linear term of the expansion is governing the expansion, i.e. the coefficient of the linear term is assumed to be more significant than the coefficients of non-linear terms. The coefficient of the constant term is not considered in the comparison process as it gives only the mean value and does not contribute to the probabilistic distribution of the responses.

Assuming that the response given by the initially generated of PC is giving a satisfactory result upto time t_1, Gerritsma et al. (2010) considered that linear term of PC expansion should govern the expansion. Authors considered that the coefficient of the linear term is comparatively dominating than the non-linear coefficients such that

$$\frac{\max(c^{(2)}, c^{(3)}, \ldots, c^{(p)})}{c^{(1)}} \leq \frac{1}{\varphi} \tag{6.26}$$

where superscript $^{(\cdot)}$ indicates the order of PC expansion and φ is a tolerance limit. In the present study, since multiple random variables are considered, the minimum of the coefficients of the first order PC expansion may be compared with the maximum of the coefficient of the higher-order PC. If this condition is violated, a new PC may be generated, which is a function of responses at time t_1 and subsequently wherever the condition is violated. Ozen and Bal (2017) considered norm ratio of the non-linear terms in the variance to the norm of the variance,

$$\rho(t) = \frac{||\sum_{|p|>1} c^2_{j,p}(.,t)||_{L^1}}{||\sum_{|p|>0} c^2_{j,p}(.,t)||_{L^1}}, \quad t \in [t_{j-1}, t_{j-1} + \Delta t_{j-1}] \tag{6.27}$$

In the first criterion, the authors considered the effect of only one of the higher-order terms and ignored the importance of all other coefficients. Similarly, in the case of the second criterion, though the effects of all the coefficients are considered, it is physically difficult to assign a limiting value to ensure that the contribution of linear terms is significantly higher than non-linear terms. Thus, in the present study, a slightly modified criterion is proposed (Eq. 6.28), which is defined as the ratio of the RMS of the coefficient of the non-linear terms of PC expansion to the RMS of the linear terms. Thus,

$$\frac{\sqrt{\text{Mean}\left({}^{(>1)}\boldsymbol{c}^2\right)}}{\sqrt{\text{Mean}\left({}^{(1)}\boldsymbol{c}^2\right)}} < \frac{1}{\varphi} \tag{6.28}$$

where $\boldsymbol{c}$ are the coefficients of PC expansion (Eq. 6.5). The left superscript indicates the order of PC expansion and right superscript indicate the square of of $\boldsymbol{c}$. The new criterion assigns equal weightage to all the coefficients, while adoption of a limit is also relatively simple. A parametric study is conducted in section 6.5.1 for accurate evaluation of responses with different values of φ for the proposed updation criterion.

6.4.3 Updation of initial condition

At the time instant $n_1\Delta t$ of updation of polynomial, the stochastic equations are solved where initial conditions are reconstructed for obtaining solution at $(n+1)\Delta t$. This can be considered as a new problem to be solved using the updated PC from time $t = (n_1+1)\Delta t$ onwards until the accuracy criterion fails. The responses at time $t = n_1\Delta t$ are the initial condition for the evaluation of responses at time $t = (n_1+1)\Delta t$. However, these must be expressed in terms of new PC coefficients. The new PC coefficients can be calculated from Eqs. 6.5-6.7 considering the new PC expansion $\Psi_j[\xi_r(\theta)_{\text{new}}]$. The left-hand sides of Eqs. 6.5-6.7 are the ensemble of responses at the previous time step ($t = n_1\Delta t$).

6.4.4 Algorithm of TDgPC

The basic philosophy, updation criterion and related discussion for TDgPC are presented in the previous sections. The stepwise algorithm for TDgPC for structural mechanics problem is described below.

Stepwise algorithm of TDgPC

A4-1 Perform KL expansion on the random field.

$$\boldsymbol{E}(x,\theta) = E_0\left(1+\sum_{n=1}^{Q}\xi_n(\theta)\sqrt{\lambda_n}f_n(x)\right)$$

A4-2 Evaluate number of random variables (Q) of KL expansion based on % expected energy consideration.

{

while energy $\leq$threshold

$Q = Q + 1$

energy=energy+$\lambda_Q / sum(\lambda)$

end while

}

A4-3 In case of non-Gaussian random field

(a) Generate $\xi_n(\theta)$ iteratively as discussed in section 4.2.1.

(b) Perform ICA on the random variables of KL expansion.

$$\xi_n(\theta)_{\text{Dependent}} \xrightarrow{\text{using Fast ICA}} \xi_n(\theta)_{\text{Independent}}$$

(c) Transform the independent random variable to same distribution using non-linear transformation. (Also in the case of non-Gaussian random variable problem and different distribution problems.)

$$\xi_n(\theta)_{\text{Independent}} \xrightarrow{\text{Non-linear transformation}} \xi_n(\theta)_{\text{Same disctribution}}$$

A4-4 Formulate stiffness matrix as discussed in sections 3.2.2 and 4.2.3 for Gaussian and non-Gaussian random field respectively.

A4-5 Formulate mass matrix as discussed in section 6.2.1.

A4-6 Formulate damping matrix as discussed in section 6.2.1.

A4-7 Chose an order of PC expansion,p.

A4-8 Construct the random vector considering randomness from both stiffness and mass $\xi_r(\theta) = \{\xi_n^{(M)}(\theta), \xi_n^{(K)}(\theta)\}$.

A4-9 Construct PC expansion using Gram-Schmidt orthogonalization process as discussed in section 3.4.3, considering $\xi_r(\theta)$ as the random variables.

A4-10 Approximate responses using PC expansion using Eqs. 6.5-6.7.

A4-11 Convert the stochastic equation to a set of simultaneous deterministic equation using Galerkin projection.

A4-12 Apply initial conditions as discussed in section 6.3.3.

A4-13 Solve the transformed deterministic equation using Newmark-β,

A4-14 Check for accuracy criteria as par Eq. 6.28.

A4-15 If accuracy calculated in step A4-14 is within limit, continue evaluation of dynamic responses using Newmark-β

A4-16 If accuracy calculated in step A4-14 exceeds the desired limit, PC are reconstructed.

(a) Evaluate dominant random variables, ($\xi_i(\theta)_{\text{disp}}$) using KL expansion of covariance function ($\boldsymbol{C}_{\boldsymbol{u}_1\boldsymbol{u}_2}$) of displacement responses.

$$\xi_i(\theta)_{\text{disp}} = \frac{1}{\sqrt{\lambda_{\text{new}_i}}} \boldsymbol{u}_{\text{mean}} E_{\text{vector new}_i}$$

where λ_{new_i} and $E_{\text{vector new}_i}$ are the eigenvalue and eigenvector of the covariance function of the responses. $\boldsymbol{u}_{\text{mean}}$ is the matrix of zero mean responses. The covariance function of responses is calculated as,

$$\boldsymbol{C}_{u_1 u_2} = \mathbb{E}[(u_1 - \text{mean}(u_1))(u_2 - \text{mean}(u_2))]$$

(b) Evaluate dominant random variables, ($\xi_i(\theta)_{\text{load}}$) using KL expansion of covariance function of transformed loading ($\boldsymbol{q}^{\text{equiv}}$) evaluated using Eq. 6.22.

$$\xi_i(\theta)_{\text{load}} = \frac{1}{\sqrt{\lambda_{\text{new}_i}}} \boldsymbol{q}^{\text{equiv}}_{\text{mean}} E_{\text{vector new}_i}$$

where λ_{new_i} and $E_{\text{vector new}_i}$ are the eigenvalue and eigenvector of the covariance function of the random forces. $\boldsymbol{q}^{\text{equiv}}_{\text{mean}}$ is the matrix of zero mean loading. The covariance function of responses is calculated as,

$$\boldsymbol{C}_{q_1^{\text{equiv}} q_2^{\text{equiv}}} = \mathbb{E}[(q_1^{\text{equiv}} - \text{mean}(q_1^{\text{equiv}}))(q_2^{\text{equiv}} - \text{mean}(q_2^{\text{equiv}}))]$$

(c) Construct vector of random variables $\xi(\theta)_{\text{new}} = \{\xi_i(\theta)_{\text{disp}}, \xi_i(\theta)_{\text{load}}\})$

(d) Construct the basis vectors for Gram-Schmidt process by considering tensor product of the random variables $\{\xi(\theta)_{\text{new}}\}$ as discussed in section 3.4.3.

(e) Construct new PC ($\Psi_j[\xi_r(\theta)_{\text{new}}]$) using Gram-Schmidt orthogonalization as discussed in section 3.4.3.

(f) Approximate responses using new PC ($\Psi_j[\xi_r(\theta)_{\text{new}}]$) expansion using Eqs. 6.5-6.7

(g) Perform Galerkin projection

(h) Update initial conditions as discussed in section 6.4.3.

(i) Go to step A4-13

It is also important to note that the new random variables $\{\xi(\theta)_{\text{new}}\}$ are considered only to approximate responses and updation of initial condition at the location of updation of PC. The random variables describing the randomness of material and geometric properties do not change as these quantities are considered as time invariant.

6.5 Numerical examples

6.5.1 Deflection of truss under cyclic loading

The first example considered is a 2-D cantilever truss as shown in Fig. 6.1. The area and Young's modulus of the members are considered to have independent Gaussian distribution with parameters as shown in Table 6.1.

The structure is subjected to a cyclic loading ($q(t)$) at the free end. The load-time history is shown in Fig. 6.2 and is given by Eq. 6.29

$$q(t) = \begin{cases} \sin(2\pi\omega_q t)\ \text{N}, & \text{if } 0 \leq t \leq 10, \quad \omega_q = 2 \\ 0, & \text{otherwise} \end{cases} \tag{6.29}$$

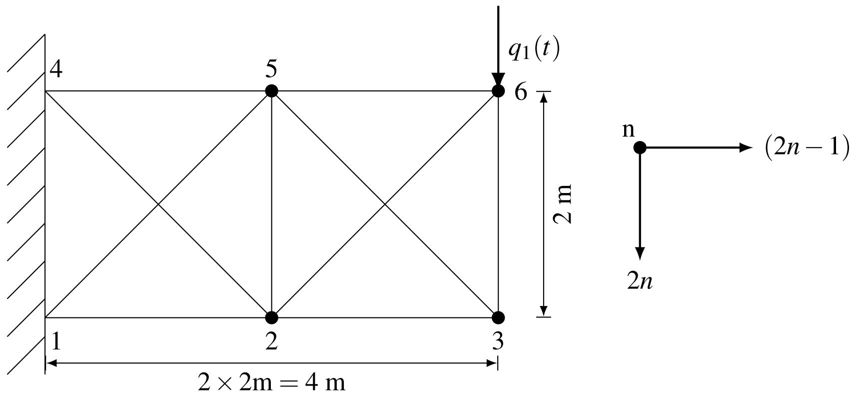

Fig. 6.1: Cantilever truss with loading.

Table 6.1: Distribution of random parameters of truss structure.

Member	Parameter	Unit	Mean	SD	Distribution
Bottom	Area, A_1	m^2	2×10^{-3}	2×10^{-4}	Gaussian
Cord	Youngs's modulus, E_1	Pa	2.1×10^{11}	2.1×10^{10}	Gaussian
Top Cord	Area A_2	m^2	2×10^{-3}	2×10^{-4}	Gaussian
	Youngs's modulus, E_2	Pa	2.1×10^{11}	$2.1\times^{10}$	Gaussian
Vertical	Area A_3	m^2	1×10^{-3}	1×10^{-4}	Gaussian
Member	Youngs's modulus, E_3	Pa	2.1×10^{11}	2.1×10^{10}	Gaussian
Inclined	Area A_4	m^2	1×10^{-3}	1×10^{-4}	Gaussian
Member	Youngs's modulus, E_4	Pa	2.1×10^{11}	2.1×10^{10}	Gaussian

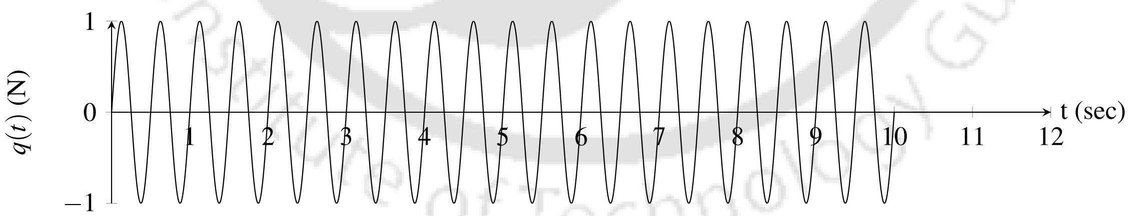

Fig. 6.2: Imposed cyclic load on truss.

The input random parameters are Gaussian in nature. However, these are of different mean and standard deviation and hence these input variables are transformed to standard Gaussian distribution by subtracting the mean and dividing by the standard deviation of the corresponding random variable. The transformed random variables are shown in Fig. 6.3 and are considered only to generate PC. The random variables, characterising the input material and geometric properties however remain the same. The properties and the covariance of the transformed random variables are shown in Tables 6.2 and 6.3 respectively. The mass matrix for each member is given by

$$\boldsymbol{M}_i = \rho L_i A_i(\theta)/6 \begin{bmatrix} 2 & 0 & 1 & 0 \\ 0 & 2 & 0 & 1 \\ 1 & 0 & 2 & 0 \\ 0 & 1 & 0 & 2 \end{bmatrix} \tag{6.30}$$

where ρ is the mass density of the member, $A_i(\theta)$ is the area of each member and considered as Gaussian random variable in the present study. L_i is the length of each member. Two additional masses of 22.5×10^4 kg and 11.25×10^4 kg are considered at node 5 and 6 respectively, which corresponds to superimposed dead load. The first frequency is found to be 1.108 Hz. The time steps for analysis is considered as 0.01 second based on acceptable modal mass participation. Modal damping of 1% is considered for all the modes. As the area is considered as random, the mass matrix is also random. However, for simplicity, the damping matrix is not considered random and evaluated considering the deterministic part of stiffness and mass matrices. The dynamic equation can be written as

$$\left(\overline{\boldsymbol{M}} + \sum_{i=1}^{S} \boldsymbol{M}_i(A_i(\theta)) \right) \ddot{\boldsymbol{u}} + \boldsymbol{D}\dot{\boldsymbol{u}} + \sum_{i=1}^{S} \boldsymbol{K}_i(A_i(\theta), E_i(\theta))\boldsymbol{u} = \boldsymbol{q}(t) \tag{6.31}$$

where $\overline{\boldsymbol{M}}$ is mass matrix due to superimposed dead load at node 5 and 6.

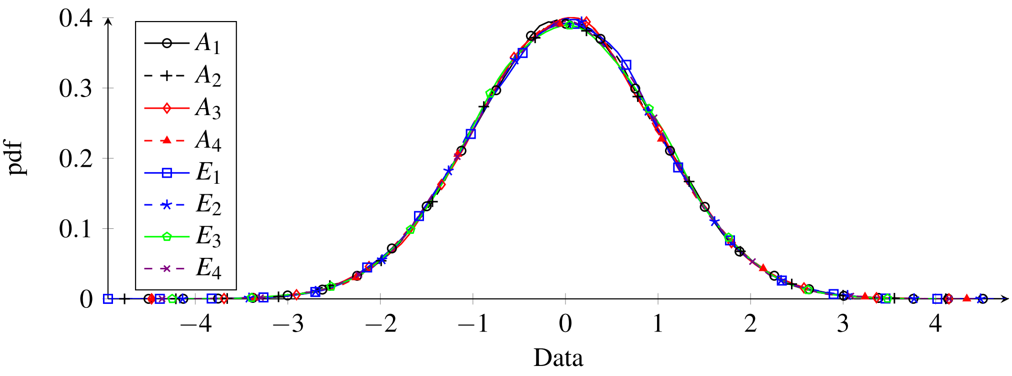

Fig. 6.3: pdfs of transformed random variables.

Table 6.2: Properties of the transformed random variables of truss structure.

	Mean	SD	Skewness	Kurtosis
A_1	6.544×10^{-11}	1.000	-6.092×10^{-03}	2.992
A_2	1.216×10^{-10}	1.000	-4.048×10^{-03}	3.017
A_3	-2.703×10^{-10}	1.000	-5.196×10^{-03}	3.034
A_4	-6.406×10^{-11}	1.000	4.656×10^{-02}	3.019
E_1	1.311×10^{-10}	1.000	-2.079×10^{-02}	2.981
E_2	-1.404×10^{-11}	1.000	2.228×10^{-02}	3.002
E_3	-1.022×10^{-11}	1.000	-1.910×10^{-02}	2.954
E_4	-4.851×10^{-11}	1.000	-1.135×10^{-02}	3.004

Table 6.3: Covariance of the transformed random variables of truss structure.

	A_1	A_2	A_3	A_4	E_1	E_2	E_3	E_4
A_1	1.00000	0.00592	-0.00614	0.00465	0.00252	0.00033	0.00257	-0.00041
A_2	0.00592	1.00000	0.00093	0.00704	-0.01236	-0.00265	0.00212	0.00168
A_3	-0.00614	0.00093	1.00000	0.01232	-0.00028	-0.00255	-0.00348	0.01417
A_4	0.00465	0.00704	0.01232	1.00000	0.00084	-0.01035	0.00748	-0.00397
E_1	0.00252	-0.01236	-0.00028	0.00084	1.00000	-0.01035	0.00285	0.00627
E_2	0.00033	-0.00265	-0.00255	-0.01035	-0.01035	1.00000	-0.00255	0.00025
E_3	0.00257	0.00212	-0.00348	0.00748	0.00285	-0.00255	1.00000	0.00455
E_4	-0.00041	0.00168	0.01417	-0.00397	0.00627	0.00025	0.00455	1.00000

6.5.1.1 Evaluation of Responses using mPC and Newmark-β method

The truss is analysed for the given loading, while the statistical responses are approximated using PC. The PCs are generated using the transformed random variables and using Gram-Schmidt orthogonalization process as discussed in section 3.4.3 and these are designated as mPC. The deterministic equation formed after Galerkin projection is solved using Newmark-β method. A sample size of 3×10^4 is considered for analysis. The same seeds of random variables are used in all the analyses so that there would not be any anomaly in input while comparing the responses. Though the input variables are Gaussian, the responses may not be Gaussian due to the non-linear relation between the input and the responses. Thus, higher-order statistical moments (skewness and kurtosis) of responses are also compared with MCS responses along with mean and SD of responses. As discussed in previous sections, the responses approximated using PC based method may not agree well with MCS responses, and hence, the problem is further analysed using TDgPC in the next section. Results obtained using different orders of PC expansions are discussed along with the results from TDgPC in the following section.

6.5.1.2 Responses using TDgPC and Newmark-β method

In the previous section, the problem is solved considering PC approximation of responses. In this section the problem is solved using TDgPC scheme. In TDgPC, the PCs are updated wherever it fails to approximate the response with a pre-assumed accuracy. The PCs in all these cases are mPC, generated using Gram-Schmidt orthogonalization process as discussed in section 3.4.3.

The transformed equation after Galerkin projection (Eq. 6.13) is deterministic in nature and is solved using Newmark-β method. At each time steps, the coefficients of PC expansion for displacement at free end (DOF=12) are checked for accuracy using accuracy criterion as given by Eq. 6.28. At a time instant where the criterion fails, the PCs are updated. The ensemble of displacement is considered to updated the random variables to generate PC expansion. As shown in Eq. 6.22, the randomness in the responses $(\ddot{\boldsymbol{u}}, \dot{\boldsymbol{u}}, \boldsymbol{u})$ generate an ensemble of loading forces. Two random variables from the displacement and two random variables from random forces are considered in the updation of new PC. The random variables are evaluated using KL expansion of displacements and forces. The initial conditions are updated based on the new PC expansion as discussed in section 6.4.3. In order to study the effect of order of PC expansion and value of tolerance limit (φ), three different values $\varphi = \{6,\ 8.\ 10\}$ are considered with 2^{nd},3^{rd},4^{th} order of PC expansion.

The time history of statistical parameters of vertical displacement at the free end (DOF=12) of truss when solved using different orders of PC in TDgPC scheme with tolerance limit of φ are checked for accuracy with respect to the responses of MCS and compared with responses of mPC expansion. Figs. 6.4-6.6 show the time history of statistical parameters of displacements where order of PC is varied from 2 to 4.

It can be observed from time history (Figs. 6.4-6.6) that in case of responses of different order of PC expansion, as the order increases the mean and standard deviation converges toward MCS with the increase in order of PC. However, the same is not observed in the case of skewness, kurtosis and envelop of displacement.

The responses of TDgPC converges as the value of φ increases for all the three orders considered. However, a minimum order of PC expansion is required for attaining good agreement with responses of MCS. The responses of TDgPC is observed to be having far higher agreement with MCS than responses of mPC of same order or even higher order PC for all the statistical parameters considered.

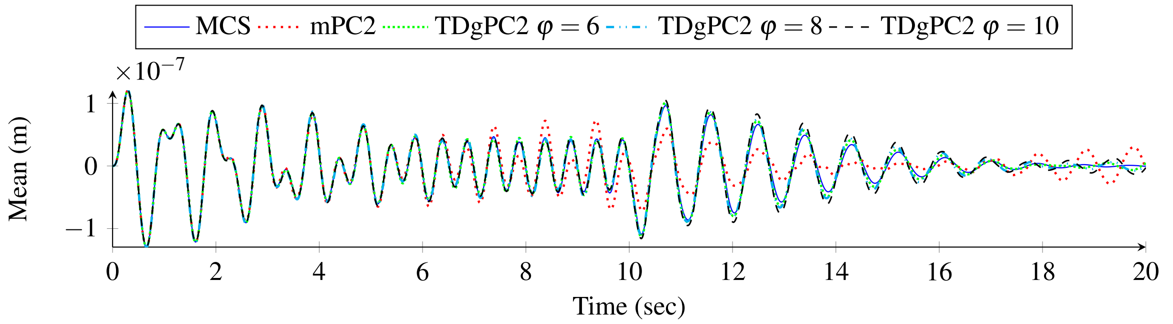

(a) Mean of displacement.

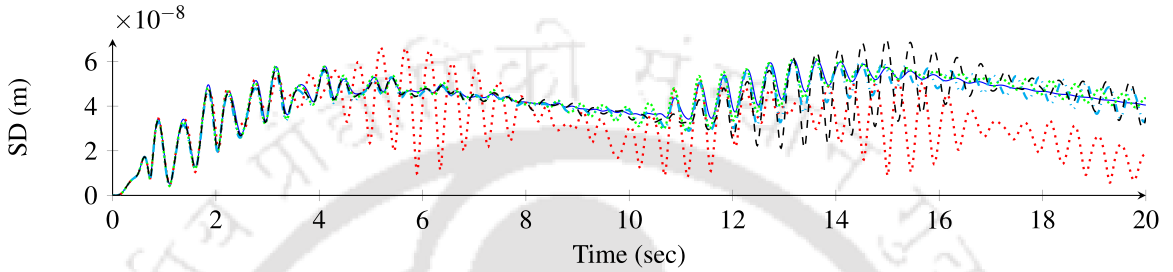

(b) SD of displacement.

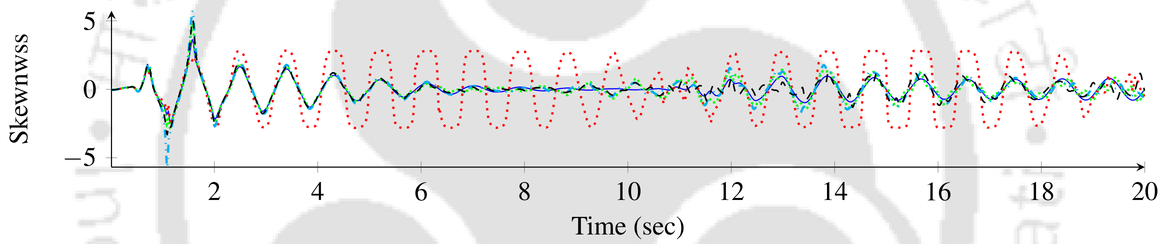

(c) Skewness of displacement.

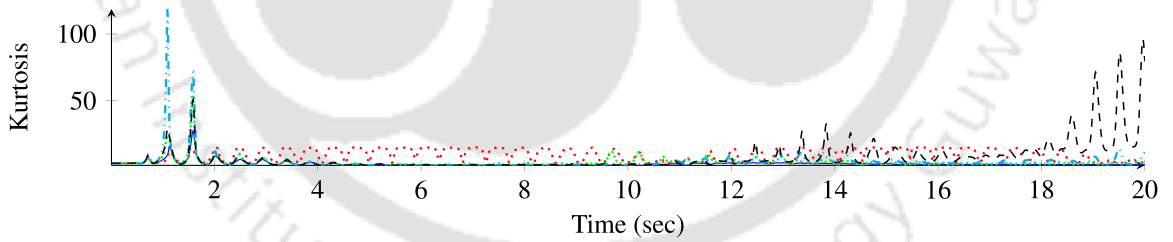

(d) Kurtosis of displacement.

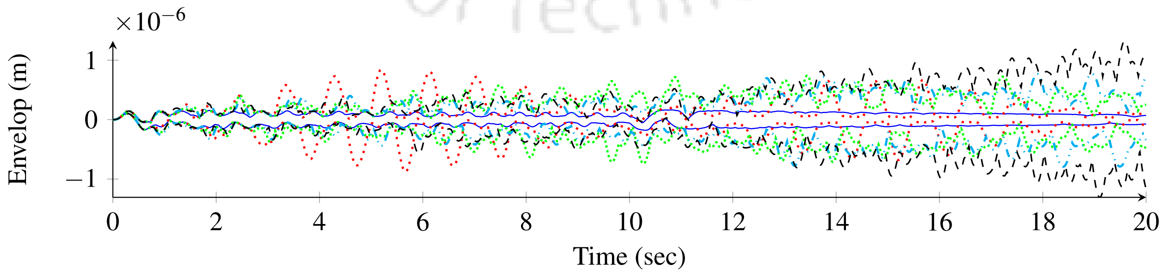

(e) Envelop of displacement.

Fig. 6.4: Time history of statistical parameters of vertical deflection at the free end (DOF=12) for different values of tolerance limit (φ) with order of PC equal to 2.

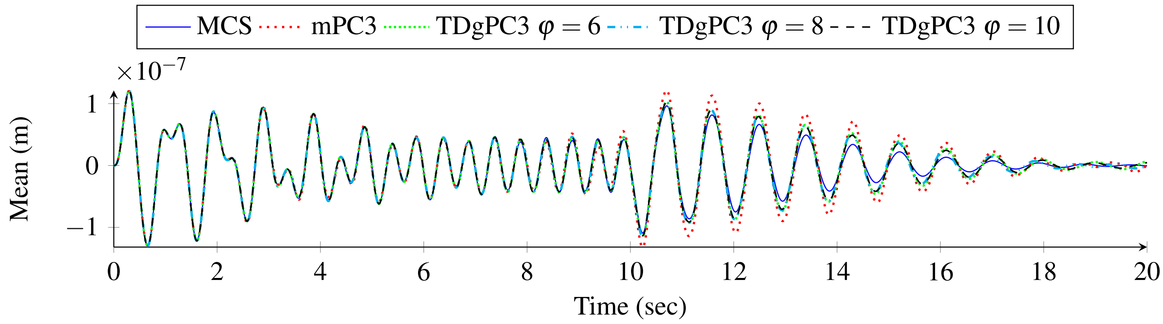

(a) Mean of displacement.

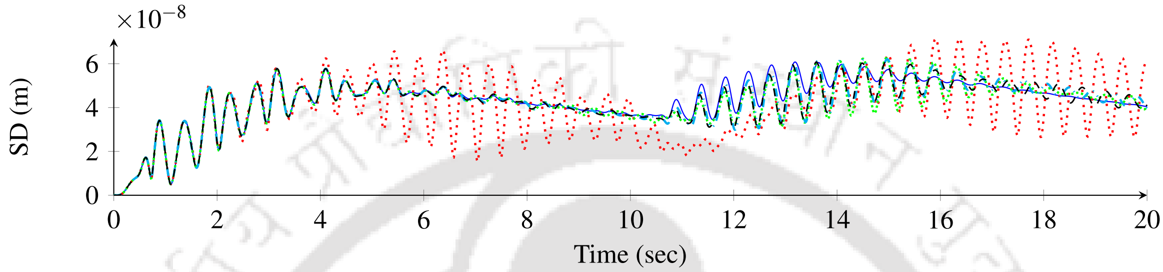

(b) SD of displacement.

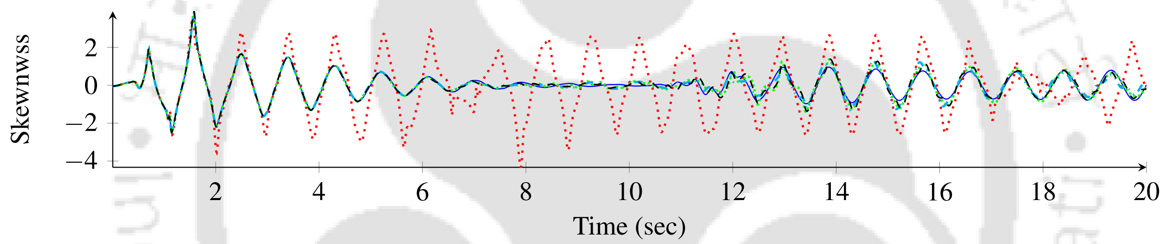

(c) Skewness of displacement.

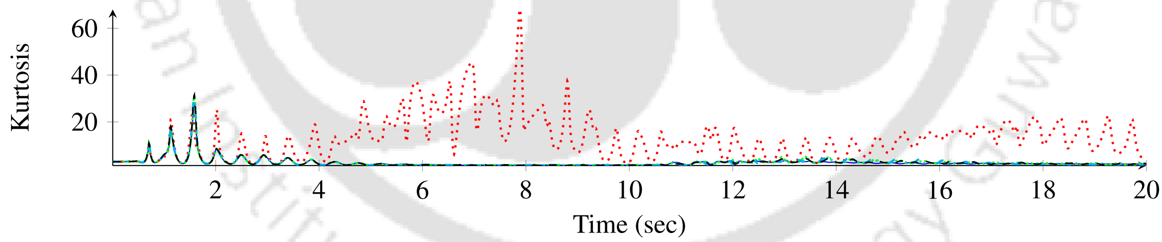

(d) Kurtosis of displacement.

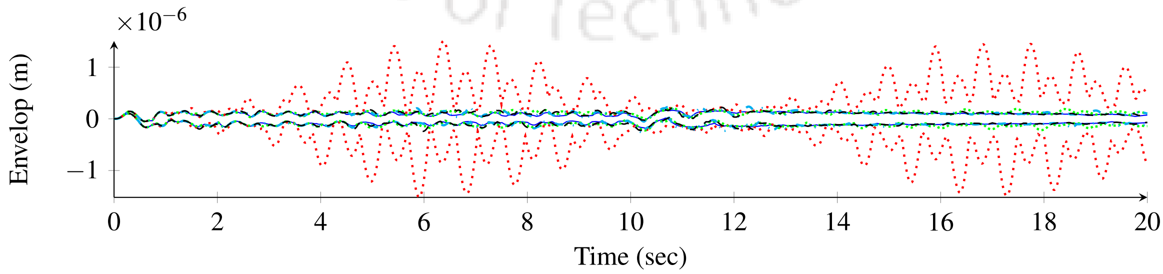

(e) Envelop of displacement.

Fig. 6.5: Time history of statistical parameters of vertical deflection at the free end (DOF=12) for different values of tolerance limit (φ) with order of PC equal to 3.

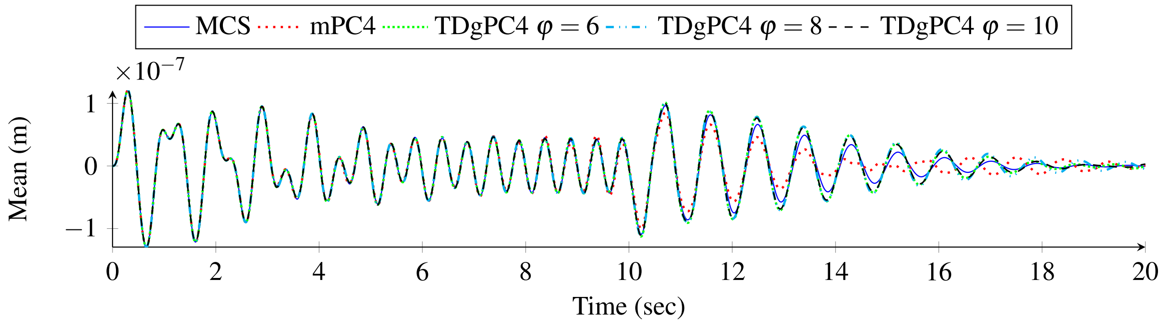

(a) Mean of displacement.

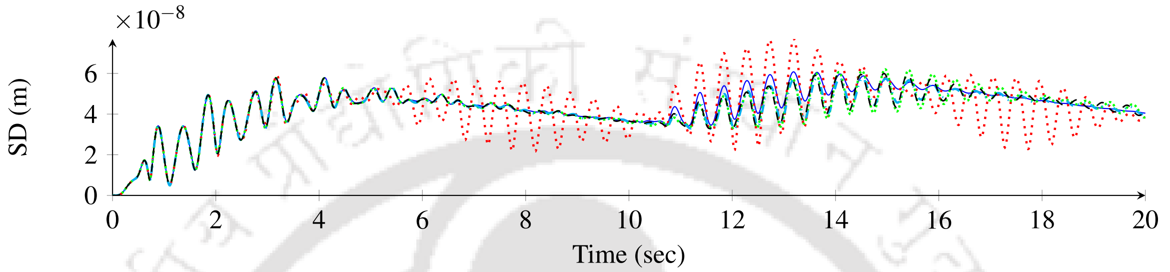

(b) SD of displacement.

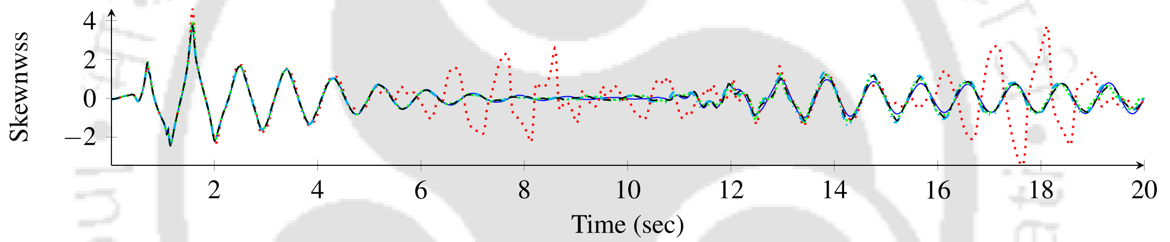

(c) Skewness of displacement.

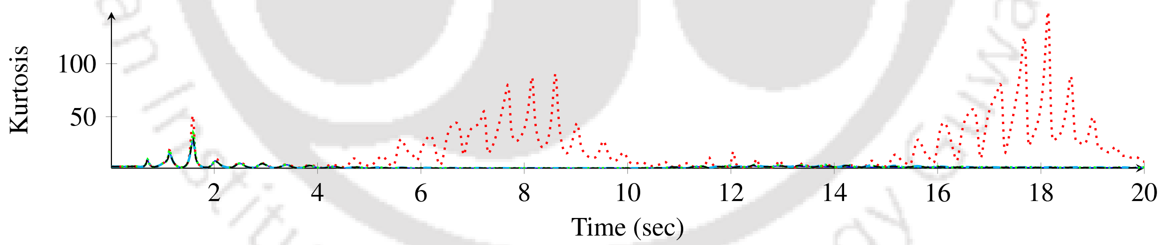

(d) Kurtosis of displacement.

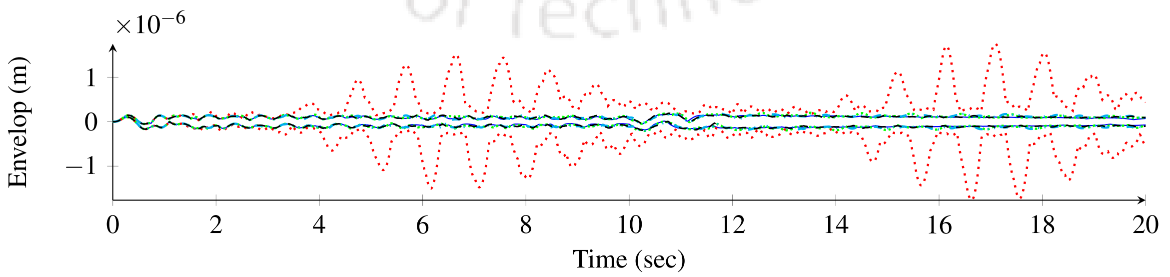

(e) Envelop of displacement.

Fig. 6.6: Time history of statistical parameters of vertical deflection at the free end (DOF=12) for different values of tolerance limit (φ) with order of PC equal to 4.

The fact that the higher-order moments are not correctly calculated even by the fourth-order PC expansion is also verified from the plots of pdf at time instant $t = \{0.1,\ 2,\ 4,\ 6\}$ s. The pdfs of displacement at the free end at time instant $t = \{0.1,\ 2,\ 4,\ 6\}$ s evaluated using mPC of different orders of PC are shown in Fig. 6.7 and compared with pdfs of MCS. It can be observed that at time instant $t = 0.1$ s, the pdfs of displacement evaluated using different order mPC matches very well with pdf of MCS. However, as time progresses, these pdfs differ from MCS as can be seen from pdfs at time instant $t = \{2,\ 4,\ 6\}$ s. This is because, at time instant $t = 0.1$ s, the responses are nearer to Gaussian and thus initially considered PC expansion can approximate the response with some good degree of accuracy. However, as the statistical properties of displacement changes over time, the initially considered PC approximation is not appropriate to represent the responses. The initially considered PC can approximate the responses only upto a certain duration of time.

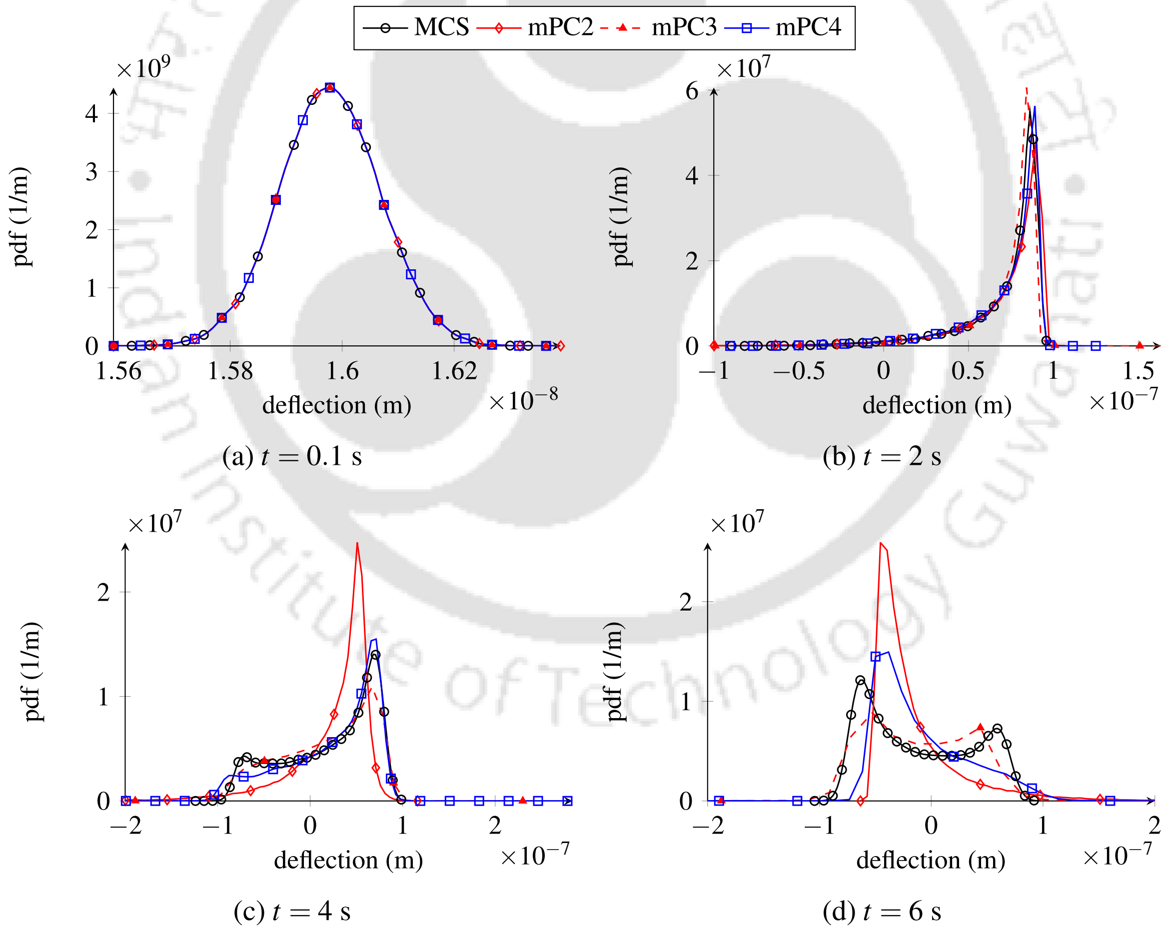

(a) $t = 0.1$ s (b) $t = 2$ s (c) $t = 4$ s (d) $t = 6$ s

Fig. 6.7: pdf of displacement at free end at different time instant, evaluated using different order of mPC.

The pdfs of displacement at free end at different time instant $t = \{2,\ 4,\ 6,\ 8\}$ s are shown in Fig. 6.8 when solved using TDgPC scheme with different orders of PC expansion. It can be observed that the pdfs are in good agreement with pdfs of MCS. Thus, it can be concluded that the PC bases at these time instant in TDgPC are optimal.

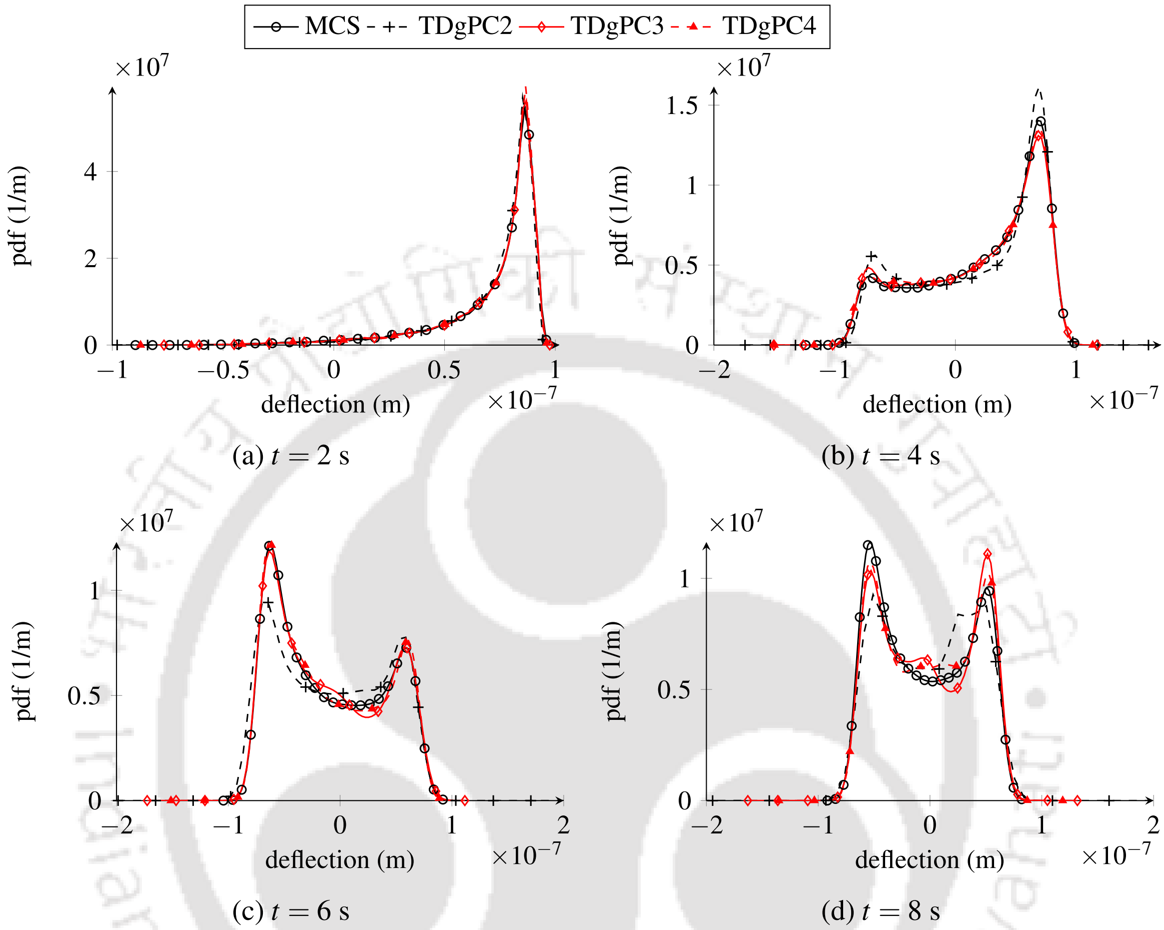

Fig. 6.8: pdf of displacement at free end at different time instant, evaluated using different order of TDgPC ($\varphi = 6$).

The accuracy of responses evaluated using mPC and TDgPC scheme are checked using RMS error with respect to MCS. The calculated RMS are further normalized by mean of responses evaluated using MCS. Thus, RMS error is defined as

$$\mathrm{RMS}(t) = \frac{\sqrt{\mathrm{Mean}\left[\left(u_{\mathrm{MCS}}(t) - u(t)\right)^2\right]}}{\left|\mathrm{Mean}(u_{\mathrm{MCS}}(t))\right|} \tag{6.32}$$

The RMS errors of displacement at the free end are evaluated for different order of PC expansion when solve using mPC and TDgPC scheme and are shown in Fig. 6.9. It can be observed that the error in the case of TDgPC scheme is lesser than mPC scheme.

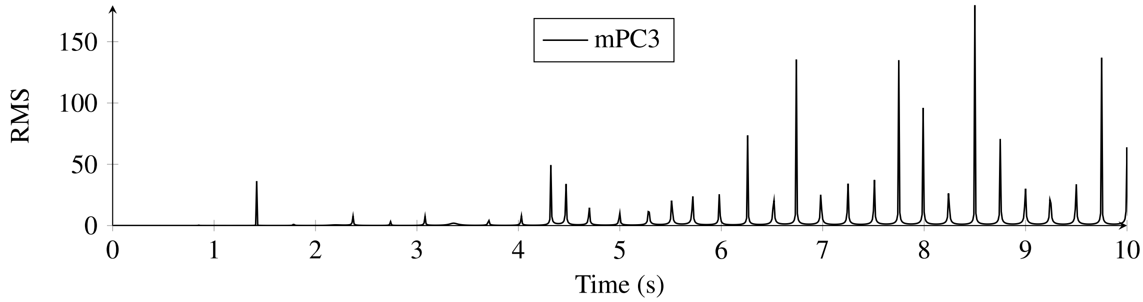

(a) mPC of 3rd order.

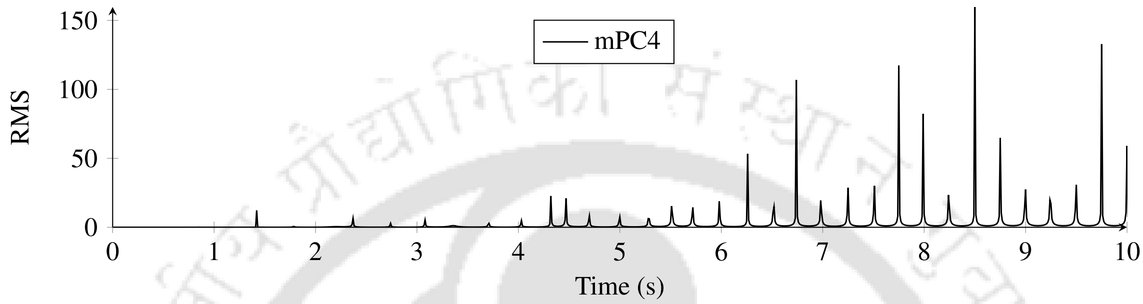

(b) mPC of 4th order.

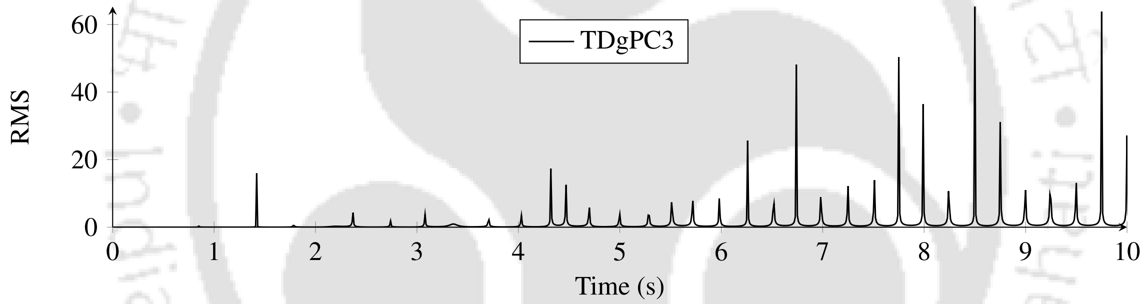

(c) TDgPC scheme of 3rd order PC ($\varphi = 6$).

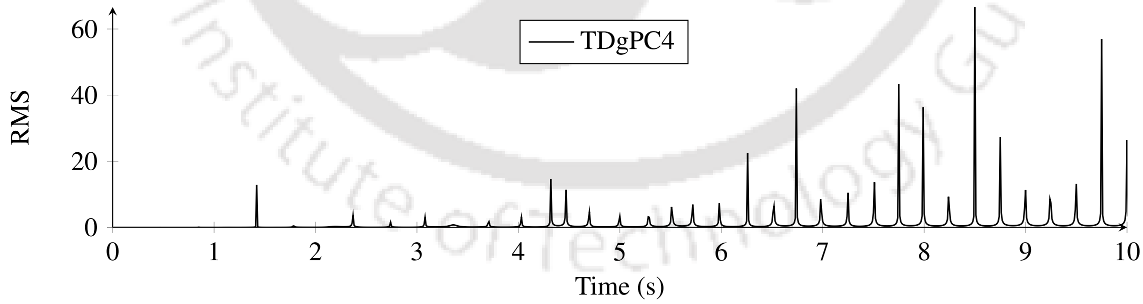

(d) TDgPC scheme of 4th order PC ($\varphi = 6$).

Fig. 6.9: RMS of deflection at free end (DOF=12) evaluated using different order of PC using mPC and TDgPC scheme.

The location of updation of PC for TDgPC of different orders and different values of φ are shown in Table 6.4. It can be observed that as the value of the tolerance limit φ increases, the location of initial updation is observed to move backwards and thus increases the accuracy of responses. This can be observed for all the three orders of PCs considered in this study. It is observed that as the order increases, the initial responses are also better. Thus the location of initial updation is observed to move forward with an increase in the order of PC expansion. However, as the tolerance limit increases, the criterion becomes more and more stringent, and thus the total number of updations increases with increase in the value of the tolerance limit. It can be observed from the responses that as the value of φ increases, the responses are in better agreement with those from MCS. It can be observed from Table 6.4 that only for $\varphi = 6$ and order of PC expansion as 4, the initial location is significantly different.

Table 6.4: Location of updation of PC in case of TDgPC (truss problem)

Order	2			3			4		
φ	6	8	10	6	8	10	6	8	10
Initial upation instant (s)	0.70	0.69	0.68	0.73	0.72	0.71	1.12	0.74	0.74

From the previous discussion, it is observed that the responses of PC expansion deviate from MCS as time propagates. This discrepancy in responses with time has however been reduced by considering TDgPC. The requirement of computer memory (RAM), actually depends on the number of terms in the expansion, which depends on both the number of random variables and order of expansion considered. It is further observed that the agreements in responses till the first update are quite acceptable even with a lower order of PC. Thus, the method can be made more efficient by considering a relatively lower order of PC until the first updation is done. The maximum size of a problem that can be solved with an available computer infrastructure depends on the memory requirement, which is governed by the number of terms in the PC expansion considered at the very first time step. Since the number of random variables reduces to four from eight in post updation, the order of initial expansion thus govern the computational requirement.

Fig. 6.10 shows the statistical parameter of displacement at the free end (DOF=12) when solved using TDgPC with 3rd order PC upto first updation and with 4^{th} order PC afterwards. For comparison of responses, 4^{th} order mPC results are also plotted on the same figures. It is observed that responses of TDgPC is in better agreement with MCS than those from 4^{th} order mPC expansion.

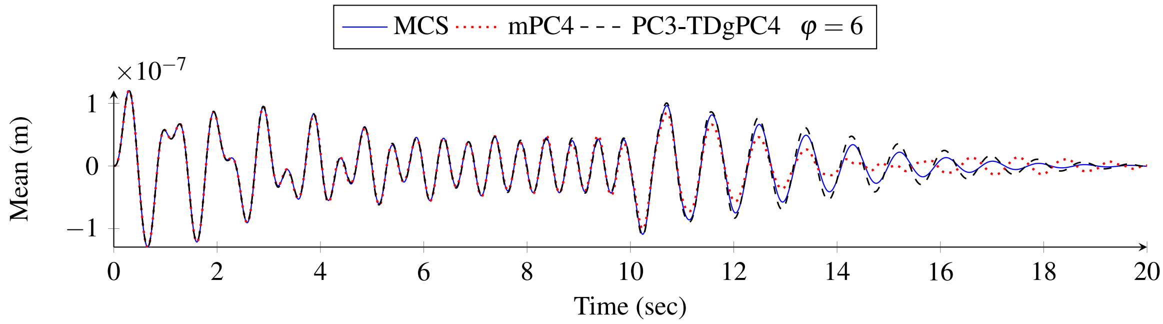

(a) Mean of displacement.

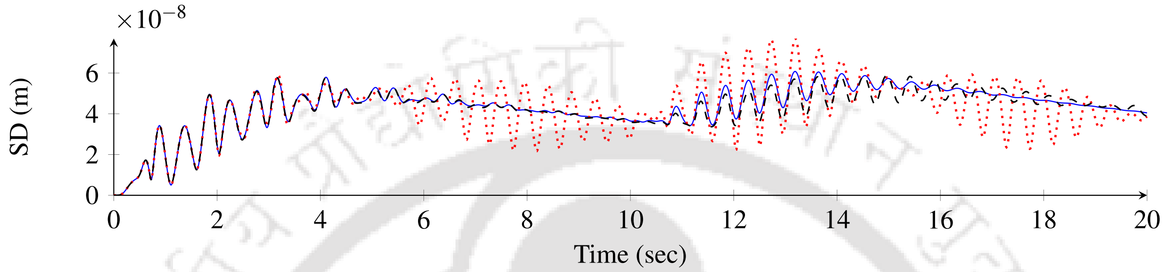

(b) SD of displacement.

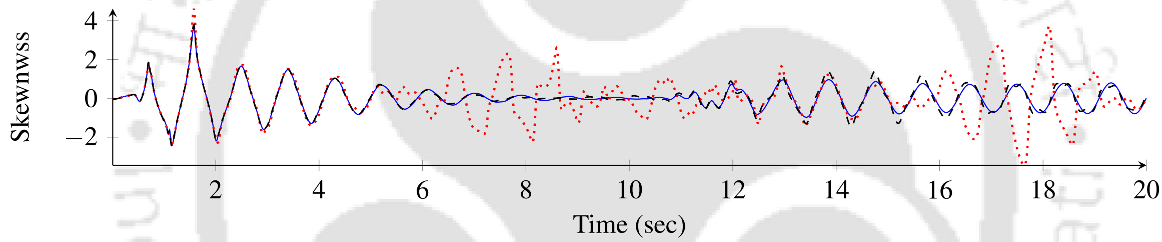

(c) Skewness of displacement.

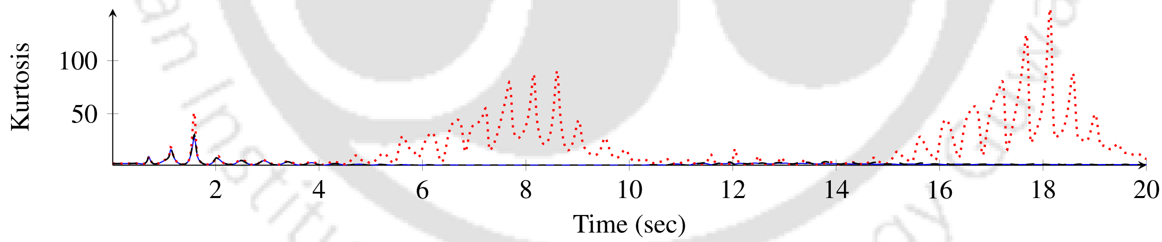

(d) Kurtosis of displacement.

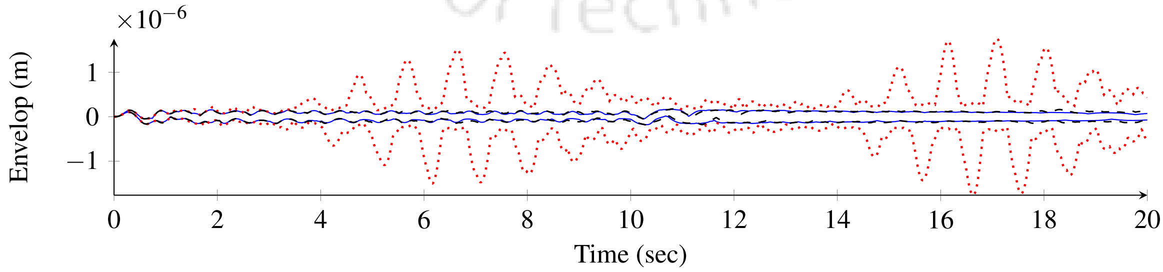

(e) Envelop of displacement.

Fig. 6.10: Time history of statistical parameters of vertical deflection at free end (DOF=12) when solve using 3rd order PC upto first instant of TDgPC and 4th order afterwards ($\varphi = 6$).

6.5.2 Cantilever beam under dynamic loading

The second problem considered is a cantilever beam of dimension as shown in Fig 6.11, subjected to a deterministic dynamic loading at the free end. A step load of 1 N up-to a time instant of 2 sec (Fig. 6.12) is applied at the free end and given by Eq. 6.33

$$q(t) = \begin{cases} 1 \text{ N}, & \text{if } 0 \leq t \leq 2, \\ 0, & \text{otherwise} \end{cases} \tag{6.33}$$

A uniformly distributed mass of 9.08 kg/m including self weight of beam is considered along the length of the beam. The beam is analysed considering a 1-D log-normal random field for Young's modulus along the length of the beam of the form

$$E(x,\theta) = E_0[1+\alpha(x,\theta)] \tag{6.34}$$

where E_0 is the mean value of the random field and $\alpha(x,\theta)$ is a homogeneous zero mean log-normal random field with an exponential covariance function as

$$\boldsymbol{C}(x_1,x_2) = \sigma^2 \exp\left(\frac{-|x_1-x_2|}{L_c}\right) \tag{6.35}$$

where σ is the standard deviation of the random field. L_c is the correlation length and is considered as $L/2$. The beam is analysed for $\sigma = 0.2$.

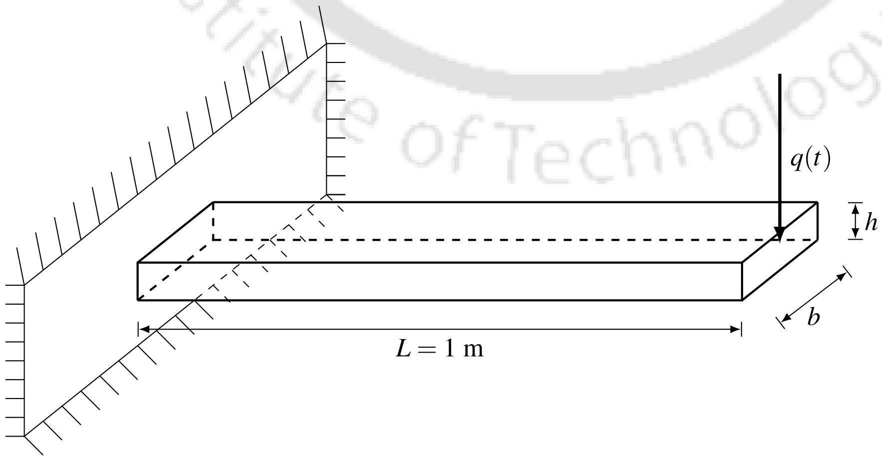

- b=39 mm.
- h=5.93 mm.
- $E_0 = 2 \times 10^{11}$ Pa.

Fig. 6.11: Cantilever beam subjected to a dynamic loading at the free end.

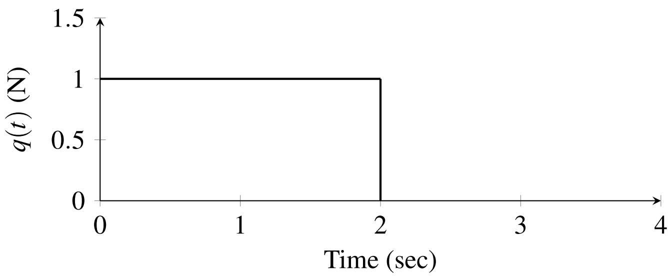

Fig. 6.12: Applied dynamic load at the free end of cantilever beam (Fig. 6.11).

The beam is discretized into 30 element of equal length and modelled using 2 nodded Euler-Bernoulli beam. The lump mass matrix is considered as deterministic and is written as,

$$M_i = \frac{\rho A_i l_i}{78}\begin{bmatrix} 39 & 0 & 0 & 0 \\ 0 & l_i^2 & 0 & 0 \\ 0 & 0 & 39 & 0 \\ 0 & 0 & 0 & l_i^2 \end{bmatrix} \tag{6.36}$$

where A_i and l_i are the area and length of each member and ρ is the mass density of the member. Boundary conditions are applied at the fixed end of the beam by restraining all the degrees of freedom. The beam is first analysed deterministically considering the mean value of Young's modulus. The distribution of natural frequencies are shown in Fig. 6.13.a and the corresponding model mass are shown in Fig. 6.13.b. It can be observed that most of the model masses are concentrated within the first few modes. The significant mode is calculated based on 90% model mass participation which corresponds to 6^{th} mode with frequency 181.59 Hz. The fundamental frequency of the system is observed to be 2.16 Hz. The size of the time step for Newmark-β is chosen as 1/600 sec. The damping matrix of the system is calculated from deterministic part of stiffness and mass matrices considering a 1% constant model damping for all the modes.

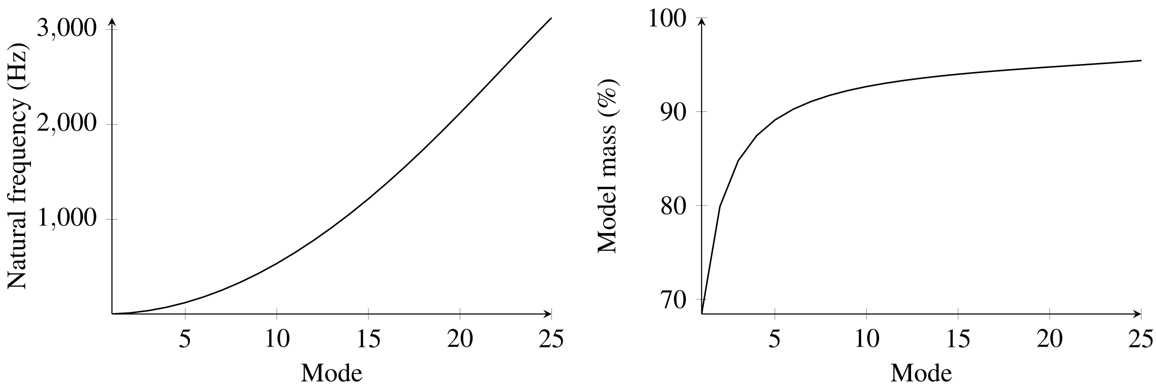

(a) Natural frequencies (b) Model mass participation

Fig. 6.13: Dynamic properties of the cantilever beam when solve deterministically considering mean value of Young's modulus.

6.5.2.1 Discretization and generation of random field using KL expansion

The principle and methodology for discretization of non-Gaussian random field is discussed in section 4.2.1. In particular, the discretization and simulation of random field for log-normal distribution is studied in the numerical example discussed in Chapter 4, section 4.4.2.1. Since, in the present case, the same beam, covariance function and log-normal distribution are considered, the random variables generated in section 4.4.2.1 are considered in the present numerical example also. Thus six random variables are considered in the representation of random field. The generated random variables are not independent and thus ICA is performed to transform these to independent variables. The application of ICA to random field generation is discussed in detail in numerical example in section 4.4.2.1. The random variable after ICA are not of same distribution. Thus, these are transformed to standard Gaussian random variables and are considered to generate PC expansion only.

6.5.2.2 Response calculated using PC and Newmark-β method

Similar to the truss problem, the beam is analysed for the given load using Newmark-β method and statistical properties of the responses are approximated using PC expansion. The beam is analysed for different orders of PC expansion and the statistical parameters of responses are compared with those of MCS. The PC is generated using Gram-Schmidt orthogonalisation (as in section 3.4.3) considering the transformed random variables evaluated from random variables after performing ICA (as in section 4.4.2.1). A sample size of 3×10^4 is considered in all the analysis. The time history for different statistical parameters of vertical deflection at free end when calculated using different orders of PC expansion for $\sigma = 0.2$ of Young's modulus are shown in Fig. 6.14. It can be observed that during the initial time duration, the responses agree well with responses of MCS. However, as time progresses, these responses are observed to deviate from MCS. It can be observed that as the order of PC expansion increases, the mean and standard deviation of responses converge towards MCS, while the skewness and kurtosis still lack proper convergence. Fig 6.15 shows pdfs of vertical deflection at free end using MCS and mPC for different order of PC expansion. It can be observed that the pdfs corresponding to mPC differ with those from MCS over time, thus requires a new PC approximation to represent these responses more accurately. To overcome loss of accuracy in responses, the problem is analysed using TDgPC scheme in the next section.

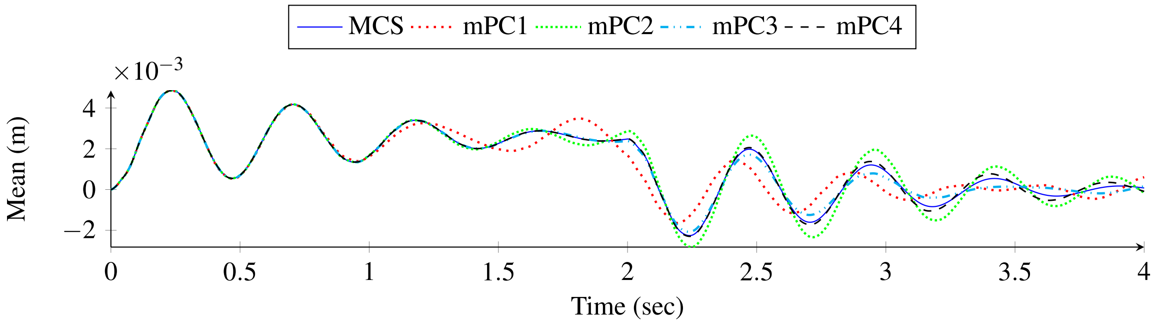

(a) Mean of displacement.

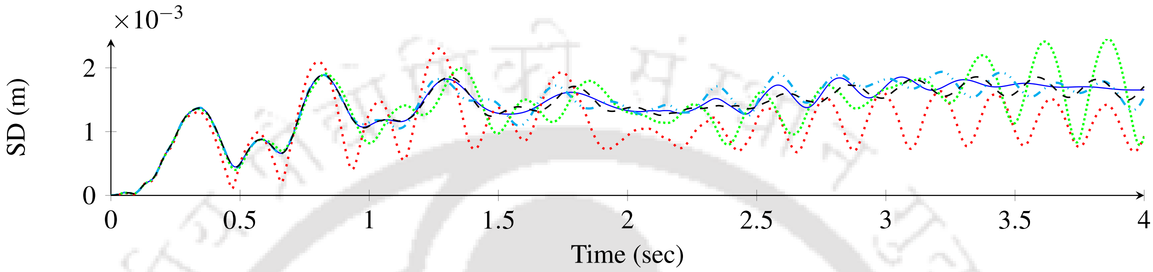

(b) SD of displacement.

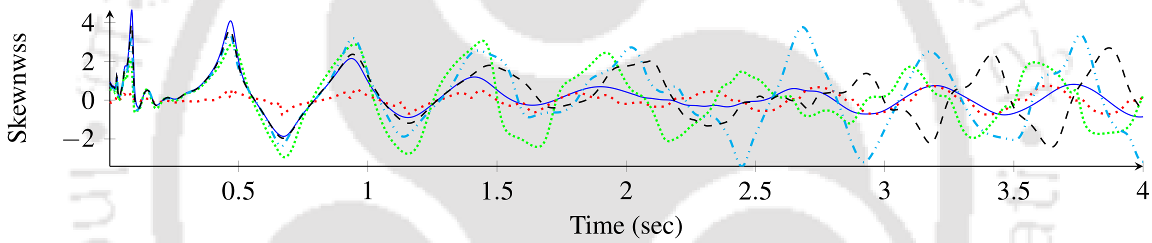

(c) Skewness of displacement.

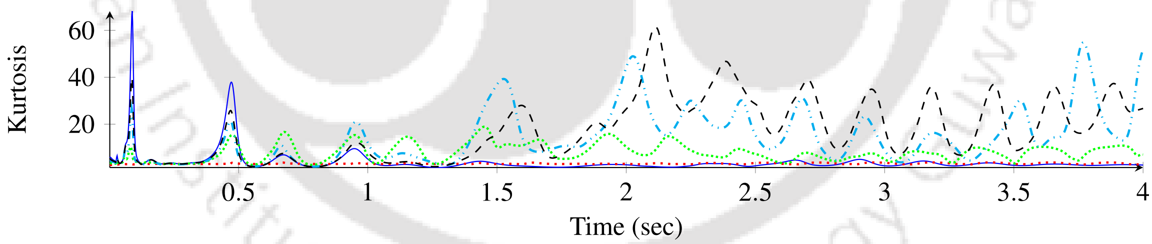

(d) Kurtosis of displacement.

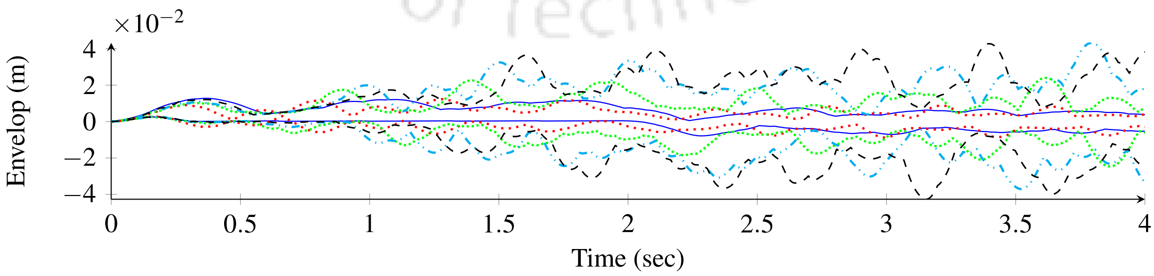

(e) Envelop of displacement.

Fig. 6.14: Time history of statistical parameters of vertical deflection at free end for different orders of PC expansion ($\sigma = 0.2$).

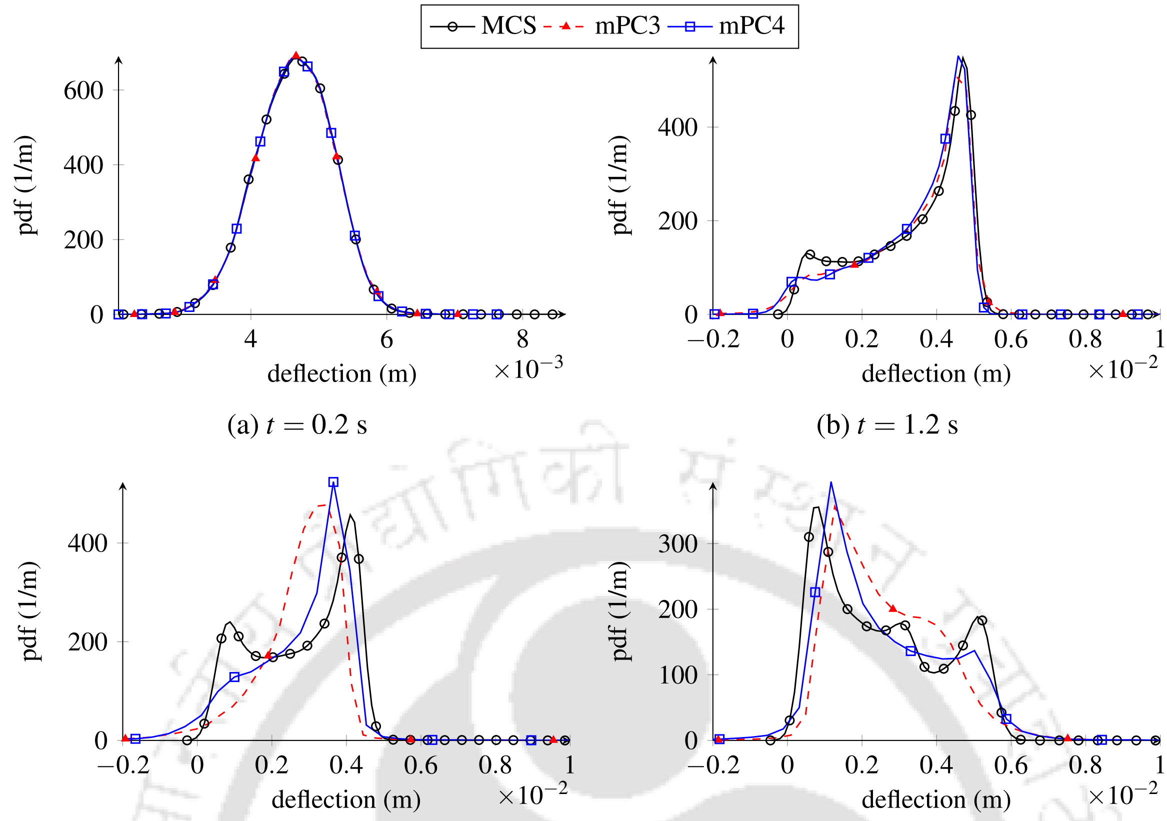

(a) $t = 0.2$ s

(b) $t = 1.2$ s

(c) $t = 1.6$ s

(d) $t = 1.8$ s

Fig. 6.15: pdf of displacement at free end at different time instant, evaluated using different orders of mPC ($\sigma = 0.2$).

6.5.2.3 Response calculated using TDgPC and Newmark-β method

It is observed that the responses of PC based method deviate from MCS as the time progresses. The problem is thus analysed using TDgPC scheme. The PCs are updated based on updation criterion as given by Eq. 6.28 with a tolerance limit (φ) equal to 6. The time history of the statistical parameters are shown in Fig. 6.16. It can be observed that the responses are in better agreement with MCS than mPC response. The pdfs of vertical deflection at free end at time instant $t = \{1.2, 1.4, 1.6, 1.8\}$ s are shown in Fig. 6.17. It can be observed that these are also in better agreement with MCS than what is observed in Fig. 6.15 for mPC. The fact that pdfs of responses change over time, reduces the optimality of PC expansion when considered for long duration of loading. Thus, TDgPC provides a framework to change the PC expansion as and when required.

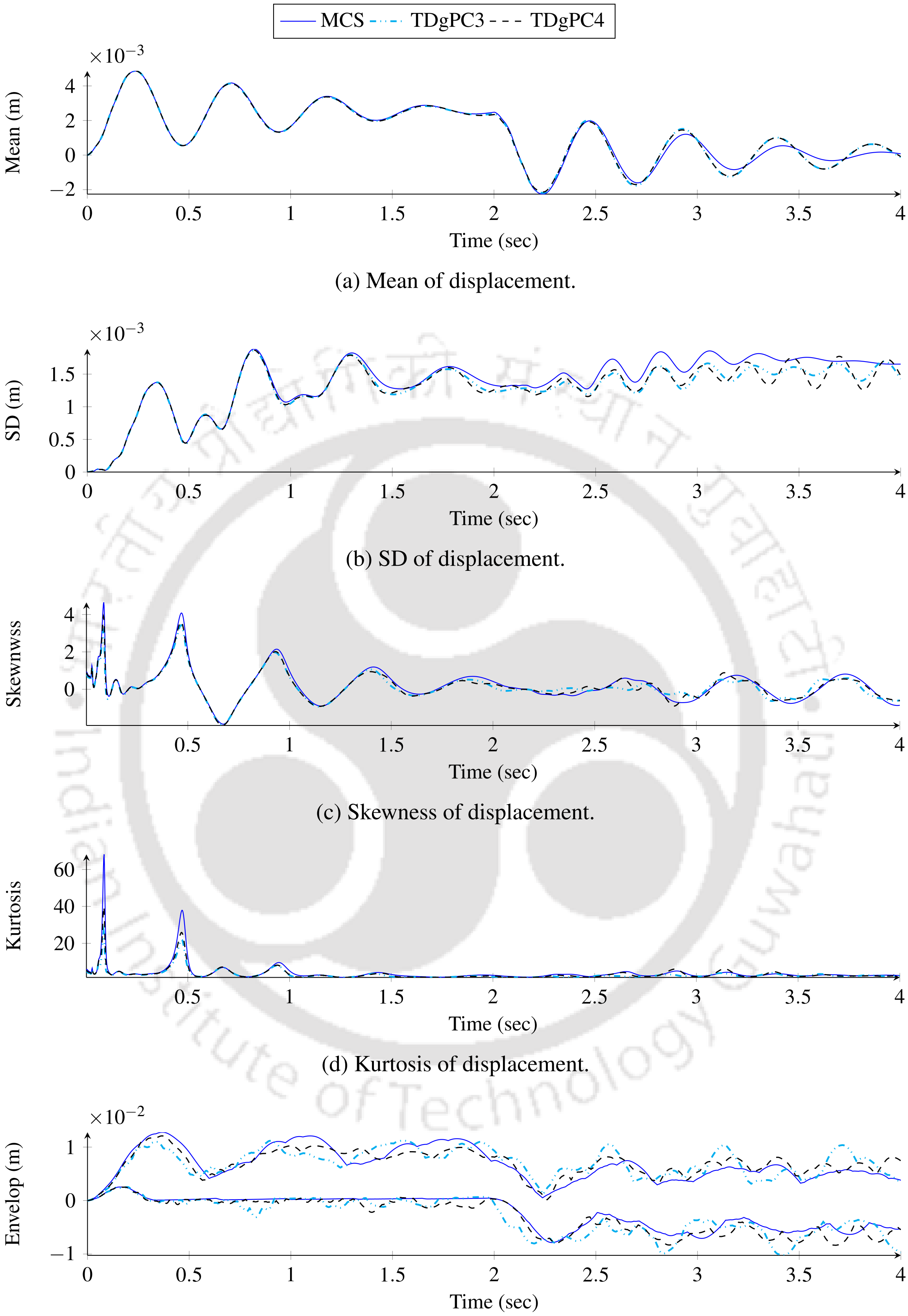

(a) Mean of displacement.

(b) SD of displacement.

(c) Skewness of displacement.

(d) Kurtosis of displacement.

(e) Envelop of displacement.

Fig. 6.16: Time history of statistical parameters of vertical deflection at free end for different orders of PC expansion solved using TDgPC scheme ($\varphi = 6$) ($\sigma = 0.2$).

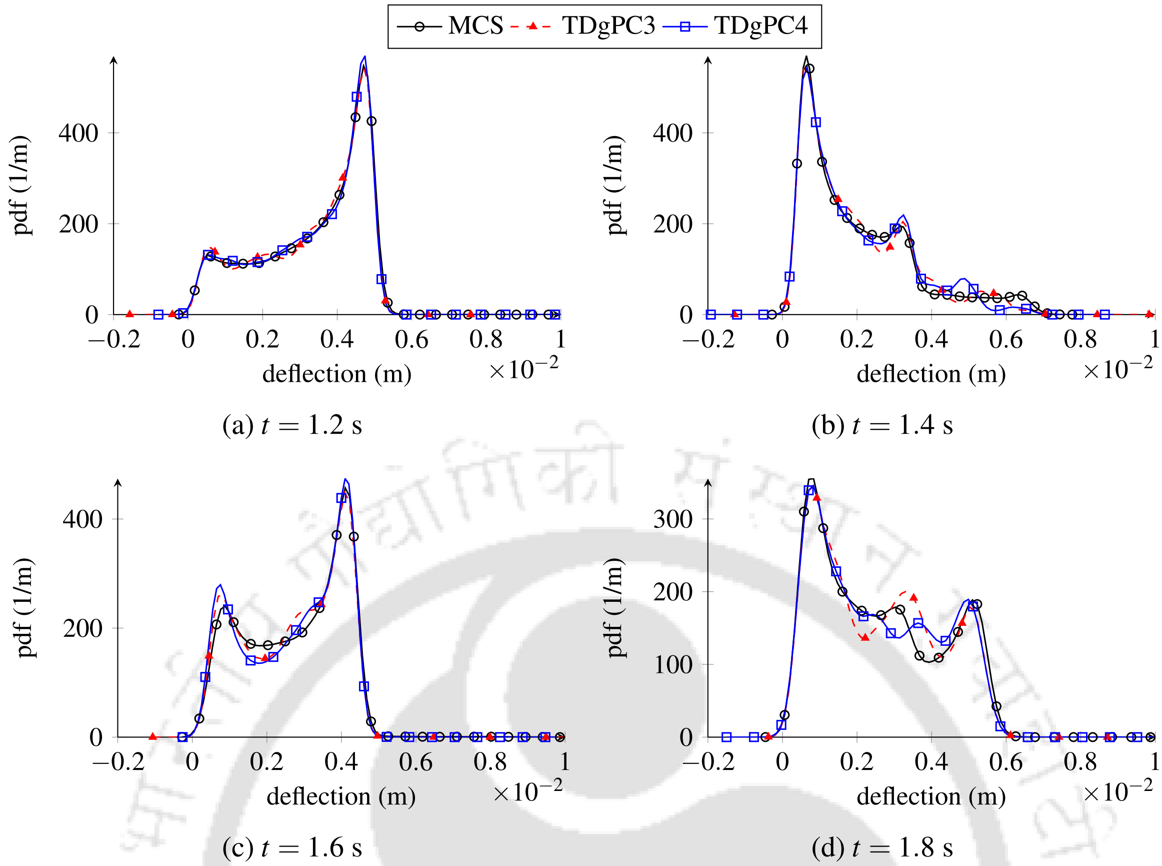

Fig. 6.17: pdf of displacement at free end at different time instant, evaluated using different orders of TDgPC ($\varphi = 6$) ($\sigma = 0.2$).

6.6 Conclusions

Structural mechanics problems under deterministic dynamic loading and random system parameters are analysed using TDgPC. It is observed that the statistical properties of the responses change over time. Thus, initially considered PC expansion loses it optimality. Thus even with increase in order of expansion in the PC based method, the responses are not in good agreement with response of MCS after some duration of analysis. Moreover, with increase in order, computation cost increases exponentially without much advantage. The problem is further studied using TDgPC, where PCs are updated based on some accuracy criterion. An updation criterion based on the RMS value of linear and non-linear coefficients of PC expansion is studied. From the numerical studies on two linear structural mechanics problems, it is observed that the responses of TDgPC are in a better agreement with MCS than mPC. Thus, TDgPC can be considered as an alternative method to solve linear structural mechanics problem, where PC based method fails to approximate the responses properly.

7

Adaptive discretization of random fields using KL expansion

Contents

7.1 Introduction

In the previous chapters, the formulation and solution of SFEM are discussed in details. In the case of consideration of material property (e.g. Young's modulus) as a random field, the same needs to be discretized for integration with SFEM. In particular, the random fields in civil engineering application are assumed to be weakly homogeneous and hence the same is generally represented using marginal distribution, mean and covariance function (Allaix and Carbone, 2009). A discretization method converts the continuous parameter random field to a set of random variables. The various discretization schemes available are already discussed in section 2.3. Truncated Karhunen-Loève (KL) expansion is one of the popular methods for the discretization of a random field and the same is considered in the present study. The applications of KL expansion are discussed in Chapter 3 and 4 for Gaussian and non-Gaussian random field, respectively. The basic philosophy of KL expansion is discussed in section 3.2.1, which is applicable to a Gaussian field and iterative KL expansion is discussed in section 4.2.1, which is applicable to a non-Gaussian random field. The need and the application of ICA in the case of a non-Gaussian random field are discussed in section 4.2.2. In all the numerical examples addressed so far, a discretization is considered based on the expected energy consideration. In this chapter, a detailed study is conducted regarding the number of element and number of terms to be considered in the discretization process for an assumed accuracy level. Further, an adaptive discretization scheme is also proposed.

An accurate discretization of random field can be achieved by considering a fine mesh along with a large number of terms. However, an increase in discretization and/or inclusion of more terms leads to an increase in computational cost. It is also found that only an increase in the number of terms in the expansion or number of elements alone does not provide an accurate representation of the random field. Moreover, as the number of terms increases, the size of the system matrix increases. Even in the case of Monte Carlo simulation (MCS), as the number of random variables increases, the sample size increases. Thus, an optimal order of expansion and discretization are always desired.

An efficient discretization using KL expansion should consider both accuracy and computational cost requirement. The accuracy of continuous parameter random field representation can be easily achieved by dividing the domain into a fine mesh along with all the terms in the expansion. However, this will increase the computational cost as popular approaches like SFEM, stochastic finite difference will have a large system matrix to be solved. It has been further observed that the contributions of the initial few terms of the expansion are significantly higher than the later terms and hence the expansion is truncated at some suitable number. An appropriate discretization is thus sought along with an appropriate number of terms of the expansion to represent the random field.

KL expansion can be considered to discretize Gaussian random field and is also applicable for generation of non-Gaussian random field using an iterative process (Phoon et al., 2005). However, as discussed above, an appropriate combination of a number of eigenvectors and discretization is necessary for accurate representation. Allaix and Carbone (2009) considered a genetic algorithm to evaluate an optimal number of random variables by minimizing truncation order, while keeping the constraint that the global discretization error should be less than an admissible limit. Further, Allaix and Carbone (2010, 2012) proposed an adaptive discretization scheme considering local error in variance. Members with the highest errors in variance are discretized further when the global error in variance is more than a prescribed value.

The present study thus considers investigations on the selection of number of terms and appropriate discretization to represent the random field at its best possible manner. As already considered in previous numerical examples, the value of the random field is considered at two Gauss-points rather than mid-point or node-points of an element to improve the representation of the random field. This will better represent random field without increasing the computation cost of finite element and can be directly implemented in FE framework. If the random field is considered at nodal points, it has to be interpolated between nodes, which increases the order of integration. Moreover, if it is considered at mid-point, it reduces the number of points resulting in a poor approximation of the random field. Further, an adaptive discretization scheme has been presented to automatically arrive at a discretized domain while keeping all the possible errors under control for the best representation of random fields.

The chapter is organized as follows. Discretization of random field using KL expansion is discussed in section 7.2. The implementation of the discretized random field to SFEM is discussed in section 7.3. Section 7.4 discusses the quantification of various errors in the simulated random field due to discretization. Mesh sizes and adaptive discretization are discussed in section 7.5, followed by numerical study in section 7.6. The final conclusion are made in section 7.7.

7.2 Discretization of random field using KL expansion

The basic principle of discretization of random field using KL expansion is discussed in section 3.2.1. As discussed, the KL expansion is often truncated at some suitable number Q based on the expected energy criterion of the covariance function. The variance and covariance function for truncated expansion is given by

$$\mathrm{Var}[\hat{\alpha}(x,\theta)] = \hat{\boldsymbol{C}}(x,x) = \sum_{i=1}^{Q} \lambda_i f_i^2(x) \tag{7.1}$$

$$\hat{\boldsymbol{C}}(x_1,x_2) = \sum_{n=1}^{Q} \lambda_n f_n(x_1) f_n(x_2) \tag{7.2}$$

The truncation of KL expansion introduces error in the simulated random field. An efficient discretization using KL expansion should consider both accuracy and computational cost requirement. The accuracy of continuous parameter random field representation can be easily achieved by dividing the domain in to a fine mesh along with all the terms in the expansion. However, this will increase the computational cost as popular approach like SFEM, stochastic finite difference will have a large system matrix to be solved. It has been further observed that the contributions of initial few terms of the expansion are significantly higher than the latter terms and hence the expansion is truncated at some suitable number. An appropriate discretization is thus sought along with an appropriate number of terms of the expansion to represent the random field. In the subsequent sections, a detailed study on effect of discretization on the accuracy of simulated data is carried out considering all the possible measures.

7.3 Finite element considerations

The approximation of random field through discretization using KL expansion acts as a mathematical framework to convert a continuous random field to a set of random variables, which enable it to implement in SFEM. However, the implementation of a stochastic mesh into FEM mesh is slightly involved as the two meshes are generated based on two different criteria and one may end up getting two different meshes. The stochastic mesh is based on the variability of the random field, which can be apparently quantified using correlation length parameter. On the other hand, the FE meshes are based on stress gradient. There may be three ways to consider these two different meshes. First, the finer of the two meshes considering both the criteria may be considered as the final mesh. There may be a demand for a local discretization in different areas in the two meshes, the finer of the two are considered as the final mesh. This type of mesh is generally considered in most of the cases and the same approach is also considered in numerical studies in Chapter 3 and 4. The second one considers two different meshes based on the above mentioned criteria and considers the random field mesh as a block of finite element meshes such that each block contains one or more finite elements as an integer multiplier (Kiureghian and Ke, 1988). The third approach considers completely two independent meshes as suggested by Schenk and Schuëller (2003). Two different meshes are mapped using an interpolation function like bicubical interpolation (Schenk and Schuëller, 2003) or bivariate interpolation (Charmpis and Papadrakakis, 2005).

Consideration of same mesh for both random field and FE is simpler and convenient to implement in a numerical scheme. Moreover, two independent meshes do not automatically guarantee any appreciable reduction in computational cost without compromising the accuracy requirement of either random field or FE discretization. Further, computational cost primarily depends on FE mesh and hence, the same mesh is generally preferred satisfying the requirement of discretization of both random field and FE analysis.

The formulation of stochastic finite element is similar to that of deterministic counterpart, and are discussed in section 3.2.2 and 4.2.3.

7.4 Discretization error quantification: Accuracy of statistical parameters

It has been observed that the most of the expected energy is concentrated within the first few eigenvalues and thus the expansion is often truncated at a suitable number based on the desired level of accuracy. This introduces error in statistical parameters (e.g variance, covariance) of the random field. The mean value is not affected by the truncation operation. The expected energy can be calculated from eigenvalues and expected energy associated with each modes is expressed as (Huang et al., 2001),

$$\text{Expected Energy}_i = \frac{\lambda_i}{\sum_{k=1}^{\infty} \lambda_k} \tag{7.3}$$

The evaluated expected energy provides an estimate of overall accuracy, but does not specify point wise errors in statistical parameters. Thus, it is also important to establish a point wise error measure. Moreover, it will act as a measure for judgement in adaptive discretization. The point wise error in variance and covariance can be defined by comparing the truncated parameter with the continuous parameter. Thus, point wise error in variance $\varepsilon_{\sigma_{\hat{\alpha}}^2}(x)_Q$ is defined as,

$$\varepsilon_{\sigma_{\hat{\alpha}}^2}(x)_Q = \frac{\mathrm{Var}[\alpha(x,\theta)] - \mathrm{Var}[\hat{\alpha}(x,\theta)]}{\mathrm{Var}[\alpha(x,\theta)]} \tag{7.4}$$

where $\mathrm{Var}[\hat{\alpha}(x,\theta)]$ is calculated from truncated expansion using Eq. 7.1. The point wise error in variance is a positive quantity as the truncated variance underestimate its value (Allaix and Carbone, 2009). In case of a constant variance the point wise variance can be written respectively as,

$$\varepsilon_{\sigma^2_{\hat{\alpha}}}(x)_Q = 1 - \frac{\sum_{i=1}^{Q} \lambda_i f_i^2(x)}{\sigma^2} \tag{7.5}$$

The global error in variance is evaluated by integrating the point wise error over the domain (Ω) and normalized by its domain. Thus global error in variance, $\overline{\varepsilon}_{\sigma^2_{\hat{\alpha}_Q}}$ is given by,

$$\overline{\varepsilon}_{\sigma^2_{\hat{\alpha}_Q}} = \frac{1}{\Omega} \int_{\Omega} \varepsilon_{\sigma^2_{\hat{\alpha}}}(x)_Q d\Omega = 1 - \frac{\sum_{j=1}^{Q} \lambda_j \int_{\Omega} f_i^2 d\Omega}{\Omega \times \sigma_w^2} \tag{7.6}$$

Similarly, the point wise error in covariance ($\varepsilon_{\boldsymbol{C}(x_1,x_2)}(x)_Q$) can be calculated by comparing truncated covariance (given by Eq. 7.2) with the actual one and given as

$$\varepsilon_{\boldsymbol{C}_{\alpha,\alpha}}(x_1,x_2)_Q = \frac{\left| \boldsymbol{C}(x_1,x_2) - \hat{\boldsymbol{C}}(x_1,x_2) \right|}{\boldsymbol{C}(x_1,x_2)} \tag{7.7}$$

The point wise error in covariance is not always positive and the actual covariance at some places may be zero. Thus, point wise error in covariance is generally calculated using Eq. 7.8 (Allaix and Carbone, 2010). The global error in covariance is evaluated using integrating over the domain and normalized by its domain, given by Eq. 7.9.

$$\varepsilon_{\boldsymbol{C}_{\alpha,\alpha}}(x_1,x_2)_Q = \frac{\left| \boldsymbol{C}(x_1,x_2) - \hat{\boldsymbol{C}}(x_1,x_2) \right|}{\sqrt{\mathrm{Var}[\alpha(x_1,\theta)\mathrm{Var}[\alpha(x_2,\theta)]}} \tag{7.8}$$

$$\overline{\varepsilon}_{\boldsymbol{C}_{\alpha,\alpha_Q}} = \frac{1}{\Omega^2} \int_{\Omega} \varepsilon_{\boldsymbol{C}(x,x)}(x)_Q d\Omega d\Omega \tag{7.9}$$

In case of stationary random field variance at x_1 and x_2 are same, thus $\sqrt{\mathrm{Var}[\alpha(x_1,\theta)\mathrm{Var}[\alpha(x_2,\theta)]}$ can be considered as $\mathrm{Var}[\alpha(x,\theta)] = \sigma^2$. The global discretization error in variance and covariance gives a prospective of the accuracy of the discretized domain and number of terms considered. However, Allaix and Carbone (2010) observed that the global error in covariance is small compare to error in variance, thus generally not considered for determination of accuracy.

It is also important to note that for a particular discretized mesh, point wise error in variance can be reduced by considering additional eigenvectors. However, as the number of eigenvectors increases, the discretization should also accordingly increase for better representation of eigenvectors.

The other important parameters which influence the accuracy of the simulated random field are the accuracy of eigenvectors and eigenvalues. Allaix and Carbone (2010) considered calculation of error in eigenvalue and eigenvector by comparing with two different iterations. For eigenvalues, the authors considered absolute difference between the two values. However, in case of eigenvectors, the authors considered square root of the integral value of square of differences between two random vectors from coarse and fine meshes. Further, Allaix and Carbone (2012) updated the error criteria by considering a single quantity for both eigenvalue and eigenvector instead of two and calculate the error as,

$$\varepsilon_{\lambda f} = \frac{\left[\int_D (\mathrm{Var}_i^{(\mathrm{FINE})}[\hat{\alpha}(x,\theta)] - \mathrm{Var}_i^{(\mathrm{COARSE})}[\hat{\alpha}(x,\theta)])^2 dx\right]^{1/2}}{\left[\int_D (\mathrm{Var}_i^{(\mathrm{FINE})}[\hat{\alpha}(x,\theta)])^2 dx\right]^{1/2}} \tag{7.10}$$

where $\mathrm{Var}_i[\hat{\alpha}(x,\theta)]$ indicate variance of truncated random field considering up to the i^{th} term and (FINE) and (COARSE) indicate the calculation are done in coarse mesh and then subsequently in fine mesh.

As observed from Eq. 3.1, eigenvalue and eigenvector can be combined to form a single quantity as $\hat{f}_n(x) = \sqrt{\lambda_n} f_n(x)$. The accuracy of eigenvector may be estimated using Modal Assurance Criterion (MAC) defined as,

$$\mathrm{MAC}_n = \frac{\left|\hat{f}_n^{(i)}(x)^T \hat{f}_n^{(i+1)}(x)\right|^2}{\hat{f}_n^{(i)}(x)^T \hat{f}_n^{(i+1)}(x) \hat{f}_n^{(i+1)}(x)^T \hat{f}_n^{(i+1)}(x)} \tag{7.11}$$

where subscript n indicates a particular number of eigenvector and superscripts (i) and $(i+1)$ indicate a coarse and fine mesh respectively. The fine mesh is considered to have relatively more correct eigenvectors. In case of an adaptive scheme, MAC is calculated with respect to meshes of two subsequent iterations.

MAC provides a measure of accuracy of eigenvectors and the value ranges from 0 to 1, one being the perfect match with the target eigenvector.

An iterative adaptive scheme is discussed in the subsequent section, which controls both the continuity requirement of the random field and point wise accuracy in statistical parameters.

7.5 Mesh size and adaptive discretization

An accurate discretization of random field is important to represent the continuous parameter random field accurately. However, it is also important to note the increase in computational demand as the discretization increases. Kiureghian and Ke (1988) obtained a stochastic mesh size of $L_c/4$ to $L_c/2$ size by repeatedly evaluating the reliability index of a beam with stochastic rigidity using meshes with decreasing element size. Li and Der Kiureghian (1993), Zeldin and Spanos (1998) also studied the discretization process by calculating the power spectrum density of the random field before and after discretization and obtained similar conclusion. However, it has also been observed in literature that a very large number of discretization is considered with very small number of eigenvectors. Such consideration can accurately describe the continuity requirement of continuous random field, but would fail to represent the statistical parameter accurately as point wise errors are likely to be more in this case. Moreover, only very few eigenvectors in KL expansion would not produce a proper spatial variability. Allaix and Carbone (2012) proposed an adaptive discretization scheme in KL expansion where domain is discretized adaptively based on the error in point variance. However, as the author considered the value of random field at node points, all the member common to the node are needed to be discretized if error at the node is higher than the prescribed value. This can be avoided by considering values of the random field at mid-points instead of nodes. However, the numbers of point to represent the eigenvectors are one per element.

The present study differs from the previous study that it considers the values of the random field at Gauss points. As higher and higher number of eigenvectors are considered, the discretization requirement increases to properly represent the same. Thus, if Gauss points are considered rather than nodes to represent eigenvector, it contains more number of points to property represent eigenvectors without increasing the size of the stiffness matrix. Moreover, considering random field at Gauss points, the re-discretization of element is required only in the particular element, which has a point wise error more than the prescribed value. The most significant advantage is that random field can be directly considered in finite element analysis during numerical integration using Gauss quadrature method, whereas in nodal point discretization, an approximation between node is necessary. On the other hand in case of mid point, the value is common for the entire length of the member, which may be a bit coarse representation of random variable along the domain.

7.6 Implementation and Numerical examples

The simulated data are studied for error due to discretization by considering two examples. The first one is a 1-D random field problem representing Young's modulus of Euler-Bernoulli beam and the second one is a plane stress problem considering Young's modulus as 2-D random field. Further, the implementation to non-Gaussian random field is also discussed in section 7.6.3. A good discretization method should consider both finite element requirement and discretization requirement from random field. The requirement of discretization based on random field is studied in this paper. The requirement of discretization due to finite element can be studied by considering mesh convergence for the deterministic problem. A unified mesh can be formulated based on these two criteria.

As discussed in section 2.2, two of the most commonly considered covariance functions in structural engineering are exponential covariance function given by Eq.7.12 (Type-1) and square exponential covariance function given by Eq. 7.13 (Type-2), where σ is the standard deviation of the random field. x_1, x_2 are the coordinates within the limit $[-a, a]$, where a is known as length of the process and the value is half of the length (L) of the member. L_c is the correlation length and acts as a normalizing factor to the length of the process. The shape of the covariance functions are shown in Fig. 7.1 (for a value of $L_c = 0.5$).

$$\boldsymbol{C}(x_1, x_2) = \sigma^2 \exp\left(-\frac{|x_1 - x_2|}{L_c}\right) \tag{7.12}$$

$$\boldsymbol{C}(x_1, x_2) = \sigma^2 \exp\left(-\left(\frac{x_1 - x_2}{L_c}\right)^2\right) \tag{7.13}$$

The correlation length, L_c plays an important role in the accuracy of simulated random field. Figs. 7.2a and 7.2b show respectively Type-1 and Type-2 covariance functions for different values of correlation length. If the value of correlation length is very small, it approaches to a delta-correlation process known as white noise. On the other hand, for large values of correlation length compared to domain under consideration, the process becomes a random variable. Huang et al. (2001) observed that the accuracy of the simulated data is more when the ratio of length of the process to correlation length is low. Thus, higher the value of L_c, lesser number of terms are required for a same level accuracy. This can also be observed from decay of eigenvalues and cumulative % expected energy as shown in Figs. 7.3 and 7.4 for covariance functions Type-1 and Type-2 respectively. In both the cases, it can be observed that as the value of L_c increases, more expected energy are concentrated within the first few modes. Thus, for a same level of expected energy, lesser number of terms are required when the value of L_c is more. Moreover, Type-2 covariance has more expected energy in first few modes than Type-1, thus requires lesser number of terms as compared to Type-1. The decay rate of covariance function is increases with reduction in correlation length. The decay rate of the covariance function can be related to the number of terms required in the expansion to achieve a desired level of accuracy. If the decay rate is more, number of terms required is higher for a desired accuracy (Ghanem and Spanos, 1991b). Thus, as the value of L_c increases the random field becomes lesser and lesser correlated. All the subsequent studies are carried out by considering correlation length L_c as $L/2$.

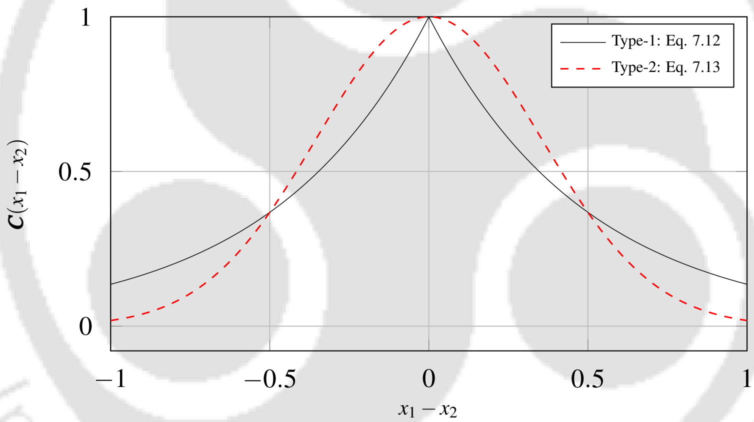

Fig. 7.1: Exponential and square exponential covariance function.

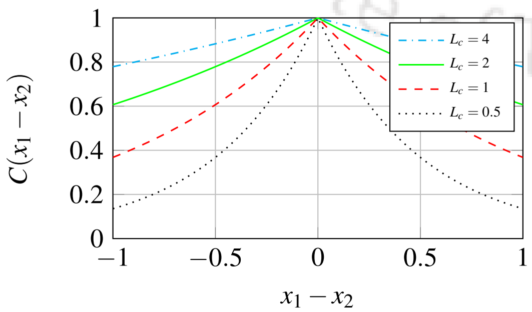

(a) Exponential covariance, Type-1.

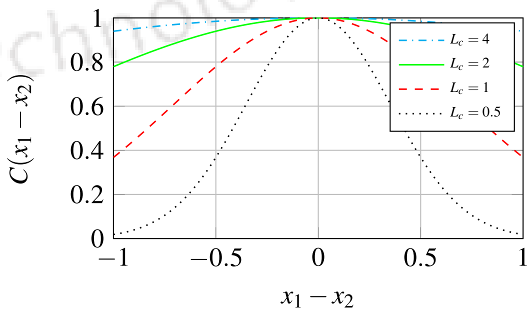

(b) Square exponential covariance, Type-2.

Fig. 7.2: Covariance functions for different values of correlation length.

7.6.1 Effect of Discretization on accuracy of simulated random field

7.6.1.1 Beam problem with 1-D random field

In the previous sections some salient points are discussed regarding the effect of shape of covariance function and correlation length on the accuracy of simulated data. Further, it is also discussed in section 7.1 that a good approximation of random field should have both sufficient number of elements and sufficient number of eigenvectors. In order to develop more insight, a beam modelled using 2 noded Euler-Bernoulli beam is considered as shown in Fig. 7.5 with covariance function (Type-1) as described in Eq. 7.12. The random field may be represented at mid point and at 2-Gauss points of elements. It can be easily seen that if two Gauss points are considered to represent the random field, more number of point are available to represent the random field than mid point based representation. Thus, naturally a better representation of random field through representation of eigenvectors of covariance function. The beam is discretized into 100 elements of equal length to have a very fine mesh and is considered as target mesh to compare shape of eigenvectors of covariance function with different discretization. In order to obtain an accurate representation of random field, three criteria namely (1) sufficient number of terms in the KL expansion; (2) sufficient number of elements and (3) proper representation of eigenvectors are considered essential. The adequacy of first criterion can be evaluated from expected energy consideration. The second and third criteria ensure proper representation of random field while sufficient number of elements are required for proper representation of eigenvectors. Further, expected energy depends on total number of eigenvalues which again depends on the discretization. Thus, while considering all the three criteria in a holistic manner, an appropriate limit of % cumulative energy may be set to obtain a satisfactory representation of random field in terms of random variables.

Similarly, the beam can be analysed deterministically to find a converged FE mesh and finer of the stochastic and FE mesh is adopted for the stochastic finite element analysis.

Fig. 7.5 also shows a typical realization of the random field with 8 and 16 elements when all the terms of the expansion are considered, while considering the values of the random field at two Gauss points. It can be observed that 16 element random field has a better spatial randomness along its length. However, consideration of only a finer discretization without proper attention to number of terms will not produce a random field with an appropriate random signature. It is intuitive that if for a fine mesh, only one eigenvector is considered all the realizations will have same spatial variability along length, the only difference would be the magnitude. On the other hand, if all the eigenvectors are considered, the computational cost will invariably increase. Thus, a combination of appropriate refinement and number of eigenvectors are desired.

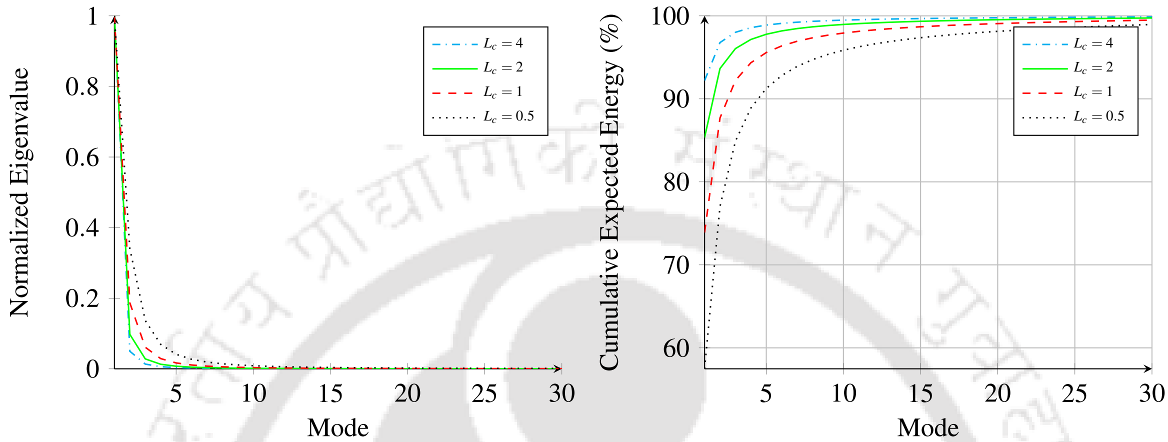

(a) Decay of eigenvalues. (b) Cumulative expected energy *vs* modes.

Fig. 7.3: Relative properties of the eigenvalues and cumulative % expected energy of Type-1 covariance function.

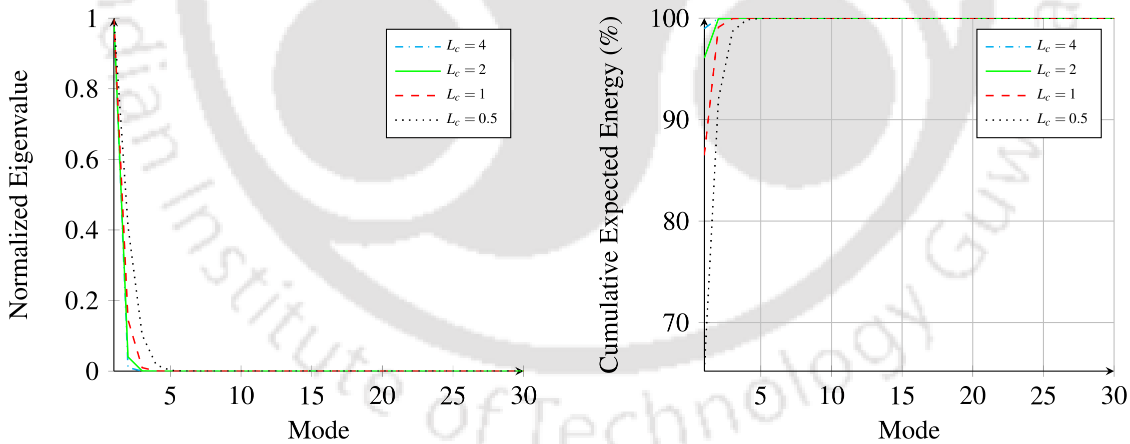

(a) Decay of eigenvalues. (b) Cumulative expected energy *vs* modes.

Fig. 7.4: Relative properties of the eigenvalues and cumulative % expected energy of Type-2 covariance function.

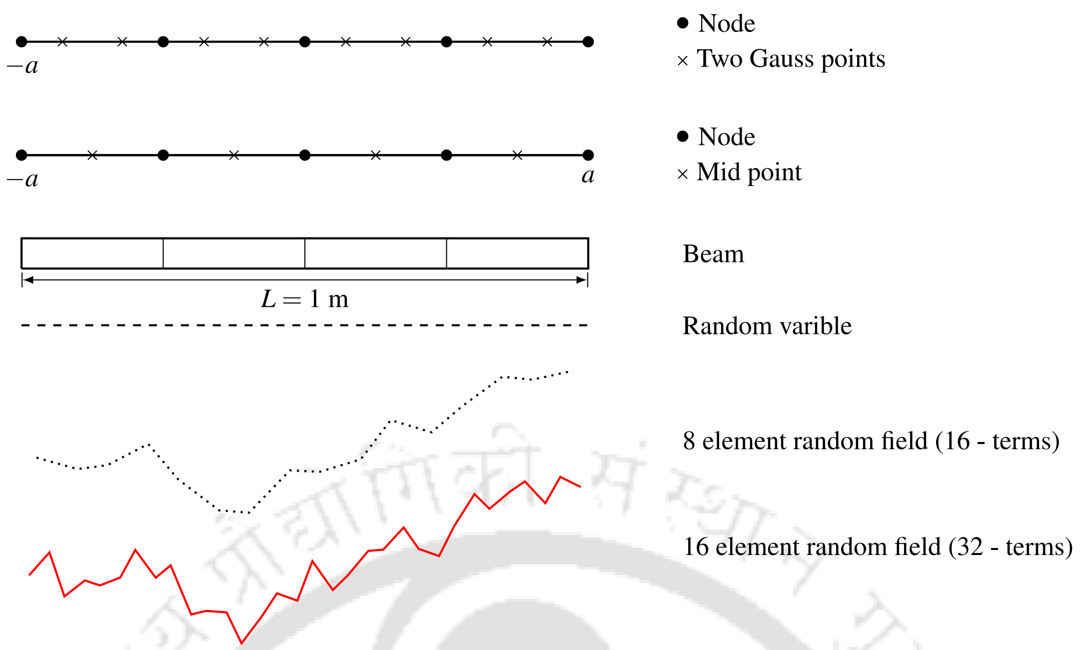

Fig. 7.5: Beam showing mid point and two Gauss points along with random field corresponding to 8 and 16 elements.

Tables 7.1 and 7.2 show the % expected energy for different number of elements and modes when the random field is considered at two Gauss points and mid points respectively. It can be observed that most of the expected energy is concentrated with in a first few modes and as the number of elements increase, the expected energy for each mode reduces slightly. The share of total expected energy per mode reduces as the number of modes increases with increase in number of elements. Moreover, with same number of elements, the expected energy corresponding to each mode for random field being represented at two Gauss points is lesser than that of similar consideration at mid point. This is because even with same number of elements, random field with two Gauss points consideration has more modes than mid point consideration. However, it may also be noted that the % expected energy with two Gauss point representation is almost of same order as that of mid point representation, while the considered discretization of the former is half of the later case. This is going to be advantageous as admissible % expected energy can be achieved with a discretized domain having lesser number of elements. Further an integrated approach involving other parameters like continuity and error in variance as well as covariance should be adopted to have best possible representation of the random field.

Table 7.1: % Expected energy with random field representation at two Gauss points.

No. of	Modes							
Ele	1	2	3	4	5	6	7	8
4	58.02	78.12	86.55	91.13	94.54	96.67	98.43	100.00
6	57.71	77.51	85.61	89.85	92.47	94.32	95.88	96.92
8	57.60	77.29	85.28	89.40	91.91	93.60	94.85	95.84
10	57.55	77.19	85.13	89.20	91.65	93.29	94.48	95.38
12	57.53	77.14	85.05	89.09	91.51	93.12	94.28	95.15
14	57.51	77.10	85.00	89.03	91.43	93.02	94.16	95.01
16	57.50	77.08	84.97	88.98	91.37	92.96	94.08	94.92
18	57.49	77.07	84.95	88.95	91.34	92.91	94.03	94.86
100	57.47	77.01	84.87	88.85	91.20	92.75	93.84	94.65

Ele$\longrightarrow$ Element

Table 7.2: % Expected energy with random field representation at Mid point.

No. of	Modes							
Ele	1	2	3	4	5	6	7	8
8	58.15	78.36	86.82	91.40	94.38	96.58	98.39	100.00
12	57.77	77.61	85.73	89.96	92.58	94.38	95.74	96.83
16	57.64	77.35	85.35	89.47	91.97	93.65	94.89	95.84
20	57.57	77.23	85.17	89.24	91.69	93.32	94.50	95.40
24	57.54	77.16	85.08	89.12	91.54	93.15	94.30	95.16
28	57.52	77.12	85.02	89.05	91.45	93.04	94.17	95.02
32	57.51	77.10	84.99	89.00	91.39	92.97	94.09	94.93
36	57.50	77.08	84.96	88.97	91.35	92.92	94.04	94.87
200	57.47	77.01	84.87	88.85	91.20	92.75	93.84	94.65

To study the continuity requirement and accuracy of eigenvector, the evaluated eigenvectors are checked for accuracy by comparing with target eigenvectors which are evaluated for 100 elements for two Gauss points and 200 elements for mid point consideration. Tables 7.3 and 7.4 show the MAC values for different eigenvectors and different element numbers when random fields are considered at two Gauss points and mid point respectively. Further, Fig 7.6 shows the eighth eigenvector of covariance function with different element numbers and compared with target shape when random fields are approximated at mid point and two Gauss points. It can be observed that in both the cases, MAC values converge towards 1 when number of elements increase. However, for the same number of elements, the MAC is better for the case when random field is considered at two Gauss points. Thus, with lesser number of element, a better MAC can be obtained when considered at two Gauss points per element.

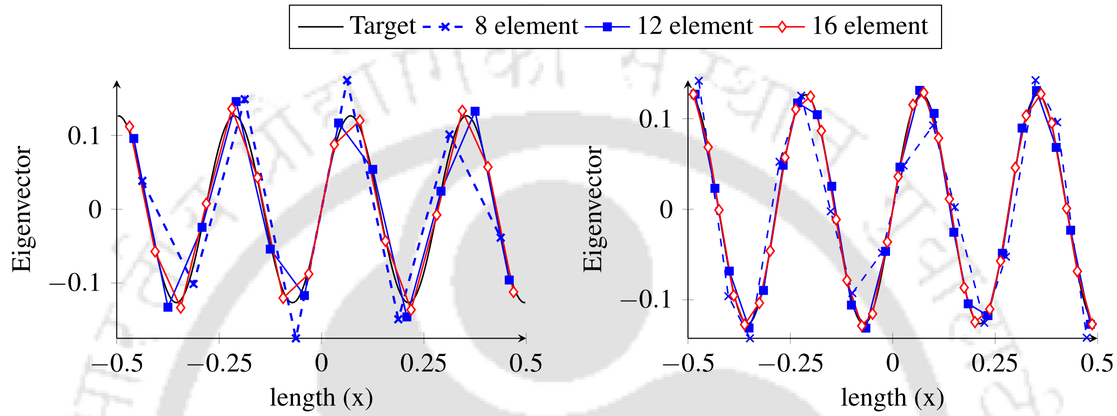

(a) Mid point (b) Gauss Point

Fig. 7.6: Eighth eigenvector of covariance function with different element number.

Table 7.3: MAC for different eigenvectors for various discretized domain with random field representation at two Gauss points.

No. of	Modes								
Ele	1	2	3	4	5	6	7	8	9
4	1.0000	0.9992	0.9917	0.9475	0.9662	0.9097	0.8923	0.7765	-
6	1.0000	0.9999	0.9989	0.9946	0.9807	0.9184	0.9742	0.8737	0.9078
8	1.0000	1.0000	0.9997	0.9987	0.9958	0.9885	0.9687	0.8867	0.9786
10	1.0000	1.0000	0.9999	0.9995	0.9986	0.9964	0.9918	0.9817	0.9551
12	1.0000	1.0000	1.0000	0.9998	0.9994	0.9985	0.9968	0.9936	0.9872
14	1.0000	1.0000	1.0000	0.9999	0.9997	0.9993	0.9985	0.9971	0.9946
16	1.0000	1.0000	1.0000	1.0000	0.9999	0.9996	0.9992	0.9985	0.9972
18	1.0000	1.0000	1.0000	1.0000	0.9999	0.9998	0.9995	0.9991	0.9985
100	1.0000	1.0000	1.0000	1.0000	1.0000	1.0000	1.0000	1.0000	1.0000

Table 7.4: MAC for different eigenvectors for various discretized domain with random field representation at Mid point.

No. of	Modes								
Ele	1	2	3	4	5	6	7	8	9
8	1.0000	0.9990	0.9925	0.9759	0.9519	0.9272	0.8944	0.7984	-
12	1.0000	0.9999	0.9988	0.9952	0.9878	0.9763	0.9612	0.9435	0.9215
16	1.0000	1.0000	0.9997	0.9987	0.9964	0.9923	0.9859	0.9774	0.9667
20	1.0000	1.0000	0.9999	0.9995	0.9987	0.9971	0.9944	0.9905	0.9853
24	1.0000	1.0000	1.0000	0.9998	0.9994	0.9987	0.9975	0.9956	0.9930
28	1.0000	1.0000	1.0000	0.9999	0.9997	0.9994	0.9987	0.9978	0.9964
34	1.0000	1.0000	1.0000	1.0000	0.9999	0.9997	0.9995	0.9991	0.9985
38	1.0000	1.0000	1.0000	1.0000	0.9999	0.9999	0.9997	0.9995	0.9991
200	1.0000	1.0000	1.0000	1.0000	1.0000	1.0000	1.0000	1.0000	1.0000

The statistical parameters of the random field are checked for accuracy. In order to study the effect of discretization and truncation on the accuracy of simulated data, permissible error in % expected energy of 5% is considered. The global error in variance and covariance are calculated using Eqs. 7.6 and 7.9 respectively and are shown in Tables 7.5 and 7.6 for different number of elements when random fields are considered at two Gauss points and mid point respectively. It can be observed that global error in variance reduces as the % expected energy increases, which can also be seen from Eq. 7.6.The reduction in % expected energy with refinement can be improved by inclusion of additional eigenvectors in the representation of discretized domain. On the other hand, the global error in covariance is observed to reduce consistently simultaneous increase in refinement and increase in number of eigenpairs are considered. Moreover, it is also observed that both the errors in variance and covariance are lesser in case of random field consideration at two Gauss points. The minimum value of local variance and error in local covariance (except diagonal terms) are also shown. It can be observed that as the expected energy reduces, the minimum value of local variance also reduces. However, maximum error in local covariance reduces with simultaneous increase in number of element and % expected energy.

Table 7.5: Error in calculated variance and covariance for random field represented at two Gauss points.

No. of Ele	Q	% ExpEn	$\overline{\varepsilon}_{\sigma^2_{\hat{\alpha}_Q}}$ $\times 10^{-2}$	$\overline{\varepsilon}_{C_{\alpha,\alpha_Q}}$ $\times 10^{-2}$	Min Var$[\hat{\alpha}(x,\theta)]$	Max $\varepsilon_{C_{\alpha,\alpha}}(x_1,x_2)$
4	6	96.67	3.6670	2.1610	0.9480	0.0466
6	7	95.88	4.3610	1.2610	0.9455	0.0422
8	8	95.84	4.2920	1.2180	0.9504	0.0258
10	8	95.38	4.6520	0.9520	0.9441	0.0350
12	8	95.15	4.8470	0.8560	0.9410	0.0349
14	8	95.01	4.9650	0.8140	0.9431	0.0379
16	9	95.58	4.4000	0.6630	0.9496	0.0336
18	9	95.52	4.4610	0.6590	0.9450	0.0326
100	9	95.27	4.7120	0.6200	0.9132	0.0665

ExpEn$\longrightarrow$ Expected energy

Table 7.6: Error in calculated variance and covariance for random field represented at mid points.

No. of Ele	Q	% ExpEn	$\overline{\varepsilon}_{\sigma^2_{\hat{\alpha}_Q}}$ $\times 10^{-2}$	$\overline{\varepsilon}_{C_{\alpha,\alpha_Q}}$ $\times 10^{-2}$	Min Var$[\hat{\alpha}(x,\theta)]$	Max $\varepsilon_{C_{\alpha,\alpha}}(x_1,x_2)$
8	6	96.58	3.7970	2.2530	0.9480	0.0455
12	7	95.74	4.4790	1.4560	0.9405	0.0357
16	8	95.84	4.2830	1.0810	0.9467	0.0331
20	8	95.40	4.6580	0.9350	0.9467	0.0333
24	8	95.16	4.8530	0.8560	0.9407	0.0310
28	8	95.02	4.9680	0.8110	0.9431	0.0355
32	9	95.59	4.4050	0.6580	0.9499	0.0315
36	9	95.52	4.4630	0.6500	0.9464	0.0315
200	9	95.27	4.7090	0.6200	0.9145	0.0679

The influence of number of eigenvectors and number of elements on accuracy of simulated data are studied. It is observed that an integrated approach is required considering all the parameters like % expected energy, correctness of eigenvectors and errors in statistical parameters like variance and covariance. From Table 7.1, 7.3 and 7.5 corresponding to two

Gauss points representation and from Table 7.2,7.4 and 7.6 for mid point representation of random field and from Fig. 7.6, it can be observed that two Gauss points representation of random field is better than mid point representation. The second and third parameters are more likely to be governed by local error at element level. Thus, it may be more economical to carry out discretization locally, where only the elements with unacceptable error level are discretized further. The next section discusses the effect of local discretization in an adaptive manner. As it is observed that two Gauss points representation of random field is better than mid point representation, subsequent studies are carried out considering two Gauss points representation only.

7.6.2 Adaptive discretization

From the previous section, it has been observed that a combination of number of eigenvectors and number of elements is necessary for accurate representation of random field along with proper representation of those considered eigenvectors. However, a mesh with uniform element size may not be proper choice. It may be more economical to consider a suitable adaptive discretization scheme where elements which lack accuracy are only discretized further. As discussed in section 7.3, there can be three ways to combine FE mesh and random field mesh. The present study considers the random field representation at Gauss point of element and thus it will be more appropriate to consider random field discretization and FE discretization as same.

The present adaptive algorithm is shown as a flowchart in Fig. 7.7. The discretization process starts with four input parameters, namely, the covariance function of the random field to be discretized, a target % expected energy to be used for monitoring global error in discretization, a target local variance to be used for enforcing local level refinement, and an initial discretized mesh. The next step is to discretize the random field using KL expansion and evaluate the eigenpairs of the covariance function. The number of eigenvectors to be considered is calculated based on the target % expected energy. Variances of the random field along the length are calculated using Eq. 7.1 based on the considered number of eigenvectors. If the magnitude of variance in any element is less than the assumed local target variance, the concerned element is discretized into two elements of equal length. The next step is to discretize the random field based on the new discretized domain and the process continues until all the elements satisfy the local variance limit. The eigenvectors are finally checked for accuracy using MAC with respect to a new mesh with each element of the last admissible discretized domain subdivided into two elements of equal length.

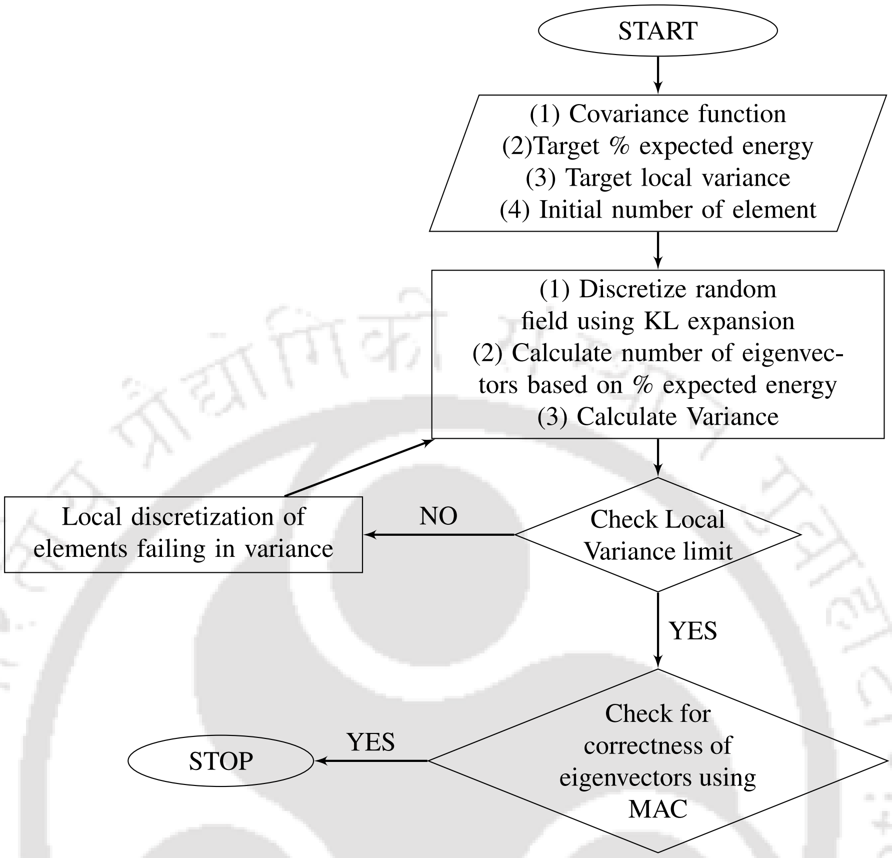

Fig. 7.7: Flow chart for adaptive discretization.

An adaptive discretization scheme was proposed by Allaix and Carbone (2010, 2012), where the elements having the highest error in local variance were further discretized when the global error in variance is more than a permitted value. Since subsequent refinements are done only on the basis of global error in variance, elements with unacceptable error in variance at local level may be left out. Thus some modification in the proposed adaptive strategies are suggested in the current study for more effective discretization of random field. It has been observed from the previous section that the global error in variance can be correlated to % expected energy. Thus, without any bias, it can be assumed that instead of considering global error in variance, % expected energy can be considered for global error in variance, which enables to relate global error in variance from eigenvalue itself. Further, a local error in covariance is related to two points in the physical domain, thus rendering it to be an inappropriate criterion for any adaptive discretization. Thus, a local error in variance is considered in the present study as criteria for further discretization.

7.6.2.1 Implementation and numerical study

7.6.2.1.1 1-D random field representing Young's modulus of beam element

The same beam problem with exponential covariance function (Type-1) is considered for further study. Two numerical case studies are conducted with CASE-(1) a target expected energy of 95% and a point-wise error in variance of 5.05% (94.95% accuracy) CASE-(2) a target expected energy of 95.5% and a point-wise error in variance of 5% (95% accuracy). Two cases with slight variation are done to appreciate the effectiveness of the adaptive strategy. It is also important to note that the two limits on % expected energy and minimum point-wise error are correlated to each other. A big difference in these two limits may result in discretization in an infinite loop or may not discretize at all. it is not however difficult to appreciate that the local accuracy level in variance should be marginally lesser than its target expected energy, which is a global representation of the expected accuracy level of the simulated random field. For both the cases, an initial mesh of 4 elements is considered with two nodes for each element. Elements are discretized locally where the point-wise error in variance is more than the prescribed value. As the number of elements increase, the eigenvectors required for attaining prescribe expected energy may also increase and is considered accordingly.

CASE-(1) :

The discretized domain with different iterations are shown in Fig. 7.8 and the corresponding local variances along the length are shown in Fig. 7.9. It can be observed that the elements whose local variances are below the target limit are discretized further in the next iteration. The number of eigenvectors required to achieve the desired level of % expected energy for each iteration are shown in Table 7.7 along with global errors in variance as well as covariance and the magnitude of minimum variance. It can be observed that in the first iteration, the global error in variance is less than that of other iterations. Thus, if only global error in variance is considered as discretization criterion Allaix and Carbone (2010, 2012), the domain may not have been discretized further. It is however seen that the error in local variance is more than the prescribed value. Thus, based on local variance, elements of the domain are further discretized. The global error in covariance is more in the initial iteration and reduces as iteration increases. MAC for different eigenvectors are calculated with respect to the next iteration and are shown in Table 7.8. In the case of the last iteration, MAC values are evaluated with respect to eigenvector for covariance matrix generated by considering a mesh obtained by dividing each of the elements of the last iteration into two of equal length. Thus, for the present case, the number of elements for the last iteration is 16, MACs are calculated with respect to 32 elements generated by dividing each element into two elements of equal length. It is also important to note that the global errors in variance and covariance can be reduced by considering additional eigenvectors.

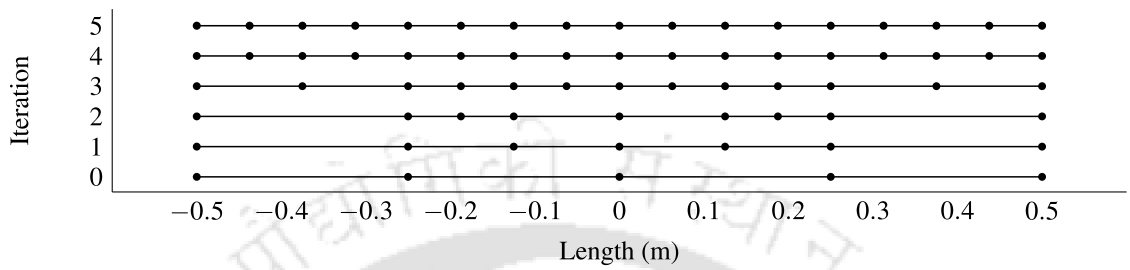

Fig. 7.8: Adaptive discretization of random field over a beam with different iterations (CASE-(1)).

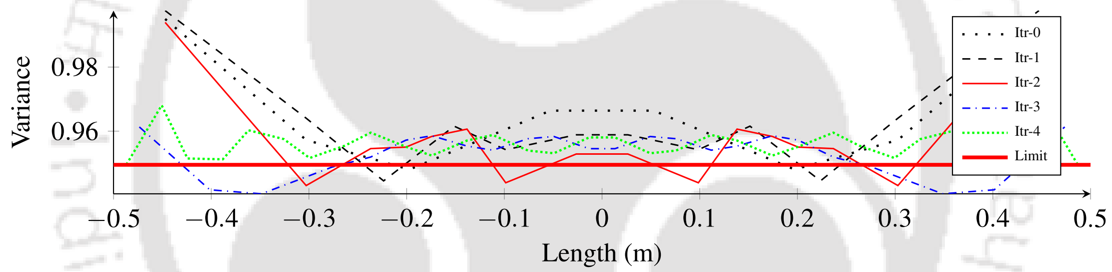

Fig. 7.9: Calculated variances along length for different iterations (CASE-(1)).

Table 7.7: Various parameters in the discretized domain for CASE-(1)

Itr	No. of Ele	Q	% ExpEn	$\overline{\varepsilon}_{\sigma^2_{\hat{\alpha}_Q}}$ $\times 10^{-2}$	$\overline{\varepsilon}_{C_{\alpha,\alpha_Q}}$ $\times 10^{-2}$	Min Var$[\hat{\alpha}(x,\theta)]$
1	6	7	96.35	3.629	1.133	0.944
2	8	7	95.78	4.255	1.194	0.943
3	12	8	95.33	4.847	0.966	0.940
4	16	9	95.58	4.400	0.663	0.950
5	16	9	95.58	4.400	0.663	0.950

Itr⟶ Iteration

Table 7.8: MAC for different eigenvectors for different iterations (CASE-(1))

Itr	Modes								
	1	2	3	4	5	6	7	8	9
0	0.9985	0.9919	0.9089	0.8714	0.9518	0.7986	0.7195	-	-
1	0.9999	0.9950	0.9987	0.9214	0.9312	0.9816	0.9483	-	-
2	0.9999	0.9955	0.9966	0.9153	0.9189	0.9435	0.9736	0.8505	-
3	0.9983	0.9941	0.9110	0.8662	0.8909	0.8596	0.7867	0.7395	0.7689
4	1.0000	1.0000	1.0000	1.0000	1.0000	1.0000	1.0000	1.0000	1.0000
5	1.0000	1.0000	1.0000	1.0000	0.9999	0.9997	0.9993	0.9986	0.9975

CASE-(2) :

Similar to CASE-(1), the domain is discretized iteratively considering the limits specified. Figs. 7.10 and 7.11 respectively show the discretized domain and local variance along the length with different iterations. Elements whose local variances are below the target limit are further discretized in the next iteration. The number of eigenvectors required to achieve the desired level of % expected energy for each iteration are shown in Table 7.9 along with global errors in variance and covariance and minimum variance. It can be observed that in the initial, iteration the global error in variance is least. However, global error in covariance is more and minimum value of local variance is lesser than the prescribe accuracy limit. As the iteration progresses the global covariance reduces and minimum variance is observed to reach within the target limit. MAC for different eigenvectors are calculated with respect to the next iteration and are shown in Table 7.10. In the case of the last iteration, MACs are evaluated with respect to eigenvector for covariance matrix generated by considering discretization of all the elements of the last iteration. Thus, for the present case, the number of elements for the last iteration is 36, MACs are calculated with respect to 72 elements generated by dividing each element into half. It can also be observed from Table 7.9 that in case of adaptive discretization, % expected energy is higher and local error in covariance is lesser than those corresponding to uniform discretization. Thus, the adaptive scheme can automatically arrive at the required mesh in an efficient manner.

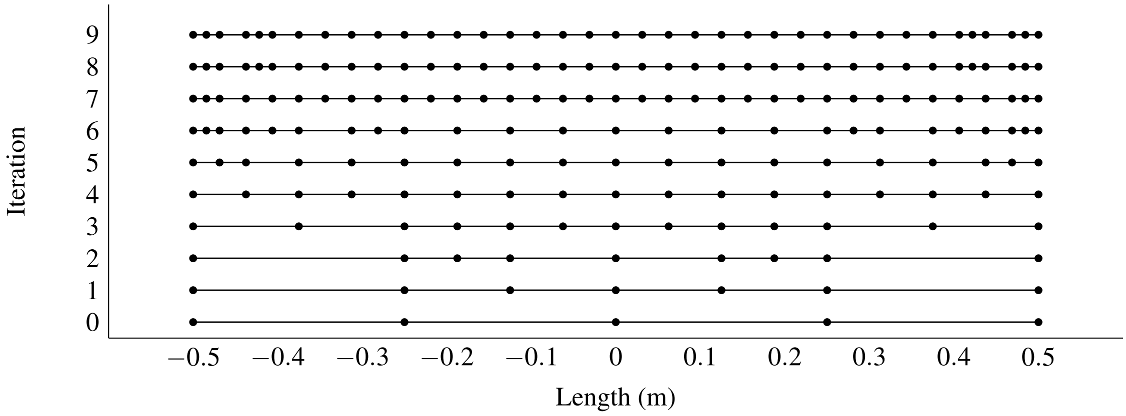

Fig. 7.10: Adaptive discretization of random field over a beam with different iterations (CASE-(2)).

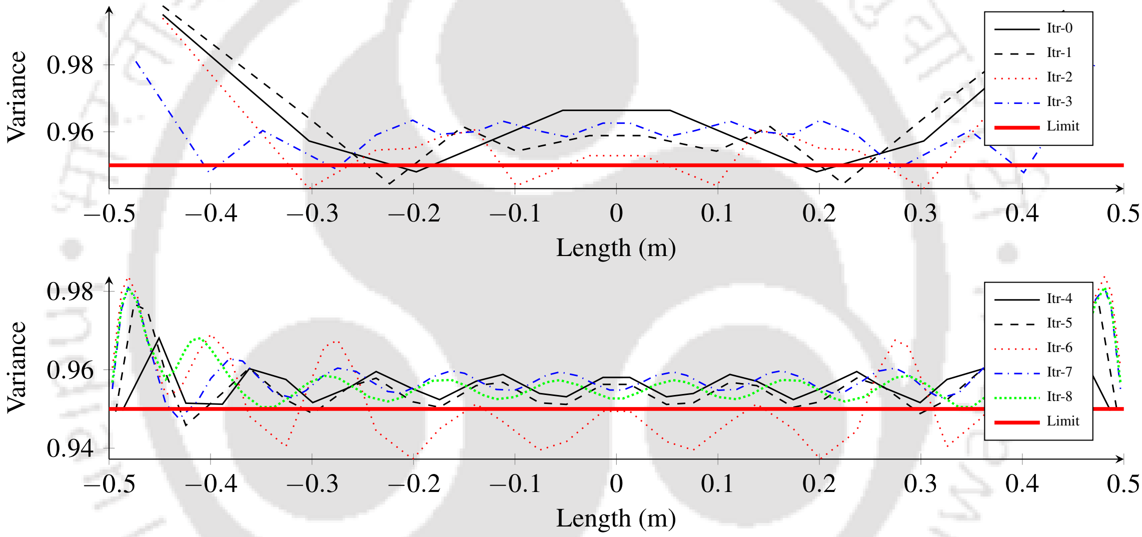

Fig. 7.11: Calculated variances along length for different iterations (CASE-(2)).

Table 7.9: Various error measures in the discretized domain (CASE-(2))

Itr	No. of Ele	Q	% ExpEn	$\bar{\varepsilon}_{\sigma^2_{\hat{\alpha}_Q}}$ $\times 10^{-2}$	$\bar{\varepsilon}_{C_{\alpha,\alpha_Q}}$ $\times 10^{-2}$	Min Var$[\hat{\alpha}(x,\theta)]$
1	6	7	96.35	3.629	1.133	0.944
2	8	7	95.78	4.255	1.194	0.943
3	12	9	96.04	4.086	0.838	0.948
4	16	9	95.58	4.400	0.663	0.950
5	18	9	95.61	4.489	0.684	0.946
6	24	9	95.69	4.791	0.689	0.937
7	34	10	95.88	4.204	0.539	0.947
8	36	10	95.87	4.257	0.553	0.950
9	36	10	95.87	4.257	0.553	0.950
Uniform	36	10.00	95.83	4.1480	0.5230	0.9359

Table 7.10: MAC for different eigenvectors for different iterations (CASE-(2))

Itr	Modes									
	1	2	3	4	5	6	7	8	9	10
0	0.9985	0.9919	0.9089	0.8714	0.9518	0.7986	0.7195	-	-	-
1	0.9999	0.9950	0.9987	0.9214	0.9312	0.9816	0.9483	-	-	-
2	0.9999	0.9955	0.9966	0.9153	0.9189	0.9435	0.9736	0.8505	0.7827	-
3	0.9983	0.9941	0.9110	0.8662	0.8909	0.8596	0.7867	0.7395	0.7689	-
4	0.9994	0.9974	0.9750	0.9427	0.9165	0.9019	0.8974	0.8988	0.9016	-
5	0.9987	0.9994	0.9463	0.9688	0.9585	0.9034	0.8565	0.8268	0.7420	-
6	0.9979	0.9976	0.9037	0.9284	0.9089	0.8665	0.8649	0.8141	0.6875	0.6423
7	0.9999	0.9997	0.9947	0.9925	0.9959	0.9996	0.9985	0.9881	0.9675	0.9402
8	1.0000	1.0000	1.0000	1.0000	1.0000	1.0000	1.0000	1.0000	1.0000	1.0000
9	1.0000	1.0000	1.0000	1.0000	1.0000	1.0000	1.0000	1.0000	1.0000	0.9999

7.6.2.1.2 2-D random field representing Young's modulus of plane stress problem

The second problem considered is a plane stress problem of square domain of length 1m.

The randomness is considered in both the direction with covariance function

$$\boldsymbol{C}(x_1,x_2;y_1,y_2) = \sigma^2 \exp\left(-\frac{(x_1-x_2)^2}{L_{c_x}^2} - \frac{(y_1-y_2)^2}{L_{c_y}^2}\right) \tag{7.14}$$

where L_{c_x} and L_{c_y} are the correlation length in X and Y directions and values are considered as $L_x/2$ and $L_y/2$ respectively. The eigenvalues and eigenvectors of 2-D covariance function can be evaluated from 1-D eigenvalues and eigenvectors considering 1-D covariance function $\boldsymbol{C}(x_1,x_2) = \sqrt{\sigma^2}\exp(-(x_1-x_2)^2/L_{c_x}^2)$. Thus, the 2-D eigenvalues and eigenvectors are evaluated as $\lambda(x,y) = \lambda_x\lambda_y$ and $f(x,y) = f(x)f(y)$ respectively, where λ_x and λ_y are the eigenvalues in X and Y direction respectively. Similarly, $f(x)$ and $f(y)$ are the eigenvector in X and Y directions. A target expected energy of 90% and an allowable point-wise error in variance of 10.5% (89.5% accuracy) are considered for each direction. Similar to the previous beam problem, an initial mesh of 4 elements are considered in each direction.

The adaptive discretization for each 1-D case is studied considering the above parameter. Only the results in X direction are discussed. The discretization in X-direction for different iterations are shown in Fig. 7.12 and the corresponding variance in X-direction are shown in Fig. 7.13. The number of eigenvectors considered in each iteration with global errors in variance, covariance and the minimum local variance are shown in Table 7.11. It may be noted that the adaptive discretization starts with a mesh and determines the number of eigenvectors required to satisfy the target % expected energy. However, a simultaneous examination of error in variance at element level shows that elements with higher level of errors than set target exists and hence needs more discretization. Thus, if only % expected energy is considered as criterion, any further discretization would not have happened and some elements with unacceptable level of errors would have existed. From Figs.7.12 and 7.13, it can be observed that in the first iteration, elements which have a local variance less than the prescribed allowable error are discretized further. Once all the local variance values are more than the minimum value considered, the iteration process stops. Thus, the proposed adaptive discretization scheme is considered to be more effective in the representation of random field as both global as well as local errors are utilized. Similar to the beam problem, the eigenvectors are checked for accuracy using MAC and are shown in Table 7.12. The two dimensional discretized domain is shown in Fig. 7.14. A comparison with the case of uniform discretization with the same number of elements and eigenvectors indicate that the minimum value of local variance is lesser than that of the adaptively discretized domain, though % expected energy is marginally higher.

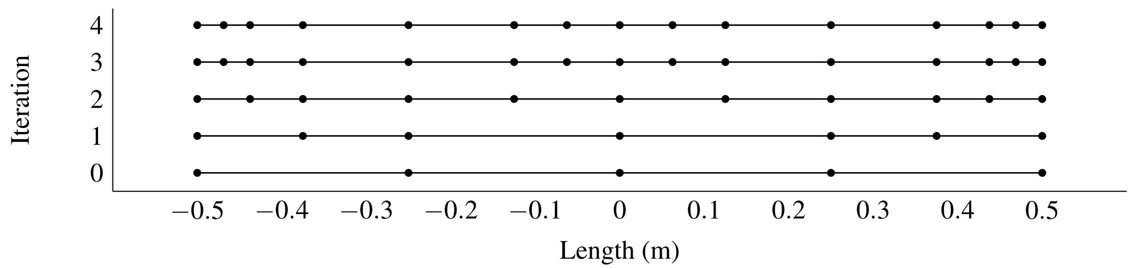

Fig. 7.12: Adaptive discretization of random field over plane stress domain in X direction with different iterations.

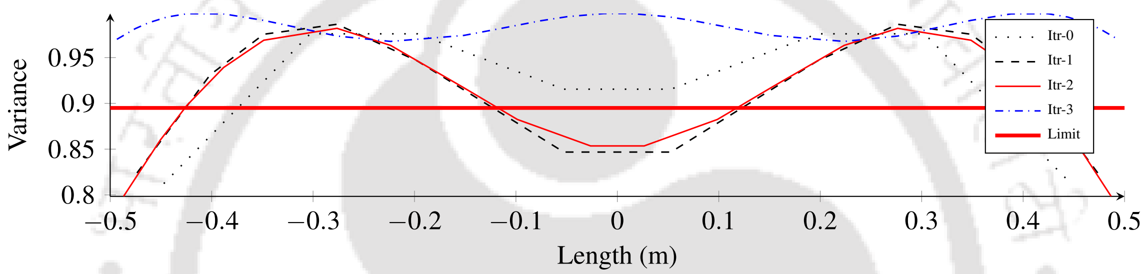

Fig. 7.13: Calculated variances along X-direction for different iterations (Plane stress domain).

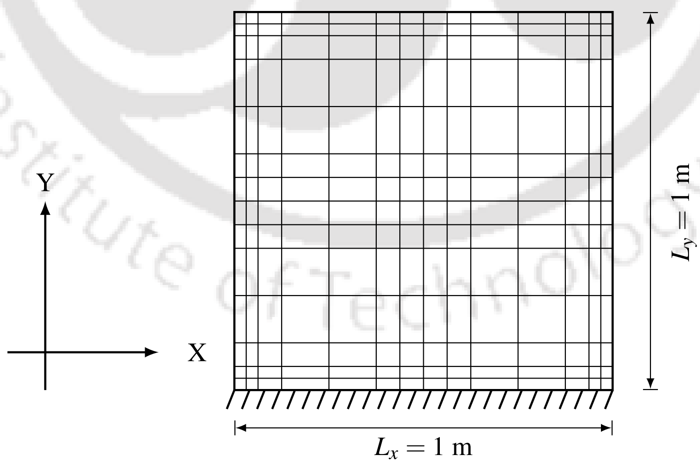

Fig. 7.14: Final mesh for adaptive discretization of 2-D random field for plane stress problem.

Table 7.11: Various error measures in the discretized domain along X direction.

Itr	No. of Ele	Q	% ExpEn	$\overline{\varepsilon}_{\sigma^2_{\hat{\alpha}_Q}}$ $\times 10^{-2}$	$\overline{\varepsilon}_{C_{\alpha,\alpha_Q}}$ $\times 10^{-2}$	Min Var$[\hat{\alpha}(x,\theta)]$
1	6	2	91.84	8.101	5.419	0.824
2	10	2	90.62	8.289	5.687	0.798
3	14	3	98.58	1.585	1.118	0.968
4	14	3	98.58	1.585	1.118	0.968
Uniform	14	3	98.71	1.166	0.792	0.946

Table 7.12: MAC for different eigenvectors for different iteration.

Itr	Modes		
	1	2	3
0	0.9986	0.9996	-
1	0.9999	0.9999	-
2	0.9999	0.9999	0.9964
3	1.0000	1.0000	1.0000
4	0.9960	0.9979	0.9899

7.6.3 Non-Gaussian random field

In the previous section, discussion are made regarding the discretization of random fields when the same is idealized as a Gaussian distribution. However, physical quantities like Young's modulus and area are more realistically represented if the distribution is assumed as non-Gaussian. There are mainly two categories of generation of non-Gaussian random fields. The first one is a translation process, while the second one is a direct generation using KL expansion. In both the cases, it is sought to evaluate the non-Gaussian random field iteratively. In the case of KL expansion, the difference with Gaussian one is that the random variables ($\xi_i(\theta)$ in Eq. 3.1) of KL expansion need to be generated iteratively. Phoon et al. (2005), Huang et al. (2000) proposed the generation of these random variables iteratively. The advantage of direct generation of non-Gaussian fields over translation process is that the covariance function of the former one (direct generation) always matches with the theoretical one, thus requires to match only the marginal distribution in the iteration process. In the context of achieving an appropriate discretization for the non-Gaussian random field representation, the adopted procedure for Gaussian random field can be considered, as the variance and covariance are independent of the random variable, $\xi_i(\theta)$. Once a proper discretization is obtained, the iteration process to generate the random variables can be carried out. However, the generated random variables after the iteration process are not necessarily independent though uncorrelated. The dependency among the random variables can be reduced by considering independent component analysis (ICA) (Comon, 1994, Hyvärinen and Oja, 2000) which replaces the random variables by a linear combination of independent random variables. Khalil and Sarkar (2008, 2014) considered ICA to ensure that the random variables are independent. The discussion on iterative KL expansion for simulation of non-Gaussian random field and application of ICA are already presented in sections 4.2.2 and 4.4.2.1.

7.7 Conclusion

This chapter presents various issues related to discretization of random fields in structural mechanics problem using truncated KL expansion. The influence of parameters like correlation length, type of covariance function, % expected energy on the accuracy of discretization of random field are studied. The accuracy with respect to truncation of KL expansion is also studied in details. It is observed that the global error in variance is correlated to % expected energy. A higher value of % expected energy reduces the global error in variance. Thus, % expected energy is considered for limiting global error in variance. The global error in covariance is observed to improve with the increase in both the number of elements and number of eigenpairs considered. Further, an adaptive discretization scheme is presented where the desired limiting values of % expected energy and a co-related limiting value of error in variance at element level are used as controlling parameter. The advantage of adaptive discretization is that the desired accuracy on % expected energy can be related automatically while ensuring that each element of the discretized domain are conforming to minimum accuracy set for variance. The applicability of the adaptive discretization scheme and appropriate modification required for a non-Gaussian random field is also discussed.

8

Conclusions and recommendations for future research

Contents

8.1 Summary

The standard FEM is a potent mathematical tool considered to analyse engineering problems numerically. However, it does not consider the random nature of physical parameters in the analysis. SFEM is one of the branches of the FEM, where an approximate solution of the stochastic system is sought to be evaluated combining with a probabilistic model. PC based method is one of the solution methods of SFEM, where the responses are approximated using known orthogonal functions, random in nature and unknown coefficients. Thus, the calculations of stochastic responses become equivalent to the evaluation of unknown coefficients.

It is observed that as the SD of the input variables increase, the responses become non-Gaussian even though the input variables are Gaussian in nature. These responses can be approximated using PC expansion. Xiu and Karniadakis (2002) observed that orthogonal polynomial in PC are optimal for the representation of a random process when the weight functions for some orthogonal polynomials are identical to the probability density functions. However, the probabilities of the responses are not known before solving the problems. Thus, to represent the response accurately using Hermite Polynomial, a higher order expansion is required. In this context, it may be appropriate to approximate the responses using gPC.

However, in order to consider an appropriate variant of gPC, the distributions of responses are not available *apriori*. Moreover, as the order and/or the number of random variables increases, the number of terms in the PC expansion also increases exponentially. It is known as the curse of dimensionality and one of the major drawbacks of PC expansion.

An iterative PC based method in the intrusive framework is proposed to overcome the curse of dimensionality. The method solves the problem iteratively using smaller sizes of PC expansion. The proposed method iteratively generates PC, based on the responses of the previous iteration. First-order PC expansion is considered in the initial iteration. As the PC is generated from the responses of the previous iteration, the PC is a function of non-Gaussian random variables. Hence, a non-Gaussian response is approximated using a PC expansion of an appropriate non-Gaussian type. Thus, the updated PC expansion can be considered as more appropriate to approximate the responses. Since the PC approximation is more appropriate to represent the responses, it requires lesser order of expansion.

Moreover, it is also proposed to consider iteration within the same order after the initial iteration, and convergence can be achieved within the same order with an increase in iterations. The number of random variables is also reduced by considering only the dominant components of the responses and are evaluated using KL expansion. Thus, a non-Gaussian response is approximated using PC of non-Gaussian nature with a reduced number of random variables. Hence, a lower order of expansion is observed to be adequate to have the same level of accuracy.

In the case of random field problem, the random field is discretised using KL expansion. The size of the stiffness matrix is reduced by considering the random field at Gauss points rather than midpoint or nodes of members. Thus there are more numbers of points to represent the random field with the same size of the stiffness matrix. The size of the stiffness matrix is further reduced by considering an eigen decomposition of the stiffness matrix and considering only the dominant component as proposed by Pascual and Adhikari (2012).

The method is further explored to consider non-Gaussian random material properties. The discretisation and simulation of non-Gaussian random fields are carried out by considering iterative KL expansion as proposed by Huang et al. (2000), Phoon et al. (2002, 2005). However, the random variables generated to represent the non-Gaussian random field may not be independent. Thus, ICA (Comon, 1994) is considered to obtain a set of independent random variables.

Different types of numerical examples have been solved to demonstrate the efficiency of the proposed method considering both Gaussian and non-Gaussian randomness. The responses are observed to be in good agreement with those of MCS. The proposed iterative scheme is observed to be an effective strategy for addressing linear elastostatic structural mechanics problems considered in this study. The proposed method can be considered as an alternative to computationally demanding MCS. The proposed method is observed to exhibit significant reduction in curse of dimensionality of the PC based method without compromising the accuracy in the evaluated responses.

The issues related to large dimension of stochastic system matrix can be reduced by considering PDD, where multidimensional response are represented using a linear combination of responses of mean, univariate, bivariate and higher variate components. A hybrid approach of PDD and iterative PC based methods are considered to solve SFE equations. From the numerical studies of linear structural mechanics problems with both Gaussian and non-Gaussian randomness, it is observed that the proposed hybrid strategy of PDD and iterative method can be considered as an efficient alternative method for the solution of structural mechanics problem compared to PDD-PC based approach.

Another drawback of PC expansion is the loss of optimality as observed in the case of time-dependent problems. In the case of dynamically loaded structural problem, the responses can be evaluated using Newmark-β method while the stochasticities of responses are approximated using PC expansion. However, the statistical parameters of responses change over time. Thus PC loses its efficiency over time integration as responses are approximated using PC of initially considered bases. TDgPC (Gerritsma et al., 2010) is considered to overcome this drawback. From the numerical study, it is observed that even though the order of PC expansion is increased, the responses do not converge towards MCS responses. However, responses of TDgPC are observed to converge toward MCS responses.

A detailed study has been carried out for discretisation of random field using truncated KL expansion. The influence of parameters like correlation length, type of covariance function, % expected energy on the accuracy of discretisation of the random field are studied. From the numerical study, it is observed that the global error in variance is correlated to % expected energy. A higher value of % expected energy yields lower value of error in global variance. Further, an adaptive discretisation scheme is presented considering a % expected energy to control global error and a correlated limiting value of variance at element level to control local discretisation. The advantage of an adaptive discretisation is that the desired accuracy on % expected energy is achieved automatically, while ensuring that each element of the discretised domain are conforming to minimum prescribed accuracy for variance.

8.2 Conclusions

The major conclusions ascribed to the present study may be summarized as follows:

- The statistical responses as evaluated using the proposed method are observed to be in better agreement with those from MCS as compared to PC expansion of same order.
- The proposed method can accurately evaluate the responses with much lesser computational complexity as compared to MCS and conventional PC (mPC).
- The proposed iterative method demands much lesser RAM requirement as compared to mPC and hence can be used to solve relatively larger problem with available computational infrastructure.
- Convergence study carried out with respect to MCS responses can lead to the determination of optimal order of PC expansion required for accurate evaluation of responses. Similarly, convergence study carried out using responses of two successive iterations and orders of PC can lead to accurate evaluation of responses even in the absence of MCS responses.
- Combination of PDD and ImPC is observed to be computationally more efficient than conventional PDD-PC.
- TDgPC can be considered as an effective alternative method for structural mechanics problems under dynamic loading, where PC based method may fail to evaluate responses accurately.
- The adaptive strategy for discretization of random field can ensure to provide an appropriate discretized domain, while keeping all the possible errors within the acceptable limit.

8.3 Recommendations for future research

The present study addresses the curse of dimensionality of PC based method at multiple levels. The future scope of study may include the following:

- With the advancement in computer facility, the demand for parallel computation is increasing in order to reduce the computational time. Future study may explore the potential of parallel algorithm of the proposed method. The stiffness matrices representing the deterministic part and each of the stochastic parts are independent and can be formulated independently. The calculations of ensembles of responses from PC coefficients for each DOFs are independent. Further, application of Polynomial Dimensional Decomposition decouples the problem to multiple smaller dimensional problems which can be solved individually. A detailed study can be carried out to evaluate the computational advantage and scope of parallel computation.

- The proposed method is an iterative procedure for the evaluation of responses. The coefficients of the PC expansion are evaluated using Galerkin projection known as intrusive formulation. The future study may be extended to the non-intrusive iterative formulation. In the case of non-intrusive formulation, the coefficients of the PC expansion are evaluated using regression, where a limited number of MCS responses are considered.

- With the advancement of computer science, machine learning and its application to different branches of engineering are increasing day by day. The least square regression generally considered in non-intrusive formulation is more prone to over-fitting for higher order polynomials. Thus, future study may be focussed in developing efficient machine learning algorithm to study the effect of uncertainty in structural system in an iterative non-intrusive framework so that more reliable design can be carried out.

- Study may include higher values of standard deviation of input random quantities and its effect on response statistics of structural system.

- Studies can be targetted towards more involved real time structural problems from field in a computationally efficient manner.

- The present study considers only linear structural mechanics problem under static and dynamic loadings. Issues related to dimensional curse, computational efficacy and accuracy are addressed. The future study can be extended to include non-linear static and structural dynamics problems in a computationally efficient manner.
- The present study considers structural mechanics problem with random properties. Future study can be extended in exploring the possibility of extending other field of problem including coupled problems.

List of Publications

Published in Journals

- **Nath, K.**, Dutta, A., and Hazra, B. (2019). An iterative polynomial chaos approach for solution of structural mechanics problem with Gaussian material property. *Journal of Computational Physics*, 390:425-451, https://doi.org/10.1016/j.jcp.2019.04.014

- **Nath, K.**, Dutta, A., and Hazra, B. (2019). An iterative polynomial chaos approach toward stochastic elastostatic structural analysis with non-Gaussian randomness. *International Journal for Numerical Methods in Engineering*, 119(11):1126-1160, https://doi.org/10.1002/nme.6086

Under Review in Journals

- **Nath, K.**, Dutta, A., and Hazra, B. (-). An adaptive scheme for random field discretization using KL expansion, *ASCE-ASME Journal of Risk and Uncertainty in Engineering Systems, Part A: Civil Engineering* UNDER REVIEW

- **Nath, K.**, Dutta, A., and Hazra, B. (-). A Polynomial Dimensional Decomposition-Iterative Polynomial Chaos approach towards solution of structural mechanics problems with random material properties, *Probabilistic Engineering Mechanics* UNDER REVIEW

- **Nath, K.**, Dutta, A., and Hazra, B. (-). Long duration response evaluation of linear structural system with random system properties using time dependent polynomial chaos, *Journal of Computational Physics* UNDER REVIEW

References

Adhikari, S. (2011). Doubly spectral stochastic finite-element method for linear structural dynamics. *Journal of Aerospace Engineering*, 24(3):264–276.

Allaix, D. L. and Carbone, V. I. (2009). Discretization of 2d random fields: A genetic algorithm approach. *Engineering Structures*, 31(5):1111 – 1119.

Allaix, D. L. and Carbone, V. I. (2010). Numerical discretization of stationary random processes. *Probabilistic Engineering Mechanics*, 25(3):332 – 347.

Allaix, D. L. and Carbone, V. I. (2012). Development of a numerical tool for random field discretization. *Advances in Engineering Software*, 51:10 – 19.

Ang, A. and Tang, W. (2014). *Probability Concepts in Engineering: Emphasis on Applications to Civil and Environmental Engineering*. Wiley India Pvt Ltd, second edition edition.

Arnst, M., Ghanem, R., Phipps, E., and Red-Horse, J. (2014). Reduced chaos expansions with random coefficientsin reduced-dimensional stochastic modeling of coupled problems. *International Journal for Numerical Methods in Engineering*, 97(5):352–376.

Baroth, J., Bressolette, P., Chauvire, C., and Fogli, M. (2007). An efficient SFE method using lagrange polynomials: Application to nonlinear mechanical problems with uncertain parameters. *Computer Methods in Applied Mechanics and Engineering*, 196(4548):4419 – 4429.

Bathe, K.-J. (1996). *Finite element procedures*. Prentice Hall, Englewood Cliffs, NJ.

Betz, W., Papaioannou, I., and Straub, D. (2014). Numerical methods for the discretization of random fields by means of the KarhunenLoѐve expansion. *Computer Methods in Applied Mechanics and Engineering*, 271:109 – 129.

Bjerager, P. (1988). Probability integration by directional simulation. *Journal of Engineering Mechanics*, 114(8):1285–1302.

Blatman, G. and Sudret, B. (2008). Sparse polynomial chaos expansions and adaptive stochastic finite elements using a regression approach. *Comptes Rendus Mcanique*, 336(6):518 – 523.

Blatman, G. and Sudret, B. (2010). An adaptive algorithm to build up sparse polynomial chaos expansions for stochastic finite element analysis. *Probabilistic Engineering Mechanics*, 25(2):183 – 197.

Blatman, G. and Sudret, B. (2011). Adaptive sparse polynomial chaos expansion based on least angle regression. *Journal of Computational Physics*, 230(6):2345 – 2367.

Brenner, C. E. and Bucher, C. (1995). A contribution to the SFE-based reliability assessment of nonlinear structures under dynamic loading. *Probabilistic Engineering Mechanics*, 10(4):265 – 273.

Chakraborty, S. and Dey, S. (1995). Stochastic finite element method for spatial distribution of material properties and external loading. *Computers & Structures*, 55(1):41 – 45.

Charmpis, D. C. and Papadrakakis, M. (2005). Improving the computational efficiency in finite element analysis of shells with uncertain properties. *Computer Methods in Applied Mechanics and Engineering*, 194(12):1447 – 1478. Special Issue on Computational Methods in Stochastic Mechanics and Reliability Analysis.

Chen, Y., Jakeman, J., Gittelson, C., and Xiu, D. (2015). Local polynomial chaos expansion for linear differential equations with high dimensional random inputs. *SIAM Journal on Scientific Computing*, 37(1):A79–A102.

Cheng, K. and Lu, Z. (2018). Adaptive sparse polynomial chaos expansions for global sensitivity analysis based on support vector regression. *Computers and Structures*, 194:86–96.

Comon, P. (1994). Independent component analysis, a new concept? *Signal Processing*, 36(3):287 – 314. Higher Order Statistics.

Deodatis, G. (1990). Bounds on response variability of stochastic finite element systems: effect of statistical dependence. *Probabilistic Engineering Mechanics*, 5(2):88 – 98.

Deodatis, G. (1991). Weighted integral method. I: Stochastic stiffness matrix. *Journal of Engineering Mechanics*, 117(8):1851–1864.

Deodatis, G. and Micaletti, R. C. (2001). Simulation of highly skewed non-gaussian stochastic processes. *Journal of Engineering Mechanics*, 127(12):1284–1295.

Deodatis, G. and Shinozuka, M. (1991). Weighted integral method. II: Response variability and reliability. *Journal of Engineering Mechanics*, 117(8):1865–1877.

Doostan, A., Ghanem, R. G., and Red-Horse, J. (2007). Stochastic model reduction for chaos representations. *Computer Methods in Applied Mechanics and Engineering*, 196(37):3951 – 3966. Special Issue Honoring the 80th Birthday of Professor Ivo Babuka.

Doostan, A. and Owhadi, H. (2011). A non-adapted sparse approximation of pdes with stochastic inputs. *Journal of Computational Physics*, 230(8):3015 – 3034.

Florian, A. (1992). An efficient sampling scheme: Updated latin hypercube sampling. *Probabilistic Engineering Mechanics*, 7(2):123 – 130.

Gerritsma, M., van der Steen, J.-B., Vos, P., and Karniadakis, G. (2010). Time-dependent generalized polynomial chaos. *Journal of Computational Physics*, 229(22):8333 – 8363.

Ghanem, R. and Spanos, P. (1991a). Spectral stochastic finite element formulation for reliability analysis. *Journal of Engineering Mechanics*, 117(10):2351–2372.

Ghanem, R. and Spanos, P. (1991b). *Stochastic Finite element: A spectral approach*. Spinger-Verlag, New Yark.

Ghanem, R. and Spanos, P. D. (1990). Polynomial chaos in stochastic finite elements. *Journal of Applied Mechanics*, 57(1):197–202.

Gill, P. E. and Miller, G. F. (1972). An algorithm for the integration of unequally spaced data. *The Computer Journal*, 15(1):80–83.

Golub, G. H. and Van Loan, C. F. (1983). *Matrix Computations*. The Johns Hopkins University Press, Baltimore, Maryland-21218.

Graham, L. and Deodatis, G. (2001). Response and eigenvalue analysis of stochastic finite element systems with multiple correlated material and geometric properties. *Probabilistic Engineering Mechanics*, 16(1):11 – 29.

Grigoriu, M. (1984). Crossings of non-gaussian translation processes. *Journal of Engineering Mechanics*, 110(4):610–620.

Grigoriu, M. (1998). Simulation of stationary non-gaussian translation processes. *Journal of Engineering Mechanics*, 124(2):121–126.

Gurley, K. R., Tognarelli, M. A., and Kareem, A. (1997). Analysis and simulation tools for wind engineering. *Probabilistic Engineering Mechanics*, 12(1):9 – 31.

Huang, S., Phoon, K.-K., and T. Quek, S. (2000). Digital simulation of non-gaussian stationary processes using Karhunen - Loève expansion. In *8th ASCE Specialty Conference on Probabilistic Mechanics and Structural Reliability*.

Huang, S. P., Quek, S. T., and Phoon, K. K. (2001). Convergence study of the truncated Karhunen - Loève expansion for simulation of stochastic processes. *International Journal for Numerical Methods in Engineering*, 52(9):1029–1043.

Hyvärinen, A. and Oja, E. (2000). Independent component analysis: algorithms and applications. *Neural Networks*, 13(4):411 – 430.

Jakeman, J., Eldred, M., and Sargsyan, K. (2015). Enhancing ℓ_1-minimization estimates of polynomial chaos expansions using basis selection. *Journal of Computational Physics*, 289:18 – 34.

Jakeman, J., Narayan, A., and Zhou, T. (2017). A generalized sampling and preconditioning scheme for sparse approximation of polynomial chaos expansions. *SIAM Journal on Scientific Computing*, 39(3):A1114–A1144.

Khalil, M. and Sarkar, A. (2008). Independent component analysis for uncertainty representation of stochastic systems. In *49th AIAA/ASME/ASCE/AHS/ASC Structures, Structural Dynamics, and Materials Conference, 16th AIAA/ASME/AHS Adaptive Structures Conference, 10th AIAA Non-Deterministic Approaches Conference, 9th AIAA Gossamer Spacecraft Forum, 4th AIAA Multidisciplinary Design Optimization Specialists Conference*, page 1891.

Khalil, M. and Sarkar, A. (2014). Independent component analysis to enhance performances of Karhunen-Loève expansions for non-gaussian stochastic processes: Application to uncertain systems. *Journal of Sound and Vibration*, 333(21):5600 – 5613.

Kiureghian, A. D. and Ditlevsen, O. (2009). Aleatory or epistemic? does it matter? *Structural Safety*, 31(2):105 – 112. Risk Acceptance and Risk Communication Risk Acceptance and Risk Communication.

Kiureghian, A. D. and Ke, J.-B. (1988). The stochastic finite element method in structural reliability. *Probabilistic Engineering Mechanics*, 3(2):83 – 91.

Kundu, A. and Adhikari, S. (2014). Transient response of structural dynamic systems with parametric uncertainty. *Journal of Engineering Mechanics*, 140(2):315–331.

Kundu, A., DiazDelaO, F., Adhikari, S., and Friswell, M. (2014). A hybrid spectral and metamodeling approach for the stochastic finite element analysis of structural dynamic systems. *Computer Methods in Applied Mechanics and Engineering*, 270:201 – 219.

Lagaros, N. D., Stefanou, G., and Papadrakakis, M. (2005). An enhanced hybrid method for the simulation of highly skewed non-gaussian stochastic fields. *Computer Methods in Applied Mechanics and Engineering*, 194(45):4824 – 4844.

Li, C. and Der Kiureghian, A. (1993). Optimal discretization of random fields. *Journal of Engineering Mechanics*, 119(6):1136–1154.

Li, H. and Zhang, D. (2013). Stochastic representation and dimension reduction for non-gaussian random fields: review and reflection. *Stochastic Environmental Research and Risk Assessment*, 27(7):1621–1635.

Li, J., Tian, Y., and Cassidy, M. J. (2015). Failure mechanism and bearing capacity of footings buried at various depths in spatially random soil. *Journal of Geotechnical and Geoenvironmental Engineering*, 141(2):04014099.

Liu, W. K., Belytschko, T., and Mani, A. (1986a). Probabilistic finite elements for nonlinear structural dynamics. *Computer Methods in Applied Mechanics and Engineering*, 56(1):61 – 81.

Liu, W. K., Belytschko, T., and Mani, A. (1986b). Random field finite elements. *Int. J. Numer. Meth. Engng.*, 23:1831 – 1845.

Liu, W. K., Mani, A., and Belytschko, T. (1987). Finite element methods in probabilistic mechanics. *Probabilistic Engineering Mechanics*, 2(4):201 – 213.

Loeve, M. (1977). *Probability Theory I*. Springer-Verlag New York.

Ma, X. and Zabaras, N. (2011). A stochastic mixed finite element heterogeneous multiscale method for flow in porous media. *Journal of Computational Physics*, 230(12):4696 – 4722.

Matthies, H. G., Brenner, C. E., Bucher, C. G., and Soares, C. G. (1997). Uncertainties in probabilistic numerical analysis of structures and solids-stochastic finite elements. *Structural Safety*, 19(3):283 – 336. Devoted to the work of the Joint Committee on Structural Safety.

Melchers, R. (1989). Importance sampling in structural systems. *Structural Safety*, 6(1):3 – 10.

Nair, P. (2001). On the theoretical foundations of stochastic reduced basis methods. In *19th AIAA Applied Aerodynamics Conference. June: 19*, pages 161–174.

Nair, P. B. and Keane., A. J. (2002). Stochastic reduced basis methods. *American Institute of Aeronautics and Astronautics*, 40(8):1653–1664.

Navarro, M., Witteveen, J., and Blom, J. (2014). Polynomial chaos expansion for general multivariate distributions with correlated variables. *arXiv preprint arXiv:1406.5483*.

Newland, D. E. and Newland, D. (1984). *An introduction to random vibrations and spectral analysis*, volume 2. Longman New York.

Nickel, R. E. (1971). On the stability of approximation operators in problems of structural dynamics. *International Journal of Solids and Structures*, 7(3):301 – 319.

Noh, H.-C. (2004). A formulation for stochastic finite element analysis of plate structures with uncertain poisson's ratio. *Computer Methods in Applied Mechanics and Engineering*, 193(4547):4857 – 4873.

Ozen, H. and Bal, G. (2016). Dynamical polynomial chaos expansions and long time evolution of differential equations with random forcing. *SIAM/ASA Journal on Uncertainty Quantification*, 4(1):609–635.

Ozen, H. C. and Bal, G. (2017). A dynamical polynomial chaos approach for long-time evolution of spdes. *Journal of Computational Physics*, 343:300 – 323.

Pascual, B. and Adhikari, S. (2012). A reduced polynomial chaos expansion method for the stochastic finite element analysis. *Sadhana*, 37(3):319–340.

Phoon, K., Huang, H., and Quek, S. (2005). Simulation of strongly non-gaussian processes using Karhunen-Loève expansion. *Probabilistic Engineering Mechanics*, 20(2):188 – 198.

Phoon, K., Huang, S., and Quek, S. (2002). Simulation of second-order processes using Karhunen-Loève expansion. *Computers & Structures*, 80(12):1049 – 1060.

Popescu, R., Deodatis, G., and Nobahar, A. (2005). Effects of random heterogeneity of soil properties on bearing capacity. *Probabilistic Engineering Mechanics*, 20(4):324 – 341.

Pranesh, S. and Ghosh, D. (2016). Addressing the curse of dimensionality in SSFEM using the dependence of eigenvalues in KL expansion on domain size. *Computer Methods in Applied Mechanics and Engineering*, 311:457 – 475.

Pranesh, S. and Ghosh, D. (2018). Cost reduction of stochastic galerkin method by adaptive identification of significant polynomial chaos bases for elliptic equations. *Computer Methods in Applied Mechanics and Engineering*, 340:54 – 69.

Rahman, S. (2006). A solution of the random eigenvalue problem by a dimensional decomposition method. *Int. J. Numer. Meth. Engng.*, (67):13181340.

Rahman, S. (2008). A polynomial dimensional decomposition for stochastic computing. *International Journal for Numerical Methods in Engineering*, 76(13):2091–2116.

Rahman, S. (2017). Wiener-Hermite polynomial expansion for multivariate gaussian probability measures. *Journal of Mathematical Analysis and Applications*, 454(1):303 – 334.

Rahman, S. (2018a). Mathematical properties of polynomial dimensional decomposition. *SIAM/ASA Journal on Uncertainty Quantification*, 6(2):816–844.

Rahman, S. (2018b). A polynomial chaos expansion in dependent random variables. *Journal of Mathematical Analysis and Applications*, 464(1):749 – 775.

Rahman, S. and Xu, H. (2004). A univariate dimension-reduction method for multi-dimensional integration in stochastic mechanics. *Probabilistic Engineering Mechanics*, 19(4):393 – 408.

Reusch, F. and Estrin, Y. (1998). FE-analysis of mechanical response of simple structures with random non-uniformity of material properties. *Computational Materials Science*, 11(4):294 – 308.

Sachdeva, S. K., Nair, P. B., and Keane, A. J. (2006). Comparative study of projection schemes for stochastic finite element analysis. *Computer Methods in Applied Mechanics and Engineering*, 195(1922):2371 – 2392.

Sakamoto, S. and Ghanem, R. (2002). Polynomial chaos decomposition for the simulation of non-gaussian nonstationary stochastic processes. *Journal of Engineering Mechanics*, 128(2):190–201.

Sarma, P., Durlofsky, L. J., and Aziz, K. (2008). Kernel principal component analysis for efficient, differentiable parameterization of multipoint geostatistics. *Mathematical Geosciences*, 40(1):3–32.

Schenk, C. and Schuëller, G. (2003). Buckling analysis of cylindrical shells with random geometric imperfections. *International Journal of Non-Linear Mechanics*, 38(7):1119 – 1132.

Shao, Q., Younes, A., Fahs, M., and Mara, T. A. (2017). Bayesian sparse polynomial chaos expansion for global sensitivity analysis. *Computer Methods in Applied Mechanics and Engineering*, 318:474–496.

Shinozuka, M. (1972). Probabilistic modeling of concrete structures. *ASCE J Eng Mech Div*, 98:1433–1451.

Shinozuka, M. and Deodatis, G. (1988). Response variability of stochastic finite element systems. *Journal of Engineering Mechanics*, 114(3):499–519.

Shinozuka, M. and Lenoe, E. (1976). A probabilistic model for spatial distribution of material properties. *Engineering Fracture Mechanics*, 8(1):217 – 227.

Sobol, I. M. (1998). On quasi-Monte Carlo integrations. *Mathematics and Computers in Simulation*, 47(2):103 – 112.

Soize, C. and Ghanem, R. G. (2009). Reduced chaos decomposition with random coefficients of vector-valued random variables and random fields. *Computer Methods in Ap-*

plied Mechanics and Engineering, 198(21):1926 – 1934. Advances in Simulation-Based Engineering Sciences Honoring J. Tinsley Oden.

Spanos, P. and Ghanem, R. (1989). Stochastic finite element expansion for random media. *Journal of Engineering Mechanics*, 115(5):1035–1053.

Stefanou, G. (2009). The stochastic finite element method: Past, present and future. *Computer Methods in Applied Mechanics and Engineering*, 198(9):1031 – 1051.

Sudret, B. and Kiureghian, A. D. (2002). Comparison of finite element reliability methods. *Probabilistic Engineering Mechanics*, 17(4):337 – 348.

Takada, T. (1990a). Weighted integral method in multi-dimensional stochastic finite element analysis. *Probabilistic Engineering Mechanics*, 5(4):158 – 166.

Takada, T. (1990b). Weighted integral method in stochastic finite element analysis. *Probabilistic Engineering Mechanics*, 5(3):146 – 156.

Vanmarcke, E. and Grigoriu, M. (1983). Stochastic finite element analysis of simple beams. *Journal of Engineering Mechanics*, 109(5):1203–1214.

Vanmarcke, E., Shinozuka, M., Nakagiri, S., Schuller, G., and Grigoriu, M. (1986). Random fields and stochastic finite elements. *Structural Safety*, 3(3):143 – 166.

Wall, F. and Deodatis, G. (1994). Variability response functions of stochastic plane stress/strain problems. *Journal of Engineering Mechanics*, 120(9):1963–1982.

Wan, X. and Karniadakis, G. E. (2005). An adaptive multi-element generalized polynomial chaos method for stochastic differential equations. *Journal of Computational Physics*, 209(2):617 – 642.

Wan, X. and Karniadakis, G. E. (2006a). Beyond Wiener-Askey expansions: Handling arbitrary pdfs. *Journal of Scientific Computing*, 27(1-3):455–464.

Wan, X. and Karniadakis, G. E. (2006b). Long-term behavior of polynomial chaos in stochastic flow simulations. *Computer Methods in Applied Mechanics and Engineering*, 195(41):5582 – 5596. John H. Argyris Memorial Issue. Part II.

Wan, X. and Karniadakis, G. E. (2006c). Multi-element generalized polynomial chaos for arbitrary probability measures. *SIAM Journal on Scientific Computing*, 28(3):901–928.

Wiener, N. (1938). The homogeneous chaos. *American Journal of Mathematics*, 60(4):897–936.

Witteveen, J. A., Sarkar, S., and Bijl, H. (2007). Modeling physical uncertainties in dynamic stall induced fluid-structure interaction of turbine blades using arbitrary polynomial chaos. *Computers & Structures*, 85(11):866 – 878.

Xiu, D. and Karniadakis, G. E. (2002). The Wiener-Askey polynomial chaos for stochastic differential equations. *SIAM Journal on Scientific Computing*, 24(2):619–644.

Xu, H. and Rahman, S. (2004). A generalized dimension-reduction method for multidimensional integration in stochastic mechanics. *International Journal for Numerical Methods in Engineering*, 61(12):1992–2019.

Yadav, V. and Rahman, S. (2014). Adaptive-sparse polynomial dimensional decomposition methods for high-dimensional stochastic computing. *Computer Methods in Applied Mechanics and Engineering*, 274:56 – 83.

Yamazaki, F., Member, A., Shinozuka, M., and Dasgupta, G. (1988). Neumann expansion for stochastic finite element analysis. *Journal of Engineering Mechanics*, 114(8):1335–1354.

Yamazaki, F. and Shinozuka, M. (1988). Digital generation of non-Gaussian stochastic fields. *Journal of Engineering Mechanics*, 114(7):1183–1197.

Yin, S., Yu, D., Luo, Z., and Xia, B. (2018). An arbitrary polynomial chaos expansion approach for response analysis of acoustic systems with epistemic uncertainty. *Computer Methods in Applied Mechanics and Engineering*, 332:280 – 302.

Zeldin, B. A. and Spanos, P. D. (1998). On random field discretization in stochastic finite elements. 65(2):320–327.

Zhang, J. and Ellingwood, B. (1994). Orthogonal series expansions of random fields in reliability analysis. *Journal of Engineering Mechanics*, 120(12):2660–2677.

Zhu, W., Ren, Y., and Wu, W. (1992). Stochastic FEM based on local averages of random vector fields. *Journal of Engineering Mechanics*, 118(3):496–511.